

EVALUATION OF METHODS FOR THE ASSESSMENT OF *IN VITRO* NEUROTOXICITY

Calcium homeostasis as target for insecticides

Marieke Meijer

2016

**EVALUATION OF METHODS FOR THE ASSESSMENT
OF *IN VITRO* NEUROTOXICITY**

Calcium homeostasis as target for insecticides

**EVALUATIE VAN METHODEN VOOR HET
BEOORDELEN VAN NEUROTOXICITEIT *IN VITRO***

Calcium homeostase als neurotoxisch aangrijpingspunt
voor bestrijdingsmiddelen

(met een samenvatting in het Nederlands)

Proefschrift

ter verkrijging van de graad van doctor aan de Universiteit Utrecht op
gezag van de rector magnificus, prof. dr. G.J. van der Zwaan, ingevolge
het besluit van het college voor promoties in het openbaar te verdedigen

op dinsdag 24 mei 2016 des middags te 2.30 uur

door

Marieke Meijer

geboren op 2 april 1988 te Beverwijk

Evaluation of methods for the assessment of *in vitro* neurotoxicity
Calcium homeostasis as target for insecticides

Copyright © Marieke Meijer

ISBN: 978-90-393-6536-6

Layout and printing: Proefschrift-aio.nl

Cover design and illustrations: Eko Baskoro Harimulyo

The studies described in this thesis were performed at the Neurotoxicology
Research Group, Toxicology Division, at the Institute for Risk Assessment
Sciences (IRAS), Faculty of Veterinary Medicine, Utrecht University.

Promotor: Prof. dr. M. van den Berg
Copromotor: Dr. R.H.S. Westerink

This thesis was accomplished with financial support of the European Union project DENAMIC (Developmental Neurotoxicity Assessment of Mixtures in Children), grant agreement FP7-env-2011-282957

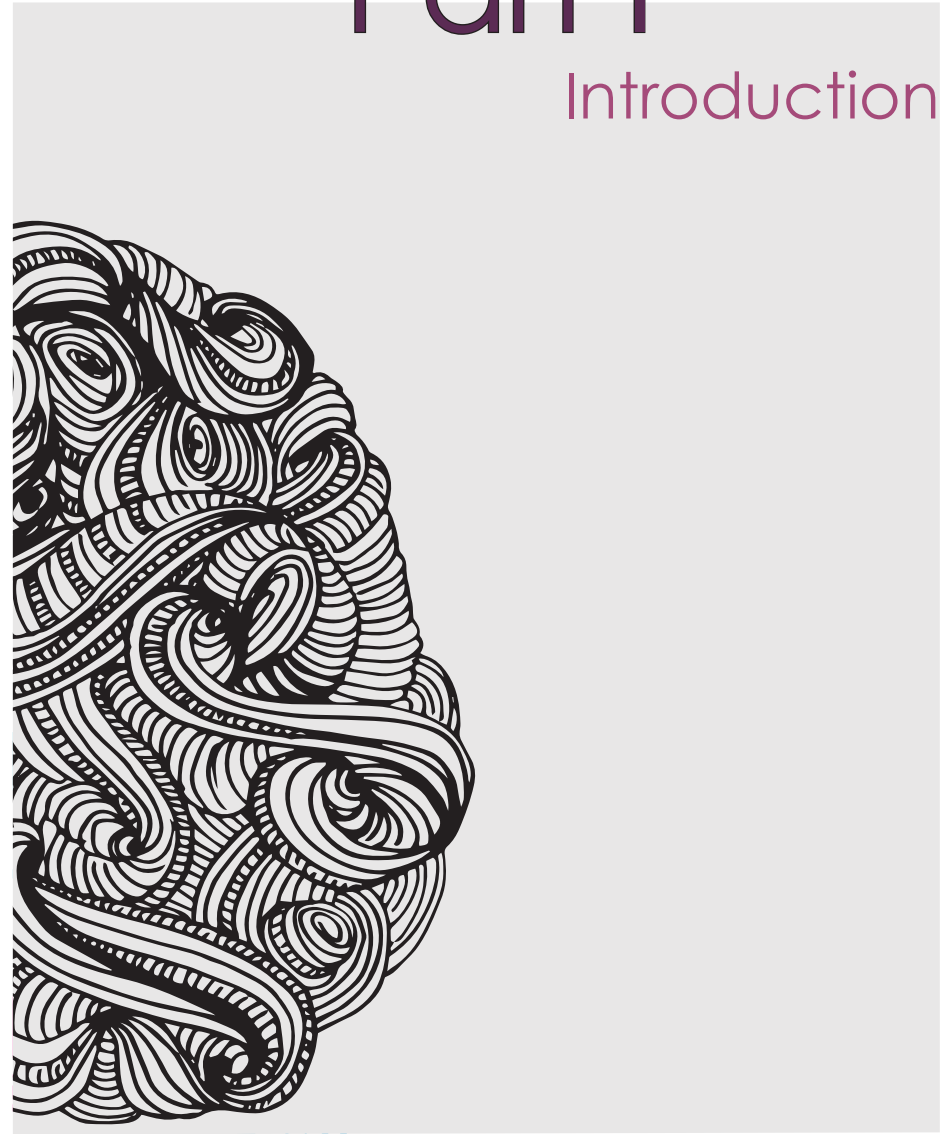
CONTENTS

<hr/>		
Part 1 Introduction		8
Chapter 1	Introduction and outline of the thesis	11
<hr/>		
Part 2 Cell viability and methods for assessing neurotoxicity		26
Chapter 2	Screening for effects on cell viability (concentration-range finding)	29
Chapter 3	Evaluation of assays for the investigation of oxidative stress	49
Chapter 4	Experimental approaches to study neurotransmitter release <i>in vitro</i>	73
Chapter 5	Comparison of plate reader-based methods with fluorescence microscopy for measurements of intracellular calcium levels for the assessment of <i>in vitro</i> neurotoxicity	83
<hr/>		
Part 3 Screening for effects of insecticides on calcium homeostasis		100
Chapter 6	Acute disturbance of calcium homeostasis in PC12 cells as a novel mechanism of action for (sub)micromolar concentrations of organophosphate insecticides	103
<hr/>		
Chapter 7	Inhibition of voltage-gated calcium channels as common mode of action for (mixtures of) distinct classes of insecticides	121
Chapter 8	Inhibition of voltage-gated calcium channels after subchronic and repeated exposure of PC12 cells to different classes of insecticides	139
<hr/>		
Part 4 Ex vivo study		162
Chapter 9	Effects of a single, oral dose of chlorpyrifos during a critical period of brain development in mice on hippocampal long-term potentiation	165
<hr/>		
Part 5 Summary, discussion and recommendations		174
Chapter 10	Summary and discussion	177
References		192
Appendix	Nederlandse samenvatting	217
	Dankwoord	225
	Curriculum Vitae	228
	List of publications	228



Part I

Introduction



Chapter 1

INTRODUCTION AND OUTLINE OF THE THESIS

1.1 REGULATORY NEUROTOXICITY TESTING

In developed countries the production, use and application of chemicals is regulated to protect human and environmental health. In Europe, a variety of chemical regulations have been replaced by one regulation, entitled REACH (Registration, Evaluation and Administration of Chemicals). Previous European Union (EU) legislation distinguished between “existing” (chemicals reported on the European market between 1971 and 1981; > 100,000 chemicals) and “new” chemicals (chemicals introduced on the market after 1981; > 3,800 chemicals) and required that only new chemicals are tested for their safety before being allowed on the market. In contrast, the new REACH regulation requires companies to provide safety information of all chemicals produced or imported in high-volume (> 1000 kg/year; EC EU, 2015). Consequently, more toxicity studies are needed that are performed according to regulatory test guidelines described by the Organization for Economic Co-operation and Development (OECD; OECD, 2015a) or the EU (ECHA, 2015b). Many of these toxicity studies are performed with animals (*in vivo* studies), for example, the study described in OECD test guideline 443 that evaluates reproductive and developmental effects of pre- and postnatal chemical exposure and systemic toxicity in pregnant and lactating females and offspring (OECD, 2015b). Furthermore, studies performed according to this guideline provide an indication of other types of chemical-induced toxicity. In case of indications of chemical-induced toxicity of the nervous system (neurotoxicity), an additional study should be performed according to OECD test guideline 426 or 424. These test guidelines investigate chemical-induced effects on the developing and adult nervous system, respectively (OECD, 2015c,d). Specifically, the tests described by test guideline 426 and 424 evaluate chemical-induced neurobehavioral changes of cognitive, sensory, and motor functions and changes in neuropathology in animals (OECD, 2015c,d). With the results of these studies the safety of the chemical is evaluated by the European Chemicals Agency (ECHA) or by the member states (ECHA, 2015a).

1.2 THE EUROPEAN UNION PROJECT DEVELOPMENTAL NEUROTOXICITY ASSESSMENT OF MIXTURES IN CHILDREN (DENAMIC)

Recently, there has been concern that the current regulatory neuro(developmental) toxicity studies are not sufficiently sensitive for the detection of (developmental) neurotoxicity (e.g. Coecke et al., 2007; Vorhees and Makris, 2015). There is particular concern that (environmental) exposure to low levels of neurotoxic chemicals (and mixtures thereof) contributes to the observed increase in learning and developmental disorders. Multiple epidemiological studies have indicated that exposure to known neurotoxicants can impair neurodevelopment in children (e.g. Boucher et al., 2013; Forns et al., 2012; Keil et al., 2014; Muñoz-Quezada et al., 2013; Sagiv et al., 2010). In addition, current regulatory studies require many animals (at least 80 animals/experiment), are expensive, and time-consuming (28 days-1 year). Subsequently, there is societal pressure and a need for better (more sensitive, cheaper and faster) and animal-free (*in vitro*; developmental) neurotoxicity studies that predict human hazard more accurately (Bal-Price et al., 2008, 2010; Coecke et al., 2007). Therefore, the aim of the DENAMIC project was to develop tools and methods for screening chemicals for neurotoxicity, to support and improve EU legislation for the identification of (potential) neurotoxicants.

The DENAMIC project consisted of two pillars; exposure/epidemiology and hazard characterization. These pillars will be used together for risk assessment. The research described in this thesis was part of the hazard characterization and focused on the development of tools and methods for *in vitro* neurotoxicity screening. Within the DENAMIC project, insecticides from different classes, that are well-known for their neurotoxicity and presence in food, were selected as reference chemicals (the organochlorine endosulfan, the organophosphate chlorpyrifos, the pyrethroid cypermethrin and the carbamate carbaryl). Also, the neonicotinoid imidacloprid and the organophosphates parathion, paraoxon-ethyl (metabolite of parathion), paraoxon-methyl (metabolite of methyl parathion) and chlorpyrifos-oxon (metabolite of chlorpyrifos) were studied in this thesis.

1.3 IN VITRO NEUROTOXICITY TARGETS

The nervous system is a complex structure with specialized cells (neurons) that transports, receives, integrates and translates signals into cellular actions that determine the functioning and behavior of an organism. Neurons can communicate with each other via neurotransmission with signaling molecules (e.g. neurotransmitters and neurohormones) and electrical signals (action potentials). To study neurotoxicity, *in vitro* models of neurons (neuronal cells) and neural cells (other cells of the nervous system, such as glial cells) can be used to investigate chemical-induced changes of cellular and molecular processes that are essential for neuronal function. Essential neuronal functions that are studied in this thesis are neuronal cell viability, oxidative stress, neurotransmitter release, and calcium homeostasis. *In vitro* assays are potentially more sensitive, cheaper and faster methods than *in vivo* methods and are therefore the focus of this research.

1.3.1 Cell viability

Chemical-induced molecular and cellular changes of neur(on)al cells may ultimately result in cell death (cytotoxicity) and can be assessed by the study of cell viability. Since the assessment of chemical-induced molecular and cellular changes is biased at concentrations that induce cytotoxicity, cell viability studies are often performed as concentration-range finding studies. With concentration-range finding studies in neur(on)al cells, concentrations are identified below which a specific neurotoxic effect could be detected without cytotoxicity (Westerink, 2014). Several measures can be used to study cytotoxicity, which are generally divided in active and passive measures of cell viability. Examples of active measures of cell viability are ATP levels and mitochondrial activity, whereas passive measures of cell viability assess, e.g., membrane integrity and the percentage of viable neurons (Johnson et al., 2013). In general, a combination of active and passive measures of cell viability assays is and should be used.

1.3.2 Oxidative stress

Cellular oxidative stress is the imbalance between reactive oxygen species (ROS) and the antioxidant defense capacity and could be the result of chemical exposure. ROS play an important role in cellular signaling and an excessive ROS level (oxidative stress) can damage DNA, proteins and lipids. As a result, it can cause impaired cellular functioning and, consequently, cell death (Dai et al., 2014). Not surprisingly, oxidative stress is involved in neurodegenerative disorders, such as Alzheimer's disease and Parkinson's disease (e.g. Popa-Wagner et al., 2013).

1.3.3 Neurotransmission

Upon arrival of an action potential, (presynaptic) neurons release neurotransmitters at the end of their axon, which in many cases is in the vicinity of dendrites or the soma of neighboring (postsynaptic) neurons via specialized connections (synapses). Generally, action potentials are electrical signals that carry their information (encoded in their firing pattern) along axons to their presynaptic parts. In the presynaptic plasma membrane, voltage-gated calcium channels (VGCCs) open upon arrival of the action potential, thereby allowing a rapid influx of extracellular calcium ions and, thereby a strong increase of the intracellular calcium concentration ($[Ca^{2+}]_i$; Fig. 1). This rapid increase of $[Ca^{2+}]_i$ triggers the release of neurotransmitters. Neurotransmitters are stored in vesicles in the presynaptic neuron and are released into the synaptic cleft via fusion of the vesicle membrane with the presynaptic plasma membrane, a process called exocytosis. (Fig. 1). On the opposite side of the synaptic cleft, at the postsynaptic neuron, the released neurotransmitters bind and activate their receptors, resulting in cellular signal transduction (Fig. 1). Signal transduction is terminated by reuptake (presynaptic neurotransmitter transporters) or degradation of the neurotransmitters (neurotransmitter esterases and oxidases). There are different types of neurotransmitters, such as acetylcholine, dopamine, gamma-aminobutyric acid (GABA), glutamate and serotonin, and a wide variety of neuropeptides, each of which plays a (only partly known) role in brain functions, such as memory, attention, learning and behavior.

Calcium homeostasis

Calcium homeostasis plays an important role in numerous cell functions, such as neuronal cell signaling (neurotransmission), neur(on)al development and gene expression. Consequently, cells tightly regulate their $[Ca^{2+}]_i$ (e.g. Leclerc et al., 2011). Basal $[Ca^{2+}]_i$ is kept low and stable and is locally increased in the cell by influx of extracellular Ca^{2+} upon depolarization of the cell membrane via VGCCs, or upon activation of calcium-permeable receptors via ligand-binding. VGCCs can be divided in two major categories: low-voltage activated (LVA) calcium channels, which are activated at small membrane depolarizations, and high-voltage activated (HVA) calcium channels, which are activated at stronger membrane depolarizations. T- ($Ca_v3.1$ - $Ca_v3.3$) type VGCCs are LVA channels and are rapidly inactivated. L- ($Ca_v1.1$ - 1.4), N- ($Ca_v2.1$), P/Q- ($Ca_v2.2$) and R- ($Ca_v2.3$) type channels are HVA channels and are more slowly inactivated. All calcium channels can trigger neurotransmitter release and the different calcium channels produce different release dynamics. N- and P/Q- type channels are involved in fast synaptic transmission, L- type channels in tonic and slower neurotransmitter release, and T- type channels in low-threshold exocytosis (Simms and Zamponi, 2014).

VGCCs function and activity are essential for proper neurotransmission. VGCCs dysregulation is linked to a variety of neurological disorders (Simms and Zamponi, 2014) and disturbed calcium signaling has been shown to play a role in neurodegenerative diseases, such as Parkinson's disease (Cali et al., 2014; Egorova et al., 2015).

1.3.4 Cell models

To study *in vitro* neurotoxicity, different neur(on)al models can be used, such as neur(on)al cell lines and primary neur(on)al cells. Neur(on)al cell lines are commonly derived from tumors and have neur(on)al characteristics. They are proliferative, relatively stable and reproducible cells. Rat PC12 cells are derived from a pheochromocytoma, have characteristics of dopaminergic neurons and are often used for neuroscience/neurotoxicity studies (Westerink and Ewing, 2008). PC12 cells express L-, N-, and P/Q-type VGCCs (Dingemans et al., 2009; Heusinkveld et al., 2010), have calcium homeostasis similar to that of neurons and can release neurotransmitters upon depolarization (Westerink and Ewing, 2008). They are easily cultured and can form networks upon differentiation with neurite growth factor

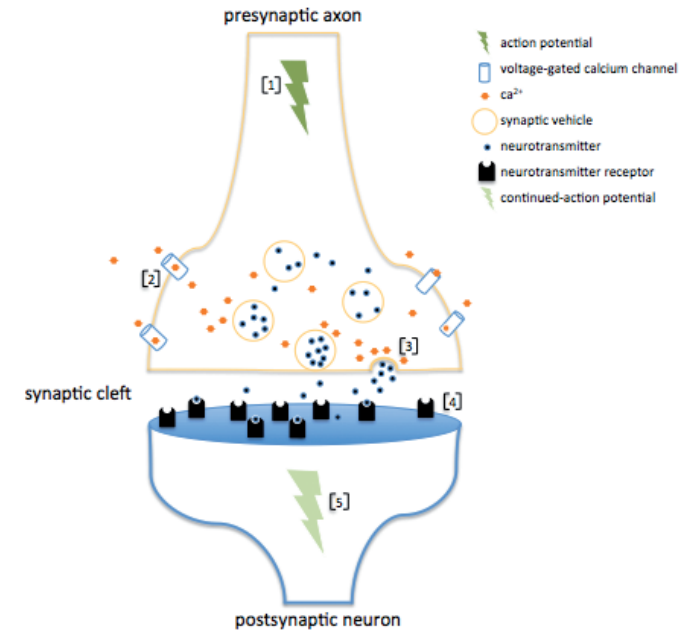


Figure 1: Simplified representation of neurotransmission. When an action potential reaches the synapse (1), VGCCs open allowing a rapid increase of the intracellular calcium concentration $[Ca^{2+}]_i$ (2). This rapid increase in $[Ca^{2+}]_i$ triggers the fusion of vesicles with the cell membrane, thereby releasing neurotransmitters into the synaptic cleft (3). The released neurotransmitters activate their neurotransmitter receptor located at the postsynaptic neuron (4). In the postsynaptic neuron the activated neurotransmitter receptors trigger intracellular signaling cascades or evoke a new action potential (5).

(NGF; Greene and Tischler, 1976). PC12 cells are thus suitable cells to study neurotransmitter release and calcium homeostasis. Primary neur(on)al cells are isolated from brain tissue and are cultured *in vitro* directly after isolation. Cells can be isolated from distinct parts of the brain, e.g. the cerebellum, the midbrain and the cortex. In culture, primary neurons differentiate and form functional heterogeneous networks and have spontaneous electrical activity. However, generally they do not proliferate (Harry et al., 1998). Primary neur(on)al cultures are useful cell models

to study neurotransmission and developmental processes. Since these cultures are heterogeneous, i.e., consist of various neural cell types, they are less suitable for the study of a single, specific cellular mechanism, such as chemically-induced inhibition of VGCCs.

Other models that can be used to study neurotoxicity are stem cells that can be stimulated to differentiate into neur(on)al cells. With stem cells, disturbances in neur(on)al differentiation at an early time-point in development can be studied. In addition, neur(on)al progenitor cells, which are stem cells already directed into the neur(on)al pathway, can be used for (developmental) neurotoxicity studies (Breier et al., 2010).

Cell lines and primary neur(on)al cells are single cells, which could form networks when cultured *in vitro*. However, cultured networks are often single layers of cells and have less cell-cell interactions than those present in the complex cellular matrix of multiple cell layers of the nervous system. Therefore, for specific studies brain slices are preferred since they consist of multiple non-dissociated cell layers. In a brain slice, the brain tissue remains relatively intact and represents a small part of a functional brain that could be used for e.g. electrophysiology studies (Lynch and Schubert, 1980).

1.4 CHEMICALS OF CONCERN FOR (DEVELOPMENTAL) NEUROTOXICITY

Humans are exposed to a wide variety of neurotoxic chemicals in their environment. Neurotoxic chemicals are present in and on food due to e.g. contamination with pesticides or heavy metals, or by natural toxins in specific foods, e.g. tetrodotoxin (TTX; a very potent neurotoxin present in, among others, pufferfish). Exposure to neurotoxic chemicals can also occur by drug use (e.g. drugs of abuse), working with industrial chemicals like organic solvents or contact with environmental pollutants present in e.g. consumer products. Generally, humans are exposed to multiple (neurotoxic) chemicals at the same time and interactions between such chemicals may increase toxicity.

1.4.1 Environmental pollutants

Environmental pollutants, that are well-known for their neurotoxicity, include polychlorinated biphenyls (PCBs), polybrominated diphenyl ethers

(PBDEs), heavy metals, such as methylmercury and lead, and pesticides. PCBs were used for many industrial applications and in particular as dielectric fluids in capacitors because of their specific physical and chemical properties (Ross, 2004). PBDEs were used as flame retardants (Costa et al., 2014) and methylmercury had various applications, such as medicine, dental amalgam, and as preservative in latex paint and in pesticides (Clarkson and Magos, 2006). Lead has various applications e.g. in building construction, paint, batteries and as radiation shield (Bressler et al., 1999). Pesticides are chemicals used for pest control in agriculture and households. Because PCBs, PBDEs, heavy metals and various pesticides are very persistent, can accumulate in the environment, and are (neuro)toxic, their use is either restricted or prohibited (Costa et al., 2014; Ross, 2004). Particularly pesticides that target insects (insecticides) are of concern for (developmental) neurotoxicity, since human exposure to pesticides often occurs due to their widespread use in agriculture and households. Another source of exposure to pesticides is via residues that are present on food.

Insecticides

Insecticides are well-known potent neurotoxicants to insects. However, most insecticides are not species-specific and can also target the mammalian nervous system. Therefore, the widespread use of insecticides in households and agriculture may pose a threat to human health. Various types of insecticides exist, which have different physical and chemical properties and are classified by their molecular structure and well-known modes of action.

Organochlorines

Organochlorines are very persistent, bioaccumulate in the environment and are poorly metabolized by humans (Mrema et al., 2013). They can be divided into two subtypes: DDT-type insecticides and chlorinated alicyclic insecticides. DDT-type insecticides prevent the deactivation or closing of voltage-gated sodium channels (VGSCs) in neurons and the chlorinated alicyclic insecticides inhibit Cl⁻ influx mediated by the GABA receptor, resulting in depolarization leading to hyper-excitation (Coats, 1990). Several studies have demonstrated an association between developmental exposure to organochlorines and impaired neurodevelopment in children (Boucher et al., 2013; Eskenazi et al., 2008; Forns et al., 2012; Sagiv et al.,

2008, 2010). Although organochlorine insecticides have been banned in Europe, residues of the chlorinated alicyclic organochlorine endosulfan are still frequently found in food at levels that exceed the maximum residue level (MRL) allowed on food products demonstrating their persistency in the environment (EFSA, 2014, 2015). Besides inhibition of GABA receptors, endosulfan has many other targets in animals involved in neurological functions. It can alter the expression of the neuronal proteins vesicular monoamine transporter 2 (VMAT2), dopamine transporter (DAT), tyrosine hydroxylase (TH), dopamine 2 (D2) receptor, vesicular glutamate transporter (vGlut) and glutamate N2B (GluN2B) receptor in the frontal cortex of male offspring of rodents (Wilson et al., 2014). Also, endosulfan increases the amplitude of evoked potential in rat cortex (Scremin et al., 2011) and reduces cholinesterase activity in dams and their male offspring when exposed during mating, pregnancy and lactation (Silva de Assis et al., 2011). After developmental exposure of zebrafish to endosulfan, touch response (Stanley et al., 2009) and acetylcholinesterase (AChE) activity were reduced, which was accompanied by a reduction in exploratory performance (Pereira et al., 2012). Moreover, endosulfan induced lipid peroxidation (Jia and Misra, 2007; Qiao et al., 2005; Slotkin et al., 2007b) and P450 enzymes (e.g. Casabar et al., 2010) *in vitro*.

Organophosphates

Organophosphate insecticides are well-known irreversible inhibitors of acetylcholinesterase (AChE). The termination of neurotransmission by acetylcholine (ACh) occurs by intrasynaptic degradation of ACh by AChE. If AChE is no longer present or not functional, ACh continues to activate its postsynaptic receptors, which can cause hyperexcitation. The neurotoxic potential of organophosphate insecticides (inhibition of AChE) is strongly increased by bioactivation to their -oxon metabolites (Eaton et al., 2008). Organophosphates have been widely used and exposure to these chemicals has been associated with neurodevelopmental disorders in children (reviewed by Muñoz-Quezada et al., 2013). An organophosphate that has been extensively studied for its neurotoxicity and that frequently exceeds the MRL on food, is chlorpyrifos (EFSA, 2015). Chlorpyrifos induces neurochemical and neurobehavioral changes in (developing) rodents (e.g. Icenogle et al., 2004; Moser et al., 2005; Padilla et al., 2005) and in zebrafish (Richendrer et al., 2012; Sledge et al., 2011) following various exposure

scenarios. *In vitro* studies with neurons have demonstrated numerous neurotoxic effects for chlorpyrifos, including inhibition of neurite outgrowth (e.g. Howard et al., 2005; Sachana et al., 2001, 2005; Yang et al., 2008) and of nicotinic acetylcholine receptor (nAChR) functioning (Smulders et al., 2004), induction of oxidative stress (Crompton et al., 2000; Lee et al., 2012; Slotkin et al., 2007b; Slotkin and Seidler, 2009b, 2010), programmed cell-death (apoptosis; Lee et al., 2012; Raszewski et al., 2014), and phosphorylation of transcription factor CREB (Schuh et al., 2002). Additionally, chlorpyrifos has been reported to reprogram adenylyl cyclase signaling (Adigun et al., 2010a), reduce dopamine content (Xu et al., 2012) and change choline acetyl transferase (ChAT) and tyrosine hydroxylase (TH) activity and gene expression (Jameson et al., 2006; Slotkin and Seidler, 2009a,b). Moreover, additional gene expression studies have been performed *in vitro* and *in vivo* that showed changes in expression of various other genes after chlorpyrifos exposure (Adigun et al., 2010b; Betancourt et al., 2006; Estevan et al., 2013; Slotkin et al., 2010; Slotkin and Seidler, 2009a,b, 2010, 2011, 2012). In addition to effects of chlorpyrifos on neuronal cells, several studies have implicated an important role for glial cells in the neurotoxicity of chlorpyrifos (Garcia et al., 2001, 2005; Guizzetti et al., 2005; Qiao et al., 2001; Sachana et al., 2008; Zurich et al., 2004) and a direct role for the -oxon metabolites of organophosphates (e.g. chlorpyrifos-oxon) in developmental neurotoxicity (Flaskos, 2012).

Carbamates

Carbamates are known as reversible inhibitors of AChE. Comparable with organophosphates, the inhibition of AChE will increase the ACh level in the synaptic cleft, resulting in overexcitation. Some studies have indicated that children exposed to carbamates have an increased risk for neurodevelopmental disorders (Ostrea et al., 2012; Shelton et al., 2014). On food, the carbamate carbaryl has been found at concentrations that exceed the MRL (EFSA, 2014). In animals, carbaryl affects several functional and behavioral outcomes (McDaniel et al., 2007; Moser, 1995; Moser et al., 2010, 2015). Besides inhibition of AChE, carbaryl can block nAChRs (Nagata et al., 1997; Smulders et al., 2003, 2004), inhibit nitric oxide synthase (NOS; Rao et al., 1999) and neurite outgrowth (Flaskos et al., 1999), and also induces changes in electrical neuronal activity *in vitro* and *in vivo* (Alloisio et al., 2015; Freeborn et al., 2015).

Pyrethroids

Pyrethroids are well-known for their ability to delay the inactivation of VGSCs resulting in depolarization and subsequent overexcitation (Choi and Soderlund, 2006; Meacham et al., 2008). They are rapidly metabolized in humans (e.g. Leng et al., 2006) and other mammals (Wolansky and Harrill, 2008). Nevertheless, some epidemiological studies have found an association between exposure to pyrethroids and neurodevelopmental disorders in children (Oulhote and Bouchard, 2013; Shelton et al., 2014; Wagner-Schuman et al., 2015). Residues of the pyrethroid cypermethrin have been found on food at concentrations that exceed the MRL (EFSA, 2013). In rodents, cypermethrin was shown to induce behavioral changes, such as spontaneous behavior in mice (Lee et al., 2015b), motor activity (Crofton and Reiter, 1988; Wolansky et al., 2006), changes in the functional observational battery (FOB; McDaniel and Moser, 1993; Weiner et al., 2009) and in schedule-controlled behavior in rats (Peele and Crofton, 1987). In addition to changes in behavior, cypermethrin alters the expression/level of tau (Lee et al., 2015b; Maurya et al., 2015), glutamate receptor 1 (GluR1; Lee et al., 2015b), GABA (Han et al., 2014), glial fibrillary acidic protein (GFAP; Malkiewicz et al., 2006), and glutathione (GSH; Giray et al., 2001) in different brain tissues. Furthermore, cypermethrin induced lipid peroxidation (Giray et al., 2001; Tiwari et al., 2010) and apoptosis, and affected the mitochondria in brain tissues (Agrawal et al., 2015). In animals, the pyrethroids permethrin and cypermethrin also reduced the dopamine level (Nasuti et al., 2007). Beside their effects on VGSCs (Choi and Soderlund, 2006; Meacham et al., 2008), cypermethrin suppressed the open state of voltage-gated chloride channels (Burr and Ray, 2004) and altered the delayed rectifier potassium current (Yu-Tao et al., 2009) in *in vitro* models.

Neonicotinoids

Neonicotinoids are well-known for their activation of nAChRs, resulting in overexcitation (Matsuda et al., 2009). Their human health risk is presumably low due to their high selectivity for insect nAChRs compared with mammals (Tomizawa et al., 2000), though a possible association between imidacloprid and autism spectrum disorders has been reported (Keil et al., 2014). Furthermore, rat offspring of imidacloprid exposed dams showed sensorimotor impairments and increased GFAP expression (Abou-

Donia et al., 2008), whereas zebrafish exposed to imidacloprid showed neurobehavioral changes (Crosby et al., 2015). *In vitro*, imidacloprid acted as an agonist on human (Li et al., 2011) and rat nAChRs (Kimura-Kuroda et al., 2012). Moreover, imidacloprid was shown *in vitro* to activate the extracellular-regulated kinase (ERK) cascade (Tomizawa and Casida, 2002) and to cause a depolarization shift of the membrane potential (Bal et al., 2010).

1.5 THESIS OUTLINE

This thesis consists of **5 parts**. **Part 1** is aimed at introducing the subject and reference compounds of this thesis. **Part 2** describes the concentration-range finding and the evaluation of methods used. **Part 3** consists of *in vitro* studies that have extensively investigated the effects of insecticides on calcium homeostasis. In **part 4**, an *ex vivo* study is described, which investigated the effect of neonatal chlorpyrifos exposure on a neurophysiological measure of learning and memory. In **part 5**, the data presented in **parts 2-4** are summarized and discussed.

More specifically, **part 1 (chapter 1)** has described the background of this project and the investigated chemicals and targets of interest for screening for neurotoxicity. **Part 2** describes a concentration-range finding (cell viability) study of chemicals in PC12 cells (**chapter 2**), followed by reports on the development and applicability of assays for screening for oxidative stress (**chapter 3**) and neurotransmitter release in neuronal cells (**chapter 4**). Next, it was evaluated if a high-throughput approach with a plate reader-based method for $[Ca^{2+}]_i$ measurements would yield similar results as measurements obtained with a low- to medium- throughput fluorescence microscopy-based approach (**chapter 5**). The evaluated assays for the detection of oxidative stress and neurotransmitter release did not appear suitable for screening for chemical-induced effects. For $[Ca^{2+}]_i$ measurements, it was demonstrated that results obtained with a plate reader-based method yielded different results compared with data obtained with a fluorescence microscopy-based method and it appeared that experiments with a plate reader-based method yielded unreliable results. Therefore, in **part 3** studies on calcium homeostasis were performed with a fluorescence microscopy-based method. Effects of insecticides on calcium homeostasis, in particular on VGCCs, were investigated. First,

effects of acute exposure to organophosphate insecticides, a carbamate insecticide and mixtures thereof on calcium homeostasis in PC12 cells were studied (**chapter 6**). Several -oxon metabolites of the organophosphates were included in the study because data on AChE inhibition demonstrated that organophosphates are particularly potent AChE inhibitors upon bioactivation. Next, the effects of acute exposure to an organochlorine (endosulfan), organophosphate (chlorpyrifos), pyrethroid (cypermethrin) and neonicotinoid (imidacloprid) and mixtures of these chemicals on calcium homeostasis in PC12 cells were investigated as a common mode of action for different types of insecticides (**chapter 7**). Since exposure to insecticides generally occurs subchronically and repeatedly, the effects of subchronic and repeated exposure to insecticides on calcium homeostasis were investigated in PC12 cells (**chapter 8**). Moreover, to investigate differences between cell models, studies on calcium homeostasis were also performed with primary neuronal cortical cultures to compare with the studies performed with PC12 cells (**chapter 8**).

In a collaboration with different partners of the DENAMIC project, an *ex vivo* study was performed to correlate *in vivo* and *in vitro* data (**part 4**). To this end, mice were exposed to a single, oral dose of chlorpyrifos at a critical period of brain development, which is known to induce changes in spontaneous behavior at 4 months of age. Effects on long-term potentiation, a measure of learning and memory, were investigated in hippocampal brain slices of these mice at ~5 months of age (**chapter 9**).

The data presented in this thesis are summarized and placed in context of the existing literature in **part 5 (chapter 10)**, which is a summary and discussion of the information presented in **chapters 2-9** followed by conclusions and recommendations for future research.

Handwritten physics notes and diagrams:

- $U = \epsilon B$
- low resistance: $R_1 = 13.5 \Omega$, $R_2 = 3 \Omega$, $R_3 = 20 \Omega$
- $F_A = \rho g V$, $w = D \uparrow$, $w = 0$, $z = u$
- $P = \bar{S}$
- Graph: X_{in} vs ω showing a resonance peak labeled "Plank".
- $\omega^2 = \frac{mgL}{I}$; $T = \frac{2\pi}{\omega} = 2\pi \sqrt{\frac{I}{mgL}}$
- $x = \rho \cos \varphi$, $y = \rho \sin \varphi$
- $\rho = \sqrt{x^2 + y^2}$
- $q = \frac{h}{\lambda} = \frac{h}{v \cdot T} = \frac{h}{v} \cdot \frac{1}{T} = \frac{h}{v} \cdot \frac{\omega}{2\pi}$
- $s = 10m$, $\frac{h}{v} = \frac{h}{c} = \frac{h}{3 \times 10^8}$
- Equations of motion: $x' = x_0 + mt'$, $y' = y_0 + nt'$, $z' = z_0 + pt'$
- Formula for s : $1) T = \frac{t}{n}$, $2) v = \frac{c}{n}$, $3) T = \frac{t}{n}$, $4) v = \frac{c}{n}$, $5) v = \frac{2\pi r}{T}$
- Diagram: A vertical rod with a mass m and a spring constant k .
- Diagram: A circuit with a battery \mathcal{E} , a resistor R , and a capacitor C .
- Diagram: A circuit with a battery \mathcal{E} , a resistor R , and a capacitor C in parallel.
- Diagram: A circuit with a battery \mathcal{E} , a resistor R , and a capacitor C in series.
- Equation: $\frac{p}{v} + \gamma \frac{dv}{v} = 0$
- Equation: $I = \frac{U}{R}$
- Equation: $\downarrow \uparrow \rightarrow \text{const}$, $\uparrow \downarrow \rightarrow \text{const}$
- Equation: $D = \frac{p \cdot l}{S}$
- Equation: $S = ?$

Part II

Cell viability and methods for assessing neurotoxicity



Chapter 2

SCREENING FOR EFFECTS ON CELL VIABILITY (CONCENTRATION-RANGE FINDING)

Marieke Meijer, Remco H.S. Westerink and Milou M.L. Dingemans

Adapted from:

“D2.1 Report on direct neurotoxicity screening”

(deliverable DENAMIC, FP7-ENV-2011 project nr. 282957, June 2013)

Author(s)

Marieke Meijer, Remco H.S. Westerink, Milou M.L. Dingemans
(IRAS) Timo Hamers, Ronald E. van Kesteren (VU)

SUMMARY

This report describes the effects of selected pesticides and environmental pollutants on cell viability *in vitro*. The investigated pesticides include organophosphates, carbamates, pyrethroids, organochlorines, bipyridyls and neonicotinoids. Additionally, the effects of a number of halogen-free flame retardants, brominated flame retardants, phthalates, perfluorinated chemicals are investigated. Methylmercury is included as a model compound for developmental neurotoxicity.

The cell viability data reported here gives insight in appropriate exposure concentrations for further *in vitro* testing. Concentrations that cause significant cell death will serve as upper limit of the concentration range to be tested in additional assays.

2.1 INTRODUCTION

Epidemiological studies revealed that environmental chemical exposure during human development can affect cognitive development (e.g. Miodovnik, 2011). Historical examples of perinatal developmental neurotoxicity in humans are lead and methylmercury (MeHg). Exposure to these environmental metals has long been known to be detrimental to neurodevelopment, and the recognized adverse effects include impaired cognitive function and behavioral disturbances in exposed children (Chen et al., 2011). Neurodevelopmental effects of exposure to polychlorinated biphenyls (PCBs) have been well-described (e.g. Jacobson and Jacobson, 1996; Park et al. 2009), but also prenatal exposure to polybrominated diphenyl ethers (PBDEs) has recently been associated with neurodevelopmental effects in children (Roze et al., 2009; Herbstman et al., 2010).

While some pollutants have already been banned (including PCBs and PBDEs), other chemicals that are suspected to affect neurodevelopment are still widely produced and used. Cognitive and/or behavioral effects in humans have been identified for several environmental contaminants, including pesticides that are regularly used within the EU. Exposure to organophosphate pesticides have been associated with neurodevelopmental effects in humans (Mackenzie Ross et al., 2013). Prenatal exposure to organochlorine pesticides have been associated with the occurrence of autism spectrum disorders (Roberts et al., 2007). Perfluorooctanoic acid (PFOA), one of the perfluorinated chemicals, is associated with increased occurrence of ADHD in children (Hoffman et al., 2010). Exposure to phthalates associated with house dust is another example of a recently identified possible risk factor for autism spectrum disorders (Larsson et al., 2009).

This report summarizes the effects of a set of environmental chemicals on *in vitro* cytotoxicity in PC12 cells (Greene and Tischer, 1976) for concentration-range finding.

2.2 MATERIALS AND METHODS

2.2.1 Chemicals

An initial test set of chemicals was specified by the DENAMIC project (Table 1). To investigate the possible influence of metabolism (which is not expected to occur to a large extent in the cell systems) on toxicity, a number of metabolites were also included. Also, a number of reference chemicals were determined as representatives for the different pesticide classes based on exposure information. MeHg is included as a developmental neurotoxicity model compound.

The tested chemicals (at the highest achievable purity) were purchased from different companies (annex 1). Suppliers of chemicals for cell culture and assays are indicated in the methods. All other chemicals were obtained from Sigma-Aldrich (Zwijndrecht, The Netherlands), unless otherwise noted.

Most chemicals were dissolved in DMSO at 100 mM and further diluted to obtain different concentrations. The final concentration of DMSO in exposure media was 0.1% (v/v). Paraquat was dissolved in H₂O.

2.2.2 Cell culture and exposure

PC12 cells

The pheochromocytoma rat (PC12) cell line is a widely used model to assess neurotoxicity and neuronal function (for review see Westerink and Ewing, 2008). PC12 cells (Greene and Tischler, 1976) were cultured for maximal 10 passages in RPMI 1640 medium (Invitrogen, Breda, The Netherlands) supplemented with 5% fetal bovine serum and 10% horse serum (ICN Biomedicals, Zoetermeer, The Netherlands), 100 U/ml penicillin and 100 mg/ml streptomycin (ICN Biomedicals, Zoetermeer, The Netherlands) as described previously (Hendriks et al., 2012; Hondebrink et al., 2011). Cells were grown in a humidified incubator at 37°C and 5% CO₂ and subcultured one day prior to measurements of cell viability. For measurements of cell viability, undifferentiated PC12 cells were seeded in 48-wells plates (Greiner Bio-one, Solingen, Germany) at a density of 3·10⁵ cells/well (500 µl per well). All culture flasks, dishes and plates were coated with poly-L-lysine (PLL) (50 µg/ml). Medium was replaced every 2-3 days.

For cell viability studies, cells were exposed to concentrations up to 100 µM. In all studies, no-observed-effect concentrations (NOECs) were determined. In most studies, cells were exposed for 24h. Additional experiments were performed in which cells were exposed for 48h.

Table 1: DENAMIC chemicals.

Chemical class	parent chemical (* pesticide class reference chemical)	metabolite(s)	
Pesticides	chlorpyrifos *	chlorpyrifos-oxon	
	parathion-ethyl	paraoxon-ethyl + paraoxon-methyl	
	organophosphates	dimethoate	dimethoate-oxon (omethoate)
		diazinon	diazinon-O-analog
		dichlorvos	-
		carbaryl *	-
	carbamates	aldicarb	-
		pirimicarb	-
		methomyl	-
		alpha-cypermethrin *	-
	pyrethroids	cypermethrin (isomeric mixture)	-
		permethrin	-
		bioallethrin	-
	organochlorines	endosulfan *	-
		dicofol	-
bipyridyls	paraquat	-	
neonicotinoids	imidacloprid	-	
Environmental chemicals	phosphate based plasticizers/ flame retardants	tris(1,3-dichloro-2-propyl)phosphate (TCPP)	-
		tri-ortho-cresyl phosphate (TOCP)	-
	other halogen-free flame retardants	dihydro-oxa-phosphaphenanthrene-oxide (DOPD)	-
	brominated flame retardants	brominated diphenyl ether 47 (BDE-47)	hydroxylated brominated diphenyl ether 47 (6-OH-BDE-47)
		dibutyl phthalate (DBP)	-
	phthalates	diethylhexyl phthalate (DEHP)	monoethyl hexyl phthalate (MEHP)
	perfluorinated chemicals	perfluor octanoic acid (PFOA)	-
	perfluor octanesulfonic acid (PFOS)	-	
heavy metals	methylmercury **	-	

* Reference chemicals for pesticide classes. The reference chemicals were chosen based on exposure levels as described by EFSA 2008

** Developmental neurotoxicity reference chemical

2.2.3 Cell viability assays

Alamar Blue assay combined with CFDA or Neutral Red assay

The effects of the pesticides and environmental chemicals on viability of PC12 cells were determined with a combined Alamar Blue (aB; Magnani and Bettini, 2000) and CFDA-AM assay (Bopp and Lettieri, 2008). In experiments with MeHg, the CFDA-AM assay was replaced by the Neutral Red assay (Repetto et al., 2008) due to interference of MeHg with the CFDA-AM measurement. The aB assay, which is based on the ability of the cells to reduce resazurin to resorufin, records mitochondrial activity of the cells as a measure of cell viability. Both the CFDA and neutral red (NR) assay measure membrane integrity, with the difference that CFDA can be measured simultaneously with aB, while the NR assay requires additional incubation and washing steps. Both combinations of assays allow for the measurement of two independent measures of cell viability: chemical effects on metabolic/mitochondrial activity (associated with oxidative stress) and acute cytotoxicity (membrane integrity).

Cell viability was assessed in 48-wells (PC12) plates (Greiner Bio-one, Solingen, Germany). Wells in which the cells were lysed with a SDS/DMF lysis buffer were used for background values. Briefly, following exposure to the chemicals of interest, cells were incubated for approximately 30 min in 11 μM resazurin and 3.6 μM CFDA-AM (Invitrogen, Breda, The Netherlands) solution in phenol-red free and serum-free medium (at 37°C, 5% CO₂; protected from light). Resorufin and CFDA were measured spectrophotometrically at 540/590 nm (excitation/emission) and at 493/541 nm, respectively with a Tecan Infinite M1000 plater reader equipped with a 10W Xenon flash light source (Tecan Group Ltd; Männedorf, Switzerland).

After removal of the aB solution, cells were incubated for approximately 1h with 100 μl NR solution (Invitrogen, Breda, The Netherlands; 12 μM in DMEM). Following incubation, the NR solution was carefully removed, and cells were lysed in 100 μl extraction solution (1% glacial acetic acid, 50% ethanol, and 49% H₂O). After 30 min extraction, NR was measured spectrophotometrically at 530 and 645 nm (excitation/emission) with a Tecan Infinite M1000 plater reader (Tecan Group Ltd; Männedorf, Switzerland). Data were processed with iControl software (version 7.1).

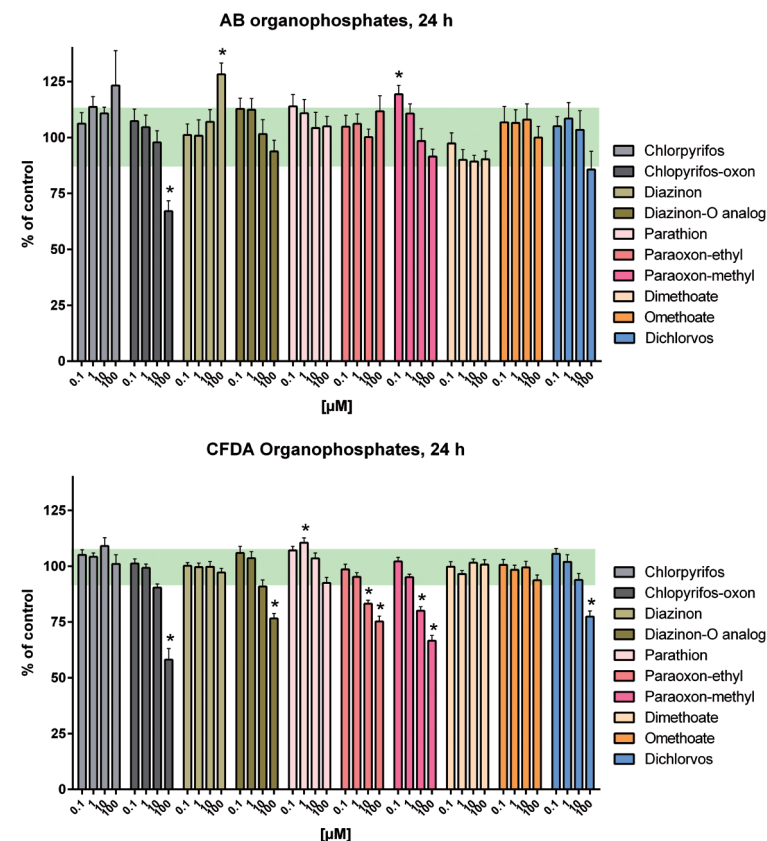


Figure 1: Summary graph of cell viability effects of organophosphates measured with an aB (top) and CFDA assay (bottom). Bars represent mean cell viability measured after 24h exposure compared to time-matched controls (set at 100%) \pm SEM ($n = 12-16$ wells/concentration). * $p < 0.05$ versus control. Effects are considered relevant when exceeding control \pm SD (indicated by the green shaded area).

2.2.4 Data analysis and statistics

All aB and NR data were corrected for background by subtracting data from wells containing lysed cells. Cell viability data are normalized to data from control wells (exposed to DMSO). Data are presented as mean \pm standard error or standard deviation (as indicated in the figures) from the number

of wells (*n*) indicated, derived from multiple independent experiments (*N*; as indicated in the figures). The concentration-dependence of chemical effects was determined by one-way ANOVA and *posthoc* Bonferroni tests. A *p*-value of < 0.05 was considered statistically significant. Statistical analyses were performed with SPSS 20 (SPSS, Chicago, IL).

2.3 RESULTS

2.3.1 Cytotoxicity of individual chemicals

Organophosphate pesticides

Non-significant effects were observed for the organophosphates (OP) dimethoate and its metabolite omethoate and parathion. All other chemicals showed either a significant effect in the aB or CFDA assay. Diazinon and paraoxon-methyl increased mitochondrial activity significantly at 100 (128.2% ± 5.1 of control) and 0.1 μM (119.3% ± 4.0) while chlorpyrifos-oxon decreased mitochondrial activity significantly at 100 μM (67.1% ± 4.6; Fig. 1). The effect of chlorpyrifos-oxon on mitochondrial activity after 48h exposure was not different from the effect after 24h exposure. Although chlorpyrifos did not result in effects after 24h exposure, chlorpyrifos significantly increased mitochondrial activity at 100 μM after 48h (113.6% ± 5.3; Fig. 2). A similar effect was observed for parathion, which increased mitochondrial activity at 100 μM only after 48h exposure (115.0% ± 4.1; Fig. 2).

Membrane integrity was decreased significantly by chlorpyrifos-oxon at 100 μM (58.1% ± 5.0), diazinon-O analog at 100 μM (76.6 ± 2.2), paraoxon-ethyl and -methyl at 10 (83.2% ± 1.5 and 80.0 ± 1.8) and 100 μM (75.2% ± 2.3 and 66.6 ± 2.3) and dichlorvos at 100 μM (77.4% ± 2.6; Fig. 1). Chlorpyrifos exposure did not result in effects on membrane integrity after either 24h or 48h exposure. The effect of chlorpyrifos-oxon on membrane integrity after 48h exposure was not different from the effect after 24h exposure.

Carbamate pesticides

Methomyl did not exert significant effects (Fig. 3). Pirimicarb showed a significant decrease in mitochondrial activity at 100 μM (85.4% ± 2.2) but did not affect membrane integrity. In contrast, aldicarb and carbaryl significantly reduced membrane integrity without altering mitochondrial activity at 100 μM (89.7% ± 2.0 and 88.4% ± 2.4; Fig. 3). When exposed for 48h however, carbaryl significantly decreased aB (81.9% ± 2.7; Fig. 2).

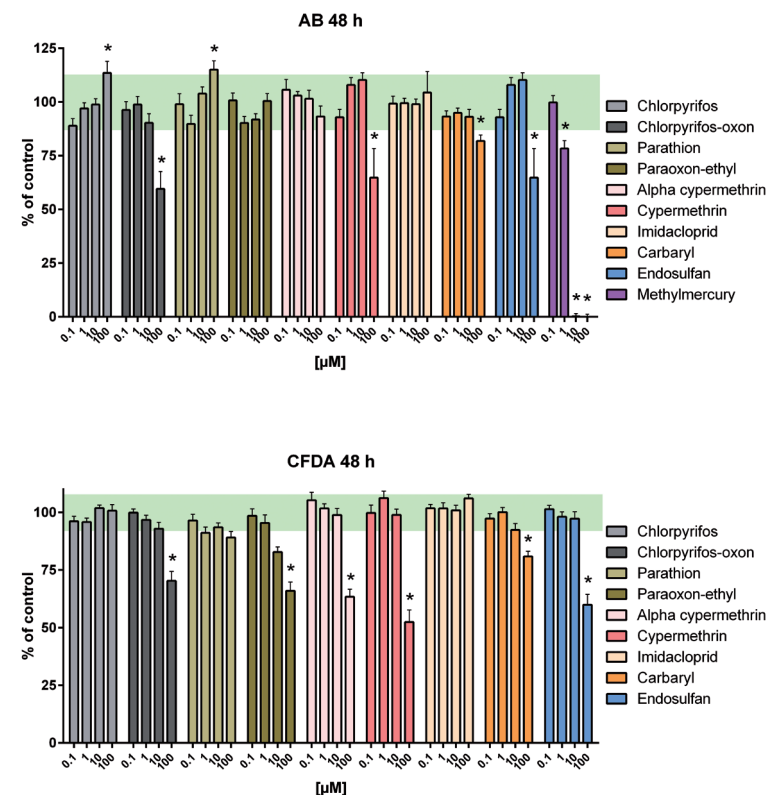


Figure 2: Summary graph of cell viability effects of pesticides measured with an aB (top) and CFDA assay (bottom). Bars represent mean cell viability measured after 48h exposure compared to time-matched controls (set at 100%) ± SEM (*n* = 12-25 wells/concentration). * *p* < 0.05 versus control. Effects are considered relevant when exceeding control ± SD (indicated by the green shaded area).

Pyrethroid pesticides

The pyrethroid bioallethrin increased mitochondrial activity significantly already at 10 μM (135.3% ± 10.9) followed by a large and significant decrease at 100 μM (19.5% ± 4.6), although no effects on membrane integrity at 100 μM were observed (Fig. 4). Of the pyrethroids tested, permethrin did not

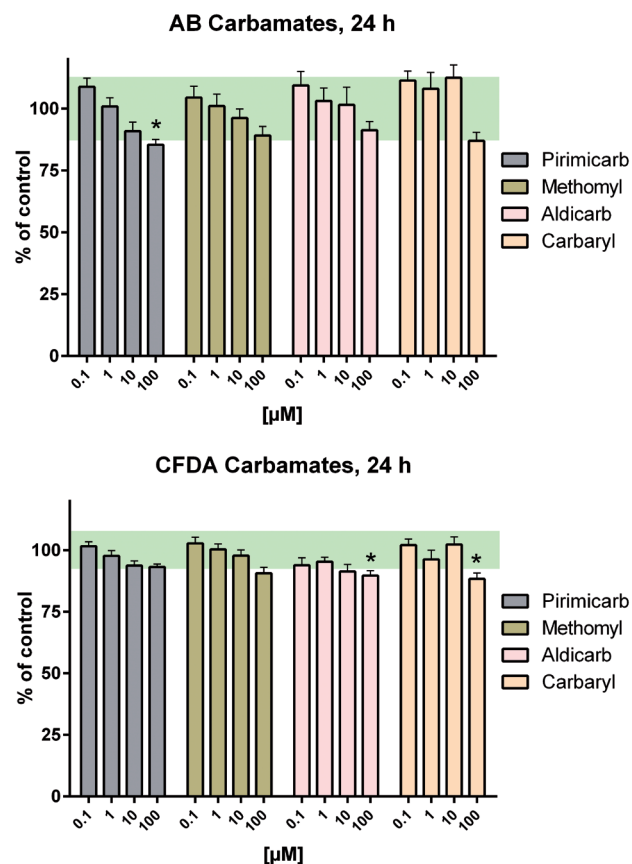


Figure 3: Summary graph of cell viability effects of carbamates measured with an aB and CFDA assay. Bars represent mean cell viability measured after 24h exposure compared to time-matched controls (set at 100%) ± SEM ($n = 11-12$ wells/concentration). * $p < 0.05$ versus control. Effects are considered relevant when exceeding control ± SD (indicated by the green shaded area).

affect mitochondrial activity or membrane integrity (Fig. 4). Cypermethrin and alpha-cypermethrin only reduced membrane integrity at 100 μM ($53.7\% \pm 2.9$ and $73.1\% \pm 2.6$, respectively; Fig. 4). While the aB assay did not show effects of cypermethrin after 24h exposure, cypermethrin significantly decreased aB at 100 μM after 48h ($64.8\% \pm 13.6$; Fig. 2).

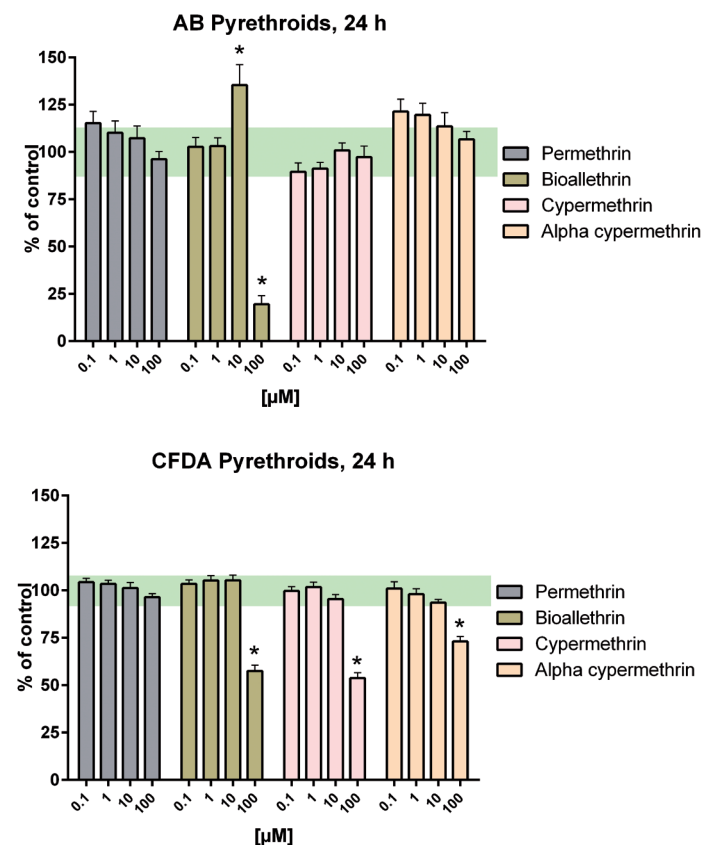


Figure 4: Summary graph of cell viability effects of pyrethroids on PC12 cells measured with an aB (left) and CFDA assay (right). Bars represent mean cell viability measured after 24h exposure compared to time-matched controls (set at 100%) ± SEM ($n = 12-16$ wells/concentration). * $p < 0.05$ versus control. Effects are considered relevant when exceeding control ± SD (indicated by the green shaded area).

Organochlorine pesticides

Endosulfan displayed no significant effects on aB or CFDA after 24h exposure (Fig. 5). After 48h exposure however, endosulfan significantly decreased aB ($64.8\% \pm 13.6$; Fig. 2), and strongly reduced membrane integrity at 100 μM ($59.9\% \pm 4.6$).

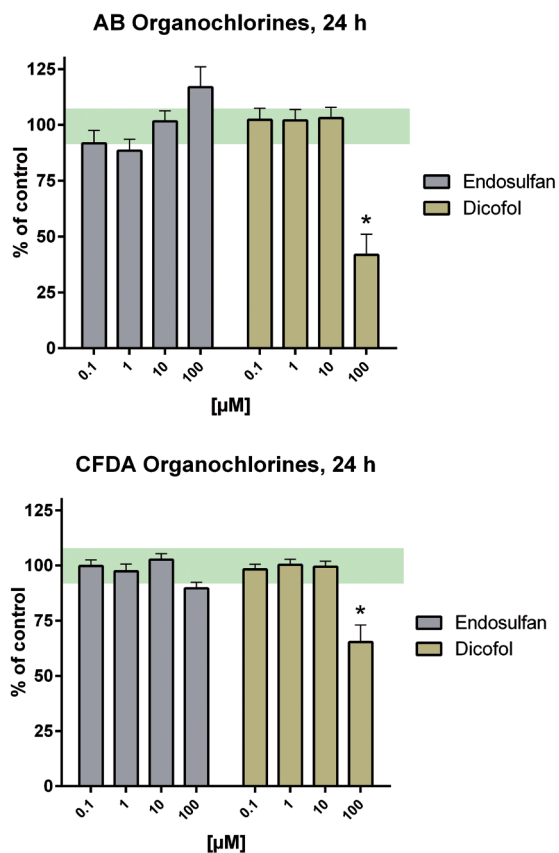


Figure 5: Summary graph of cell viability effects of organochlorines measured with an aB (left) and CFDA assay (right). Bars represent mean cell viability measured after 24h exposure compared to time-matched controls (set at 100%) ± SEM ($n = 12-20$ wells/concentration). * $p < 0.05$ versus control. Effects are considered relevant when exceeding control ± SD (indicated by the green shaded area).

The other organochlorine, dicofol, decreased mitochondrial activity and membrane integrity significantly at 100 µM ($41.8\% \pm 9.1$ and $65.3\% \pm 7.8$ for aB and CFDA, respectively; Fig. 5).

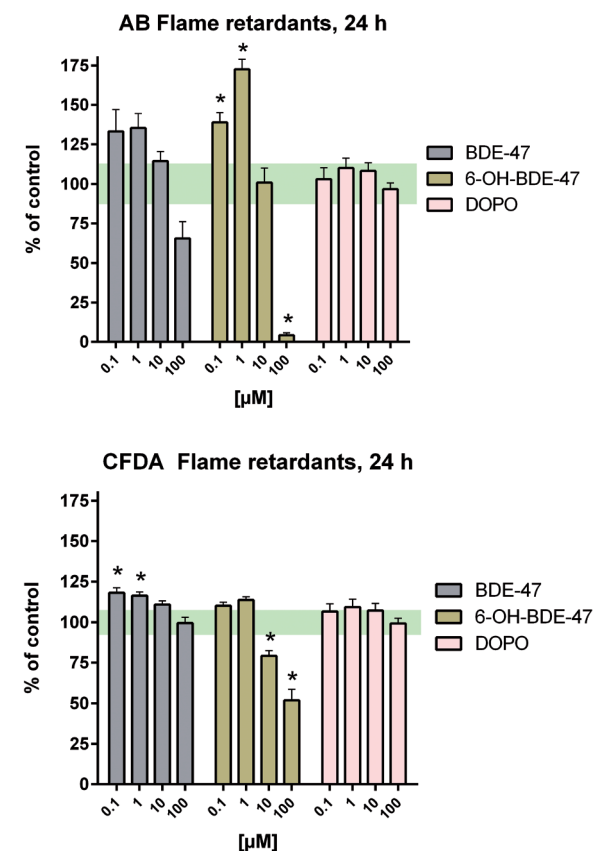


Figure 6: Summary graph of cell viability effects of flame retardants measured with an aB (left) and CFDA assay (right). Bars represent mean cell viability measured after 24h exposure compared to time-matched controls (set at 100%) ± SEM ($n = 12-20$ wells/concentration). * $p < 0.05$ versus control. Effects are considered relevant when exceeding control ± SD (indicated by the green shaded area).

Flame retardants

Halogen-free flame retardant DOPO did not affect cell viability after 24h exposure (Fig. 6). In contrast, the brominated flame retardant BDE-47 and its metabolite 6 OH-BDE-47 were highly potent in affecting cell viability as mitochondrial activity was significantly

increased from 0.1 μM ($139.0\% \pm 6.2$ and 172.5 ± 6.3 at 0.1 μM and 1 μM , respectively; Fig. 6).

Other pesticides

Paraquat did not show effects in the aB and CFDA assay after 24h exposure (Fig. 7), whereas imidacloprid exposure also did not result in effects on cell viability (24-48h exposure; Fig. 2 and 7).

Other chemicals

Phthalates DEHP increased mitochondrial activity significantly at 100 μM ($124.4\% \pm 4.1$; Fig. 7). On the other hand, exposure (24h) to DBP and DEHP-metabolite MEHP did not result in effects on cell viability.

Phosphate-based plasticizers O-TCP increased mitochondrial activity after 24h exposure (aB) at 10 μM ($138.8\% \pm 6.1$) but did not significantly decrease membrane integrity (CFDA). On the other hand, TDCPP did not affect mitochondrial activity but significantly decreased membrane integrity ($72.3\% \pm 4.8$; Fig. 7).

Perfluorinated chemicals The perfluorinated chemical PFOA did not affect mitochondrial activity or membrane integrity after 24h exposure in contrast with PFOS, which significantly reduced mitochondrial activity and membrane integrity at 100 μM ($44.9\% \pm 5.0$ and $91.5\% \pm 2.0$, respectively; Fig. 7).

Methylmercury The heavy metal and developmental neurotoxic chemical methylmercury was the most potent chemical of the test set in disturbing cell viability after 24h of exposure. Already at 0.1 μM a significant increase in mitochondrial activity was observed ($124.1\% \pm 8.7$), which was significantly decreased at 10 μM ($8.5\% \pm 2.3$) and at 100 μM ($2.4\% \pm 1.1$; Fig. 7). After 48h of exposure to methylmercury, the increase in mitochondrial activity was no longer observed. The mitochondrial activity decreased from 1 μM ($78.4\% \pm 3.7$) and was completely inhibited at 10 μM (Fig. 2).

Since methylmercury interfered with the CFDA assay, a NR assay was performed instead as a measure of membrane integrity. The NR assay showed that methylmercury decreased cell viability significantly at 10 μM ($10.9\% \pm 4$; $n=12$, $N=3$; data not shown).

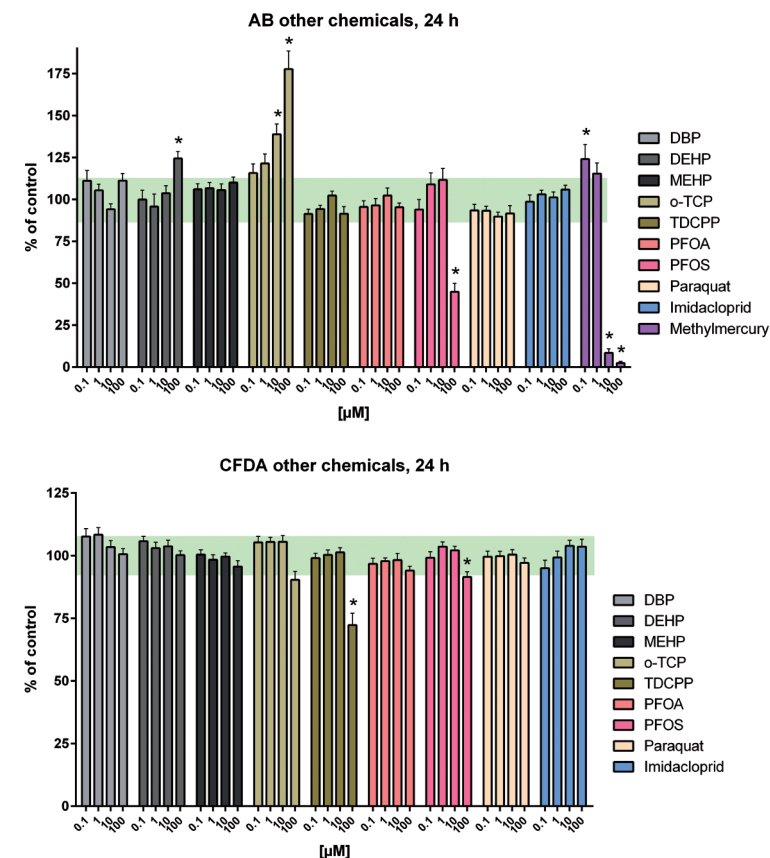


Figure 7: Summary graph of cell viability effects of environmental chemicals measured with an aB (top) and CFDA assay (bottom). Bars represent mean cell viability measured after 24h exposure compared to time-matched controls (set at 100%) \pm SEM ($n = 11-20$ wells/concentration). * $p < 0.05$ versus control. Effects are considered relevant when exceeding control \pm SD (indicated by the green shaded area).

2.4 CONCLUSIONS

Little effects on cell viability were observed for pesticides up to 10 μM . Effects of pesticides on cell viability were mostly observed at 100 μM . Most other compounds showed no or only (small) effects on cell viability at 100 μM , with the exception of ToCP, 6-OH-BDE-47 and MeHg. ToCP increased mitochondrial activity at 10 μM . BDE-47 metabolite 6-OH-BDE-47 showed a very potent effect on cell viability from 0.1 μM . Similarly, the DNT reference chemical MeHg also showed effects on cell viability at 0.1 μM .

The data reported here give insight in appropriate exposure concentrations for further *in vitro* testing. Concentrations that cause significant cell death will serve as upper limit of the concentration range to be tested in additional assays. Accordingly, maximum test concentrations of 10 μM were used for most additional studies.

Table 2: LOECs of pesticides and MeHg on cell viability.

Chemical class pesticides	Compound	PC12 (24-48h exposure)	
organophosphates	chlorpyrifos	>100 ^a	
	chlorpyrifos-oxon	100 (mit. activity ↓; membr. integrity ↓)	
	parathion	>100 ^a	
	paraoxon-ethyl	10 (membr. integrity ↓)	
	paraoxon-methyl	0.1 (mit. activity ↑); 10 (membr. integrity ↓)	
	dimethoate	>100	
	omethoate	>100	
	diazinon	100 (mit. activity ↑)	
	diazinon-O-analogue	100 (membr. integrity ↓)	
	dichlorvos	100 (membr. integrity ↓)	
	carbamates	aldicarb	100 (membr. integrity ↓)
		carbaryl	100 (membr. integrity ↓) ^a
methomyl		>100	
pirimicarb		100 (mit. activity ↓)	
pyrethroids	alpha-cypermethrin	100 (membr. integrity ↓)	
	cypermethrin (isomeric mixture)	100 (membr. integrity ↓) ^a	
	permethrin	>100	
	bioallethrin	10 (mit. activity ↑)	
organochlorines	dicofol	100 (mit. activity ↓; membr. integrity ↓)	
	endosulfan	>100 ^a	
neonicotinoids	imidacloprid	>100	
bipyridyls	paraquat	>100	
heavy metals	methylmercury (CH_3Hg)	0.1 (mit. activity ↑↓) ^a	

^a Effect appeared or increased when cells were exposed for a longer duration (48h)

Annex 1 - information of used chemicals

Compound	Supplier	Order no.	Grade	Purity (%)	Lot no.	MW (g/mol)	Remarks
chlorpyrifos	Sigma-Aldrich	45395	Pestanal	99.9	SZBA141XV	350.59	
parathion-ethyl	Sigma-Aldrich	45607	Pestanal	98.8	SZBA249XV	291.26	
aldicarb	Sigma-Aldrich	33386	Pestanal	99.9	SZBB329XV	190.26	
pirimicarb	Sigma-Aldrich	45627	Pestanal	98.5	SZBA236XV	238.29	
permethrin	Sigma-Aldrich	45614	Pestanal	98.3	SZBB206XV	391.29	Cis/Trans
bioallethrin	Sigma-Aldrich	31489	Pestanal	96.7	SZBA284XV	302.41	
dicofol	Sigma-Aldrich	36677	Pestanal	97.2	SZB9077XV	370.49	
endosulfan	Sigma-Aldrich	32015	Pestanal	99.9	SZB8163XV	406.93	Alpha + Beta 2:1
diazinon	Sigma-Aldrich	45428	Pestanal	98.3	SZB8170XV	304.35	
dichlorvos	Sigma-Aldrich	45441	Pestanal	98.9	SZBA223XV	220.98	
cypermethrin	Sigma-Aldrich	36128	Pestanal	95.1	SZB7197XV	416.30	
dimethoate	Sigma-Aldrich	45449	Pestanal	99.6	SZB9243XV	229.26	
methomyl	Sigma-Aldrich	36159	Pestanal	99.9	SZB8197XV	162.21	
omethoate	Sigma-Aldrich	36181	Pestanal	97.0	SZB9125XV	213.19	
paraoxon-ethyl	Sigma-Aldrich	36186	Pestanal	97.6	SZBB192XV	275.20	
paraoxon-methyl	Sigma-Aldrich	46192	Pestanal	96.0	SZE9113X	247.14	
chlorpirifos-oxon	Accustandard	P-700N		93.5	22748	334.52	
diazinon-O analog	Accustandard	P-640N		98.2	22796	228.28	
alpha-cypermethrin	Sigma-Aldrich	45806	Pestanal	99.7	SZBA068XV	416.30	Mixture of isomers
Carbaryl	Sigma-Aldrich	32055	Pestanal	99.5	SZBB165XV	201.22	
imidacloprid	Sigma-Aldrich	37894	Pestanal	99.9	SZB9112XV	255.66	
BDE-47	Ake Bergmann			100.0		485.60	
60H-BDE-47	Ake Bergmann			100.0		501.82	
Methylmercury chloride	Sigma-Aldrich	33368	Pestanal	99.9	SZBA172XV	251.08	
paraquat	Sigma-Aldrich	36541	Pestanal	99.9	SZBB348XV	257.16	
Tri-o-tolyl phosphate	ACROS	366460250		96.0	A0250944	368.36	
DEHP	Sigma-Aldrich	P-6699	GC	99.0	37H3473	390.60	
PFOS	Sigma-Aldrich	77282		98.0	1246519	538.22	
DOPO	KremsChemie	21906100		98.0	MIG 1	216.17	
PFOA	ACROS	373930050		96.0	A0201677	414.07	
TDCPP	Sigma-Aldrich	32951	Oekanal	96.0	SZBA265XV	430.90	
Dibutyl phthalate	Sigma-Aldrich	36736	Pestanal	99.8	SZB8149XV	278.34	

Chapter 3

EVALUATION OF ASSAYS FOR THE INVESTIGATION OF OXIDATIVE STRESS

Marieke Meijer, Milou M.L. Dingemans and Remco H.S. Westerink

Adapted from:

“D2.3 Report on *in vitro* screening for effects on intra- and intercellular signaling”

(deliverable DENAMIC, FP7-ENV-2011 project nr. 282957, September 2014)

Author(s)

Marieke Meijer, Milou M.L. Dingemans, Remco H.S. Westerink (IRAS) Timo Hamers (VU)

Oxidative stress is the imbalance between reactive oxygen species (ROS) and antioxidants. ROS are formed as a by-product of mitochondrial respiration during the oxidative phosphorylation and the generation of ROS is especially increased at high metabolic rate and mitochondrial dysfunction. Other causes of oxidative stress are membrane-bound NADPH oxidases that can catalyze the formation of superoxides, and dysregulation of iron metabolism (Milton and Sweeny, 2012).

ROS are highly reactive molecules that play an important role in cell signaling and in the immune system. In homeostasis, ROS levels are maintained at low levels by cellular antioxidant activity. However, at elevated levels, ROS can oxidize lipids, proteins and nucleic acids and thereby induce cellular damage and dysfunction. Consequently, oxidative stress is associated with adverse health effects such as aging, cancer and neurodegenerative disorders (Dai et al., 2014).

To investigate if the selected reference chemicals of the DENAMIC project induce neurotoxicity via oxidative stress, assays for the investigation of oxidative stress were evaluated. Markers for oxidative stress are increased levels of ROS, decreased levels of antioxidants and oxidative damage to lipids, proteins and DNA. Due to the short life span of ROS, only assays that allow for measurements over time were included for evaluation. One assay was selected that measures ROS (H_2DCFDA) and one assay that measures lipid peroxidation as marker for oxidative stress (BODIPY).

3.12;7'-DICHLORODIHYDROFLUORESCEIN DIACETATE (H_2DCFDA) ASSAY

3.1.1 Introduction

The H_2DCFDA assay is a widely used assay for the investigation of elevated intracellular ROS levels. H_2DCFDA is a molecule that is converted into a fluorescent molecule (DCF) upon reaction with ROS (Fig. 1). The fluorescent light emitted by DCF was detected by a fluorescence microplate reader (Infinite M200, 10W Xenon flash light source, Tecan Trading AG, Männedorf, Switzerland) allowing high-throughput measurements. We evaluated the applicability of this assay for the investigation of chemical-induced ROS production. The different protocols and test chemicals used are described below. All experiments included rotenone, a mitochondrial complex 1 inhibitor, as a positive control and were performed with PC12 or primary cortex cells in 48-wells or 96-wells plates, respectively.

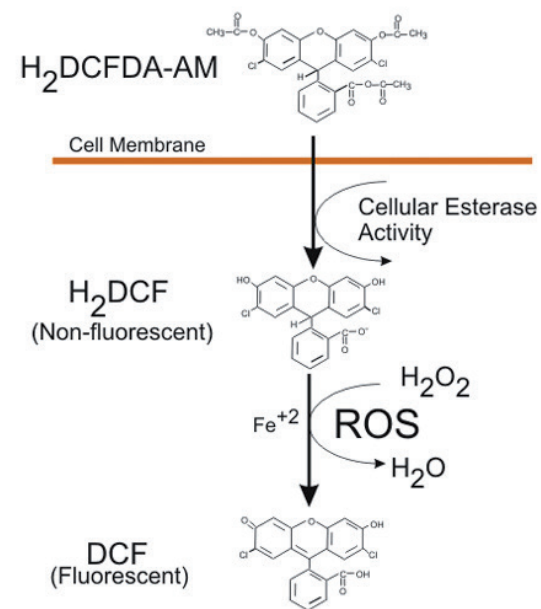


Figure 1: Transformation of H_2DCFDA -AM by cellular esterases and ROS to the fluorescent compound DCF (Biotek, 2014).

3.1.2 Protocol test 1

The first protocol evaluated is adapted from the literature (e.g. Heusinkveld et al., 2013; de Groot and Westerink, 2014; Hendriks et al., 2012). PC12 cells were seeded in 48-wells plates and after cell attachment, medium was removed and cells were loaded with 1.5 μM H_2DCFDA (Molecular Probes, Invitrogen, Breda, The Netherlands) in 250 μL colorless and serum-free RPMI1640 medium (Invitrogen). After 30 min incubation at 37°C, 250 μL medium containing test chemical was added to the wells (in this case chlorpyrifos, endosulfan, or α -cypermethrin and positive control rotenone; all obtained from Sigma-Aldrich, Zwijndrecht, The Netherlands). Fluorescence was measured immediately after addition of the test chemical and after 3, 6, 24 and 48h. Each test compound was measured at 4 different concentrations (0.1-100 μM) in quadruplicate in two different 48-wells plates. Each plate included 100 μM rotenone in duplicate. Fluorescence of each well/time point was expressed relatively to the fluorescence measured at 0h and was normalized to their time-matched controls.

3.1.3 Results

No increase in ROS was observed for endosulfan at concentrations $\leq 10 \mu\text{M}$ after 3, 6 and 24h of exposure (Fig. 2). A time-dependent increase in ROS was observed for endosulfan amounting to $124 \pm 3\%$ at 100 μM (Fig. 2). Rotenone caused a small increase, which was maximal after 6h of exposure ($110 \pm 6\%$; Fig. 2).

When cells were exposed to α -cypermethrin, no increase in ROS was observed (Fig. 3). In contrast to the previous data (Fig. 2), rotenone now increased ROS to $134 \pm 2\%$ and $133 \pm 4\%$ after 3 and 6h and to $142 \pm 9\%$ and $143 \pm 8\%$ after 24 and 48h (Fig. 3).

ROS levels were increased after exposure to 100 μM chlorpyrifos for 3 and 6h ($116 \pm 2\%$ and $113 \pm 5\%$, respectively; Fig. 4). Rotenone increased ROS after 3, 6, 24 and 48h of exposure to $134 \pm 5\%$, $136 \pm 6\%$, $129 \pm 5\%$ and $172 \pm 25\%$, respectively (Fig. 4).

In conclusion, the results of the H_2DCFDA assay, as measured by this protocol, only indicated that endosulfan slightly induces ROS over time. The positive control rotenone did induce a large increase in ROS in some

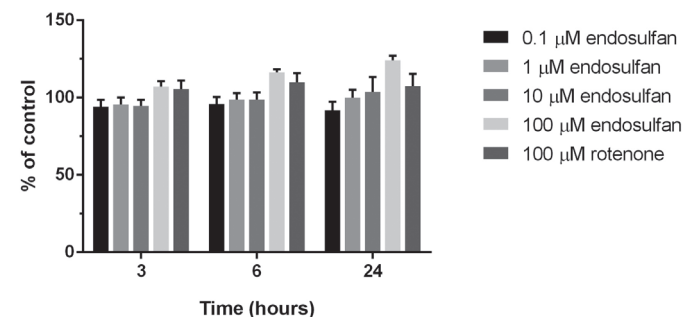


Figure 2: Relative ROS levels measured with protocol 1 after exposure to endosulfan (0.1-100 μM) for 3, 6 and 24h. Data are expressed as % of their time-matched control.

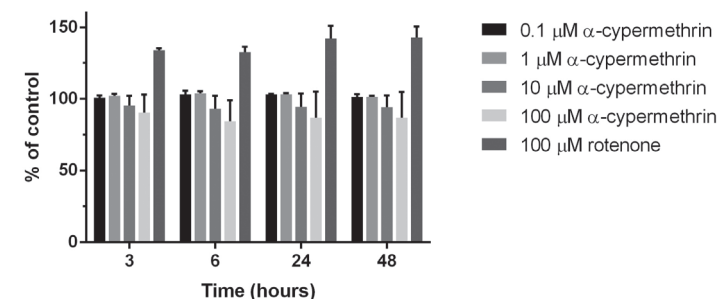


Figure 3: Relative ROS levels measured with protocol 1 after exposure to α -cypermethrin (0.1-100 μM) for 3, 6, 24 and 48h. Data are expressed as % of their time-matched control.

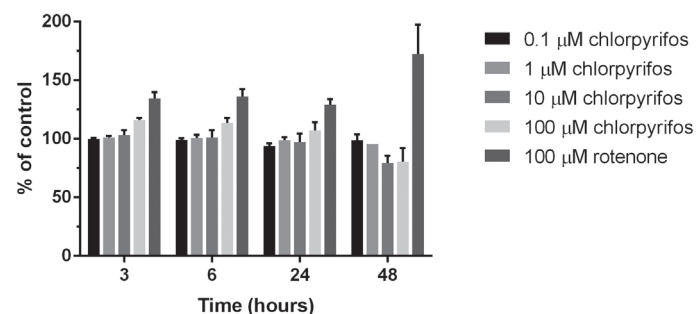


Figure 4: Relative ROS levels measured with protocol 1 after exposure to chlorpyrifos (0.1-100 μM) for 3, 6, 24 and 48h. Data are expressed as % of their time-matched control.

experiments (to 172% of the control after 48h of exposure; Fig. 4), but in some experiments the increase in ROS was small (107% compared to the control after 24h of exposure; Fig. 2).

3.1.4 Test for interference

A disadvantage of the above-described protocol is that H₂DCFDA and the test chemical are incubated simultaneously. We hypothesized that chemicals can interact with H₂DCFDA and thereby influence its fluorescence independent of whether or not there is an increase in ROS. α -cypermethrin, carbaryl, imidacloprid, paraoxon-ethyl, methylmercury, endosulfan, chlorpyrifos, parathion and rotenone were investigated for possible interferences with H₂DCFDA by performing the assay with protocol 1 in a cell-free system (Fig. 5). A clear (and concentration-dependent) reduction in H₂DCFDA fluorescence was observed when carbaryl and H₂DCFDA were incubated together (Fig. 5A). Endosulfan, chlorpyrifos and parathion also appear to reduce H₂DCFDA fluorescence, though to a lesser extent compared to carbaryl (Fig. 5B). Methylmercury (Fig. 5B) imidacloprid, paraoxon-ethyl and α -cypermethrin (Fig. 5C) did not reduce the H₂DCFDA fluorescence.

3.1.5 Protocol test 2A

To prevent possible interferences with the test chemicals, protocol 1 was repeated with a slight modification in the experimental set-up. After loading the cells with 1.5 μ M H₂DCFDA for 30 min at 37°C, all medium was removed. Next, 500 μ L of medium containing test chemical was added to the wells. However, compared to protocol 1 this resulted in very low fluorescence (in arbitrary units) and high variance, which is unfavorable to reliably distinguish chemical-induced ROS (Fig. 6). Interestingly, in contrast to previous data shown in Fig. 3, α -cypermethrin tested with protocol 1 now appears to increase ROS (Fig. 6).

3.1.6 Protocol test 2B

To increase the fluorescence with the protocol described in test 2A, cells were incubated overnight with different concentrations H₂DCFDA in 250- or 500 μ L/well. H₂DCFDA concentrations tested were 0.15-, 0.75- and 1.5 μ M. After incubation with the dye overnight, medium was replaced by 500 μ L medium containing chlorpyrifos, endosulfan and rotenone.

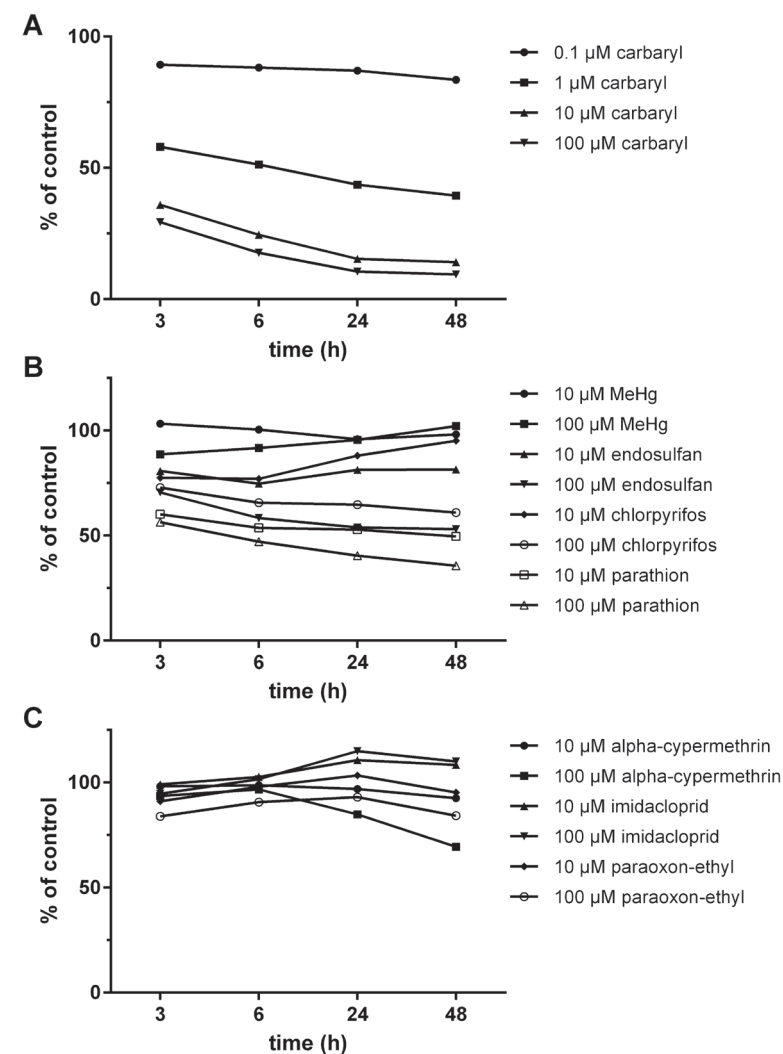


Figure 5: Test for interference of the test chemicals with H₂DCFDA after 3, 6, 24 or 48h.

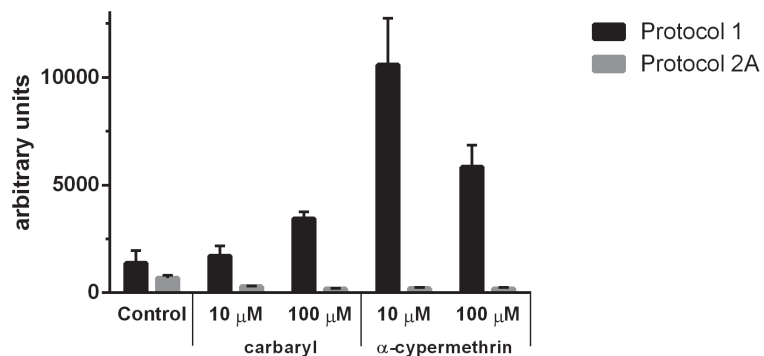


Figure 6: Comparison of fluorescence (arbitrary units) measured with H_2DCFDA with protocol 1 and 2A after 24h of exposure to 10- and 100 μ M carbaryl and α -cypermethrin.

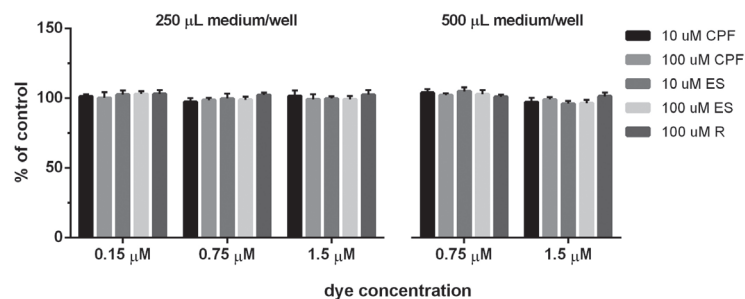


Figure 7: Relative ROS levels measured after 3h of exposure to chlorpyrifos (CPF), endosulfan (ES) or rotenone (R) with different test conditions (250 μ L: 0.15 μ M, 1 plate; 0.75- and 1.5 μ M, 4 plates; 500 μ L: 0.75- and 1.5 μ M, 3 plates (quadruplicate/plate)). Data are expressed as % compared to their time-matched control.

3.1.7 Results

Compared to protocol 2A, incubation overnight with H_2DCFDA increased the fluorescence at all different H_2DCFDA concentrations (data not shown). After 3h of exposure, for none of the test conditions an increase in ROS was observed compared to the control (Fig. 7).

After 6h of exposure, only after loading with 0.75 μ M H_2DCFDA in 500 μ L of exposure medium an increase in ROS levels was observed (Fig. 8). However,

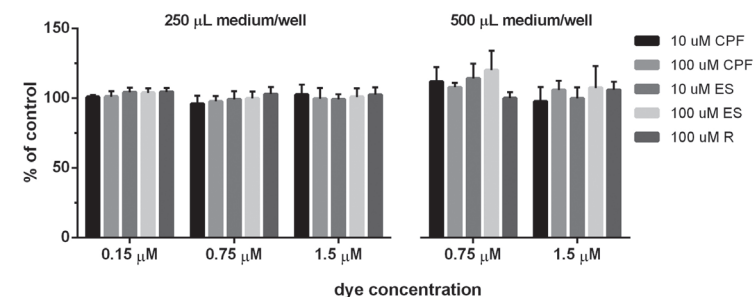


Figure 8: Relative ROS levels measured after 6h of exposure to chlorpyrifos (CPF), endosulfan (ES) or rotenone (R) with different test conditions. Data are expressed as % compared to their time-matched control.

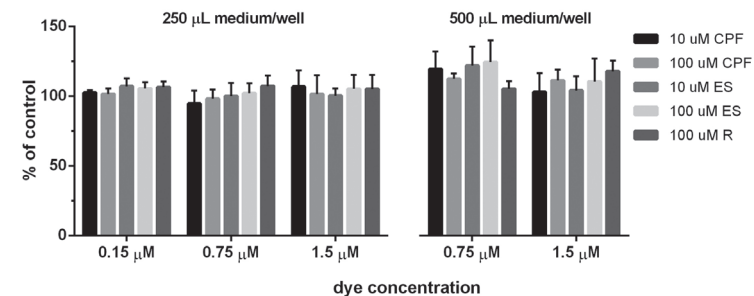


Figure 9: Relative ROS levels measured after 24h of exposure to chlorpyrifos (CPF), endosulfan (ES) or rotenone (R) with different test conditions. Data are expressed as % compared to their time-matched control.

effects were small ($120 \pm 14\%$ at 100 μ M endosulfan) and no effect was observed for the positive control rotenone ($100 \pm 4\%$; Fig. 8).

The effects of 100 μ M endosulfan on ROS slightly increased after 24h of exposure to $124 \pm 15\%$ (Fig. 9) and after 48h of exposure to $133 \pm 46\%$ (Fig. 10). A small effect of rotenone was observed after loading with 1.5 μ M H_2DCFDA after 24h ($118 \pm 8\%$; Fig. 9) and after loading with 0.75- and 1.5 μ M H_2DCFDA after 48h of exposure ($130 \pm 19\%$ and $134 \pm 12\%$; Fig. 10).

3.1.8 Screening chemicals for ROS with protocol 2B in PC12 cells

Chlorpyrifos, chlorpyrifos-oxon, parathion, paraoxon-ethyl, carbaryl, imidacloprid, cypermethrin, α -cypermethrin, endosulfan and methylmercury were investigated for effects on ROS with the H_2DCFDA dye by use of protocol 2B. Protocol 2B was used because with protocol 1 chemicals may interfere with H_2DCFDA and compared to protocol 2A, 2B had the highest fluorescence. Dye loading concentration was $2.3 \mu M$ in $500 \mu L$ medium for all experiments. Only for parathion, carbaryl and methylmercury a significant concentration- and time dependent increase in ROS was observed after 24- or 48h of exposure (data not shown). However, increases in ROS were small (8-11%) but comparable to rotenone (9%; data not shown).

3.1.9 ROS measurements with H_2DCFDA in primary cortex cells

Since the effects observed were small or absent in PC12 cells, we also investigated if chemical-induced oxidative stress could be identified in primary cortex cells. Protocol 1 was repeated with primary cortex cells and cells were exposed to low concentrations chlorpyrifos, chlorpyrifos-oxon, carbaryl, α -cypermethrin, endosulfan and methylmercury. A concentration-dependent increase in fluorescence was observed for rotenone with a maximum increase after 24h to 144% (Fig. 11). Carbaryl increased fluorescence to 106- and 120% after 48h of exposure at 0.1 and $1 \mu M$, respectively (Fig. 11). Chlorpyrifos-oxon increased fluorescence to 107% at $1 \mu M$, whereas methylmercury appeared to decrease fluorescence to 88% after 48h of exposure at $1 \mu M$ (Fig. 11).

In a separate set of experiments, higher concentrations of these chemicals were tested with protocol 1. Interestingly, 10 and $100 \mu M$ carbaryl reduced the relative fluorescence to 87% and 70%, respectively, after 24h of exposure (Fig. 12). Endosulfan increased the fluorescence at $10 \mu M$ to 120% after 6h and to 109% after 24h and decreased the fluorescence at $100 \mu M$ to 85% after 24h (Fig. 12). Methylmercury continues to decrease the fluorescence at $10 \mu M$ to 88% but increases the fluorescence at $100 \mu M$ to 149% after 24h of exposure (Fig. 12). Chlorpyrifos-oxon further increases the fluorescence at higher concentrations ($100 \mu M$: 116% after 24h; Fig. 12). Though previous experiments did not show an effect for

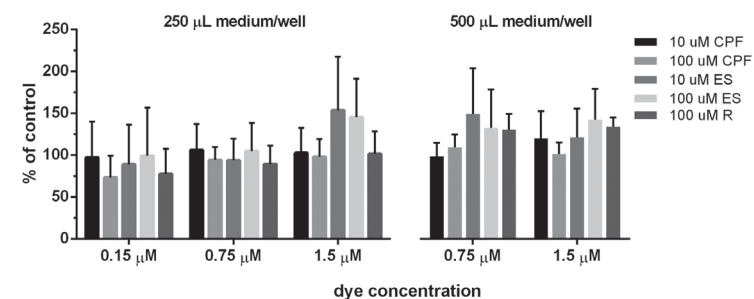


Figure 10: Relative ROS levels measured after 48h of exposure to chlorpyrifos (CPF), endosulfan (ES) or rotenone (R) with different test conditions. Data are expressed as % compared to their time-matched control.

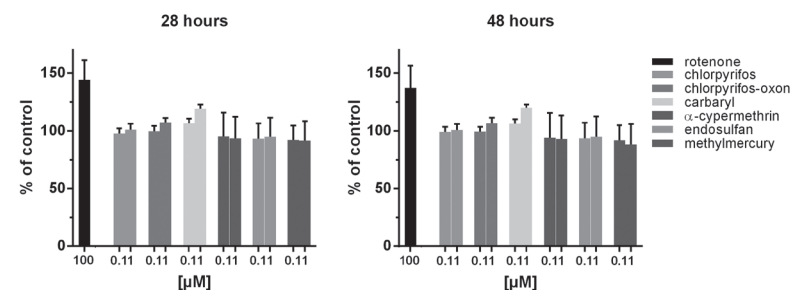


Figure 11: Relative ROS levels measured after 28 and 48h of exposure to rotenone, chlorpyrifos, chlorpyrifos-oxon, carbaryl, α -cypermethrin, endosulfan and methylmercury in cortex cells with protocol 1.

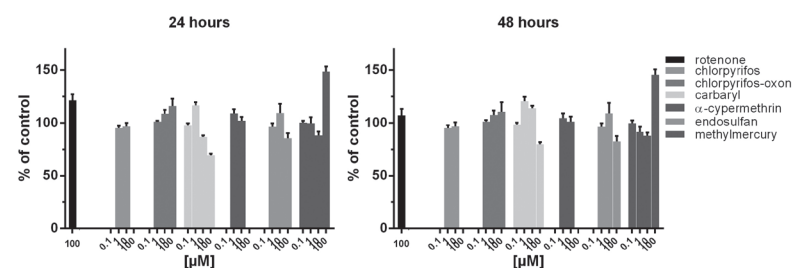


Figure 12: Relative ROS levels measured after 24 and 48h of exposure to rotenone, chlorpyrifos, chlorpyrifos-oxon, carbaryl, α -cypermethrin, endosulfan and methylmercury in cortex cells with protocol 1.

α -cypermethrin, now an increase in fluorescence was observed at 1 μ M (115% after 6h). Comparable to the previous experiments, chlorpyrifos did not demonstrate effects on the fluorescence (Fig. 12).

Next, protocol 1 was tested with 3h of dye loading instead of 30 min of dye loading with chlorpyrifos-oxon, carbaryl and rotenone. Interestingly, strong effects were now observed for chlorpyrifos-oxon (142% at 10 μ M after 24h). Carbaryl and rotenone did not show large changes in fluorescence (data not shown).

Also, protocol 2B was applied to the primary cortex cells, similar to the screening of chemicals in PC12 cells. The investigated chemicals were chlorpyrifos, chlorpyrifos-oxon, carbaryl, endosulfan and methylmercury. The largest increase in fluorescence was observed after 24h of exposure to rotenone (18% increase) followed by carbaryl (12%; 48h) and chlorpyrifos-oxon (6%; 48h; data not shown).

3.1.10 ROS measurements with H₂DCFDA in non-neuronal MCF-7 cells and new H₂DCFDA stock

Different experiments were performed with a new stock solution of the H₂DCFDA dye to confirm that our stock was working properly. Also, MCF-7 cells were used as a non-neuronal model with a slightly different protocol from a fellow research group (protocol 1 and 2A with 2h loading instead of 30 min). Results show that MCF-7 cells increase H₂DCFDA fluorescence after rotenone exposures comparable with PC12 and cortex cells, indicating that the 'old' H₂DCFDA stock solution was working properly. More importantly, these results also indicate that effects are dependent on the type of protocol used. For example, exposure to 10 μ M chlorpyrifos-oxon for 24h did not affect the relative fluorescence when tested with protocol 1 with 2h (99%) or 30 min (104%) of dye loading, but when tested with protocol 2 after dye loading for 2h, the relative fluorescence was increased to 121% and to 119% after 30 min of dye loading (data not shown).

3.1.11 Discussion

We were not able to establish a proper protocol for the ROS-sensitive dye H₂DCFDA. Protocol test 1 demonstrated that results are poorly reproducible and that chemicals can interfere with H₂DCFDA. Protocol test 2A, in which H₂DCFDA was not present during exposure, yielded not

enough fluorescence to reliably discriminate effects from the control. Protocol test 2B did demonstrate that fluorescence can be increased by increasing the dye concentration and loading time. With this protocol, a small, concentration-dependent increase in ROS was observed for endosulfan as well as for the positive control rotenone. Rotenone was used as a positive control for this assay because it is a well-known mitochondrial complex 1 inhibitor and thereby induces the production of ROS. Previously, it was shown that fluorescence in the H₂DCFDA assay increases when exposed to rotenone (to ~180% of control; Heusinkveld et al., 2013; de Groot and Westerink, 2014). A comparable increase in fluorescence was observed in this study with protocol 1 (~170% of control; Fig. 4). However, the other tested protocols showed an increase in fluorescence of ~15% after rotenone exposure. Next, a small chemical screening test for ROS with protocol 2B was performed. This screening test only identified carbaryl, parathion and methylmercury as possible inducers of ROS and in cortex cells also chlorpyrifos-oxon, though the effects observed were small (~10%). Chlorpyrifos and endosulfan did not show an increase in ROS in this screening test with protocol 2B. Interestingly, chlorpyrifos and endosulfan were shown in other studies to induce ROS by use of the H₂DCFDA assay (e.g. Saulsbury et al., 2009, dye loading after chemical exposure; e.g. Jia and Misra, 2007, comparable protocol with 2B). Also, DNA synthesis inhibition by chlorpyrifos was partly prevented by antioxidant vitamin E (e.g. Slotkin et al., 2007a) and by use of the TBARS assay; endosulfan was shown to increase levels of malondialdehyde (MDA; marker of lipid peroxidation; e.g. Jia and Misra, 2007). This suggests that chlorpyrifos and endosulfan may induce oxidative stress but that the H₂DCFDA assay performed with protocol 1 or 2B, may not be sufficiently sensitive to demonstrate oxidative stress. Protocol 1 did indicate a possible concentration- and time-dependent increase in ROS by endosulfan, but not for chlorpyrifos. Also, data generated using protocol 1 may be less reliable due to possible interference with the test chemicals (Fig. 5). The lack of sensitivity appeared not cell-model dependent as also in primary cortex cells only small increases in fluorescence were observed when protocol 1 or 2B was used. Moreover, a test with non-neuronal cells demonstrated that effects depend on the protocol used and that low sensitivity appears independent of the cell type used.

H₂DCFDA is a widely used assay and it is well known that care should be taken with this assay as H₂DCFDA can leak out of cells and is subsequently oxidized by air and other factors (The Molecular Probes Handbook, 2010). A large part of the obtained fluorescence is therefore likely not related to chemical-induced ROS but due to reaction with other factors. With proper controls it should be possible to discriminate a fluorescence increase for chemical-treated cells. However, in case of protocol 1, interference may occur and cannot be controlled for. Also, limited effects were observed in our screening study by use of protocol 2B. This could be explained by different reasons: PC12 and cortex cells may be limited in H₂DCFDA uptake or H₂DCFDA is internalized in organelles and in that way, not enough H₂DCFDA was available to react with ROS, ROS are unstable and could react with other targets before they can react with H₂DCFDA, H₂DCFDA may be very unstable (due to cleavage of the -AM group) when taken up by the cells and it could be possible that the plate reader is not sufficiently sensitive to detect the fluorescence changes. Flow cytometry or fluorescent microscopy may allow for higher resolution for the detection of H₂DCFDA fluorescence as it eliminates background fluorescence. However, these approaches limit high-throughput application and problems with the interference of chemicals with H₂DCFDA and instability of H₂DCFDA can still occur.

In conclusion, we were not able to accurately determine oxidative stress induced by the test chemicals with the H₂DCFDA assay, which was at least partly due to the interference of chemicals with H₂DCFDA. By use of a modified protocol, that prevented the interference of chemicals with H₂DCFDA, positive control rotenone induced only a small increase in ROS (~9%), indicative for low sensitivity. Also, the use of different protocols resulted in different results questioning the reproducibility and reliability of this assay. Experiments demonstrated that our findings are not related to our H₂DCFDA stock and that our findings are not specific for neuronal cells.

Based on our findings so far, we also argue that data obtained with the H₂DCFDA assay should be interpreted with caution. It should be reported in the methods if chemicals were tested for interference with H₂DCFDA and if a positive control was included.

3.2 BODIPY® 581/591 C11 ASSAY

3.2.1 Introduction

BODIPY is a fluorescent fatty acid analogue, which measures ROS that are associated with lipid peroxidation. Lipid peroxidation is damage to lipids due to oxidation by ROS. The lipid membrane can be permanently damaged by lipid peroxidation.

BODIPY fluoresces in the red range of the visible spectrum and upon oxidation with free radical species and peroxyxynitrite, its fluorescent properties shift from red to green and thus allows for the ratiometric determination of lipid peroxidation (Drummen et al., 2002). However, BODIPY is not oxidized by nitric oxide, superoxide, transition ions and hydrogen peroxides in the absence of transition metal ions (Drummen et al., 2002). Detection of fluorescence is possible with a microplate reader (Drummen et al., 2002) allowing medium- to high-throughput measurements. Several tests were performed to evaluate the use of BODIPY as a marker for oxidative stress.

3.2.2 Results

Several excitation and emission spectra were measured to identify the appropriate excitation and emission wavelengths to measure BODIPY. 48-wells plates, 500 µL exposure medium (colorless and serum-free RPMI1640) containing 2 µM non-oxidized BODIPY/well was used to run spectra.

The excitation (ex) spectra show that at emission (em) 525 nm (green) fluorescence is highest at excitation 455 and at emission 600 nm (red) is the highest at excitation 550 nm (Fig. 13A). This was confirmed in the emission spectra, where emission was highest at 525 nm when excited with 455 nm, and emission was highest at 600 nm when excited with 550 nm (Fig. 13B).

Next, PC12 cells were exposed to chemicals that are expected to induce oxidative stress. Cells were loaded with 10 µM BODIPY for 60 min at 37 °C, washed with PBS and exposed to the test chemicals in colorless and serum-free RPMI1640 for 18.5h. Fluorescence was measured at different excitation wavelengths (370, 455, 495 and 550 nm) with em 530 nm or 600 nm (Fig. 14). The results demonstrate that fluorescence is very low when measured with ex 370, 455, and 495 nm with em 530 nm, but high when excited with 550 nm and em 600 nm (Fig. 14). Fluorescence of 100 µM rotenone and 10% H₂O₂ was significantly lower at ex/em 550/600

nm compared to the control, which indicates that BODIPY is oxidized (reduction of red fluorescence; Fig. 14A). Calculation of the ratio between ex/em 550/600 nm and ex/em 495/530 nm shows that rotenone increases the ratio up to ~800% of the control (Fig. 14B). When ex/em 550/600 nm was divided by ex/em 370 or 455/530 the ratio amounted to ~300% of the control (Fig. 14B). Hydrogen peroxide increased the ratios to ~140-200% of the control (Fig. 14B).

BODIPY fluorescence of the same cells was also measured after 24h of exposure to the different chemicals at ex/em 550/600 nm and ex/em 455/530 nm. Compared to 18.5h of exposure, no differences in fluorescence were observed at ex/em 550/600 nm and ex/em 455/530 nm after 24h of exposure (Fig. 15).

To determine if the decrease in fluorescence at ex/em 550/600 nm is due to oxidation of BODIPY, cells were exposed to different concentrations of rotenone. BODIPY fluorescence was measured after exposure to rotenone for 0, 3, 6, and 24h and excitation spectra were measured at emission 530 nm and 600 nm (Fig. 16 and 17). A concentration- and time- dependent increase in fluorescence was observed for rotenone at emission 530 (Fig. 16). However, wells without cells had similar fluorescence compared with cells treated with 10- or 100 μ M rotenone for 24h (Fig. 16). This may be due to high background fluorescence or low fluorescence of oxidized BODIPY.

At emission 600 nm, a concentration-dependent decrease in fluorescence was observed for BODIPY at excitation 550 nm (Fig. 17) suggesting that the different treatments induced a ratiometric change i.e. oxidation of BODIPY. The expected time-dependent decrease in fluorescence was not observed at ex/em 550/600 nm. Instead, fluorescence at ex/em 550/600 nm of controls, 1- and 10 μ M rotenone increased up to 6h of exposure (Fig. 18).

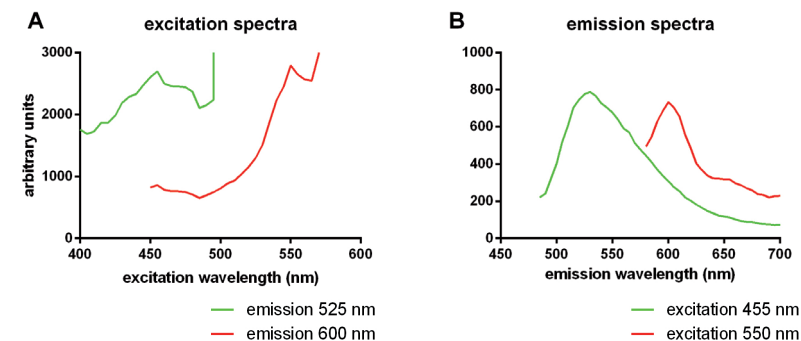


Figure 13: Excitation spectra measured at emission wavelength 525 nm and 600 nm (A) and emission spectra measured at excitation 455 nm and 550 nm (B).

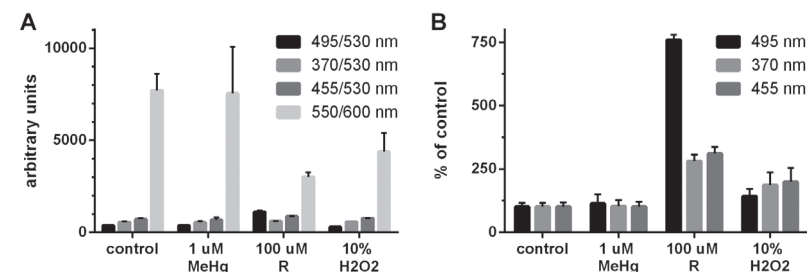


Figure 14: Effects of chemicals on BODIPY fluorescence (in arbitrary units) measured in PC12 cells at different excitation and emission wavelengths after 18.5h of exposure (A) and as ratio of ex/em 495, 370 or 455/530 nm with ex/em 550/600 nm. The ratio was normalized to the control (B).

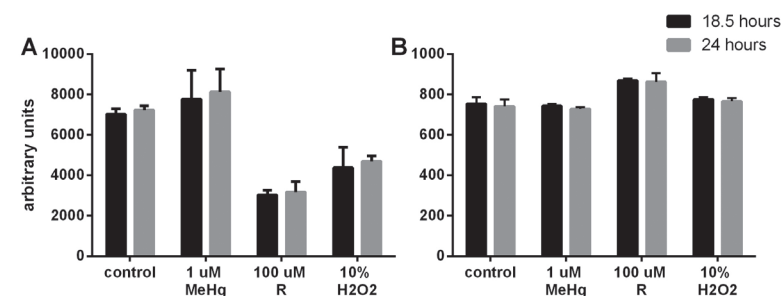


Figure 15: BODIPY fluorescence at ex/em 550/600 nm (A) and ex/em 455/530 nm (B) after 18.5 and 24h of exposure to 0.1% DMSO (control), 1 μ M methylmercury (MeHg), 100 μ M Rotenone (R) and 10% H_2O_2 (A). Note the different scales of the y-axes.

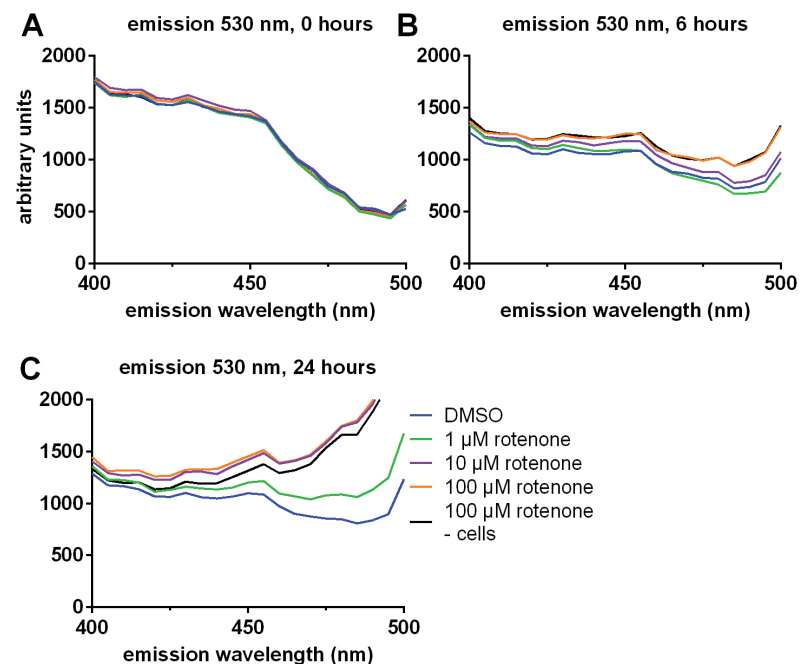


Figure 16: Excitation spectra of BODIPY measured at emission 530 nm. Fluorescence was measured after exposure to different concentrations of rotenone for 0, 3 (not shown), 6 and 24h in PC12 cells. Also, fluorescence of treated wells without cells (-cells) was measured. Control cells were exposed to 0.1% DMSO (DMSO).

As the above described data are absolute data (Fig. 18), we also expressed the data relative to the control (Fig. 19). Immediately at the start of exposure (0h), fluorescence of 1-10 μM rotenone was higher compared to the control, which was unexpected. Data of 3-24h of exposure to rotenone demonstrate a concentration- and time-dependent decrease in fluorescence compared to the control (Fig. 19).

Data shown in figures 16, 17, 18 and 19 were also expressed as ratio (Fig. 20). Fluorescence at ex 455 and 480 nm at em 530 nm was divided by the fluorescence measured at ex/em 550/600 nm (Fig. 20). Ex 480 nm was selected for this ratio calculation as differences in BODIPY fluorescence

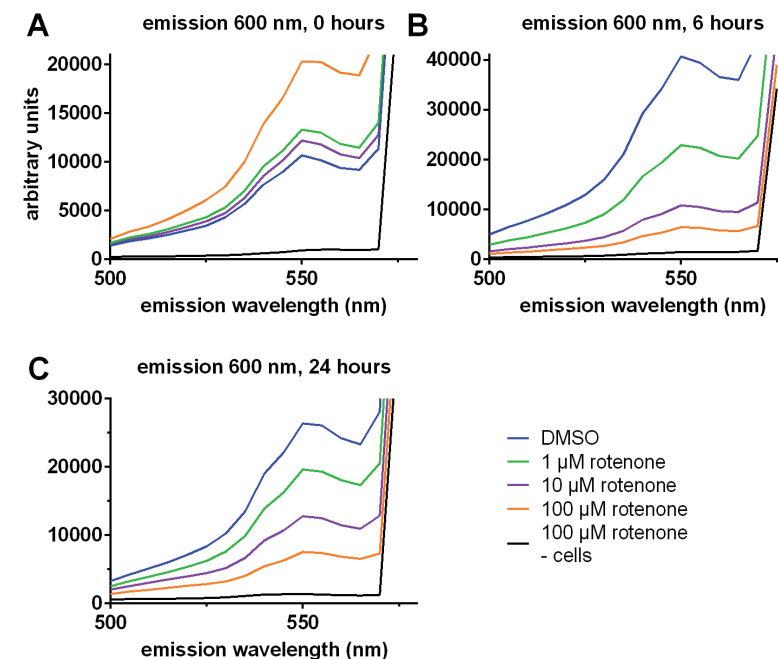


Figure 17: Excitation spectra of BODIPY measured at emission 600 nm. Fluorescence was measured after exposure to different concentrations of rotenone for 0, 3 (not shown), 6 and 24h in PC12 cells. Also, fluorescence of treated wells without cells (-cells) was measured. Control cells were exposed to 0.1% DMSO (DMSO).

were observed in the excitation spectra at em 530 nm after 24h of exposure to different concentrations of rotenone at ex 480 nm (Fig. 16). After 3-24h of exposure to 0.1% DMSO, 1- and 10 μM rotenone, ratio of ex/ex 455/550 was reduced compared to the ratio at 0h (Fig. 20A). Exposure to 100 μM rotenone increased the ex/ex 455/550 ratio from 0h (Fig. 20A). At ratio ex/ex 480/550, 0.1% DMSO decreased the ratio after 0h of exposure, whereas rotenone time- and concentration-dependently increased the ratio (Fig. 20B).

At ex/em 455/530 nm, fluorescence was low for all treatments and only small increases in fluorescence upon exposure with oxidative-stress inducing

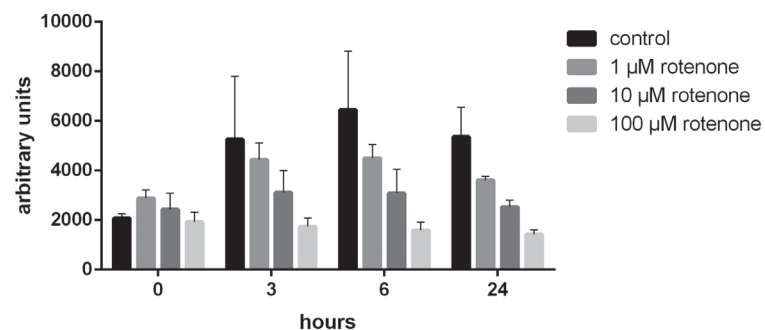


Figure 18: Fluorescence measured at ex/em 550/600 nm after exposure to 0.1% DMSO (control), 1-, 10- and 100 µM rotenone (R).

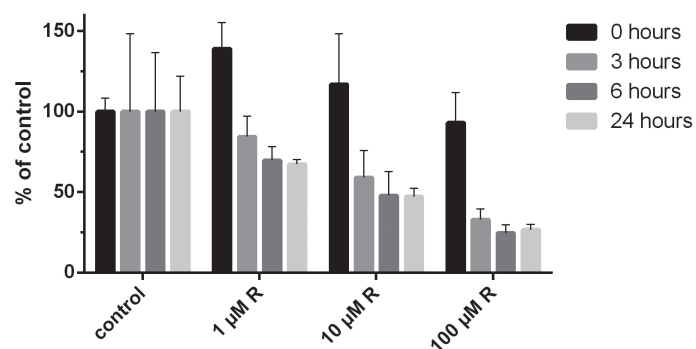


Figure 19: Data of figure 16 expressed relatively to their time-matched control.

chemicals were observed (Fig. 15B and 16). Also, fluorescence at ex/em 550/600 nm increases which was unexpected considering the ratiometric properties of BODIPY (Fig. 18). It was hypothesized that these unexpected changes in fluorescence may be due to the formation of excimers by BODIPY (Drummen et al., 2002). Excimers are non-fluorescent dimers that can be formed if fluorescent molecules are present at high concentrations and can thereby quench the fluorescent signal. Therefore, to investigate if excimers may play a role we loaded the cells with lower concentrations of BODIPY. Fluorescence at ex/em 455/530 nm and 480/530 nm changed relatively to the control independent of the different BODIPY loading concentrations

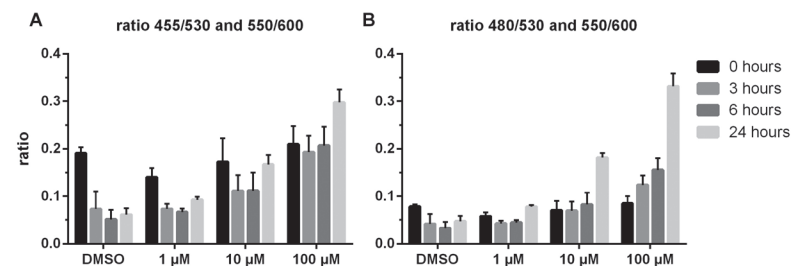


Figure 20: Data shown in figures 14 and 15 expressed as ratio. Ratios were calculated for ex/em 455/530 nm and 550/600 nm (A), and ex/em 480/530 nm and 550/600 nm (B) for 0.1% DMSO, 1-, 10-, and 100 µM rotenone.

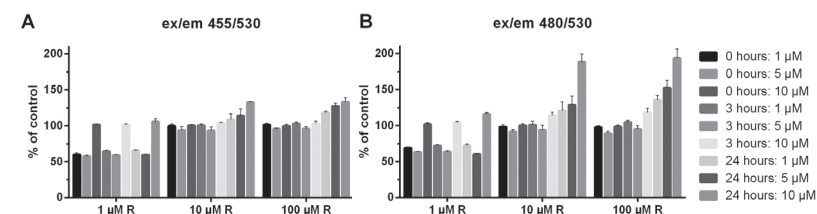


Figure 21: Effects of different BODIPY loading concentrations on the relative fluorescence measured at ex/em 455/530 (A) and ex/em 480/530 (B). Data are normalized to their time-matched controls. R is rotenone. Note: arbitrary units at ex/em 480/530 nm were approximately half of ex/em 455/530 nm. Background fluorescence was comparable to treated cells at 10 µM BODIPY loading concentrations (background not measured for 1 and 5 µM BODIPY).

(Fig. 21). At ex/em 550/600 nm, relative fluorescence did differ between BODIPY loading concentrations (Fig. 22). Because results varied somewhat at ex/em 550/600 nm for the different BODIPY loading concentrations, it was concluded that excimers may play a role in the reliable detection of fluorescence that correlates with an increase in oxidized BODIPY.

Because the absolute fluorescence of the controls increased over time at ex/em 550/600 nm (Fig. 17 and 18), we hypothesized that the cells and/or BODIPY may need some more time to stabilize after loading. Therefore, after loading with 10 µM BODIPY for 60 min, BODIPY was removed from the

cells and wells were replenished with fresh medium. After 3h, fluorescence was measured and medium replaced with exposure medium. Again, an increase in fluorescence at ex/em 550/600 nm (non-oxidized BODIPY) was observed after 3h of exposure (data not shown), indicating that BODIPY does not require a stabilization period after loading.

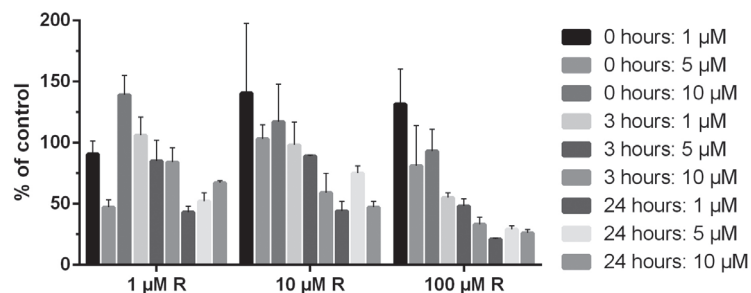


Figure 22: Effects of different BODIPY loading concentrations on the relative fluorescence measured at ex/em 550/600 nm. Data are normalized to their time-matched controls. R is rotenone.

3.2.3 Discussion

As expected from the literature, non-oxidized BODIPY fluorescence can be measured in the red spectrum (maximum emission at 600 nm). Cells treated with rotenone, which is expected to induce lipid peroxidation, demonstrated a relative decrease in non-oxidized BODIPY, which suggest that BODIPY is oxidized and a ratiometric shift occurred to the green-light spectrum. Spectra of the treatments identified several possible excitation maxima's at emission 530 nm. The ratio of emission 530/600 nm indicates a time- and concentration-dependent increase in lipid peroxidation. However, the test conditions are not yet optimal. Fluorescence at emission 530 nm is relatively low; fluorescence of non-oxidized BODIPY increases with time and high background fluorescence was detected for wells without cells. The low fluorescence at emission 530 nm and the increasing fluorescence at emission 600 nm may be due to the formation of excimers (Drummen et al., 2002). Lower BODIPY loading concentrations indicate that, relative to the control, fluorescence at emission 530 nm is somewhat increased after treatment with rotenone. Reducing the BODIPY loading

concentration and loading time, as well as increasing the cells/sample could be further explored to increase the fluorescence at emission 530 nm. Also, the increase in fluorescence at emission 600 nm may be due to the formation of excimers, as different BODIPY loading concentrations yield different results. In addition, the increase in fluorescence at emission 600 nm could be due to the disruption of the membrane by the vehicle (DMSO).

In conclusion, BODIPY displays features that are interesting for the application of BODIPY as a lipid peroxidation sensor. However, BODIPY fluorescence is not always acting as expected which may be due to the formation of excimers. Further studies are needed to determine the optimal test conditions for the use of BODIPY as a lipid peroxidation sensor.

Chapter 4

EXPERIMENTAL APPROACHES TO STUDY NEUROTRANSMITTER RELEASE *IN VITRO*

Marieke Meijer, Milou M.L. Dingemans and Remco H.S. Westerink

Adapted from:

“D2.3 Report on *in vitro* screening for effects on intra- and intercellular signaling”

(deliverable DENAMIC, FP7-ENV-2011 project nr. 282957, September 2014)

Author(s)

Marieke Meijer, Milou M.L. Dingemans, Remco H.S. Westerink (IRAS) Timo Hamers (VU)

4.1 EVALUATION OF FLUORESCENCE FALSE NEUROTRANSMITTERS TO STUDY NEUROTRANSMITTER RELEASE *IN VITRO*

4.1.1 Introduction

For the study of neurotransmitter release *in vitro*, dopamine release can be directly quantified by amperometry (Westerink and Ewing, 2008). However, amperometry is labor intensive and there is a need for more high-throughput methods for the detection of neurotransmitters. We therefore evaluated the use of optical tracers of monoamine neurotransmitters to investigate dopamine release by PC12 cells, in a medium- to high-throughput setting. Optical tracers of dopamine have recently been developed and are known as fluorescent false neurotransmitters (FFNs). These molecules are fluorescent substrates of the neuronal vesicular monoamine transporter 2 (VMAT2) and have been shown by multiphoton microscopy to accumulate in vesicles of mouse chromaffin cells (Gubernator et al., 2009). It was shown by total internal reflection fluorescence microscopy (TIRFM) that FFN511 was released upon membrane depolarization (Gubernator et al., 2009). FFNs can thus be used to study neurotransmitter release *in vitro* and potentially to study chemical-induced effects thereon. We therefore investigated the uptake and vesicular release of FFN by PC12 cells with our life-imaging fluorescence microscope and in a plate reader. The first developed FFN was FFN511 (Gubernator et al., 2009), followed by Mini202 (Lee et al., 2010) and FFN102 (Rodriguez et al., 2013) with modifications compared to FFN511. Mini202 was developed as a pH-responsive probe allowing ratiometric detection of vesicular and cytosolic dopamine (Lee et al., 2010). Vesicles have low pH (~5) and the cytosol has a higher pH (~7) and in that way a pH-sensitive probe allows for specific detection of vesicular and cytosolic neurotransmitters. FFN102 is also a pH-responsive probe but was designed as a highly polar compound to reduce nonselective labelling of tissue and passive membrane diffusion (Rodriguez et al., 2013).

4.1.2 Materials and methods

Uptake and vesicular release of FFN was investigated in undifferentiated PC12 cells, dexamethasone-differentiated PC12 cells, neuronal MES23.5 cells and in primary dopaminergic neurons. These cell types synthesize and secrete catecholamines, including dopamine, but dexamethasone-differentiated PC12 cells have larger vesicles that contain more dopamine

and exhibit a higher vesicle release frequency compared to undifferentiated PC12 cells (Westerink and Ewing, 2008). Cells were subcultured in glass-bottom dishes for imaging experiments.

Table 1: Optimum excitation wavelengths with corresponding emission wavelengths (in nm).

FFN	excitation wavelength	emission wavelength
FFN511 (Sigma-Aldrich)	410 (pH 7.3; Fig. 1A)	505
Mini202 (provided by D. Sulzer, Columbia University, NY, USA)	335 (pH 4.8); 370 (pH 7.3; Fig. 1B)	460
FFN102 (Abcam Biochemicals)	340 (pH 4.8); 370 (pH 7.3; Fig. 1C)	455

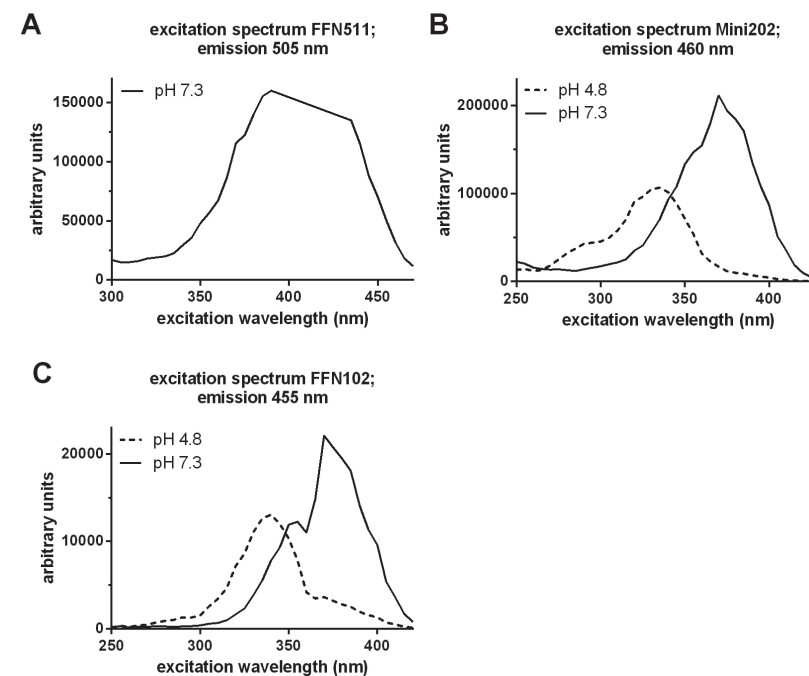


Figure 1: Excitation spectra measured for FFN511 (A), Mini202 (B) and FFN102 (C) in saline with pH 7.3 (FFN511) or at pH 4.8 and 7.3 (Mini202/FFN102) in a microplate reader.

Fluorescence was recorded with an Axiovert 35M inverted microscope (40x oil-immersion objective, NA 1.0: Zeiss, Göttingen, Germany) equipped with a TILL Photonics Polychrome IV (Xenon Short Arc lamp, 150W; TILL Photonics GmbH, Gräfelfing, Germany), an Image SensiCam digital camera (TILL Photonics GmbH) and a 410 nm long bandpass filter.

For specific experiments, fluorescence was recorded with an Infinite M200 microplate reader equipped with a 10W Xenon flash light source (Tecan Trading AG, Männedorf, Switzerland). For these experiments, 150,000 cells/well were subcultured in black, glass-bottom 96-wells plates.

Optimum excitation wavelengths were measured with solutions of FFNs in physiological saline by a microplate reader (Fig. 1; Table 1).

4.1.3 Results

FFN511. PC12 cells were loaded with 5 μ M FFN511 for 10, 20 or 60 min (Gubernator et al., 2009). Next, cells were placed under the microscope and fluorescence was measured at 370 nm while cells were continuously superfused with saline to reduce the background fluorescence and to manipulate the exposure solution. FFN511 fluorescence appeared to decrease continuously during the time course of the experiment (~45 min). When FFN511-loaded cells were viewed under the microscope without superfusion, cells were highly fluorescent, but the background fluorescence was also very high. Upon membrane depolarization with high- K^+ containing saline, no effects were observed in the background-corrected fluorescence of the cells (Fig. 2A). Also in dexamethasone-differentiated PC12 cells loaded with FFN511, no changes in fluorescence were observed after stimulation with high- K^+ containing saline (Fig. 2B). Compared to undifferentiated PC12 cells, FFN511 fluorescence was higher in dexamethasone-differentiated PC12 cells (Fig. 2). Differences in fluorescence were also not detected in the microplate reader upon membrane depolarization with high- K^+ containing saline (data not shown).

In short, we did detect that FFN511 is taken up by undifferentiated or dexamethasone-differentiated PC12 cells and exhibits fluorescence that can be measured at excitation 370 nm (Fig. 3). Changes in fluorescence that indicate release of FFN511 were however not detected in our systems upon membrane depolarization.

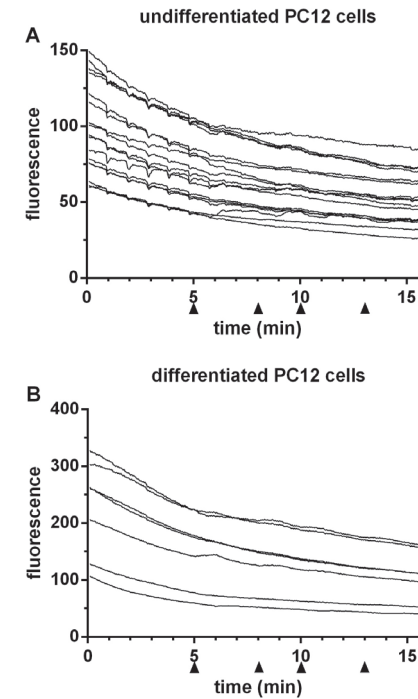


Figure 2: Background-corrected fluorescence of individual undifferentiated PC12 cells (A) and dexamethasone-differentiated PC12 cells (B). Cells were continuously superfused with saline. The arrowheads indicate the switch of superfusion to high- K^+ containing saline for 1 min to induce membrane depolarization.

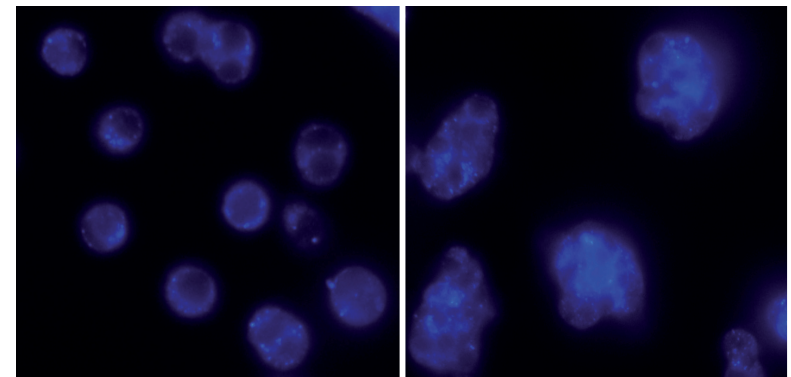


Figure 3: FFN511 fluorescence photomicrograph at excitation 370 nm in undifferentiated PC12 cells (left panel) and in dexamethasone-differentiated PC12 cells (right panel).

Mini202. Undifferentiated and dexamethasone-differentiated PC12 cells were loaded with 20 μM Mini202 for 60 min (Lee et al., 2010). In the microscope set-up, fluorescence of the cells was measured at 335, 340 and 380 nm although very little fluorescence was observed. By increasing the exposure time of the excitation light from 5 to 15 ms, the fluorescence intensity slightly increased. Also, no changes in fluorescence were observed after membrane depolarization with high- K^+ containing saline in both undifferentiated and dexamethasone-differentiated PC12 cells (data not shown). To investigate if the low fluorescence of Mini202 could be due to low uptake of Mini202 by PC12 cells, neuronal MES23.5 cells were loaded with Mini202 as well. However, results were comparable to the PC12 cell results (data not shown).

Changes in fluorescence were also not detected with the microplate reader upon membrane depolarization of undifferentiated and dexamethasone-differentiated PC12 cells (data not shown).

FFN102. Undifferentiated and dexamethasone-differentiated PC12 cells were loaded with 50 μM FFN102 for 45 min and fluorescence was measured at 340 and 370 nm (Rodriguez et al., 2013). Membrane depolarization with high- K^+ containing saline resulted in small increases in background-corrected fluorescence of the undifferentiated PC12 cells excited by 340 nm, small decreases in fluorescence excited by 370 nm and small decreases in the ratio of fluorescence excited by 340 nm and 370 nm, suggesting that FFN102 is released from the vesicles in undifferentiated PC12 cells (data not shown). These effects could however not be reproduced and were not observed in dexamethasone-differentiated PC12 cells (data not shown).

The applicability of FFN102 was also investigated with primary dopaminergic neurons. After 3, 8, 10, 11 or 15 days *in vitro* (DIV) dopaminergic neurons were loaded and investigated for FFN102 fluorescence comparable to the PC12 cells. Membrane depolarization decreased the fluorescence at 340 and 370 nm, however, no change in ratio was observed (data not shown). Stimulation of dopaminergic neurons was also induced with a combination of 1 mM acetylcholine and 50 μM glutamate. With calcium imaging experiments it was confirmed that this combination of acetylcholine and glutamate induced a strong increase in $[\text{Ca}^{2+}]_i$ in these neurons, which is a prerequisite for exocytosis. No changes in FFN102 fluorescence were observed at 340 and 370 nm

(data not shown). The absence of changes appeared independent of the DIV of the investigated dopaminergic neurons (data not shown). FFN102 fluorescence decreases over time (as was also observed for FFN511 and Mini202; Fig. 2) and it was investigated if this was due to photobleaching. To investigate this, the sample frequency was decreased with 6-fold. However, decreasing the sample frequency did not prevent the decrease in FFN102 fluorescence over time. Alternatively, FFN102 fluorescence may be reduced due to the spontaneous activity of primary dopaminergic neurons. To investigate this possibility, cells were washed in calcium-free medium after FFN102 loading to prevent spontaneous exocytosis. During measurements of FFN102 fluorescence, cells were continuously superfused with calcium-free saline, except when depolarization was induced with either acetylcholine/glutamate or high-potassium containing saline. The ratio of background-corrected F340 and F380 was slightly increased upon depolarization, however, no specific depolarization-induced changes were observed in the separate background-corrected F340 and F380 data (data not shown).

The sensitivity of FFN102 measurements may be reduced due to high fluorescence of FFN102 at pH 7.3 at excitation 340 nm. We aimed to reduce the fluorescence by decreasing the loading time of FFN102 by 3-fold. No differences in fluorescence were observed by decreasing the loading time (data not shown).

4.1.4 Discussion

In conclusion, we have not been able to detect neurotransmitter release *in vitro* using FFNs. FFNs seemed to accumulate in cells and in vesicles (Fig. 2) as indicated by background-corrected fluorescence at excitation wavelengths 370 nm (cytosolic) and 340 nm (vesicular), but we were not able to measure the release of FFNs from the cells. It is possible that FFNs are not released from the vesicles due to binding of FFNs to intravesicular storage proteins. Alternatively, the fluorescence microscope and plate reader may not be sufficiently sensitive to detect changes in fluorescence resulting from the vesicular release of FFNs. Measuring the fluorescence at a higher resolution or with confocal microscopy may increase the applicability of FFNs to investigate neurotransmitter release, but will decrease the applicability of FFNs for medium- to high-throughput screening of chemical-induced changes in neurotransmitter release, thereby limiting its use for DENAMIC.

4.2 EVALUATION OF ALTERNATIVE METHODS FOR THE DETECTION OF DOPAMINE IN BIOLOGICAL SAMPLES

4.2.1 Introduction

While FFNs allow for the study of neurotransmitter uptake and -release by mimicking monoamine neurotransmitters, direct detection of dopamine in biological samples could also be an approach for the study of neurotransmitter release. Since direct quantification by amperometry is labor intensive, we evaluated several methods that may allow more high-throughput detection of dopamine.

4.2.2 Spectrophotometric detection of dopamine

Dopamine is easily oxidized in alkaline medium to an orange/brown molecule. The color change can be quantified by measuring the absorbance with a microplate reader. Different concentrations of dopamine in physiological salt were allowed to auto-oxidize for different periods before their absorbance was measured. From 10 μM dopamine, a concentration-dependent increase in absorbance was observed (data not shown). However, at lower concentrations no concentration-dependent relationship was present, limiting the use of this method for biological samples.

4.2.3 Spectrofluometric detection of dopamine

Dopamine is also known to be auto-fluorescent in acidic solutions. Therefore, dopamine solutions in acidic buffer were prepared and fluorescence was measured for up to 1h with a microplate reader. Again, a concentration-dependent effect appeared to be present at concentrations higher than 10 μM , but not at lower dopamine concentrations (data not shown), limiting the use of this method for biological samples.

4.2.4 Amplex Ultrared assay

Dopamine can be converted by tyramine oxidase (TOD) to hydrogen peroxide. Hydrogen peroxide can react with Amplex Ultrared in the presence of horseradish peroxidase (POD). Upon reaction, Amplex Ultrared is converted in a 1:1 stoichiometry to the red-fluorescent oxidation product, resorufin. The assay was performed according to the

manufacturer's instructions. A concentration-response curve for dopamine was measured with a detection limit of $\sim 1 \mu\text{M}$ (data not shown), which is close to dopamine concentrations in biological samples (see discussion for calculation of dopamine concentrations) but not sufficiently low for reliable measurements.

4.2.5 Luminol assay

Hydrogen peroxide, which is formed after conversion of dopamine by TOD, can react with luminol in the presence of POD resulting in luminescence. A concentration-response curve for hydrogen peroxide was measured by use of this assay, which had a detection limit of 1 μM . When the assay was performed with dopamine, results varied and no increase in luminescence was observed upon membrane depolarization with high potassium containing-saline to trigger dopamine release (data not shown). Therefore, this assay is not suitable for the detection of dopamine in biological samples.

4.2.6 Discussion

The neurotransmitter dopamine can be detected by spectrophotometric, spectrofluometric or with Amplex Ultrared assays. However, detection limits are too high (lowest for Amplex Ultrared, 1 μM) for quantification of dopamine in biological samples that only contain small amounts of dopamine (PC12 cells release ~ 250 amole/cell upon exocytosis (assuming ~ 500 zmole/vesicle and ~ 500 vesicles/cell) and in case of 200,000 cells/well is 50 pmole of released dopamine; if dissolved in 100 μL , the dopamine concentration is 0.5 μM ; Westerink and Ewing, 2008). Therefore, these methods cannot be used for high-throughput investigation of chemical-induced changes in neurotransmitter release.

Chapter 5

COMPARISON OF PLATE READER-BASED METHODS WITH FLUORESCENCE MICROSCOPY FOR MEASUREMENTS OF INTRACELLULAR CALCIUM LEVELS FOR THE ASSESSMENT OF *IN VITRO* NEUROTOXICITY

Marieke Meijer^a, Hester S. Hendriks^a, Harm J. Heusinkveld^{a,b},
Wendy T. Langeveld^a, Remco H.S. Westerink^{a*}

^a Neurotoxicology Research Group, Toxicology Division, Institute for Risk Assessment Sciences (IRAS), Faculty of Veterinary Medicine, Utrecht University, P.O. Box 80.177, 3508 TD Utrecht, The Netherlands.

^b IUF - Leibniz Research Institute for Environmental Medicine, Auf'm Hennekamp 50, 40225 Düsseldorf, Germany.

Published in: *Neurotoxicology*. 2014 45C:31-37. doi: 10.1016/j.neuro.2014.09.001.

ABSTRACT

The intracellular calcium concentration ($[Ca^{2+}]_i$) is an important readout for *in vitro* neurotoxicity since calcium is critically involved in many essential neurobiological processes, including neurotransmission, neurodegeneration and neurodevelopment. $[Ca^{2+}]_i$ is often measured with considerable throughput at the level of cell populations with plate reader-based assays or with lower throughput at the level of individual cells with fluorescence microscopy. However, these methodologies yield different quantitative and qualitative results. In recent years, we demonstrated that the resolution and sensitivity of fluorescence microscopy is superior compared to plate reader-based assays. However, it is currently unclear if the use of plate reader-based assays results in more 'false negatives' or 'false positives' in neurotoxicity screening studies. In the present study, we therefore compared a plate reader-based assay with fluorescence microscopy using a small test set of environmental pollutants consisting of dieldrin, lindane, polychlorinated biphenyl 53 (PCB53) and tetrabromobisphenol-A (TBBPA). Using single-cell fluorescence microscopy, we demonstrate that all test chemicals reduce the depolarization-evoked increase in $[Ca^{2+}]_i$, whereas lindane, PCB53 and TBBPA also increase basal $[Ca^{2+}]_i$, though via different mechanisms. Importantly, none of these effects were confirmed with the plate reader-based assay. We therefore conclude that standard plate reader-based methods are not sufficiently sensitive and reliable to measure the highly dynamic and transient changes in $[Ca^{2+}]_i$ that occur during chemical exposure.

Keywords: *in vitro* neurotoxicity, intracellular calcium concentration ($[Ca^{2+}]_i$), plate reader, fluorescence microscopy, chemical screening methods, high-throughput testing strategies

5.1 INTRODUCTION

Calcium homeostasis is involved in many neuronal processes, including neurotransmission (Westerink, 2006), neurodegeneration (Mattson, 2007) and neural development (Leclerc et al., 2011). Even small changes in the intracellular calcium concentration ($[Ca^{2+}]_i$) can already result in deleterious effects (Toescu and Verkhratsky, 2007). Cells therefore tightly regulate $[Ca^{2+}]_i$ by Ca^{2+} -binding proteins, Ca^{2+} storage in mitochondria and endoplasmic reticulum (ER), Ca^{2+} transport (e.g. Na^+/Ca^{2+} exchangers) and by controlling influx of extracellular Ca^{2+} via voltage-gated calcium channels (VGCCs) and Ca^{2+} permeable neurotransmitter receptors (Westerink, 2006). Nowadays, organisms are regularly exposed to several environmental pollutants and other chemicals that can disturb Ca^{2+} homeostasis by targeting one (or more) of these Ca^{2+} controlling mechanisms. These compounds thus pose a possible risk for neuronal function and ultimately for human health. Therefore, $[Ca^{2+}]_i$ is an important readout for *in vitro* (developmental) neurotoxicity.

Real-time kinetic changes in $[Ca^{2+}]_i$ are commonly assessed with either a plate reader-based approach or with fluorescence microscopy. However, the plate reader-based approach has recently been criticized because of its low(er) temporal and spatial resolution, low sensitivity and potential pitfalls and artifacts, such as those associated with changes in volume- and osmolarity (Westerink and Hondebrink, 2010; Heusinkveld and Westerink, 2011). In contrast, single-cell fluorescence microscopy has high(er) temporal and spatial resolution, high(er) sensitivity and no artifacts associated with changes in volume and osmolarity when complemented with a superfusion system that continuously refreshes the medium. As such, fluorescence microscopy appears more appropriate for assessing chemically-induced changes in $[Ca^{2+}]_i$. Nevertheless, fluorescence microscopy is considered low- or at best medium-throughput and high-throughput plate reader-based approaches are therefore often preferred by many researchers, despite their limitations.

It has been suggested that measurements of $[Ca^{2+}]_i$ by plate reader-based techniques may be sufficiently sensitive to prioritize chemicals for further testing. However, a careful evaluation of the suitability of a plate reader-based approach for measurements of $[Ca^{2+}]_i$ is lacking and it is still unclear if this method yields 'false-negative' or 'false-positive' results. We therefore

selected a test set of chemicals based on existing fluorescence microscopy data for a direct comparison with a plate reader-based approach. The test set of chemicals consists of the organochlorine insecticides dieldrin and lindane, the polychlorinated biphenyl 53 (PCB53) and the brominated flame retardant tetrabromobisphenol-A (TBBPA), which all affect basal $[Ca^{2+}]_i$ and/or depolarization-evoked $[Ca^{2+}]_i$. In earlier studies, we demonstrated that exposure of PC12 cells to dieldrin does not affect basal $[Ca^{2+}]_i$, but reduces depolarization-evoked increase in $[Ca^{2+}]_i$ (Heusinkveld and Westerink, 2012), whereas lindane, PCB53 and TBBPA not only reduce depolarization-evoked increases in $[Ca^{2+}]_i$, but also increase basal $[Ca^{2+}]_i$ (Hendriks et al., 2012; Langeveld et al., 2012; Heusinkveld et al., 2010). The mechanisms underlying the increase in basal $[Ca^{2+}]_i$ differ largely. Lindane increases basal $[Ca^{2+}]_i$ via depolarization of the cell membrane and subsequent opening of VGCCs (Heusinkveld et al., 2010), whereas PCB53 increases basal $[Ca^{2+}]_i$ mainly by release of Ca^{2+} from the ER (Langeveld et al., 2012) and TBBPA via Ca^{2+} release from both ER and mitochondria (Hendriks et al., 2012). Careful comparison of fluorescence microscopy data of this test set of chemicals to our plate reader data indicates that the plate reader-based method is not suitable for the investigation of chemical-induced $[Ca^{2+}]_i$ changes with sufficient detail for reliable prioritization of chemicals.

5.2 MATERIALS AND METHODS

5.2.1 Chemicals

Fura-2 AM was obtained from Molecular Probes (Invitrogen, Breda, The Netherlands). PCB53 (purity >99.2%) was purchased from Neosync Inc., and possible impurities, e.g., polychlorinated dibenzodioxins/polychlorinated dibenzofurans (PCDD/Fs) and DL-PCBs, were removed by Stenberg and Andersson (Institute of Environmental Chemistry, Umeå University, Sweden) by applying a fractionation on active carbon cleanup step as described previously (Danielsson et al., 2008). Dieldrin, lindane (both purity 99.8%), TBBPA (purity >99%), and all other chemicals were obtained from Sigma-Aldrich (Zwijndrecht, The Netherlands) unless otherwise noted. Saline solutions (containing in mM: 125 NaCl, 5.5 KCl, 2 $CaCl_2$, 0.8 $MgCl_2$, 10 HEPES, 24 glucose, and 36.5 sucrose at pH 7.3, adjusted with NaOH) were prepared with deionized water (Milli-Q®; resistivity >18 MΩ cm). Stock solutions of 25-100 mM dieldrin, lindane, PCB53 and TBBPA were prepared

in DMSO and diluted in saline just prior to the experiments. All solutions used in experiments, including controls, contained 0.1% DMSO.

5.2.2 Cell culture

Rat Pheochromocytoma (PC12) cells (Greene and Tischler, 1976) were cultured for 10 passages in RPMI1640 (Invitrogen, Breda, The Netherlands) supplemented with 10% horse serum, 5% fetal bovine serum and 2% penicillin/streptomycin (ICN Biomedicals, Zoetermeer, The Netherlands) as described previously (Hendriks et al., 2012; Heusinkveld et al., 2010; Langeveld et al., 2012). All culture-ware was coated with poly-L-lysine (50 µg/mL). Cells were grown in a humidified incubator at 37°C and 5% CO_2 . Medium was refreshed every 2-3 days.

For single cell fluorescent microscopy calcium imaging experiments, undifferentiated PC12 cells were subcultured in glass-bottom dishes ($\sim 0.5 \times 10^6$ cells/dish; $\sim 75\%$ confluency; MatTek, Ashland, MA) as described previously (Hendriks et al., 2012; Heusinkveld et al., 2010; Langeveld et al., 2012). For fluorescent plate reader-based calcium measurements, undifferentiated PC12 cells (1.5×10^5 cells/well; $\sim 100\%$ confluency) were subcultured in black, clear bottom 96-wells plates (Greiner Bio-one, Solingen, Germany) as described previously (Heusinkveld and Westerink, 2011).

5.2.3 $[Ca^{2+}]_i$ measurements

Changes in $[Ca^{2+}]_i$ were measured with the calcium sensitive fluorescent ratio dye Fura-2 AM as described previously (Hendriks et al., 2012; Heusinkveld et al., 2010; Langeveld et al., 2012). PC12 cells were loaded with 5 µM Fura-2 AM for 20 min in saline followed by 15 min de-esterification in saline. All procedures and experiments were done at room temperature.

For fluorescence microscopy calcium imaging, cells were placed on the stage of an Axiovert 35 M inverted microscope (40x oil-immersion objective, NA 1.0: Zeiss, Göttingen, Germany) equipped with a TILL Photonics Polychrome IV (Xenon Short Arc lamp, 150W; TILL Photonics GmbH, Gräfelfing, Germany). Cells were continuously superfused with saline by use of a Valvelink 8.2 (Automate Scientific, CA, USA) and fluorescence, excited by 340 and 380 nm wavelengths (F_{340} and F_{380}), was collected every 3-12 s at 510 nm with an Image SensiCam digital camera (TILL Photonics GmbH, Gräfelfing, Germany). Data were processed with

TILLvisION software (version 4.01). Every experiment consisted of a 5 min baseline recording and subsequent depolarization of the cells by changing superfusion to 100 mM potassium (K^+) for 20 s. Next, cells were allowed to recover for 5-8 min before superfusion was changed to 0.1% DMSO-containing saline (control) or to saline containing dieldrin, lindane, PCB53 or TBBPA for 15-20 min. After exposure, cells were depolarized for a second time with saline containing the test substance and 100 mM K^+ . In plate reader-based approaches, depolarization for a second time is generally not possible as medium cannot be easily replaced during measurements. For comparison with the plate reader-based method, the internal control for depolarization-evoked increase in $[Ca^{2+}]_i$ in microscopy measurements is not shown in this manuscript (see Fig. 1A for example recording). Complete example recordings and concentration-response curves have been published previously in Heusinkveld and Westerink (2012; dieldrin), Heusinkveld et al. (2010; lindane), Langeveld et al. (2012; PCB53) and Hendriks et al. (2012; TBBPA).

For plate reader-based experiments, black, clear-bottom 96-wells plates with Fura-2 loaded cells (200 μ L saline/well) were placed in an Infinite M200 microplate reader equipped with a 10W Xenon flash light source (Tecan Trading AG, Männedorf, Switzerland). Fluorescence was evoked by 340 and 380 nm excitation wavelengths (F_{340} and F_{380}) and collected at 510 nm every 6 s. For all experiments a gain of 170, settle time of 100 ms, and an integration time of 40 μ Hz was used. Data were processed with iControl software (version 7.1). For every experiment, after a 3 min baseline recording 50 μ L of saline containing DMSO (0.5%; final concentration 0.1%) or test compound (dieldrin, lindane, PCB53 or TBBPA) was dispersed into the wells at a speed of 100 μ L/s. Following 15 min of exposure, cells were depolarized by adding 50 μ L of saline containing 600 mM K^+ (final concentration 100 mM). After depolarization, changes in $[Ca^{2+}]_i$ were assessed for 5 min (Fig. 1B).

For these test compounds, concentrations were selected that are known to induce a (near) maximal Ca^{2+} response and are not suspected to induce cytotoxicity within 15-20 min of exposure (Hendriks et al., 2012; Heusinkveld et al., 2010; Langeveld et al., 2012). Notably, even if a test compound would result in immediate and profound cytotoxicity it would result in the loss of cellular homeostasis and thus an increase in basal $[Ca^{2+}]_i$. For the aim of our study, i.e. a direct comparison of plate reader-based

methods with fluorescence microscopy, it would thus not even matter if compounds are acute cytotoxic.

5.2.4 Data analysis and statistics

F_{340}/F_{380} ratios were calculated and analyzed using MS-Excel 2010. For fluorescence microscopy experiments, a custom-made MS-Excel macro that calculates background-corrected F_{340}/F_{380} ratio values from the raw F_{340} and F_{380} data were used. All data are presented as mean $F_{340}/F_{380} \pm$ standard error of the mean (SEM) normalized to baseline from the number of cells ($n = 33-781$ cells from $N = 3-84$ independent experiments; fluorescence microscopy) or wells ($n = 8-11$ from $N = 8-11$ independent experiments; plate reader) indicated.

Continuous data were compared with a Student's *t*-test, paired or unpaired where applicable. A *p* value < 0.05 was considered statistically significant.

5.3 RESULTS

5.3.1 Effects on basal $[Ca^{2+}]_i$

In single-cell fluorescence microscopy experiments, (normalized) ratio levels are stable and remain unchanged upon superfusion for 15-20 min with saline containing 0.1% DMSO (1.03 ± 0.01 ; $N=84$, $n=781$; Fig. 1A). However, in the plate reader-based method (normalized) ratio levels show a gradual increase (0.52 ± 0.10 ; $N=11$, $n=11$) during the time-course of the recording (Figs. 1B and 2B, D, F, H). Additionally, a stepwise increase in normalized ratio levels is observed in the plate reader-based method immediately upon injection saline containing 0.1% DMSO (Fig. 1B). Previously, Heusinkveld and Westerink (2011) demonstrated that this is due to changes in volume and ionic conditions in the well, and also possible dye leakage from the cells. Consequently, the change in ratio upon injection of saline does not represent an actual change in $[Ca^{2+}]_i$. Therefore, also a net increase in normalized F_{340}/F_{380} ratio was calculated to correct for this volume-induced stepwise increase in fluorescence (see Heusinkveld and Westerink, 2011; Kassack et al., 2002 and Fig. 1B for further explanation). This net increase in normalized ratio upon superfusion with saline containing 0.1% DMSO amounts to 0.03 ± 0.01 ($N=84$, $n=781$; Fig. 3A) in fluorescence microscopy experiments (DMSO controls) and to 0.05 ± 0.01 ($N=11$, $n=11$; Fig. 3B) in plate reader-based experiments.

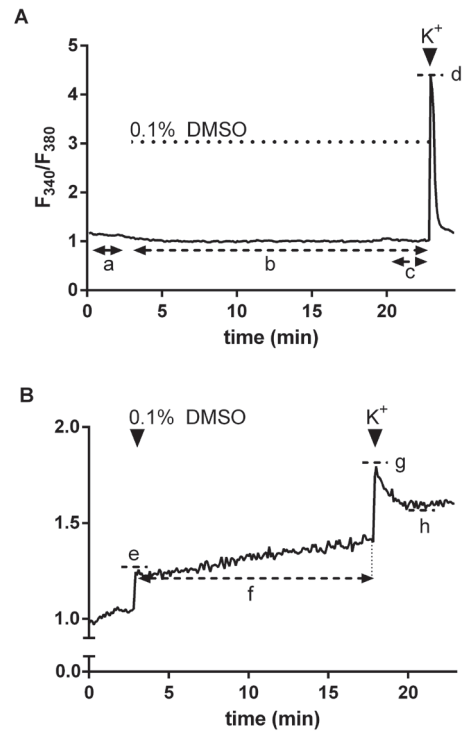


Figure 1: Example recordings of changes in normalized ratio upon DMSO (0.1%) exposure measured with the single-cell fluorescence microscopy (A) and with the plate reader-based method (B). The dotted line in the fluorescence microscopy recording (A) represents the duration of superfusion with saline containing 0.1% DMSO, whereas the arrowhead indicates the switch of superfusion to high K^+ -containing saline. The arrowheads in the plate reader-derived recording (B) represent the addition by injection of 0.1% DMSO-containing saline or high K^+ -containing saline. The basal net increase in normalized ratio of the fluorescence microscopy method (A) was calculated as: the average ratio during exposure (b) - the average ratio prior to exposure (a), whereas the depolarization-evoked net increase in normalized ratio was calculated as: the maximum amplitude upon depolarization (d) - the average ratio 1 min prior to depolarization (c). To correct for the artificial step-wise increases in fluorescence ratio in the plate reader-based method (B) the basal net increase in normalized ratio was calculated as: the average ratio during exposure (f) - the maximum amplitude upon injection (e), whereas the depolarization-evoked net increase in normalized ratio was calculated as: the maximum amplitude upon depolarization (g) - the lowest ratio after depolarization (h).

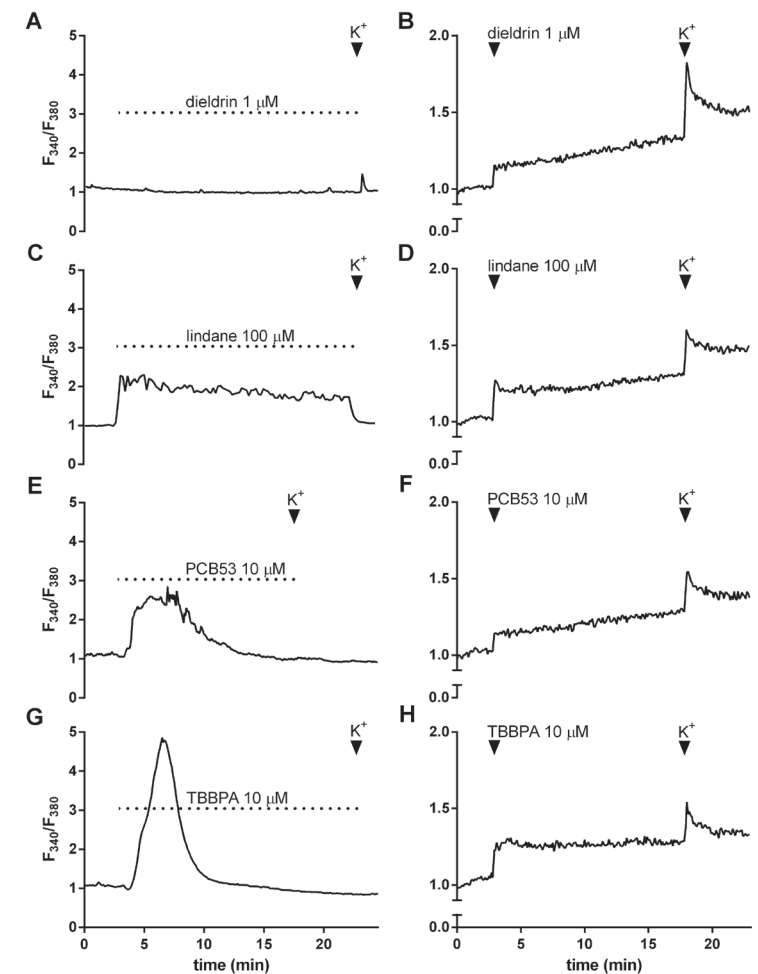


Figure 2: Example recordings of changes in normalized ratio measured with the single-cell fluorescence microscopy method (left) and the plate reader-based method (right). Changes in normalized fluorescence ratio were induced by 1 μ M dieldrin (A and B), 100 μ M lindane (C and D), 10 μ M PCB53 (E and F), and 10 μ M TBBPA (G and H). The dotted line in the recordings obtained with fluorescence microscopy represents the duration of superfusion with the test compound, the arrowhead indicates the switch of superfusion to high K^+ - and test compound-containing saline. The arrowheads in the plate reader-derived recordings represent the addition by injection of test compound-containing saline or high K^+ - and test compound-containing saline.

In single-cell fluorescence microscopy, dieldrin does not induce significant changes in basal ratios compared to DMSO controls at concentrations up to 1 μM (net increase in normalized ratio 0.00 ± 0.01 at 1 μM ; $N=5$, $n=68$; Figs. 2A and 3A). This is comparable to plate reader-based experiments where 1 μM dieldrin induces only a marginal net increase in normalized ratio of 0.07 ± 0.01 ($N=8$, $n=8$), which is not significantly different from the net increase in control conditions (Figs. 2B and 3B).

In contrast to dieldrin, in single-cell fluorescence microscopy experiments 10 and 100 μM lindane demonstrates a significant and concentration-dependent increase in normalized basal ratios (net increase in normalized ratio 0.17 ± 0.02 and 0.46 ± 0.06 ; $N=8$, $n=99$ and $N=6$, $n=63$, respectively; Figs. 2C and 3A). However, in plate reader-based experiments no significant change in normalized basal ratio is observed compared to DMSO controls at 10 μM lindane (net ratio 0.05 ± 0.01 ; $N=8$, $n=8$; Figs. 2D and 3B). At 100 μM , lindane even slightly reduces the net ratio compared to DMSO controls (0.01 ± 0.01 ; $N=8$, $n=8$; Figs. 2D and 3B).

Also, effects of PCB53 on basal ratios differ between fluorescence microscopy and plate reader-based experiments. In single-cell fluorescence microscopy, PCB53 induces a significant net increase in normalized ratio of 0.88 ± 0.07 at 1 μM and 0.63 ± 0.05 at 10 μM ($N=5$, $n=33$ and $N=8$, $n=45$; Figs. 2E and 3A). In contrast, 1 μM PCB53 in plate reader-based experiments does not affect the net ratio (0.05 ± 0.01 ; $N=8$, $n=8$; Figs. 2F and 3B) and at 10 μM , PCB53 reduces the net ratio compared to DMSO controls (-0.05 ± 0.04 ; $N=8$, $n=8$; Figs. 2F and 3B).

Comparable differences between both methods are observed for TBBPA. Single-cell fluorescence microscopy shows a very steep and concentration-dependent increase in normalized basal ratio (1.23 ± 0.17 at 10 μM and 6.06 ± 0.44 at 100 μM ; $N=11$, $n=83$ and $N=3$, $n=39$; Figs. 2G and 3A). In the plate reader, the net increase in basal ratio remains unchanged at 10 μM (0.03 ± 0.01 ; $N=8$ and $n=8$; Figs. 2H and 3B), but is reduced at 100 μM compared to DMSO controls (0.00 ± 0.02 ; $N=8$ and $n=8$; Fig. 3B).

5.3.2 Effects on depolarization-evoked increase in $[\text{Ca}^{2+}]_i$

After 15-20 min of exposure, cells were depolarized with 100 mM K^+ -containing saline. In control fluorescence microscopy experiments, the normalized ratio increases rapidly and transiently upon depolarization to 4.34 ± 0.12 ($N=84$, $n=781$; Fig. 1A). As the amplitude in ratio relies heavily

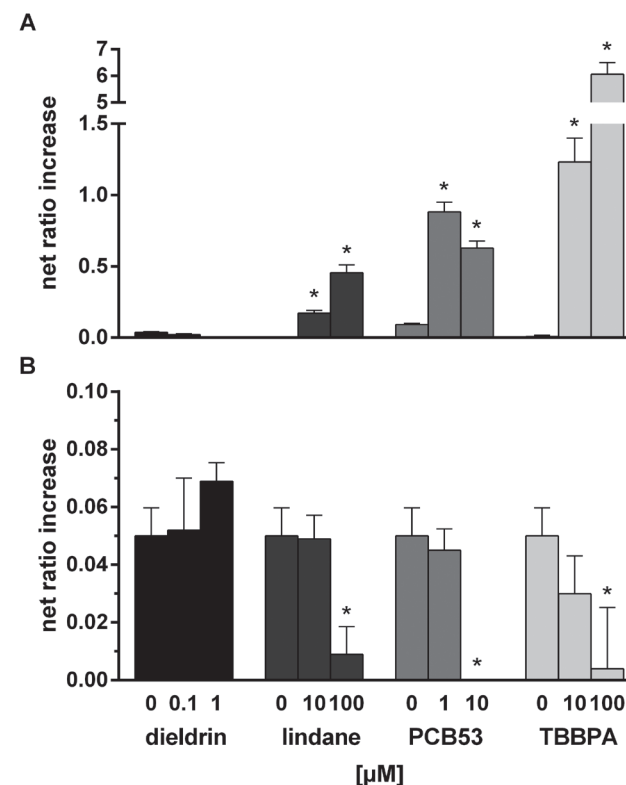


Figure 3: Chemical-induced changes in basal ratio measured with fluorescence microscopy (A) and with a plate reader-based approach (B). Data are expressed as net ratio increase and bars indicate mean \pm SEM of at least four independent experiments. Note the difference in scaling between fluorescence microscopy data (A) and plate reader data (B). * indicates a significant difference compared to control ($p < 0.05$).

on the basal increase in $[Ca^{2+}]_i$ prior to depolarization, a net ratio increase was calculated (see Fig. 1 for details). The net increase in normalized ratio upon depolarization amounts to 3.31 ± 0.12 ($N=84$, $n=781$; Fig. 4A) in fluorescence microscopy control (DMSO) experiments. Depolarization in control plate reader-based experiments increases the ratio to 1.64 ± 0.05 ($N=11$, $n=11$; Fig. 1B). Plate reader-based experiments were corrected for the fluorescence increase due to volume changes upon injection by calculation of a net increase (see Heusinkveld and Westerink, 2011; Kassack et al., 2002 and Fig. 1B for further explanation). In plate reader-based control experiments the net increase in normalized ratio amounts only to 0.16 ± 0.03 ($N=11$, $n=11$; Fig. 4B).

The four test chemicals induce a clear and concentration-dependent reduction of the depolarization-evoked increase in normalized ratio in fluorescence microscopy experiments (Figs. 2A, 2C, 2E, 2G and 4A). Compared to DMSO controls, dieldrin reduces the net increase in depolarization-evoked ratio to 2.26 ± 0.14 ($N=5$, $n=60$) and 0.43 ± 0.05 ($N=5$, $n=68$) at 0.1 and 1 μM , respectively (Fig. 4A). Similarly, lindane reduces the net increase in depolarization-evoked ratio to 0.82 ± 0.08 ($N=8$, $n=99$) and 0.25 ± 0.05 ($N=6$, $n=63$) at 10 and 100 μM , respectively (Fig. 4A). PCB53 reduces the net increase in depolarization-evoked ratio to 0.36 ± 0.11 ($N=5$, $n=33$) and 0.06 ± 0.03 ($N=8$, $n=45$) at 1 and 10 μM , respectively (Fig. 4A) and TBBPA reduces the increase in depolarization-evoked ratio to 0.29 ± 0.11 ($N=11$, $n=83$) and 0.35 ± 0.07 ($N=3$, $n=39$) at 10 and 100 μM , respectively (Fig. 4A).

However, in plate reader-based experiments, depolarization-evoked ratio levels amount to 0.19 ± 0.04 ($N=8$, $n=8$) and 0.20 ± 0.05 ($N=8$, $n=8$; Figs. 2B and 3B) for 0.1 and 1 μM dieldrin, respectively, which are not significantly different from DMSO controls. Comparable results are observed for lindane, which also does not change the net increase in depolarization-evoked ratio compared to depolarization in DMSO controls at 10 μM (0.12 ± 0.04 ; $N=8$, $n=8$) and 100 μM (0.17 ± 0.03 ; $N=8$, $n=8$), respectively (Fig. 4B). Finally, PCB53 and TBBPA induce changes in the net increase in depolarization-evoked ratio comparable to DMSO controls (1 μM PCB53: 0.15 ± 0.03 ; 10 μM PCB53: 0.19 ± 0.04 ; 10 μM TBBPA: 0.19 ± 0.03 ; 100 μM TBBPA: 0.14 ± 0.03 , all $N=8$, $n=8$; Fig. 4B).

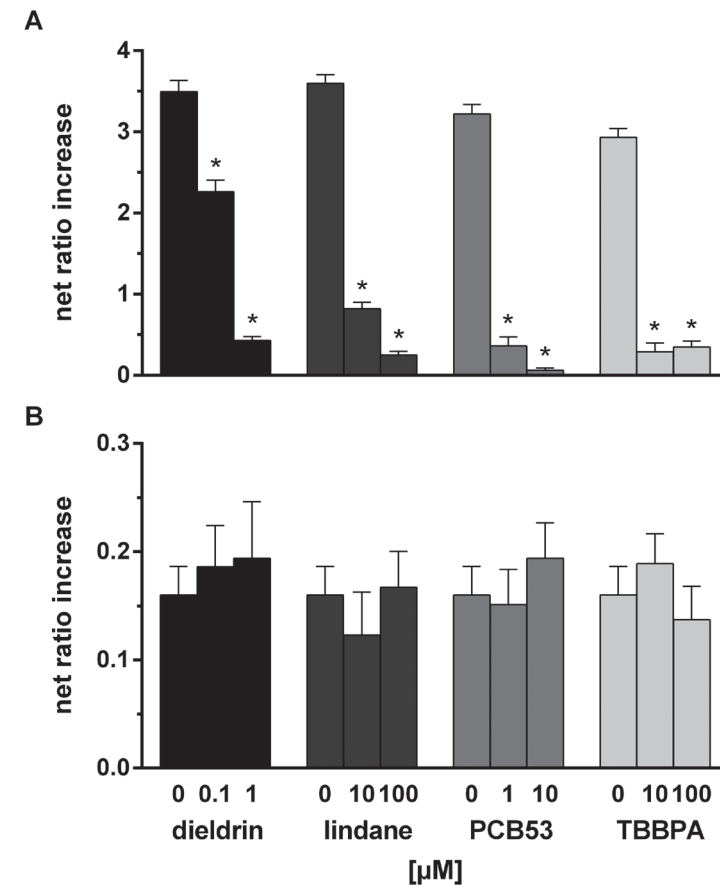


Figure 4: Depolarization-evoked increase in ratio measured with fluorescence microscopy (A) and measured with plate reader (B). Data are expressed as net ratio increase and bars indicate mean \pm SEM of at least four independent experiments. Note the difference in scaling between fluorescence microscopy data (A) and plate reader data (B). * indicates a significant difference compared to control ($p < 0.05$).

5.4 DISCUSSION

In this study we show that chemical-induced changes in $[Ca^{2+}]_i$ measured with a plate reader-based method poorly resemble those measured with single-cell fluorescence microscopy. The plate reader-based method revealed a reduction of the net increase in chemical-induced basal $[Ca^{2+}]_i$ for PCB53 (at 10 μ M), lindane and TBBPA (both at 100 μ M; Fig. 3B). These findings are different from fluorescence microscopy data which revealed an increase in chemical-induced basal $[Ca^{2+}]_i$ for PCB53 (at 1 μ M), lindane and TBBPA (both at 10 μ M; Fig. 3A; Heusinkveld et al. (2010; lindane), Langeveld et al. (2012; PCB53) and Hendriks et al. (2012; TBBPA)). Data measured with the plate reader suggest that the test compounds have no effects on the depolarization-evoked $[Ca^{2+}]_i$ (Fig. 4B) whereas fluorescence microscopy data clearly indicate that all test chemicals significantly inhibit the depolarization-evoked increase in $[Ca^{2+}]_i$ (Fig. 4A; Heusinkveld and Westerink (2012; dieldrin), Heusinkveld et al. (2010; lindane), Langeveld et al. (2012; PCB53) and Hendriks et al. (2012; TBBPA)).

Plate reader-based $[Ca^{2+}]_i$ data were corrected for known artifacts as they may severely hamper proper data analysis. Previously, we demonstrated that fluorescence intensity depends heavily on changes in volume and ionic conditions (Heusinkveld and Westerink, 2011). Therefore, upon injection of medium containing test chemical or DMSO, the observed increase in fluorescence (Figs. 1B and 2B, D, F, and H) does not necessarily represent an actual chemical-induced increase in $[Ca^{2+}]_i$. Moreover, the increase in fluorescence appeared as a stepwise increase, which does not resemble a typical increase in $[Ca^{2+}]_i$, which is fast and transient (Berridge et al., 2003; Westerink and Hondebrink, 2010; Heusinkveld and Westerink, 2011). We therefore believe that this stepwise increase in fluorescence does not represent an actual increase in $[Ca^{2+}]_i$ and, if not corrected for (see also Heusinkveld and Westerink, 2011; Kassack et al., 2002), would result in 'false positives'. Noteworthy in this respect, most plate readers are equipped with one or a limited number of injectors. Consequently, concentration-response measurements are usually performed by increasing the injection volume and may represent a volume-response curve rather than a concentration-effect curve.

A potential problem in plate reader-based measurements is dye leakage from the cells (low- Ca^{2+}) to the extracellular space (high- Ca^{2+}). Dye leakage

increases background signals and thereby reduces the signal-to-noise ratio (sensitivity). In plate reader-based experiments dye leakage is visible as a gradual increase in fluorescence over time (Figs. 1B and 2B, D, F, and H). To prevent dye leakage, occasionally probenecid (an organic anion transport blocker) is used. However, probenecid is also known to modulate several neuro(bio)logical and cardiac processes (Robbins et al., 2012) and was shown to interfere with depolarization-evoked increase in $[Ca^{2+}]_i$ (Di Virgilio et al., 1990; Heusinkveld and Westerink, 2011). The use of probenecid is therefore highly unwanted in neurotoxicity testing. In contrast to plate reader-based methods, the sensitivity of the fluorescence microscopy method is not reduced by dye leakage. The fluorescence microscope is equipped with a superfusion system and continuously refreshes the medium during the experiments. This prevents the corruption of the intracellular Ca^{2+} fluorescence by extracellular Ca^{2+} fluorescence that is caused by dye leakage. Notably, the present data were obtained with PC12 cells, which are well-characterized, have abundant expression of different types of VGCCs and are by far the most widely used cell line for *in vitro* neurotoxicity research (Westerink, 2013). However, some cell types may be more prone to dye leakage than others and as a consequence the degree of corruption of the fluorescence signal by dye leakage may vary considerably between cell types.

As described, the test compounds demonstrated different effects on basal $[Ca^{2+}]_i$ in plate reader-based and fluorescence microscopy experiments. In plate reader-based experiments, the net basal ratio for lindane, PCB53 or TBBPA appeared significantly lower than in controls (Fig. 3B). However, high resolution fluorescence microscopy convincingly revealed increases in basal $[Ca^{2+}]_i$ for lindane, PCB53 and TBBPA (Fig. 3A) through either depolarization of the membrane (lindane; Heusinkveld et al., 2010) or release of calcium by the ER and/or mitochondria (PCB53 and TBBPA; Langeveld et al., 2012, Hendriks et al., 2012). Since a reduction in basal $[Ca^{2+}]_i$ is also mechanistically not plausible, it is unlikely that the apparent reduction in basal ratio in plate-reader-based data represents an actual decrease in $[Ca^{2+}]_i$.

In addition to differences between the methods in chemical-induced changes in basal $[Ca^{2+}]_i$, we clearly identified differences in chemical-induced changes in depolarization-evoked $[Ca^{2+}]_i$ (Fig. 4). Comparable to injection of saline, injection of high K^+ -containing saline induced a

stepwise increase in the plate reader-based experiments. However, on top of this stepwise increase a small and transient signal was also visible. This transient signal was previously suggested to represent the actual change in $[Ca^{2+}]_i$ (Heusinkveld and Westerink, 2011). However, upon injection of high K^+ -containing saline in B35 (rat neuroblastoma) cells this transient signal was observed as well (not shown), while these cells lack functional voltage-gated calcium channels and thus cannot respond to depolarization with an increase in $[Ca^{2+}]_i$ (confirmed in fluorescence microscopy; data not shown). It is therefore unlikely that the transient signal on top of the stepwise increase observed upon injection of high K^+ -containing saline in B35 or PC12 cells represents an actual change in $[Ca^{2+}]_i$. Correspondingly, the net increase in ratio upon depolarization calculated for the plate reader-based method could not identify any of the chemicals that are known to (completely) inhibit the depolarization-evoked increase in $[Ca^{2+}]_i$, as shown with high resolution fluorescence microscopy. Hence, it is unlikely that a plate reader method can be used to reliably investigate the depolarization-evoked increase in $[Ca^{2+}]_i$.

In conclusion, we demonstrated that chemical-induced effects on $[Ca^{2+}]_i$ measured with a plate reader-based approach and with fluorescence microscopy differ significantly. The fluorescence microscopy approach provides high temporal resolution, which allows clear identification of differences in $[Ca^{2+}]_i$ kinetics and dynamics and translates to concentration-response relationships. This is in strong contrast with the plate reader method where differences in ratio were small and did not represent an actual chemical-induced change in $[Ca^{2+}]_i$. The plate reader-based method could not be used to identify known (neuro)toxic chemicals, while the fluorescence microscopy method convincingly identified all chemicals as (neuro)toxic. We therefore argue that the plate reader-based approach is not reliable and not sufficiently sensitive to study (and/or prioritize) chemical-induced changes in basal $[Ca^{2+}]_i$ and depolarization-evoked increases in $[Ca^{2+}]_i$ and is not a suitable method for (neuro)toxicity testing.

Acknowledgements

We gratefully acknowledge the European Union (ATHON, Grant Agreement FOOD-CT-2005-022923; ENFIRO, Grant Agreement FP7-ENV-2008-1-226563; ACROPOLIS, Grant Agreement KBBE-245163; DENAMIC, Grant Agreement FP7-ENV-2011-282957) and the faculty of veterinary medicine of Utrecht University for funding and the members of the Neurotoxicology Research Group for helpful discussions.

Conflict of interest statement: The authors declare that there are no conflicts of interest.

$U = \epsilon B$
 $R_1 = 13.5 \Omega$
 $R_2 = 3 \Omega$
 $R_3 = 20 \Omega$
 $F_A = \rho g V$
 $w = D \uparrow$
 $w = 0$
 $w = \frac{y}{BC}$
 $w = 0$
 $w = 0$

$P = \bar{S}$
 $\rho = \frac{h}{\lambda_0} C$
 $w^2 = \frac{mgL}{I}$
 $T = \frac{2\pi}{\omega} = 2\pi \sqrt{\frac{I}{mgL}}$
 $x = \rho \cos \varphi, y = \rho \sin \varphi$
 $\rho = \sqrt{x^2 + y^2}$
 $q = \frac{h}{\lambda_0} \rightarrow ?$
 $\begin{cases} x' = x_0 + mt' \\ y' = y_0 + nt' \\ z' = z_0 + pt' \end{cases}$
 \sin
 $\text{Formula for } s$
 $1) T = \frac{t}{n}$
 $2) v = \frac{c}{n}$
 $3) T = \frac{1}{f}$
 $4) \lambda = \frac{c}{f}$
 $5) v = \frac{2\pi r}{T}$
 $v = \frac{vR}{r}$
 Resistance
 $\frac{dV}{V} = 0$
 $I = \frac{U}{R}$
 $\downarrow \uparrow D = \text{const}$
 $\uparrow \downarrow a = \text{const}$
 $D = \frac{p \cdot l}{S}$
 $S = ?$

Part III

Screening for effects of insecticides on calcium homeostasis



Chapter 6

ACUTE DISTURBANCE OF CALCIUM HOMEOSTASIS IN PC12 CELLS AS A NOVEL MECHANISM OF ACTION FOR (SUB)MICROMOLAR CONCENTRATIONS OF ORGANOPHOSPHATE INSECTICIDES

Marieke Meijer^a, Timo Hamers^b, Remco H.S. Westerink^a

^a Neurotoxicology Research Group, Toxicology Division, Institute for Risk Assessment Sciences (IRAS), Faculty of Veterinary Medicine, Utrecht University, P.O. Box 80.177, NL-3508 TD Utrecht, The Netherlands

^b Institute for Environmental Studies (IVM), VU University Amsterdam, De Boelelaan 1087, NL-1081 HV Amsterdam, The Netherlands.

Published in: *Neurotoxicology*. 2014 43:110-6. doi: 10.1016/j.neuro.2014.01.008.

ABSTRACT

Organophosphates (OPs) and carbamates are widely used insecticides that exert their neurotoxicity via inhibition of acetylcholine esterase (AChE) and subsequent overexcitation. OPs can induce additional neurotoxic effects at concentrations below those for inhibition of AChE, indicating other mechanisms of action are also involved. Since tight regulation of the intracellular calcium concentration ($[Ca^{2+}]_i$) is essential for proper neuronal development and function, effects of one carbamate (carbaryl) and two OPs (chlorpyrifos, parathion-ethyl) as well as their -oxon metabolites on $[Ca^{2+}]_i$ were investigated. Effects of acute (20 min) exposure to (mixtures of) insecticides on basal and depolarization-evoked $[Ca^{2+}]_i$ were measured in fura-2-loaded PC12 cells using single-cell fluorescence microscopy. Acute exposure to chlorpyrifos and its metabolite chlorpyrifos-oxon (10 μ M) induced a modest increase in basal $[Ca^{2+}]_i$. More importantly, the tested OPs concentration-dependently inhibited depolarization-evoked $[Ca^{2+}]_i$. Chlorpyrifos already induced a ~30% inhibition at 0.1 μ M and a 100% inhibition at 10 μ M ($IC_{50} = 0.43 \mu$ M), whereas parathion-ethyl inhibited the depolarization-evoked $[Ca^{2+}]_i$ increase with ~70% at 10 μ M. Interestingly, -oxon metabolites were more potent inhibitors of AChE, but were less potent inhibitors of depolarization-evoked $[Ca^{2+}]_i$ compared with their parent compound (chlorpyrifos-oxon) or were even without effect (paraoxon-ethyl and -methyl). Similarly, acute exposure to carbaryl had no effect on $[Ca^{2+}]_i$. Exposure to mixtures of chlorpyrifos with its oxon-analog or with parathion-ethyl did not increase the degree of inhibition, indicating additivity does not apply. These data demonstrate that concentration-dependent inhibition of depolarization-evoked $[Ca^{2+}]_i$ is a novel mechanism of action of (sub)micromolar concentrations of OPs that could partly underlie OP-induced neurotoxicity.

Keywords: *in vitro* neurotoxicology, organophosphates, carbaryl, pesticide mixture toxicity, single-cell fluorescent calcium imaging, voltage-gated calcium channels.

6.1 INTRODUCTION

Organophosphates (OPs) and carbamates are insecticides used worldwide in agriculture and households. These compounds are well-known neurotoxicants that exert their adverse effect via inhibition of acetylcholine esterase (AChE), thereby inhibiting the breakdown of the neurotransmitter acetylcholine (ACh), resulting in a potentially lethal overstimulation of neurotransmission. Though the inhibition of AChE by carbamates is reversible, OPs induce an irreversible inhibition of AChE (Eaton et al., 2008; Moser et al., 2010). Moreover, some OPs inhibit neuropathy target esterase (NTE; Eaton et al., 2008), which may be responsible for some of the observed neurotoxic effects following chronic OP exposure.

Though OPs are primarily known as AChE inhibitors, animal studies demonstrated neurobehavioral effects of OPs at exposure levels that do not induce AChE inhibition (Carr et al., 2001; Dam et al., 2000; Qiao et al., 2003; Ricceri et al., 2006; Timofeeva et al., 2008), suggesting the involvement of additional mechanisms. Accordingly, *in vitro* studies demonstrated numerous effects of OPs like chlorpyrifos and parathion, including effects on neurite outgrowth (Das and Barone, 1999; Howard et al., 2005), tyrosine hydroxylase and choline acetyltransferase (Jameson et al., 2006; Monnet-Tschudi et al., 2000), muscarinic and nicotinic acetylcholine receptors (Betancourt and Carr, 2004; Guo-Ross et al., 2007; Liu et al., 2002; Slotkin et al., 2004; Smulders et al., 2004), adenylyl cyclase (Adigun et al., 2010a), DNA synthesis (Slotkin et al., 2007b), gene expression and dopamine homeostasis (Aldridge et al., 2005; Chen et al., 2011; Eells and Brown, 2009). However, most of these effects were observed at relatively high levels (~1 – 100 μ M) of thiophosphoryl OPs, i.e. parent OPs, whereas the phosphoryl OP metabolites chlorpyrifos-oxon and paraoxon were demonstrated to be 10 – 1000 times more potent in several *in vitro* assays (review by Flaskos, 2012). In contrast to OPs, carbamate insecticides do not require bioactivation and are less extensively tested *in vitro* for neurotoxic effects. Nevertheless, carbamates were also shown to affect several *in vitro* readouts, including inhibition of neurite outgrowth, cell replication (Chang et al., 2006), nicotinic acetylcholine receptor function (Smulders et al., 2003), and choline acetyltransferase (Jameson et al., 2006) at concentrations of ~2 – 100 μ M.

Although OPs and carbamates are relatively well studied, to date effects of OP and carbamate insecticides on the regulation of the intracellular calcium concentration ($[Ca^{2+}]_i$) have hardly been investigated. This is surprising considering that several of the above-mentioned endpoints, including, e.g., neurite outgrowth and gene expression, can be modulated by changes in $[Ca^{2+}]_i$ and that calcium homeostasis is essential for proper neuronal development (Leclerc et al., 2011) and function (Westerink, 2006). Notably, it has previously been shown that even small changes in $[Ca^{2+}]_i$ can already result in deleterious effects (Toescu and Verkhatsky, 2007). Neuronal cells therefore try to tightly regulate $[Ca^{2+}]_i$ by calcium binding proteins, calcium storage in mitochondria and endoplasmic reticulum (ER), and by controlling influx of extracellular calcium via voltage-gated calcium channels (VGCCs) and calcium-permeable neurotransmitter receptors (Westerink, 2006). Nevertheless, several neurotoxic chemicals (organochlorine insecticides, azole fungicides, PCBs and brominated flame retardants) have been shown to disturb basal $[Ca^{2+}]_i$ and/or inhibit the depolarization-evoked increase in $[Ca^{2+}]_i$ (Dingemans et al., 2010; Heusinkveld and Westerink, 2012; Heusinkveld et al., 2013; Langeveld et al., 2012; Westerink, 2014), indicating that regulation of $[Ca^{2+}]_i$ is an important target for many neurotoxicants and could also be involved in OP- and carbamate-induced neurotoxicity.

In the present study, we therefore investigated if (sub)micromolar concentrations of one carbamate (carbaryl) and two OPs (chlorpyrifos, parathion-ethyl) and their -oxon metabolites (chlorpyrifos-oxon, paraoxon-ethyl and paraoxon-methyl (which is a metabolite of parathion-methyl)) could disturb basal and depolarization-evoked $[Ca^{2+}]_i$. Measurements of effects of these insecticides on $[Ca^{2+}]_i$ were performed using rat PC12 cells, which are well-characterized and suitable for mechanistic neurotoxicological and neurophysiological studies (Westerink and Ewing, 2008) and express L-, N-, and P/Q-type VGCCs (Dingemans et al., 2009). Since human exposure is generally to a variety of insecticides, mixtures of OPs and carbaryl were investigated as well. Our data demonstrate that acute disturbance of depolarization-evoked $[Ca^{2+}]_i$ is a novel mechanism of action of OPs that, considering the lowest observed effect concentrations (LOEC), deserves additional attention with respect to human risk assessment.

6.2 MATERIALS AND METHODS

6.2.1 Chemicals

Fura-2 AM was obtained from Molecular Probes (Invitrogen, Breda, The Netherlands). Chlorpyrifos-oxon (purity 93.5%) was obtained from AccuStandard (New Haven, USA). Chlorpyrifos, parathion-ethyl, paraoxon-ethyl and -methyl, carbaryl (purity 99.9%, 98.8%, 97.6%, 96.0%, 99.5%, respectively) and all other chemicals were obtained from Sigma-Aldrich (Zwijndrecht, The Netherlands) unless otherwise noted. Saline solutions were prepared with deionized water (Milli-Q®; resistivity > 10 MΩ cm). Stock solutions were prepared in DMSO and test solutions (solvent concentration ≤ 0.1% DMSO) were prepared just prior to the experiments.

6.2.2 AChE measurements

Inhibition of acetylcholine esterase (AChE) activity was assessed as a decreased hydrolysis of the specific AChE substrate S-acetylthiocholine (ATC) into the products acetate and thiocholine in a down-scaled version of the original assay described by Ellman et al. (1961). Formation of thiocholine was colorimetrically determined using 5,5'-dithiobis-(2-nitrobenzoic acid) (DTNB) that reacts with the free thiol group of thiocholine. Insecticides (up to 50 μM) or 0.05% DMSO (vehicle control) were incubated with 125 mU AChE from electric eel in 2 mL phosphate buffer (0.1 M KH_2PO_4/K_2HPO_4 ; pH = 7.5) for 30 min. After incubation, 50 μL of the mixture was added to 100 μL of reaction buffer containing 0.4 mM ATC and 2.5 mM of DTNB in quadruplicate measurements per incubation. After homogenization, a spectrophotometric kinetic measurement was performed at 412 nm for 5 min on a Spectramax 340 PC platereader (Molecular Devices, USA).

6.2.3 Cell culture

Rat pheochromocytoma (PC12) cells (Greene and Tischler, 1976) were cultured for 10 passages in RPMI1640 (Invitrogen, Breda, The Netherlands) supplemented with 10% horse serum, 5% fetal bovine serum and 2% penicillin/streptomycin (ICN Biomedicals, Zoetermeer, The Netherlands) as described previously (Dingemans et al., 2010; Heusinkveld and Westerink, 2012; Langeveld et al., 2012). All culture-ware was coated with poly-L-lysine (PLL, 50 μg/mL). Cells were grown in a humidified incubator at 37 °C and 5% CO_2 . Medium was refreshed every 2-3 days. For single-cell fluorescent microscopy Ca^{2+} imaging experiments, undifferentiated PC12 cells were

subcultured in glass-bottom dishes (1.4×10^6 cells/dish; ~75% confluency; MatTek, Ashland, MA) as described previously (Dingemans et al., 2010; Heusinkveld and Westerink, 2012; Langeveld et al., 2012).

6.2.4 $[Ca^{2+}]_i$ measurements

Changes in $[Ca^{2+}]_i$ were measured using the Ca^{2+} sensitive fluorescent ratio dye Fura-2 AM as described previously (Dingemans et al., 2010; Heusinkveld and Westerink, 2012; Langeveld et al., 2012). Briefly, PC12 cells were loaded with 5 μM Fura-2 AM for 20 min in saline (containing in mM: 2 $CaCl_2$, 24 glucose, 10 HEPES, 5.5 KCl, 0.8 $MgCl_2$, 125 NaCl, and 36.5 sucrose at pH 7.3, adjusted with NaOH), followed by 15 min de-esterification of the dye in saline at room temperature. Then, cells were placed on the stage of an Axiovert 35M inverted microscope (40x oil-immersion objective, NA 1.0; Zeiss, Göttingen, Germany) equipped with a TILL Photonics Polychrome IV (Xenon Short Arc lamp, 150W; TILL Photonics GmbH, Gräfelfing, Germany). Cells were continuously superfused with saline using a Valvelink 8.2 (Automate Scientific, CA, USA) and fluorescence, excited by 340 and 380 nm wavelengths (F_{340} and F_{380}), was collected every 3 s at 510 nm with an Image SensiCam digital camera (TILL Photonics GmbH, Gräfelfing, Germany). All experiments were performed at room temperature. Every experiment consisted of a 5 min baseline recording and a subsequent depolarization of the cells by changing superfusion to 100 mM K^+ -containing saline for 21 s (to establish the viability and functionality of the cells and to serve as an internal control). Then, cells were allowed to recover for 8 min before superfusion was changed to saline containing 0.1% DMSO (vehicle control) or insecticides (0.1 – 10 μM) for 20 min. Following this 20 min exposure, cells were depolarized for a second time with K^+ -containing saline in the presence of the test substance (see Fig. 1A for example recording) to derive a treatment ratio (see below) to determine pesticide-induced effects on depolarization-evoked increases in $[Ca^{2+}]_i$. For specific experiments, the exposure duration was increased to 40 min. At the end of each recording, cells were exposed to 5 μM ionomycin and to 17 mM ethylenediamine tetraacetic acid (EDTA) to determine maximum and minimum ratios (R_{max} and R_{min}) to calculate calcium levels.

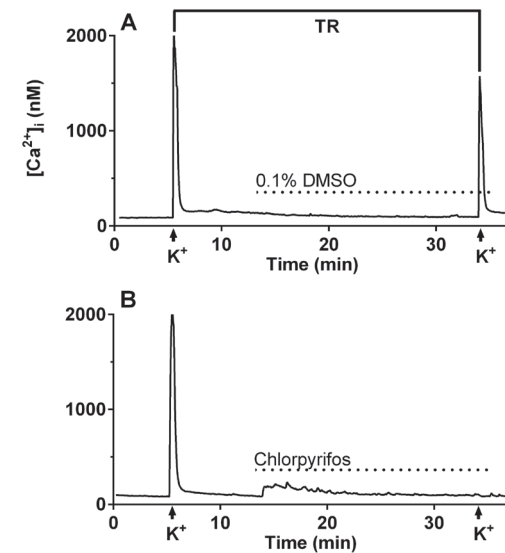


Figure 1: Representative examples of recordings of $[Ca^{2+}]_i$ from individual PC12 cells exposed to DMSO (A) or 10 μM chlorpyrifos (B). PC12 cells were exposed to saline containing test substance for 20 min (indicated by the dotted line) in between two depolarizations evoked by high K^+ -containing saline before and after exposure (indicated by the arrows). The treatment ratio (TR; 2^{nd} depolarization/ 1^{st} depolarization*100%) is used to investigate effects of insecticides on the depolarization-evoked increase in $[Ca^{2+}]_i$.

6.2.5 Data analysis and statistics

Logistic concentration-response curves with Hill slope were fitted for those insecticides showing >20% inhibition of AChE activity response at the highest test concentration using GraphPad Prism software (v6, GraphPad Software, La Jolla California, USA). Data are expressed as mean \pm SD.

Calcium-imaging data were processed with TILLVISION software (version 4.01) and further analyzed using a custom-made MS-Excel macro that calculates background-corrected F_{340}/F_{380} ratio values. Free cytosolic $[Ca^{2+}]_i$ was calculated as described previously (Dingemans et al., 2010; Heusinkveld and Westerink, 2012; Langeveld et al., 2012) using a modified Grynkiewicz's equation $[Ca^{2+}]_i = K_{d^*} \times (R - R_{min}) / (R_{max} - R)$, where K_{d^*} is the dissociation constant of Fura-2 determined in the experimental setup.

Insecticide-induced effects on basal $[Ca^{2+}]_i$ were expressed as the average increase in $[Ca^{2+}]_i$ during the first 5 min of exposure of responding cells. Only cells that displayed an increase in $[Ca^{2+}]_i$ during exposure \geq basal + SD were regarded as responding cells and were selected for quantification of basal $[Ca^{2+}]_i$ effects.

A separate analysis was performed to quantify effects on the VGCCs. Effects on the depolarization-evoked increase in $[Ca^{2+}]_i$ were expressed as a net treatment ratio (net TR: 2nd depolarization/1st depolarization*100%) as described previously (Heusinkveld and Westerink, 2012; Langeveld et al., 2012; see Fig. 1A for illustration). Data are expressed as mean \pm SEM, normalized to the control, unless otherwise noted. Cells that show effects larger than two times SD above or below average were considered to be outliers and were therefore excluded for further analysis (~15%). Per test condition at least 3 independent experiments (N) were performed to obtain at least 30 cells (n) after outlier exclusion. Concentration-response curves were fitted using GraphPad Prism software (v6, GraphPad Software, La Jolla California, USA). Data were compared with an unpaired t-test. As the SD for TR in control cells amounted to 30%, effects (at 10 μ M) were considered relevant for further concentration-response testing only if significant ($p < 0.05$) and $\geq 30\%$.

6.3 RESULTS

6.3.1 Effects of insecticides on AChE activity

Since undifferentiated PC12 cells have low basal AChE activity (Das and Barone, 1999) and to prevent confounding by other potentially present choline esterases, inhibition of AChE was assessed using purified AChE from electric eel. Chlorpyrifos did not inhibit AChE at concentrations up to 50 μ M, whereas parathion-ethyl was a weak inhibitor of AChE, yielding 50% inhibition at 27 ± 3 μ M (Table 1). In contrast, the oxon-metabolites were potent inhibitors of AChE. Chlorpyrifos-oxon caused a 50% inhibition of AChE already at 0.0093 ± 0.0014 μ M, whereas the IC_{50} values for paraoxon-ethyl and paraoxon-methyl amounted to 0.0750 ± 0.0012 μ M and 0.1830 ± 0.0064 μ M, respectively (Table 1). The carbamate insecticide carbaryl also inhibited AChE activity, with an IC_{50} of 0.99 ± 0.50 μ M (Table 1).

Table 1: IC_{50} of insecticides for inhibition of purified electric eel AChE activity, and for inhibition of depolarization-evoked increases in $[Ca^{2+}]_i$ via VGCCs in PC12 cells.

Insecticide	AChE inhibition (IC_{50} in μ M; \pm SD; n = 4, N = 2)	VGCC inhibition (IC_{50} in μ M)
chlorpyrifos	> 50	0.431 (n = 31 - 197, N = 4 - 22)
parathion	27 ± 3.0	4.13 (n = 37 - 197, N = 4 - 22)
chlorpyrifos-oxon	0.009 ± 0.0014	> 10
paraoxon-ethyl	0.075 ± 0.0012	> 10
paraoxon-methyl	0.183 ± 0.0064	> 10
carbaryl	0.990 ± 0.5000	> 10

6.3.2 Effects of insecticides on basal $[Ca^{2+}]_i$

Basal $[Ca^{2+}]_i$ in resting PC12 cells was low and stable (100 ± 1 nM; n = 197, N = 22). Upon depolarization with high K^+ -containing saline, $[Ca^{2+}]_i$ increased rapidly and transiently to 2.0 ± 0.05 μ M as a consequence of opening of VGCCs. During a subsequent 8 min recovery period, $[Ca^{2+}]_i$ returned to near resting values and was unaffected by 20 min exposure to DMSO-containing saline (Fig. 1A). When cells were exposed to saline containing 10 μ M chlorpyrifos, an immediate but small increase in $[Ca^{2+}]_i$ was observed in 42% (17 of 38 cells) of the cells (responding cells), which sustained for ~5 min and amounted to 52 ± 9 nM (n = 17, N = 5). After ~5 min, $[Ca^{2+}]_i$ returned again to near resting values for the remaining ~15 min exposure (Fig. 1B). Chlorpyrifos-oxon at 10 μ M induced a comparable transient increase in $[Ca^{2+}]_i$ in 18% (7 of 39 cells) of the cells (58 ± 7 nM, n = 7, N = 6). The increase in basal $[Ca^{2+}]_i$ was still present when cells were exposed to 10 μ M chlorpyrifos in Ca^{2+} -free medium, though the increase was less pronounced (33 ± 13 nM, n = 10 out of 34 cells, N = 3), indicating that the increase in basal $[Ca^{2+}]_i$ originates at least partly from intracellular stores. At concentrations < 10 μ M, neither chlorpyrifos nor chlorpyrifos-oxon were able to disturb basal $[Ca^{2+}]_i$ (data not shown). Moreover, at 10 μ M, the increase in basal $[Ca^{2+}]_i$ appeared specific for chlorpyrifos and chlorpyrifos-oxon as parathion-ethyl, its metabolite paraoxon-ethyl, paraoxon-methyl, and carbaryl were unable to affect basal $[Ca^{2+}]_i$ (data not shown).

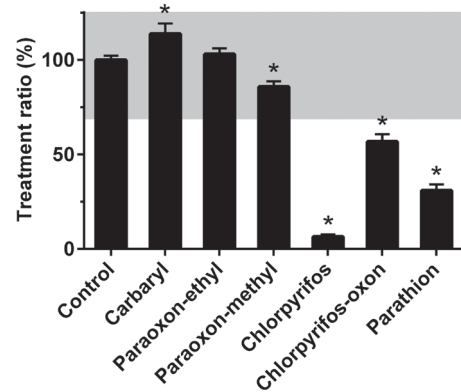


Figure 2: Summary graph of effects of several OP insecticides and carbaryl at 10 μM on the depolarization-evoked increase in $[\text{Ca}^{2+}]_i$. The shaded area indicates effects $\leq 30\%$, which were considered less relevant for further experimentation. At 10 μM , the carbamate carbaryl and both metabolites of parathion were not able to inhibit the depolarization-evoked increase in $[\text{Ca}^{2+}]_i$, whereas parathion-ethyl, chlorpyrifos and chlorpyrifos-oxon effectively inhibited the depolarization-evoked $[\text{Ca}^{2+}]_i$. Data represent mean \pm SEM ($n = 38\text{-}54$, $N = 4\text{-}6$). * indicates a significant difference compared with control ($p < 0.05$).

6.3.3 Effects of insecticides on depolarization-evoked increase in $[\text{Ca}^{2+}]_i$

Following 20 min of exposure to saline containing 0.1% DMSO (control) or insecticides, cells were depolarized for a second time with high K^+ -containing saline with 0.1% DMSO or insecticides to investigate insecticide-induced effects on the depolarization-evoked increase in $[\text{Ca}^{2+}]_i$. Because an increase in basal $[\text{Ca}^{2+}]_i$ prior to the second depolarization could influence the amplitude of the depolarization-evoked $[\text{Ca}^{2+}]_i$, a net TR was calculated (see section 6.2). In control cells, the second depolarization-evoked increase in $[\text{Ca}^{2+}]_i$ amounted to $1.5 \pm 0.04 \mu\text{M}$ ($n = 197$, $N = 22$), yielding a net TR of 72% (Fig. 1A). The net TR of control cells was set at 100% and all data were (statistically) compared with the normalized control.

Exposure to carbaryl, paraoxon-ethyl or paraoxon-methyl (all at 10 μM) did not inhibit the depolarization-evoked calcium increase in $[\text{Ca}^{2+}]_i$ compared with control cells (Fig. 2, Table 1). In contrast, exposure to

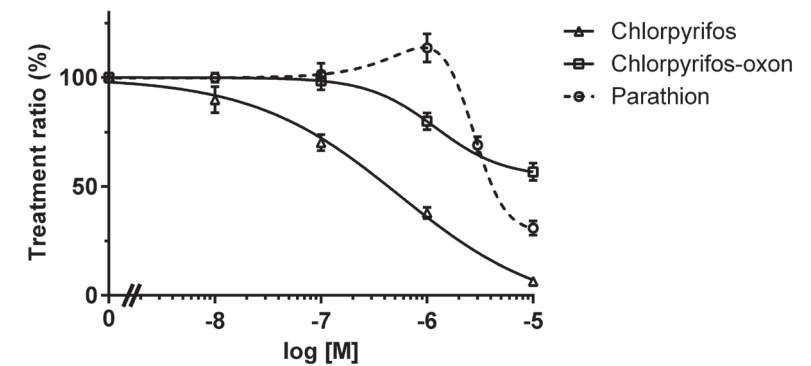


Figure 3: Concentration-response curves of the inhibition of the net TR by the OP insecticides chlorpyrifos, chlorpyrifos-oxon and parathion-ethyl. All tested OPs concentration-dependently inhibited the depolarization-evoked increase in $[\text{Ca}^{2+}]_i$, with chlorpyrifos being most potent. Data represents mean \pm SEM ($n = 31\text{-}50$, $N = 4\text{-}6$). Chlorpyrifos-oxon was significantly different from control ($p < 0.05$) at $\geq 1 \mu\text{M}$ and parathion-ethyl from $\geq 3 \mu\text{M}$, whereas chlorpyrifos was significantly different from control ($p < 0.05$) already at $\geq 0.1 \mu\text{M}$.

chlorpyrifos, chlorpyrifos-oxon or parathion-ethyl (all at 10 μM) significantly reduced the depolarization-evoked $[\text{Ca}^{2+}]_i$ increase by more than 30% (Fig. 2). Effects of these insecticides on the depolarization-evoked increase in $[\text{Ca}^{2+}]_i$ were therefore investigated in more detail.

Cells exposed to chlorpyrifos for 20 min displayed a concentration-dependent inhibition of the net TR, which decreased from $70 \pm 4\%$ ($n = 41$, $N = 4$) at 0.1 μM to $6 \pm 1\%$ ($n = 38$, $N = 5$) at 10 μM (Fig. 3, Table 1, $\text{IC}_{50} = 0.43 \mu\text{M}$). Chlorpyrifos-oxon, the active metabolite of chlorpyrifos, also induced a concentration-dependent inhibition of the TR, but was less potent than chlorpyrifos with a TR of $80 \pm 4\%$ ($n = 32$, $N = 4$) at 1 μM and $57 \pm 4\%$ ($n = 39$, $N = 6$) at 10 μM (Fig. 3, Table 1, $\text{IC}_{50} > 10 \mu\text{M}$). Finally, a concentration-dependent decrease in TR was also observed for parathion-ethyl. At 3 μM , parathion-ethyl reduced the TR to $69 \pm 4\%$ ($n = 50$, $N = 5$) and the TR was further inhibited to $31 \pm 3\%$ at 10 μM ($n = 37$, $N = 4$; Fig. 3, Table 1, $\text{IC}_{50} = 4.13 \mu\text{M}$).

6.3.4 Reversibility of OP effects on the depolarization-evoked increase in $[Ca^{2+}]_i$

To investigate reversibility of the inhibitory effects on the TR, the 20 min of insecticide exposure was followed by a 20 min wash with saline prior to the second depolarization in a separate set of experiments. Following 20 min wash, the net TR of parathion-ethyl exposed cells (10 μ M) was not significantly decreased compared with control cells exposed for 40 min to saline ($93 \pm 6\%$, $n = 39$; $N = 4$), indicating that the inhibitory effects of parathion-ethyl are fully reversible (Fig. 4). In cells exposed to chlorpyrifos (1 μ M) for 20 min, the TR was still significantly decreased ($82 \pm 5\%$, $n = 45$, $N = 4$) following 20 min wash compared with control cells, though higher than in cells first exposed to saline for 20 min and then to chlorpyrifos (1 μ M) for 20 min ($38 \pm 3\%$, $n = 37$, $N = 4$; Fig. 4), suggesting that cells recover slowly from the inhibitory effects of chlorpyrifos.

6.3.5 Effects of mixtures of insecticides on basal and depolarization-evoked increase in $[Ca^{2+}]_i$

Since human exposure is generally to a mixture of insecticides, chlorpyrifos, chlorpyrifos-oxon, parathion-ethyl and carbaryl were selected for further experiments using binary mixtures. One mixture was constituted based on the LOEC of chlorpyrifos (0.1 μ M) and parathion-ethyl (3 μ M). Comparable with the single compounds, no effects of the binary mixtures were found on basal $[Ca^{2+}]_i$ during 20 min exposure (data not shown). Following 20 min exposure to this binary mixture, the TR amounted to $65 \pm 4\%$ ($n = 42$, $N = 6$), which was not significantly different from the inhibition induced by the individual compounds at these concentrations (Fig. 5A). A second binary LOEC mixture of chlorpyrifos (0.1 μ M) and its metabolite chlorpyrifos-oxon (1 μ M) did not induce a significant inhibition in TR ($94 \pm 3\%$, $n = 42$, $N = 5$) compared with control cells, whereas the individual compounds both induced $\sim 25\%$ inhibition (Fig. 5B). Although carbaryl itself did not inhibit the TR, it may interact with other chemicals by antagonizing or potentiating their effects. Therefore, a mixture of chlorpyrifos (0.1 μ M; LOEC) and carbaryl (10 μ M; no observed effect level (NOEC)) was constituted. Following 20 min exposure to this mixture, the TR reached $91 \pm 4\%$ ($n = 40$, $N = 4$), which was significantly different from the inhibition induced by 0.1 μ M chlorpyrifos and 10 μ M carbaryl individually (Fig. 5C), but not compared with the control TR.

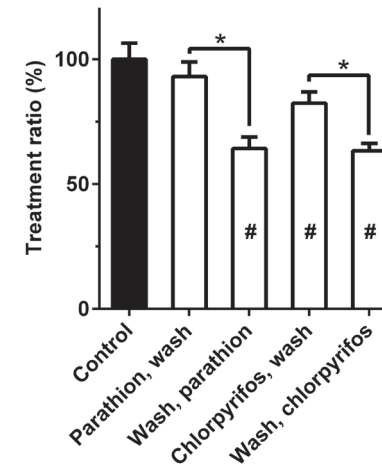


Figure 4: Reversibility of the inhibitory effects of OPs on the depolarization-evoked $[Ca^{2+}]_i$. Parathion-ethyl (10 μ M) no longer inhibited the net TR after a 20 min wash with saline demonstrating effects are reversible. After 20 min wash with saline, chlorpyrifos (1 μ M) slightly but significantly, decreased the TR indicating that the inhibitory effect of chlorpyrifos on the TR are only slowly reversible. Data represent mean \pm SEM. * indicates a significant difference compared with its corresponding washout and # a significant difference compared with control ($p < 0.05$).

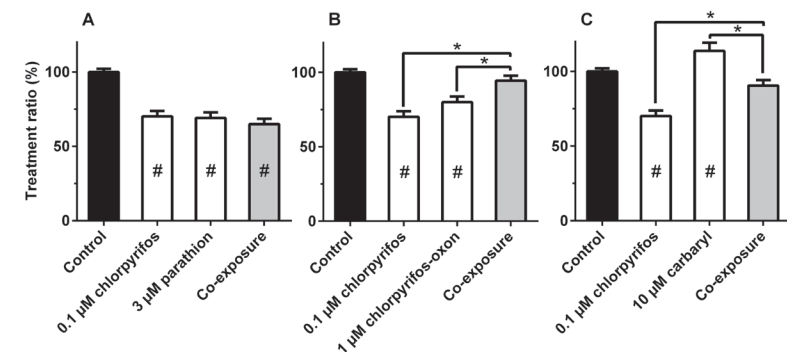


Figure 5: Effects of insecticide mixtures on the depolarization-evoked increase in $[Ca^{2+}]_i$. The LOEC mixture of chlorpyrifos (0.1 μ M) and parathion-ethyl (3 μ M) did not increase the degree of inhibition (A). The LOEC mixture of chlorpyrifos (0.1 μ M) and chlorpyrifos-oxon (1 μ M) attenuated the degree of inhibition and did not induce a significant decrease compared with control (B). The inhibitory effect of chlorpyrifos (0.1 μ M) was reduced by carbaryl (10 μ M) resulting in effects comparable with the control (C). Data represent mean \pm SEM. * indicates a significant difference compared with individual insecticides and # a significant difference compared with the control ($p < 0.05$).

6.4 DISCUSSION

The current data demonstrate that (sub)micromolar concentrations of OPs concentration-dependently inhibit the depolarization-evoked increase in $[Ca^{2+}]_i$ (Figs. 1-3). Since this inhibition is (near) complete at 10 μ M it appears due to non-specific inhibition of VGCCs, including L-, N-, and P/Q-type VGCCs that are expressed in PC12 cells. Moreover, the inhibition of depolarization-evoked Ca^{2+} -influx is at least partly reversible within 20 min (Fig. 4). At high concentrations (10 μ M), chlorpyrifos and chlorpyrifos-oxon also induced an increase in basal $[Ca^{2+}]_i$ (Fig. 1), which appears mediated by intracellular calcium stores as it is still partially present in Ca^{2+} -free saline.

In this respect it is noteworthy that calcium homeostasis is essential for proper neuronal function and development and it is well known that small changes in $[Ca^{2+}]_i$ can already result in adverse effects (Toescu and Verkhratsky, 2007). Moreover, OPs reportedly target, e.g., neurite outgrowth and differentiation, which are calcium-dependent processes (Leclerc et al., 2011), indicating calcium homeostasis could be an important target for OP-induced neurotoxicity.

Importantly, the OP-induced inhibition of depolarization-evoked Ca^{2+} -influx is not only a novel mechanism of action, but could be of particular relevance for OP-induced neurotoxicity as it occurs acutely and - for thiophosphoryl OPs, i.e. parent OPs - at levels below those for AChE inhibition (Table 1) and other cellular and molecular targets (also see section 6.1). For the oxon-metabolites and carbaryl on the other hand, inhibition of AChE appears the predominant mode of action. Notably in this respect, inhibition in PC12 cells of 'total ChE', consisting primarily of AChE and a small fraction of butyrylcholinesterase, yielded $\sim IC_{50}$ s for chlorpyrifos and chlorpyrifos-oxon amounting to $\sim 25 \mu$ M and ~ 1 nM, respectively (Das and Barone, 1999). These values are in line with the IC_{50} s values reported in section 6.3.1 for purified electric eel AChE (Table 1).

The inhibition of depolarization-evoked Ca^{2+} -influx may be specific for OPs as the tested carbamate insecticide (carbaryl) did not inhibit depolarization-evoked $[Ca^{2+}]_i$ at 10 μ M (Figs. 2 and 3). However, at this concentration carbaryl did slightly increase the treatment ratio compared with the control, suggesting carbaryl may increase opening of VGCCs or affect the recovery from the first depolarization. Interestingly, parent OPs

are more potent in inhibiting VGCCs compared with their -oxon metabolites (Figs. 2 and 3, Table 1). For OPs, metabolism usually results in bioactivation (oxon-metabolites are more potent inhibitors of, e.g., AChE; Table 1), though for the inhibition of VGCCs metabolism actually results in (partial) bioinactivation/detoxification (Table 1). This is an important finding for human risk assessment as young animals/humans have a lower rate of OP metabolism (Eaton et al., 2008). As a result, the parent compounds may persist longer in young animals/humans and thus play a more prominent role in their exposure pattern, suggesting that exposure to parent compounds could play a role in OP-induced developmental neurotoxicity. Therefore, mechanisms of action of OP parent compounds are important to investigate at low concentrations as they could (partly) explain the higher sensitivity of young animals to OPs. Additionally, toddlers were estimated to have the highest daily intake per kg bw of chlorpyrifos compared with infants and adults (Eaton et al., 2008), further increasing their risk for OP-induced (developmental) neurotoxicity. Accordingly, human studies found some adverse neurodevelopmental health effects, such as a decrease in working memory and IQ, following OP exposure (Barr et al., 2010; Eskenazi et al., 2004; Rauh et al., 2011), stressing the need for more sensitive screening methods for human risk assessment.

As human exposure is generally to a mixture of compounds rather than to individual insecticides, effects of different binary mixtures on calcium homeostasis were tested. The most potent OP in this study, chlorpyrifos, was combined at its LOEC with either its oxon-metabolite (chlorpyrifos-oxon), with parathion-ethyl, or with the carbamate carbaryl. The results indicate different interactions between these insecticides with respect to inhibition of the depolarization-evoked increase in $[Ca^{2+}]_i$ (Fig. 5). While the effects of a binary mixture of chlorpyrifos with carbaryl could be interpreted as being additive, the effects of the other two binary mixtures indicate that additivity does not apply for binary mixtures consisting of chlorpyrifos and parathion-ethyl or chlorpyrifos and chlorpyrifos-oxon. These non-additive effects were somewhat surprising as it has previously been shown in PC12 cells that mixtures of organochlorine insecticides (lindane and dieldrin; Heusinkveld and Westerink, 2012) as well as mixtures of azole fungicides (Heusinkveld et al., 2013) exert additive inhibition of VGCCs. Since the binary mixtures consisting of chlorpyrifos and parathion-ethyl or

chlorpyrifos and chlorpyrifos-oxon indicate a non-additive interaction, it is possible that competition of OPs for the different VGCCs limits the effect of the binary mixture, though this is rather unlikely considering that near IC_{20} concentrations were used. Another possibility is that the chemicals interact with each other reducing the free concentration of the active chemical that interacts with VGCCs. Though the nature of the mixture effects remains to be determined, comparable non-additive mixture effects of OPs have been found previously for *in vitro* AChE inhibition in human SH-SY5Y cells (Marinovich et al., 1996).

To conclude, the present results demonstrate that the inhibition of depolarization-evoked Ca^{2+} -influx via VGCCs is a novel mechanism of action for OP insecticides that could (partly) underlie OP-induced neurotoxicity. It appears that inhibition of VGCCs is an important common endpoint for several types of pesticides including OPs (this study), organochlorines (Heusinkveld and Westerink, 2012) and azole fungicides (Heusinkveld et al., 2013) as well as several chlorinated- and brominated persistent pollutants (Westerink, 2014). As such, this endpoint deserves additional attention with respect to human risk assessment, in particular since human exposure is generally chronic, low-dose and to mixtures.

Acknowledgements

We gratefully acknowledge the neurotoxicology research group and Dr. P.E.G. Leonards (Institute for Environmental Studies (IVM), VU University Amsterdam) for helpful discussions.

Funding

This work was supported by the European commission [DENAMIC project; grant number FP7-ENV-2011-282957] and the Faculty of Veterinary Medicine of Utrecht University.

Conflict of interest statement: The authors declare that there are no conflicts of interest.

Chapter 7

INHIBITION OF VOLTAGE-GATED CALCIUM CHANNELS AS COMMON MODE OF ACTION FOR (MIXTURES OF) DISTINCT CLASSES OF INSECTICIDES

Marieke Meijer, Milou M.L. Dingemans, Martin van den Berg and Remco H.S. Westerink

Neurotoxicology Research Group, Toxicology Division, Institute for Risk Assessment Sciences (IRAS), Faculty of Veterinary Medicine, Utrecht University, P.O. Box 80.177, NL-3508 TD Utrecht, The Netherlands.

**Published in: Toxicological Sciences 2014 141(1):103-11.
doi: 10.1093/toxsci/kfu110**

ABSTRACT

Humans are exposed to distinct structural classes of insecticides with different neurotoxic modes of action. Because calcium homeostasis is essential for proper neuronal function and development, we investigated the effects of insecticides from different classes (pyrethroid: α -cypermethrin; organophosphate: chlorpyrifos; organochlorine: endosulfan; neonicotinoid: imidacloprid) and mixtures thereof on the intracellular calcium concentration ($[Ca^{2+}]_i$). Effects of acute (20 min) exposure to (mixtures of) insecticides on basal and depolarization-evoked $[Ca^{2+}]_i$ were studied *in vitro* with Fura-2-loaded PC12 cells and high resolution single-cell fluorescence microscopy. The data demonstrate that cypermethrin, α -cypermethrin, endosulfan, and chlorpyrifos concentration-dependently decreased depolarization-evoked $[Ca^{2+}]_i$ with 50% (IC_{50}) at 78 nM, 239 nM, 250 nM and 899 nM, respectively. Additionally, acute exposure to chlorpyrifos or endosulfan (10 μ M) induced a modest increase in basal $[Ca^{2+}]_i$, amounting to 68 ± 8 nM and 53 ± 8 nM, respectively. Imidacloprid did not disturb basal or depolarization-evoked $[Ca^{2+}]_i$ at 10 μ M. Following exposure to binary mixtures, effects on depolarization-evoked $[Ca^{2+}]_i$ were within the expected effect additivity range, whereas the effect of the tertiary mixture was less than this expected additivity effect range.

These results demonstrate that different types of insecticides inhibit depolarization-evoked $[Ca^{2+}]_i$ in PC12 cells by inhibiting voltage-gated calcium channels (VGCCs) *in vitro* at concentrations comparable with human occupational exposure levels. Moreover, the effective concentrations in this study are below those for earlier described modes of action. Because inhibition of VGCCs appears to be a common and potentially additive mode of action of several classes of insecticides, this target should be considered in neurotoxicity risk assessment studies.

Keywords: *in vitro* neurotoxicity, mixture toxicity, calcium homeostasis, voltage-gated calcium channels, PC12 cells, insecticides.

7.1 INTRODUCTION

Insecticides are potent neurotoxicants, which are used in agriculture and households worldwide. In many cases, their neurotoxic mode of action is not species-specific, and the widespread use of these chemicals may thus pose a risk to human health (Mackenzie Ross et al., 2013). There are many types of insecticides, commonly classified according to their structure and mode of action.

Pyrethroids induce neuronal overexcitation by delaying the inactivation of voltage-gated sodium channels (VGSCs; Soderlund, 2012). They are rapidly metabolized in humans (e.g. Leng et al., 2006) and mammals (Wolansky and Harrill, 2008). Nevertheless, acute oral exposure to cypermethrin (and other pyrethroids) can affect behavior in mice and rats (Wolansky and Harrill, 2008) and was shown *in vitro* to have several targets, including VGSCs (Meacham et al., 2008), potassium channels (Yu-Tao et al., 2009) and ATPase (Kakko et al., 2004). Moreover, cypermethrin residues are detected in food at concentrations that exceed the maximum residue level (MRL; EFSA, 2013).

Organophosphates (OPs) are known as potent, irreversible inhibitors of acetylcholinesterase (AChE). Nonetheless, chlorpyrifos, an extensively studied OP, was demonstrated to have several additional effects *in vivo* at concentrations below those required for AChE inhibition (reviewed in Eaton et al., 2008). Moreover, chlorpyrifos induces several adverse effects in neural cells *in vitro*, such as inhibition of neurite outgrowth (reviewed in Eaton et al., 2008) and inhibition of voltage-gated calcium channels (VGCCs; Meijer et al., 2014b). Chlorpyrifos is widely used and frequently exceeds the MRL (EFSA, 2013).

Organochlorine insecticides are divided into two main groups; DDT-type insecticides that are known to target VGSCs, and chlorinated alicyclic insecticides such as endosulfan that target GABA and glycine receptors (Coats, 1990). Endosulfan can still be found in human tissues as it is poorly metabolized and highly persistent in the environment (Mrema et al., 2013). Chronic and acute exposure to endosulfan can affect behavior in adult rats (Castillo et al., 2002; Silva and Beauvais, 2010). Additionally, *in vitro* research demonstrated that endosulfan exposure affects a number of neurotoxicological targets and endpoints, such as caspase-3, NF κ B, formation of reactive oxygen species as well as GABA $_A$ and glycine-gated chlorine channels (Jia and Misra, 2007; Vale et al., 2003).

Neonicotinoid insecticides can induce neuronal overexcitation by targeting nicotinic acetylcholine receptors (nAChR; Matsuda et al., 2009). However, the human health risk associated with neonicotinoids is presumably low due to the high selectivity for insect nAChR compared with mammals (Tomizawa and Casida, 2005). Nevertheless, imidacloprid has been shown to induce neurobehavioral changes in young rats following developmental exposure (Abou-Donia et al., 2008). Moreover, some *in vitro* studies indicate that imidacloprid has additional targets in neuronal cells as it activates the extracellular signal-regulated kinase (ERK) cascade (Tomizawa and Casida, 2002) and can cause a depolarization shift of the membrane potential (Bal et al., 2010).

Calcium homeostasis is an important endpoint in neurotoxicity studies because proper regulation of the intracellular calcium concentration ($[Ca^{2+}]_i$) is critical for normal neurotransmission and neural development (Leclerc et al., 2011). Notably, even small changes in $[Ca^{2+}]_i$ can result in adverse effects (Toescu and Verkhratsky, 2007).

It has previously been shown in rat PC12 cells that inhibition of the depolarization-evoked increase in $[Ca^{2+}]_i$, which is mediated by VGCCs, is a common mode of action for several persistent environmental pollutants (Dingemans et al., 2010; Langeveld et al., 2012), the organochlorine insecticides lindane and dieldrin (Heusinkveld and Westerink, 2012), the OP insecticides chlorpyrifos and parathion (Meijer et al., 2014b) and several conazole fungicides (Heusinkveld et al., 2013).

In addition to inhibition of VGCCs, insecticides disturb calcium homeostasis through other mechanisms. Lindane and chlorpyrifos induce an increase in $[Ca^{2+}]_i$ by depolarization of the membrane and by release of calcium from intracellular calcium stores, respectively (Heusinkveld et al., 2010; Meijer et al., 2014b). On the other hand, imidacloprid can induce calcium influx through activation of calcium permeable nAChR as shown in rat cerebellar granule cells (Kimura-Kuroda et al., 2012), whereas pyrethroids, including cypermethrin, can increase sodium influx, resulting in depolarization and subsequent calcium influx via VGCCs as shown in mouse neocortical neurons (Cao et al., 2011).

To investigate if disturbance of calcium homeostasis is a common mode of action for insecticides, we investigated the effects of low concentrations (1 nM - 10 μ M) of (α -)cypermethrin, chlorpyrifos, endosulfan, and imidaclo-

prid on basal and depolarization-evoked $[Ca^{2+}]_i$ in PC12 cells. PC12 cells are well characterized and commonly used for mechanistic neurotoxicological and neurophysiological studies (Westerink, 2013; Westerink and Ewing, 2008) and express L-, N-, and P/Q-type VGCCs (Dingemans et al., 2009; Heusinkveld et al., 2010). Because humans are simultaneously exposed to multiple insecticides (EFSA, 2013) we also investigated if the effects of mixtures of insecticides are additive.

7.2 MATERIALS AND METHODS

7.2.1 Chemicals

Fura-2 AM was obtained from Molecular Probes (Invitrogen, Breda, The Netherlands). Cypermethrin (purity 95.1%), α -cypermethrin (purity 99.7%), chlorpyrifos (purity 99.9%), endosulfan (α : β 2:1; purity 99.9%), imidacloprid (purity 99.9%) and all other chemicals were obtained from Sigma-Aldrich (Zwijndrecht, The Netherlands) unless otherwise noted. Saline solutions (containing in mM: 125 NaCl, 5.5 KCl, 2 $CaCl_2$, 0.8 $MgCl_2$, 10 HEPES, 24 glucose and 36.5 sucrose at pH 7.3, adjusted with NaOH) were prepared with deionized water (Milli-Q; resistivity >18 M Ω -cm). Stock solutions were prepared in DMSO and final solutions (solvent concentration 0.1% DMSO) were prepared daily.

7.2.2 Cell culture

Rat pheochromocytoma (PC12) cells (Greene and Tischler, 1976) were cultured for up to 10 passages in RPMI 1640 medium (Invitrogen) supplemented with 10% horse serum, 5% fetal bovine serum and 2% penicillin/streptomycin (ICN Biomedicals, Zoetermeer, The Netherlands) as described previously (Dingemans et al., 2010; Langeveld et al., 2012; Meijer et al., 2014b). All cell culture material was coated with poly-L-lysine (50 μ g/mL). Cells were grown in a humidified incubator at 37 °C and 5% CO₂. Medium was refreshed every 2-3 days. For single-cell fluorescent microscopy Ca^{2+} imaging experiments, PC12 cells were subcultured (at ~75% confluency) in glass-bottom dishes (MatTek, Ashland, MA) as described previously (Dingemans et al., 2010; Langeveld et al., 2012; Meijer et al., 2014b).

7.2.3 $[Ca^{2+}]_i$ measurements

Changes in $[Ca^{2+}]_i$ were measured with the Ca^{2+} sensitive fluorescent ratio dye Fura-2 AM as described previously (Dingemans et al., 2010; Langeveld et al., 2012; Meijer et al., 2014b). Briefly, PC12 cells were loaded with 5 μ M Fura-2 AM for 20 min in saline, followed by 15 min de-esterification in saline at room temperature. Cells were placed on the stage of an Axiovert 35M inverted microscope (40x oil-immersion objective, numerical aperture 1.0; Zeiss, Göttingen, Germany) equipped with a TILL Photonics Polychrome IV (Xenon Short Arc lamp, 150W; TILL Photonics GmbH, Gräfelfing, Germany) and continuously superfused with saline using a Valvelink 8.2 (Automate Scientific, CA). Fluorescence, excited by 340 and 380 nm wavelengths (F_{340} and F_{380}), was collected every 3 s at 510 nm with an Image SensiCam digital camera (TILL Photonics GmbH). All experiments were performed at room temperature. Every experiment consisted of a 5 min baseline recording and a subsequent depolarization of the cells by superfusing with 100 mM K^+ saline (containing in mM: 5.5 NaCl, 100 KCl, 2 $CaCl_2$, 0.8 $MgCl_2$, 10 HEPES, 24 glucose and 36.5 sucrose at pH 7.3, adjusted with NaOH) for 21 s. Next, cells were allowed to recover in saline for 8 min prior to superfusion with saline containing 0.1% DMSO (vehicle control) or (mixtures of) insecticides (1 nM - 10 μ M) for 20 min to determine effects of insecticide exposure on basal $[Ca^{2+}]_i$. Following this 20 min exposure, cells were depolarized for a second time in the presence of DMSO or (mixtures of) insecticides (see Fig. 1A for example recording) to determine effects of insecticide exposure on depolarization-evoked $[Ca^{2+}]_i$. At the end of each recording, cells were permeabilized with 5 μ M ionomycin to determine the maximum ratio (R_{max}) after which all Ca^{2+} was chelated with 17 mM ethylenediamine tetraacetic acid (EDTA) to determine the minimum ratio (R_{min}) to calculate $[Ca^{2+}]_i$ (see below).

Individual insecticides were selected for the mixture experiments based on their potency to inhibit VGCCs and were combined at the (calculated) concentrations that induce an inhibition of the depolarization-evoked $[Ca^{2+}]_i$ of 20% (IC_{20}).

7.2.4 Data analysis and statistics

Data were processed with TILLvisION software (version 4.01) and further analyzed with a custom-made MS-Excel macro. A modified Grynkiewicz's equation $[Ca^{2+}]_i = K_{d^*} * (R - R_{min}) / (R_{max} - R)$, where K_{d^*} is the dissociation

constant of Fura-2 determined in the experimental setup, was used to calculate free cytosolic $[Ca^{2+}]_i$ from background-corrected F_{340}/F_{380} ratio values (Dingemans et al., 2010; Langeveld et al., 2012; Meijer et al., 2014b). Insecticide-induced effects on basal $[Ca^{2+}]_i$ were expressed as the average increase in $[Ca^{2+}]_i$ during the first 5 min of exposure of responding cells. Only cells that displayed an increase in $[Ca^{2+}]_i$ during exposure \geq basal + SD were regarded as responding cells and were selected for quantification of basal $[Ca^{2+}]_i$ effects.

Effects on the depolarization-evoked increase in $[Ca^{2+}]_i$ were expressed as a treatment ratio (TR) as described previously (Meijer et al., 2014b; see Fig. 1A for illustration). Data are expressed as mean \pm SEM (calculated from number of cells (n)), normalized to the control, unless otherwise noted. Cells that did not respond to the first depolarization (amplitude $<$ 3x basal) were excluded for further analysis. Additionally, cells that show effects outside the range of the average \pm 2x SD are considered as outliers and were excluded for further analysis (\sim 15%). Per test condition \geq 4 independent experiments (N) were performed to obtain \geq 38 cells (n) after outlier exclusion. For the calculation of IC_{20} s a non-linear regression curve with Hill-slope was fitted by use of GraphPad Prism software (v6, GraphPad Software, La Jolla, CA).

Cypermethrin, chlorpyrifos and endosulfan were used at their IC_{20} s in the mixture experiments to test if additivity applies. In view of the similar endpoint (i.e. inhibition of depolarization-evoked $[Ca^{2+}]_i$), concentration-addition could be assumed. However, this assumption cannot be confirmed because the actual underlying mechanism(s) of action is not known (i.e. different subtypes of VGCCs exist that have multiple molecular entities/binding sites that can be targeted by the individual chemicals) and the different chemicals could thus also target VGCCs via independent action. Therefore, from a theoretical point of view, effect-addition for these three insecticides cannot be excluded. Nevertheless, it has recently been suggested that in the case of effect-addition with different underlying mechanisms of action concentration-addition may also apply (Kortenkamp et al, 2012).

Effects of mixtures were considered additive if the measured effect was within the expected additivity effect range. This range was calculated from the expected inhibition (EI) of the mixtures in case of additivity (i.e., an EI of 40% for a binary IC_{20} mixture and an EI of 60% for a tertiary IC_{20} mixture)

and the sum of the confidence intervals (CI) of the $IC_{20.5}$ of the individual chemicals. Thus, the additivity effect range is $100-(EI_1+EI_2) \pm (CI_1+CI_2)$. If effects were below or above this range, the effect of the mixture was considered less or more than additive, respectively.

Data of test conditions for which the TR approached 0% are by definition not normally distributed because the TR cannot be negative. However, data from controls and from conditions that did not exert a (near) maximal effect were normally distributed (Kolmogorov-Smirnov test and Shapiro-Wilk test) and continuous data were therefore compared with an unpaired *t*-test and concentration-response curves with an one-way ANOVA. Data were considered statistically significant if $p < 0.05$.

7.3 RESULTS

7.3.1 Effects of insecticides on basal $[Ca^{2+}]_i$

Basal $[Ca^{2+}]_i$ in resting PC12 cells is low and stable (99 ± 1 nM; $n = 206$, $N = 22$). Upon depolarization with high K^+ -containing saline, $[Ca^{2+}]_i$ rapidly and transiently increased to 2.1 ± 0.1 μ M. During a subsequent 8 min recovery period, $[Ca^{2+}]_i$ returned to near resting values and was unaffected by 20 min exposure to DMSO-containing saline (Fig. 1A). When cells were exposed to 10 μ M imidacloprid (Fig. 1B), α -cypermethrin (Fig. 1C) or cypermethrin (Fig. 1D), basal $[Ca^{2+}]_i$ levels were unaffected. In contrast, in 40% of the cells exposed to 10 μ M endosulfan a small but sustained increase in $[Ca^{2+}]_i$ was observed, which lasted for 20 min and amounted to 53 ± 8 nM in the first 5 min (18 out of 45 cells (40%), $N = 6$; Fig. 1E). When cells were exposed to endosulfan in Ca^{2+} -free medium, the increase in $[Ca^{2+}]_i$ was no longer observed (data not shown). When cells were exposed to 10 μ M chlorpyrifos, 56% of the cells responded with a small but transient increase in $[Ca^{2+}]_i$ which sustained for ~ 5 min and amounted to 68 ± 8 nM (30 out of 54 cells (56%), $N = 7$; Fig. 1F). At concentrations ≤ 1 μ M, endosulfan and chlorpyrifos did not disturb basal $[Ca^{2+}]_i$ (data not shown).

7.3.2 Effects of insecticides on depolarization-evoked increase in $[Ca^{2+}]_i$

The effects of insecticide exposure on the increase in depolarization-evoked $[Ca^{2+}]_i$, which is mediated by VGCCs, were investigated by depolarization of the cells for a second time with high K^+ -containing saline following the 20 min of exposure to saline containing DMSO (control) or

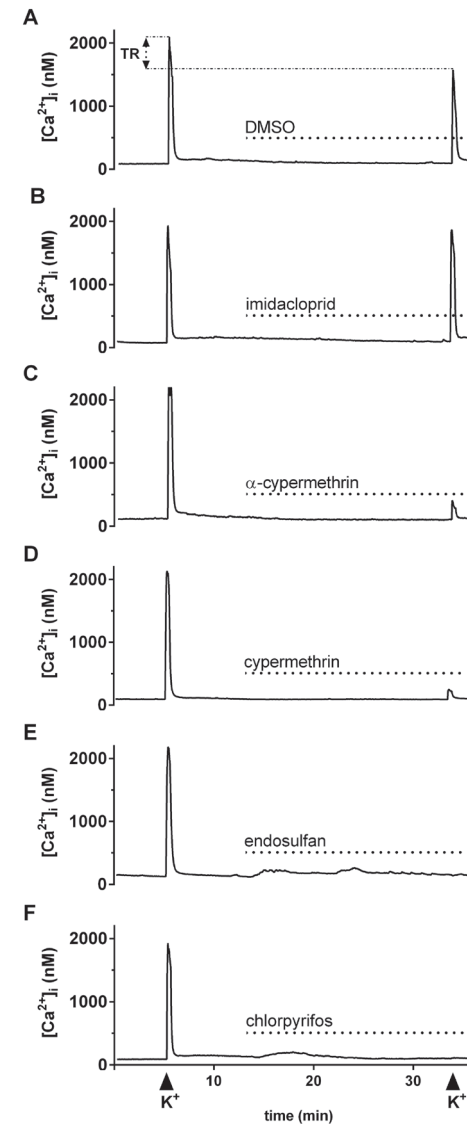


Figure 1: Representative recordings of $[Ca^{2+}]_i$ from individual PC12 cells exposed to DMSO (A), 10 μ M imidacloprid (B), α -cypermethrin (C), cypermethrin (D), endosulfan (E) and chlorpyrifos (F). PC12 cells were exposed to saline containing test compound for 20 min as indicated by the dotted line. Before and following 20 min exposure of the cells, depolarization was evoked by high K^+ -containing saline as indicated by the arrowheads below the recordings. Changes in treatment ratio (TR = amplitude 2nd depolarization/ amplitude 1st depolarization * 100%), normalized to DMSO controls, were used as a measure for effects of insecticides on the depolarization-evoked increase in $[Ca^{2+}]_i$.

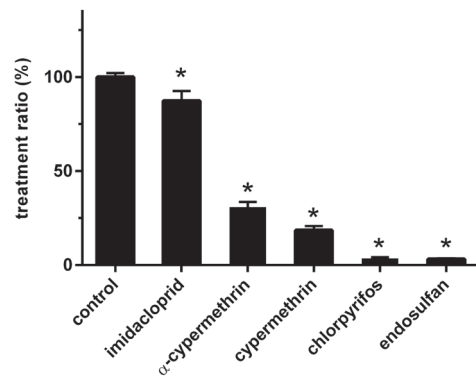


Figure 2: The inhibitory effects of insecticides on the depolarization-evoked increase in $[Ca^{2+}]_i$. At 10 μ M, α -cypermethrin, cypermethrin, chlorpyrifos, and endosulfan effectively inhibited the TR (depolarization-evoked increase in $[Ca^{2+}]_i$ after exposure compared with depolarization-evoked increase in $[Ca^{2+}]_i$ before exposure) whereas imidacloprid induced only a modest inhibition of the TR. Data represents mean \pm SEM ($n = 38$ -206, $N = 4$ -22). * indicates a significant difference compared with control ($p < 0.05$).

insecticide. In control cells, the second depolarization-evoked increase in $[Ca^{2+}]_i$ amounted to $1.5 \pm 0.05 \mu$ M ($n = 206$, $N = 22$), yielding a net TR of 69% (Fig. 1A). The TR of control cells was set to 100% and all data of insecticide-exposed cells were normalized to the control.

Effects on the depolarization-evoked increase in $[Ca^{2+}]_i$ were initially tested at 10 μ M. All tested insecticides significantly decreased the TR with endosulfan yielding the largest inhibition, reducing the TR to $3 \pm 0.5\%$ ($n = 45$, $N = 6$; $p < 0.001$; Figs. 1E and 2). At 10 μ M, chlorpyrifos yielded a comparable decrease in TR compared with endosulfan (TR: $4 \pm 1\%$; $n = 54$, $N = 7$; $p < 0.001$; Figs. 1F and 2; also see Meijer et al., 2014b). At 10 μ M, α -cypermethrin and cypermethrin reduced the TR to $31 \pm 3\%$ ($n = 57$, $N = 6$; $p < 0.001$; Figs. 1C and 2) and $18 \pm 2\%$ ($n = 50$, $N = 5$; $p < 0.001$; Figs. 1D and 2), respectively. For concentration-response curves (Fig. 3), all insecticides were tested at lower concentrations, except for imidacloprid which had only a small effect at 10 μ M (TR: $87 \pm 5\%$; $n = 38$, $N = 4$; $p < 0.03$; Figs. 1B and 2).

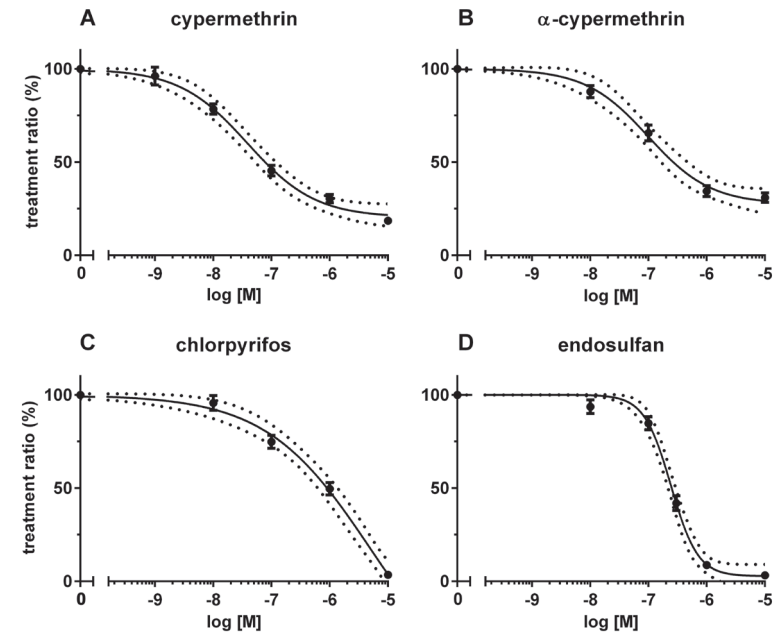


Figure 3: Concentration-response curves of inhibition of depolarization-evoked $[Ca^{2+}]_i$ by the insecticides cypermethrin (A), α -cypermethrin (B), chlorpyrifos (C) and endosulfan (D). The selected insecticides concentration-dependently inhibited the TR, with cypermethrin being most potent. The effects were significantly different from control ($p < 0.05$) at $\geq 0.01 \mu$ M (cypermethrin) and $\geq 0.1 \mu$ M (α -cypermethrin, chlorpyrifos and endosulfan). For calculated IC_{20} s and IC_{50} s, see table 1. Data represents mean \pm SEM ($n = 38$ -206, $N = 4$ -22). The dotted line indicates the 95% confidence interval of the fitted curve.

Compared to DMSO controls, cells exposed to cypermethrin for 20 min displayed a concentration-dependent inhibition of the TR ($p < 0.001$). This TR amounted to $78 \pm 3\%$ ($n = 53$, $N = 6$; $p < 0.001$) at 10 nM, $45 \pm 3\%$ ($n = 66$, $N = 5$; $p < 0.001$) at 100 nM and $30 \pm 2\%$ ($n = 63$, $N = 6$; $p < 0.001$) at 1 μ M (Fig. 3A), resulting in IC_{20} and IC_{50} values of 9 nM and 78 nM, respectively. At 100 nM, α -cypermethrin reduced the TR to $66 \pm 4\%$ ($n = 65$, $N = 8$; $p < 0.001$) and to $34\% \pm 3$ ($n = 60$, $N = 7$; $p < 0.001$) at 1 μ M (Fig. 3B; IC_{20} : 27 nM, IC_{50} : 239 nM; Table 1). Notably, the effect of cypermethrin was significantly

different from that of α -cypermethrin at $\geq 0.01 \mu\text{M}$. As also demonstrated previously (Meijer et al., 2014b), chlorpyrifos concentration-dependently decreased the TR to $75 \pm 4\%$ ($n = 52$, $N = 5$; $p < 0.001$) at 100 nM, and to $50 \pm 3\%$ ($n = 59$, $N = 6$; $p < 0.001$) at 1 μM (Fig. 3C; IC_{20} : 85 nM, IC_{50} : 899 nM; Table 1). Endosulfan also concentration-dependently decreased the TR, amounting to $85 \pm 4\%$ ($n = 59$, $N = 6$; $p < 0.001$) at 100 nM, to $42 \pm 4\%$ ($n = 39$, $N = 7$; $p < 0.001$) at 300 nM, and to $9 \pm 1\%$ ($n = 55$, $N = 7$; $p < 0.001$) at 1 μM (Fig. 3D; IC_{20} : 118 nM, IC_{50} : 250 nM; Table 1).

7.3.3 Effects of mixtures of insecticides on depolarization-evoked increase in $[\text{Ca}^{2+}]_i$

Insecticides with the highest potency (cypermethrin, chlorpyrifos, and endosulfan) were combined as binary mixtures for the investigation of additive effects on the depolarization-evoked $[\text{Ca}^{2+}]_i$. A mixture of chlorpyrifos (IC_{20}) combined with endosulfan (IC_{20}) resulted in a TR of $59 \pm 3\%$ ($n = 48$, $N = 4$), which was well within the expected additivity effect range (48-72%; Fig. 4). When chlorpyrifos (IC_{20}) and cypermethrin (IC_{20}) were combined, the TR amounted to $54 \pm 3\%$ ($n = 47$, $N = 5$), i.e., within the expected additivity effect range (49 - 71%; Fig. 4). Similarly, when endosulfan (IC_{20}) was combined with cypermethrin (IC_{20}) the TR amounted to $60 \pm 3\%$ ($n = 49$, $N = 6$), i.e. within the expected additivity effect range (48-72%; Fig. 4). However, when all three insecticides were combined, the TR amounted to $60 \pm 3\%$ ($n = 46$, $N = 4$), which was just above the expected additivity effect range (22-58%). Though the inhibitory effect of the tertiary mixture on TR is only slightly less than additive, these data indicate that mixture effects cannot completely be predicted based on additivity alone.

7.4 DISCUSSION

The present data demonstrate that the pyrethroids (α -)cypermethrin, the OP chlorpyrifos, and the organochlorine endosulfan at low concentrations acutely disturb calcium homeostasis through a concentration-dependent inhibition of VGCCs. Moreover, endosulfan and chlorpyrifos (and also its metabolite chlorpyrifos-oxon; Meijer et al., 2014b) acutely increased basal calcium levels. The effects of insecticides on basal $[\text{Ca}^{2+}]_i$ were observed only at relatively high concentrations (10 μM), whereas the IC_{50} s for inhibition of the depolarization-evoked $[\text{Ca}^{2+}]_i$ were as low as 78 nM, 239

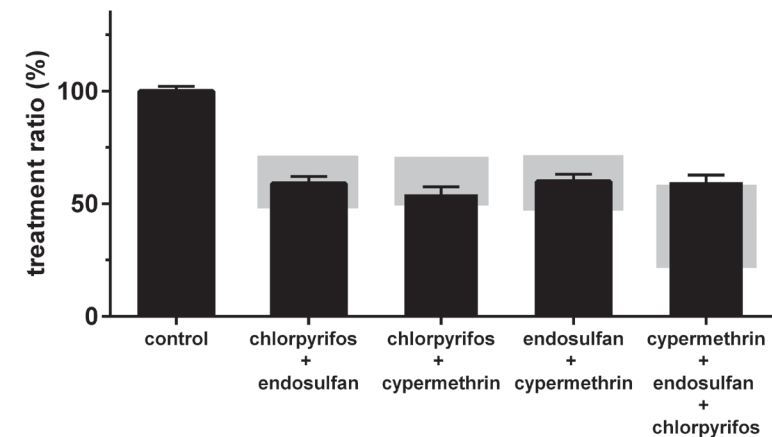


Figure 4: Effects of mixtures of insecticides on the depolarization-evoked increase in $[\text{Ca}^{2+}]_i$. Binary and tertiary mixtures of IC_{20} s were investigated to determine if the inhibitory effects of mixtures on the TR are additive. All mixtures decreased the TR significantly compared with the control. The grey shaded areas indicate the expected additivity effect range, illustrating that the binary mixtures induced an additive inhibition compared with the single compounds and that the tertiary mixture induced a less than additive inhibition. Data represents mean \pm SEM ($n = 46$ -206, $N = 4$ -22).

nM, 250 nM and 899 nM for cypermethrin, α -cypermethrin, endosulfan, and chlorpyrifos, respectively. In this study, α -cypermethrin displayed a lower potency compared with cypermethrin although α -cypermethrin has the lowest acute toxicological reference value (ARfD; EFSA, 2013).

Effects of chlorpyrifos and endosulfan on VGCCs appeared not specific for a VGCC-subtype as complete inhibition of the TR was observed at 10 μM (Fig. 3). On the other hand, a complete inhibition of VGCCs could not be reached for (α -)cypermethrin at concentrations up to 10 μM , suggesting that inhibition of VGCC by pyrethroids could be VGCC-subtype specific or that higher concentrations are required to induce a complete block. Imidacloprid did not disturb basal calcium levels and inhibited the depolarization-evoked increase in $[\text{Ca}^{2+}]_i$ only marginally. This was somewhat surprising as imidacloprid ($\geq 1 \mu\text{M}$) was reported to induce an increase in basal $[\text{Ca}^{2+}]_i$ in rat cerebellar granule cells. This effect was

mediated by $\alpha 7$, $\alpha 4\beta 2$ and $\alpha 3\beta 4$ nAChRs (Kimura-Kuroda et al., 2012), of which at least $\alpha 7$ and $\alpha 4\beta 2$ nAChRs are also expressed in PC12 cells (Mehrani and Golmanesh, 2008). However, the expression of functional (calcium permeable) nAChRs in PC12 cells is limited as acetylcholine-induced increases in $[Ca^{2+}]_i$ are relatively small (amplitude ~ 300 nM; Hondebrink et al., 2012). Possibly, the lack of effect of imidacloprid on basal $[Ca^{2+}]_i$ is due to differences in nAChR expression levels and/or functionality between PC12 cells and rat cerebellar granule cells.

Previously, several pesticides were demonstrated to potently inhibit VGCCs, including the organochlorine pesticides lindane and dieldrin (Heusinkveld and Westerink, 2012), several conazole fungicides (Heusinkveld et al., 2013) and the OP insecticides chlorpyrifos and parathion (Meijer et al., 2014b). As VGCCs are also inhibited by endosulfan and (α -) cypermethrin (Figs. 1-3), inhibition of VGCCs appears to be a common mode of action for several distinct classes of pesticides. The neonicotinoid imidacloprid (Figs. 1 and 2) and the carbamate carbaryl (Meijer et al., 2014) did not exert this effect, which indicates that there are also (classes of) insecticides that do not target VGCCs.

For chemicals with a similar mode of action effect additivity is expected. Our mixture data demonstrated that insecticide mixtures induce additive effects (Fig. 4) comparable with those observed for the conazole fungicides (Heusinkveld et al., 2013) and organochlorine insecticides (Heusinkveld and Westerink, 2012). However, when cypermethrin, endosulfan and chlorpyrifos were combined at their respective $IC_{20,s}$ in a tertiary mixture, the effect was less than additive (Fig. 4). This is in line with other mixture studies showing that additivity does not always apply for mixtures with similar modes of action. Less than additive effects of binary OP mixtures on VGCCs inhibition were observed (Meijer et al., 2014b) and also the binary mixture of PCB53 and PCB95 (which both induce an increase in basal $[Ca^{2+}]_i$) did not induce additive effects on the basal increase in $[Ca^{2+}]_i$ (Langeveld et al., 2012), indicating that effects of mixtures of chemicals with common modes of action cannot always be simply predicted by additivity.

Interestingly, effects of cypermethrin, endosulfan, and chlorpyrifos on VGCCs occur at lower concentrations compared with the presumed primary modes of action of pyrethroids, organochlorines, and OPs. For example, 10 μM cypermethrin induced a small modification in VGSC currents in *Xenopus* oocytes (Meacham et al., 2008) and endosulfan inhibited GABA-R

at 0.4 μM (IC_{50} ; Vale et al., 2003) and 1 μM (IC_{50} ; Huang and Casida, 1996) in cerebellar granule cells. These levels are higher than those required for inhibition of VGCCs (cypermethrin IC_{20} : 9 nM and endosulfan IC_{50} : 0.25 μM ; Table 1). However, it should be noted that part of the differences in sensitivity may be explained by small differences in the ion channels and/or receptors expressed in the different experimental models and potential absence of (intracellular) feedback mechanisms in *Xenopus* oocytes. Previously described effects of chlorpyrifos *in vitro* generally occur at concentrations between ~ 1 -100 μM (reviewed in Meijer et al., 2014b), which are also higher compared to the IC_{50} for inhibition of VGCCs found in this study (chlorpyrifos IC_{50} : 0.899 μM ; Table 1). The IC_{50} for inhibition of VGCCs for chlorpyrifos is somewhat higher in this study compared with Meijer et al., (2014b), which is probably due to an improvement of the curve fit as a result of the inclusion of additional data points. Nonetheless, the $IC_{50,s}$ are still in the same order of magnitude.

VGCCs are important regulators for neurotransmission and gene expression and as such they play an important role in neuronal development and function (Leclerc et al., 2011). In addition, altered expression and dysfunction of VGCCs are associated with neurological disorders, such as pain, epilepsy, migraine, and ataxia (Simms and Zamponi, 2014). Notably, some well-known neurobehavioral toxicants, such as OPs (Eaton et al., 2008), NDL-PCBs (Boix et al., 2011) and methylmercury (Bailey et al., 2013), also inhibit VGCCs. However, because these compounds have multiple effects, it is difficult to determine the contribution of inhibition of VGCC to the adverse health outcome. Nonetheless, the importance of calcium channels in neurobehavioral toxicity has been demonstrated for methylmercury because an L-type calcium channel blocker prevented or delayed the observed behavioral toxicity (Bailey et al., 2013). Yet, considering the essential role of VGCCs it is not unlikely that compensatory mechanisms prevent the manifestation of severe health outcomes unless exposure is to high concentrations and/or chronic.

To estimate the relevance of the effects observed in the present study, we compared effective concentrations for the inhibition of VGCCs by insecticides with occupational human exposure levels. α -Cypermethrin was found in Egyptian agricultural workers at an estimated daily internal dose of 0.43-1.53 $\mu g/kg/day$ (1.03-3.68 nM; Singleton et al., 2013) amounting to a margin of exposure (MOE) of 2.7-9.7 (table 1). In contrast

with α -cypermethrin, occupational exposure levels of chlorpyrifos and endosulfan were higher than the effective concentrations for the inhibition of VGCCs found in this study. For chlorpyrifos, estimated absorbed daily doses for farmers were between 2.5 and 53.2 $\mu\text{g}/\text{kg}/\text{day}$ (7.13-152 nM; Phung et al., 2012). At these concentrations, chlorpyrifos inhibits VGCCs (IC_{20} : 85 nM; table 1) and the MOE amounts only to 0.07-1.4 (table 1). Endosulfan was also found in human tissues of agricultural workers. After endosulfan is sprayed, 544.1 $\mu\text{g}/\text{L}$ (1.34 μM) was found in blood serum, resulting in a MOE of only 0.007 (table 1; Dalvie et al., 2009).

The calculated MOEs are thus insufficient to rule out effects on VGCCs in agricultural workers. However, it should be noted that for the calculation of MOEs it was assumed that the estimated absorbed daily doses and serum levels represent the insecticide concentration at the internal target sites, though the actual concentrations at the target cells *in vivo* could be different. Although more sophisticated physiologically-based pharmacokinetic (PBPK) data and/or actual measurements of the insecticide concentration at the target site are required to confirm that the MOEs are insufficient, our findings are of relevance for neurotoxicity risk assessment studies as it is also demonstrated here that additivity can occur when insecticides with common modes of action are combined.

In conclusion, the present study demonstrates that structurally diverse insecticides have inhibition of VGCCs as a common mode of action, resulting in the inhibition of the depolarization-evoked increase in $[\text{Ca}^{2+}]_i$. The tested insecticides exerted this effect at concentrations that are relevant for human (occupational) exposure situations. Our data further demonstrate that exposure to (binary) mixtures of insecticides can induce additive effects, illustrating the need to include mixture effects in human neurotoxicity risk assessment.

Acknowledgements

The authors acknowledge the European Commission [DENAMIC project; grant number FP7-ENV-2011-282957] and the Faculty of Veterinary Medicine of Utrecht University for funding, and the members of the Neurotoxicology Research Group for helpful discussions.

Funding

This work was supported by the European Commission [DENAMIC project; grant number FP7-ENV-2011-282957] and the Faculty of Veterinary Medicine of Utrecht University.

The authors declare to have no competing financial interests.

Table 1: Human exposure concentrations and (no) effect concentrations for inhibition of VGCCs of endosulfan, cypermethrin and chlorpyrifos (in μM) with the estimated margin of exposure^a.

Insecticide:	Human occupational exposure		(No-) effect concentrations for VGCC inhibition			Margin of exposure ^b
	Concentration	Estimated from	IC_{50}	IC_{20}	NOEC	
α -cypermethrin	0.0010 - 0.0037	Internal daily dose from urinary metabolite ¹	0.239	0.03	0.01	2.7 - 9.7
Chlorpyrifos	0.0071 - 0.1520	Absorbed daily dose from urinary metabolite ²	0.899	0.08	0.01	0.07 - 1.4
Endosulfan	1.3371	Blood serum ³	0.25	0.12	0.01	0.007

^aRisk estimates presented here did not take into account possible detoxification or bioactivation pathways that may influence the risk assessment

^bMargin of exposure: NOEC/exposure concentration; NOEC, no-observed-effect concentration

¹ Singleton et al., 2014

² Phung et al., 2012

³ Dalvie et al., 2009

Chapter 8

INHIBITION OF VOLTAGE-GATED CALCIUM CHANNELS AFTER SUBCHRONIC AND REPEATED EXPOSURE OF PC12 CELLS TO DIFFERENT CLASSES OF INSECTICIDES

Marieke Meijer, Joske A.R. Brandsema, Desirée Nieuwenhuis, Fiona M.J. Wijnolts, Milou M.L. Dingemans, Remco H.S. Westerink

Neurotoxicology Research Group, Toxicology Division, Institute for Risk Assessment Sciences (IRAS), Faculty of Veterinary Medicine, Utrecht University, P.O. Box 80.177, NL-3508 TD Utrecht, The Netherlands

**Published in: Toxicological Sciences 2015 147(2):607-17.
doi: 10.1093/toxsci/kfv154**

ABSTRACT

We previously demonstrated that acute inhibition of voltage-gated calcium channels (VGCCs) is a common mode of action for (sub) micromolar concentrations of chemicals, including insecticides. However, because human exposure to chemicals is usually chronic and repeated, we investigated if selected insecticides from different chemical classes (organochlorines, organophosphates, pyrethroids, carbamates and neonicotinoids) also disturb calcium homeostasis after subchronic (24h) exposure and after a subsequent (repeated) acute exposure.

Effects on calcium homeostasis were investigated with single-cell fluorescence (Fura-2) imaging of PC12 cells. Cells were depolarized with high-K⁺ saline to study effects of subchronic or repeated exposure on VGCC-mediated Ca²⁺ influx.

The results demonstrate that except for carbaryl and imidacloprid, all selected insecticides inhibited depolarization (K⁺)-evoked Ca²⁺ influx after subchronic exposure (IC₅₀'s: ~1-10 μM) in PC12 cells. These inhibitory effects were not or only slowly reversible. Moreover, repeated exposure augmented the inhibition of the K⁺-evoked increase in intracellular calcium concentration induced by subchronic exposure to cypermethrin, chlorpyrifos, chlorpyrifos-oxon, and endosulfan (IC₅₀'s: ~0.1-4 μM). In rat primary cortical cultures, acute and repeated chlorpyrifos exposure also augmented inhibition of VGCCs compared with subchronic exposure.

In conclusion, compared with subchronic exposure, repeated exposure increases the potency of insecticides to inhibit VGCCs. However, the potency of insecticides to inhibit VGCCs upon repeated exposure was comparable with the inhibition previously observed following acute exposure, with the exception of chlorpyrifos. The data suggest that an acute exposure paradigm is sufficient for screening chemicals for effects on VGCCs and that PC12 cells are a sensitive model for detection of effects on VGCCs.

Keywords: subchronic exposure, repeated exposure, *in vitro* neurotoxicology, calcium homeostasis, voltage-gated calcium channels, insecticides

8.1 INTRODUCTION

Insecticides are abundantly used because of their neurotoxicity to insects, but their mode(s) of action are often not restricted to insects. The widespread use of insecticides may therefore be of concern for (developmental) neurotoxicity in mammals, including humans (e.g. Mackenzie Ross et al., 2013). Insecticides are commonly classified according to their structure and best-known neurotoxic mode of action. Organochlorine insecticides are generally banned but very persistent and still present in the environment (Mrema et al., 2013). Organochlorines are sub-classified in two main groups; 1,1,1-Trichloro-2,2-bis(4-chlorophenyl) ethane (DDT)-type insecticides that target voltage-gated sodium channels (VGSCs) and chlorinated alicyclic insecticides that target γ-Aminobutyric acid (GABA) and glycine receptors (Coats, 1990). Pyrethroid insecticides delay the inactivation of VGSCs and thus increase the Na⁺ influx, which consequently depolarizes the cell membrane resulting in overexcitation (Soderlund, 2012). Organophosphate insecticides are best known for their irreversible inhibition of acetylcholine esterase (AChE), which results in increased levels of ACh and subsequent overexcitation (Eaton et al., 2008). Bioactivation of organophosphates via the formation of oxon metabolites strongly increases their neurotoxic potency via AChE inhibition (Eaton et al., 2008). Carbamate insecticides also inhibit AChE, but these insecticides inhibit AChE activity reversibly and do not require bioactivation (Moser et al., 2010). Neonicotinoid insecticides exert neurotoxic overexcitation via activation of nicotinic ACh receptors (nAChR; Matsuda et al., 2009).

Traditional *in vivo* tests for the investigation of neurotoxicity of such insecticides and other chemicals are expensive, laborious, may not be sufficiently sensitive and often lack information on mechanisms of toxicity (Coecke et al., 2006). Therefore, there is an increasing interest for the development of *in vitro* screening methods to test chemicals for (developmental) neurotoxicity. Voltage-gated calcium channels (VGCCs) are likely a suitable target for *in vitro* neurotoxicity screening as - together with calcium permeable neurotransmitter receptors, intracellular calcium stores, and calcium binding proteins - VGCCs tightly control the intracellular calcium concentration ([Ca²⁺]_i; Westerink, 2006). This strict control of [Ca²⁺]_i is essential for a range of cellular processes including

proper neuronal function (Simms and Zamponi, 2014; Westerink, 2006), development (Leclerc et al., 2011) and survival (Zündorf and Reiser, 2011).

PC12 cells are well characterized neuronotypical cells that are known to express L-, N-, and P/Q-type VGCCs (Dingemans et al., 2009). PC12 cells are therefore a suitable cell model for mechanistic neurophysiological and neurotoxicological (screening) studies related to these channels (Westerink, 2013; Westerink and Ewing, 2008). The effects of acute *in vitro* exposure to pesticides on VGCCs in PC12 cells are already well-studied, and it is known that acute inhibition of VGCCs is a common mode of action of organochlorine-, pyrethroid-, and organophosphate insecticides (Heusinkveld and Westerink, 2012; Meijer et al., 2014a,b) and conazole fungicides (Heusinkveld et al., 2013). Moreover, several other types of chemicals have been demonstrated to acutely inhibit VGCCs, such as brominated and halogen-free flame retardants (Dingemans et al., 2009, 2010; Hendriks et al., 2014), polychlorinated biphenyls (PCBs; Langeveld et al., 2012) and drugs of abuse (Hondebrink et al., 2011, 2012).

It is, however, largely unclear if these effects of insecticides on VGCCs persist and if subchronic or repeated exposure to insecticides increases the potency of insecticides for inhibition of VGCCs. Subchronic and/or repeated exposures are more realistic exposure scenarios because exposure to insecticides usually occurs chronically and repeatedly via occupational (e.g. agriculture) settings or consumption of food. Therefore, this study investigated the effects of subchronic (24h) and repeated (24h pre-exposure followed by a second, acute exposure) exposure to endosulfan, cypermethrin, chlorpyrifos, chlorpyrifos-oxon, carbaryl, and imidacloprid on calcium homeostasis *in vitro*.

8.2 MATERIALS AND METHODS

8.2.1 Chemicals

Fura-2 AM was obtained from Molecular Probes (Invitrogen, Breda, The Netherlands). Chlorpyrifos-oxon (purity 93.5%) was obtained from AccuStandard (New Haven). Cypermethrin (purity 95.1%), chlorpyrifos (purity 99.9%), endosulfan ($\alpha:\beta$ 2:1; purity 99.9%), imidacloprid (purity 99.9%), carbaryl (purity 99.5%), and all other chemicals were obtained from Sigma-Aldrich (Zwijndrecht, The Netherlands) unless otherwise noted. Saline solutions (containing in mM: 125 NaCl, 5.5 KCl, 2 CaCl₂, 0.8 MgCl₂, 10 HEPES, 24 glucose and 36.5 sucrose at pH 7.3, adjusted with NaOH)

were prepared with deionized water (Milli-Q; resistivity >18 M Ω -cm). Stock solutions were prepared in dimethyl-sulfoxide (DMSO), and final solutions (solvent concentration 0.1% DMSO) were prepared just prior to the experiments.

8.2.2 Cell culture

Rat pheochromocytoma (PC12) cells (Greene and Tischler, 1976) were cultured for up to 10 passages in RPMI1640 (Invitrogen) supplemented with 10% horse serum, 5% fetal bovine serum and 2% penicillin/streptomycin (ICN Biomedicals, Zoetermeer, The Netherlands) as described previously (Meijer et al. 2014a,b). Medium was refreshed every 2-3 days.

Rat primary cortical cells were isolated from brain cortices of newborn (PND1) rats (Wistar; HsdCpb:WU; Harlan Laboratories B.V.; Horst, The Netherlands). Briefly, rats were decapitated, and brains were rapidly dissected in phosphate buffered saline on ice. Tissue was dissociated to single cells by use of a cell strainer (diameter 100 μ m) and suspended in Neurobasal-A medium supplemented with 25 g/l sucrose, 450 μ M glutamine, 30 μ M glutamate, 1% penicillin/streptomycin and 10% FBS (pH 7.4). A droplet of ~400 μ l cell suspension was added to 35 mm glass-bottom dishes (to obtain a cell density of 400 000 cells/dish), and cells were allowed to adhere for ~3h prior to the addition of extra medium to obtain a total of 2.5 ml medium/dish. After day 1 in culture, medium was replaced with comparable medium, but with 2% B27 instead of FBS. After day 4 in culture, the medium was replaced with Neurobasal-A medium supplemented with 25 g/l sucrose, 450 μ M glutamine, 1% penicillin/streptomycin and 10% FBS (glutamate-free medium).

All cell culture material was coated with poly-L-lysine (50 μ g/ml). Cells were cultured in a humidified incubator at 37 °C and 5% CO₂.

For cell viability experiments, PC12 cells were seeded in 48-wells plates (0.3*10⁶ cells/well) and allowed to attach overnight. Cells were exposed to 0.1% DMSO (vehicle control) or insecticide (0.1-100 μ M) in phenol red- and serum-free RPMI1640 medium for 24h.

For single-cell fluorescent microscopy Ca²⁺ imaging experiments, undifferentiated PC12 cells were subcultured in glass-bottom dishes (MatTek, Ashland, Massachusetts) at ~0.5*10⁶ cells/dish (~75% confluency) and were allowed to attach for at least 2.5h. Rat primary cortical cells were cultured in glass-bottom dishes for 7-11 days. Then, medium of PC12 cells

was replaced with serum-free RPMI1640 medium, and medium of primary cortical cells was replaced for 50% with glutamate-free medium that contained 0.1% DMSO (vehicle control) or insecticides (1 nM to 10 μ M).

8.2.3 Cell viability (alamar Blue) and CFDA-AM

Cell viability was quantified with a combined alamar Blue (aB)/CFDA-AM assay as described previously (Heusinkveld et al., 2013) with minor modifications. The aB assay determines mitochondrial activity as a measure of cell viability based on the ability of the cells to reduce resazurin to resorufin. In the same experiment, membrane integrity was assessed by CFDA-AM, which is cleaved by nonspecific esterases in living cells to the fluorescent compound CFDA. After 24h exposure to the different pesticides (0.1-100 μ M), aB/CFDA-AM was added to the wells to obtain a final concentration of 12 and 4 μ M aB and CFDA-AM, respectively. Then, cells were incubated in the dark with the aB/CFDA-AM solution for 30 min at 37 °C. Fluorescence was measured with an Infinite M200 microplate reader (10W Xenon flash light source; Tecan Trading AG, Männedorf, Switzerland) at excitation wavelength 540 nm, emission 590 nm (aB) and excitation wavelength 493 nm, emission 541 nm (CFDA).

8.2.4 $[Ca^{2+}]_i$ measurements

Changes in $[Ca^{2+}]_i$ were measured with the Ca^{2+} -sensitive fluorescent ratio dye Fura-2 AM. PC12 cells, 24h pre-exposed to insecticides, were loaded with 5 μ M Fura-2 AM for 20 min in saline, followed by 15 min de-esterification of Fura-2 AM in saline at room temperature. Cells were placed on the stage of an Axiovert 35M inverted microscope (40x oil-immersion objective, NA 1.0; Zeiss, Göttingen, Germany) equipped with a TILL Photonics Polychrome IV (Xenon Short Arc lamp, 150W; TILL Photonics GmbH, Gräfelfing, Germany) and continuously superfused with saline by use of a Valvelink 8.2 (Automate Scientific, California). Fluorescence, excited by 340 and 380 nm wavelengths (F_{340} and F_{380}), was collected every 3-6 s at 510 nm with an Image SensiCam digital camera (TILL Photonics GmbH). All experiments were performed at room temperature. Every experiment consisted of a 5 min baseline recording and a subsequent depolarization of the cells by superfusion with saline containing 100 mM K^+ (containing in mM: 5.5 NaCl, 100 KCl, 2 $CaCl_2$, 0.8 $MgCl_2$, 10 HEPES, 24 glucose, and 36.5 sucrose at pH 7.3, adjusted with NaOH) for 24 s. Then, superfusion was reset to saline for

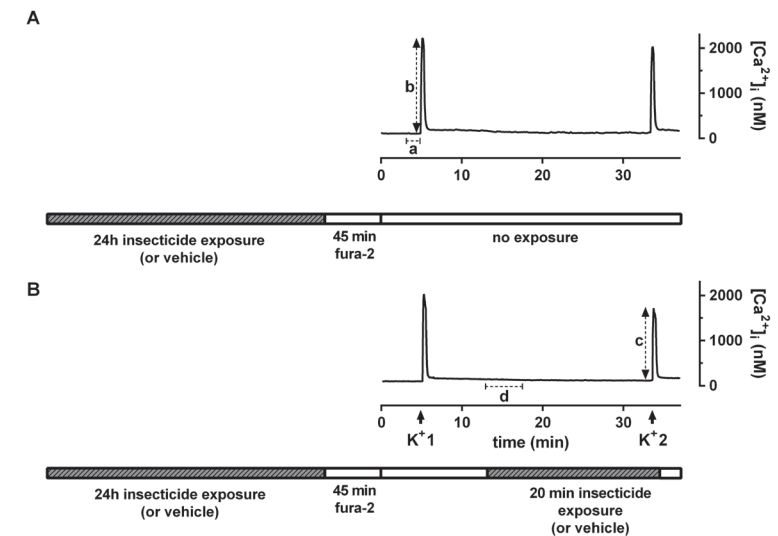


Figure 1: Example traces of control experiments. PC12 cells were pre-exposed to insecticides (or vehicle control, 0.1% DMSO) for 24h as indicated by the dashed box before the example recordings. Then, insecticide containing saline was removed to load cells with Fura-2 AM for the recording of $[Ca^{2+}]_i$. In the case of subchronic experiments, cells were not exposed during the $[Ca^{2+}]_i$ recording and during depolarization as indicated by the empty box below the example recording (A). To investigate the effects of a repeated exposure, cells were exposed for a second time for 20 min before a second depolarization (K^+2) was induced as indicated by the dashed box below the example recording (B). During the recording of $[Ca^{2+}]_i$, cells were depolarized with high K^+ -containing saline after ~5 min (K^+1) and ~33 min (K^+2). To quantify effects on basal $[Ca^{2+}]_i$ after subchronic exposure the average basal $[Ca^{2+}]_i$ of 3-5 min of the recording was used (indicated by a in Fig. 1A). To calculate effects on basal $[Ca^{2+}]_i$ for repeated exposure ~13.3-18.3 min was used (indicated by d in Fig. 1B). Effects on the depolarization-evoked increase in $[Ca^{2+}]_i$ were expressed as a net increase in $[Ca^{2+}]_i$ as indicated by b (for subchronic exposure; A) and c (for repeated exposure; B).

~28 min prior to a second depolarization with 100 mM K⁺-containing saline (see Fig. 1A). In a separate set of experiments (for repeated exposure), superfusion was changed 8 min after the first depolarization to saline containing insecticides for 20 min (acute exposure). Following this 20 min repeated acute exposure, cells were depolarized for a second time with K⁺- and insecticide-containing saline (see Fig. 1B).

At the end of each recording, cells were permeabilized with 5 μM ionomycin to determine the maximum ratio (R_{max}), after which all Ca²⁺ was chelated with 17 mM ethylenediamine tetraacetic acid (EDTA) to determine the minimum ratio (R_{min}). The obtained R_{max} and R_{min} values were used to calculate $[Ca^{2+}]_i$ (described below).

8.2.5 Data analysis and statistics

Cell viability data were analyzed by use of MS-Excel. Raw data were background-corrected and normalized to plate-matched DMSO controls. At least 3 independent experiments (N) were performed to obtain at least 12 wells (n) per condition. Data are expressed as mean ± SEM of n wells. Cell viability data were compared by use of an one-way ANOVA and a *post-hoc* Bonferroni test. Data were considered statistically significant if $p < 0.05$.

Calcium-imaging data were processed with TILLVISION software (version 4.01) and further analyzed with a custom-made MS-Excel macro that calculates background-corrected F_{340}/F_{380} ratio values and $[Ca^{2+}]_i$. To calculate free cytosolic $[Ca^{2+}]_i$ from background-corrected F_{340}/F_{380} ratio values, we used a modified Grynkiewicz's equation $[Ca^{2+}]_i = K_{d^*} * (R - R_{min}) / (R_{max} - R)$, where K_{d^*} is the dissociation constant of Fura-2 determined in the experimental setup (Meijer et al., 2014a,b).

Insecticide-induced effects on basal $[Ca^{2+}]_i$ after repeated exposure were expressed as the average increase in $[Ca^{2+}]_i$ (± SEM from n cells) during the first 5 min of re-exposure of responding cells (Fig. 1B). Responding cells are cells that displayed an increase in $[Ca^{2+}]_i$ during exposure ≥ average + SD of basal $[Ca^{2+}]_i$. Effects on the depolarization-evoked increase in $[Ca^{2+}]_i$ were expressed as a net increase (see Fig. 1 for illustration). Data were expressed as mean ± SEM (from n cells), normalized to the control, unless otherwise noted. The data were expressed in n, rather than N (independent experiments), to enable the study of single-cell calcium kinetics and oscillations. Moreover, the variation within an independent experiment (within a dish (n); CV of control repeated exposure: 0.44) was larger

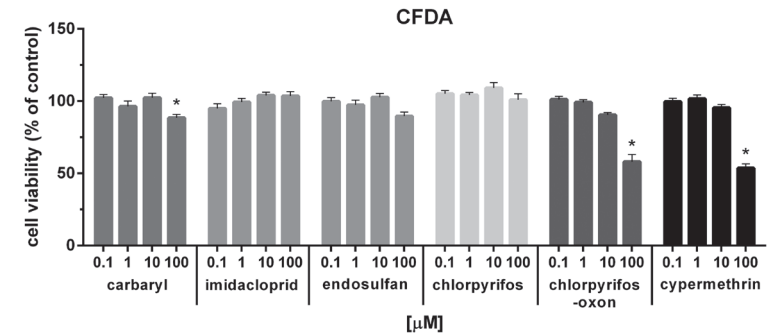


Figure 2: Cell viability following 24h of exposure to insecticides from different chemical classes. Effects on membrane integrity were investigated with a CFDA-AM assay to study the effects of insecticides on cell viability. Data, presented as mean + SEM of $n = 12-16$ obtained from $N = 3-4$, was normalized to DMSO control (%). An asterisk indicates a significant difference from the control ($p < 0.05$).

compared with the variation between the experiments (between dishes (N); CV of control repeated exposure: 0.17), which indicates that cells are independent units derived from the same population and justifies the use of n as statistical unit. Cells that showed effects over two times SD above or below average were considered as outliers and were excluded for further analysis (~13%). Per test condition at least 4 independent experiments (N) were performed to obtain ≥ 25 cells (n) after outlier exclusion. For the calculation of concentrations that induces an inhibitory effect of 20% or 50% (IC_{20} or IC_{50}), a non-linear regression curve with Hill-slope was fitted by use of GraphPad Prism software (v6, GraphPad Software, La Jolla, California). Continuous data were compared with an unpaired *t*-test. Data were considered statistically significant if $p < 0.05$.

8.3 RESULTS

8.3.1 Cytotoxicity concentration-effect range finding: effects of subchronic (24h) exposure to insecticides on cell viability in PC12 cells

Carbaryl, imidacloprid, endosulfan, chlorpyrifos, and cypermethrin did not significantly affect mitochondrial activity in PC12 cells at concentrations 0.1-100 μM after 24h of exposure as indicated by the aB assay (data not

shown). Only chlorpyrifos-oxon was able to significantly reduce the mitochondrial activity to $67 \pm 5\%$ of control at the highest concentration tested ($100 \mu\text{M}$; $n = 12$, $N = 3$; data not shown). Similarly, membrane integrity was not significantly affected by imidacloprid, endosulfan, and chlorpyrifos as indicated by the CFDA assay in PC12 cells (Fig. 2). Carbaryl modestly reduced membrane integrity to $88 \pm 2\%$ of control at $100 \mu\text{M}$ ($n = 12$, $N = 3$). At $100 \mu\text{M}$, membrane integrity compared to control was also reduced by chlorpyrifos-oxon ($58 \pm 5\%$, $n = 12$, $N = 3$) and cypermethrin ($54 \pm 3\%$, $n = 16$, $N = 4$; Fig. 2). Because cell viability is only affected by some insecticides at $100 \mu\text{M}$, the maximum concentration in subsequent experiments was kept $\leq 10 \mu\text{M}$.

8.3.2 Effects of 24h of subchronic exposure to insecticides on basal $[\text{Ca}^{2+}]_i$ and depolarization-evoked increase in $[\text{Ca}^{2+}]_i$ in PC12 cells

In control (0.1% DMSO) PC12 cells, basal $[\text{Ca}^{2+}]_i$ was low and stable ($106 \pm 2 \text{ nM}$; $n = 212$, $N = 15$; Fig. 1A). Basal $[\text{Ca}^{2+}]_i$ following subchronic (24h) exposure to insecticides was largely unchanged (ranging from $95 \pm 5 \text{ nM}$ ($10 \mu\text{M}$ cypermethrin; $n = 65$, $N = 4$) to $131 \pm 5 \text{ nM}$ ($10 \mu\text{M}$ endosulfan; $n = 59$, $N = 5$); Fig. 3).

The effects of 24h subchronic exposure to insecticides on Ca^{2+} influx via VGCCs were investigated by depolarization of the cell membrane 5 min after the start of the recording (for illustration see b in Fig. 1A). In control cells (24h subchronic exposure to 0.1% DMSO), depolarization induced a net increase in $[\text{Ca}^{2+}]_i$ of $2.1 \pm 0.08 \mu\text{M}$ ($n = 212$, $N = 15$; Fig. 1A). Carbaryl ($\leq 10 \mu\text{M}$) was not able to significantly reduce the depolarization-evoked increase in $[\text{Ca}^{2+}]_i$ ($89 \pm 6\%$ at $1 \mu\text{M}$ ($n = 57$, $N = 4$) and $92 \pm 6\%$ at $10 \mu\text{M}$ ($n = 61$, $N = 6$) compared with control; Fig. 3). Similarly, imidacloprid did not affect the depolarization-evoked increase in $[\text{Ca}^{2+}]_i$ ($96 \pm 5\%$ at $10 \mu\text{M}$; $n = 58$, $N = 4$; Fig. 3). In contrast, if depolarization was induced in cells subchronically exposed to $10 \mu\text{M}$ endosulfan, the net increase in $[\text{Ca}^{2+}]_i$ amounted only to $1.0 \pm 0.08 \mu\text{M}$, which is $46 \pm 4\%$ compared with control ($n = 59$, $N = 5$; Figs. 3 and 4A). At $1 \mu\text{M}$, endosulfan did not significantly affect the depolarization-evoked increase in $[\text{Ca}^{2+}]_i$ ($107 \pm 7\%$ compared to control; $n = 69$, $N = 4$; Fig. 4A). Chlorpyrifos did not significantly affect the depolarization-evoked increase in $[\text{Ca}^{2+}]_i$ at $0.1 \mu\text{M}$ ($96 \pm 6\%$; $n = 57$, $N = 4$; Fig. 4B). However, at $1 \mu\text{M}$, chlorpyrifos significantly reduced the net

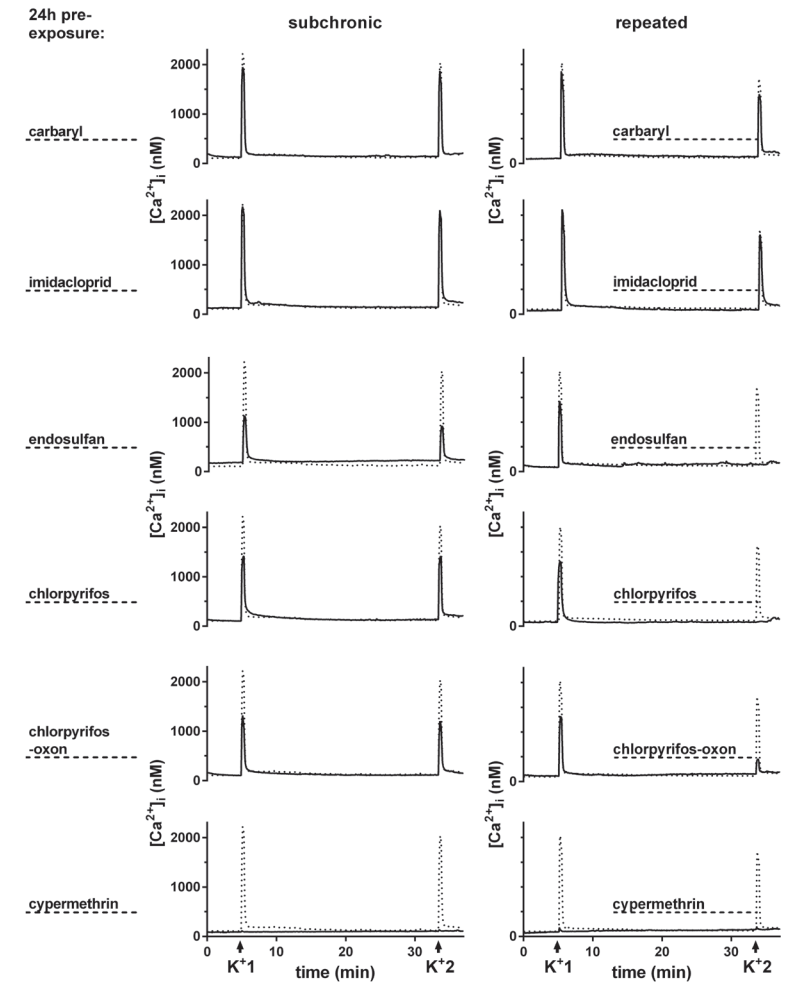


Figure 3: Representative recordings of $[\text{Ca}^{2+}]_i$ from individual PC12 cells exposed subchronic (left) and repeatedly (right) to insecticides ($10 \mu\text{M}$). PC12 cells were exposed for 24h to carbaryl, imidacloprid, endosulfan, chlorpyrifos, chlorpyrifos-oxon, and cypermethrin prior to the $[\text{Ca}^{2+}]_i$ recordings as indicated by the dashed line on the left. In a separate set of experiments (right), cells were exposed for a second time (repeated exposure) as indicated by the dashed line in the recording to the same insecticide after 24h of pre-exposure. The dotted trace in the recording shows a representative trace of a control cell. Cells were depolarized at 5 and 33.3 min as indicated by K^+1 and K^+2 .

increase in $[Ca^{2+}]_i$ to $78 \pm 6\%$ of control ($n = 59$, $N = 4$; Fig. 4B), and to $55 \pm 4\%$ of control at $10 \mu\text{M}$ ($n = 59$, $N = 5$; Figs. 3 and 4B). For chlorpyrifos-oxon, no significant reduction in the depolarization-evoked increase in $[Ca^{2+}]_i$ was observed at $0.01 \mu\text{M}$ ($92 \pm 5\%$ compared with control; $n = 54$, $N = 5$; Fig. 4C). At $0.1 \mu\text{M}$, chlorpyrifos-oxon significantly reduced the depolarization-evoked increase in $[Ca^{2+}]_i$ to $74 \pm 4\%$ ($n = 61$, $N = 5$; Fig. 4C), $62 \pm 6\%$ ($n = 62$, $N = 5$; Fig. 4C) at $1 \mu\text{M}$ and $55 \pm 3\%$ at $10 \mu\text{M}$ ($n = 64$, $N = 6$; Figs. 3 and 4C) compared with control. Cypermethrin did not significantly affect the depolarization-evoked increase in $[Ca^{2+}]_i$ at $0.1 \mu\text{M}$ ($101 \pm 6\%$ compared with control; $n = 64$, $N = 5$; Fig. 4D), but reduced the depolarization-evoked increase in $[Ca^{2+}]_i$ significantly at $1 \mu\text{M}$ to $45 \pm 4\%$ ($n = 70$, $N = 5$; Fig. 4D) and at $10 \mu\text{M}$ to $1 \pm 0.2\%$ compared with control ($n = 65$, $N = 4$; Figs. 3 and 4D). To investigate if the inhibition of the depolarization-evoked increase in $[Ca^{2+}]_i$ by insecticides is reversible, cells were depolarized ~ 28 min after the first depolarization-evoked increase in $[Ca^{2+}]_i$ for a second time. In control experiments, this second depolarization-evoked increase in $[Ca^{2+}]_i$ amounted to $1.9 \pm 0.07 \mu\text{M}$ ($n = 212$, $N = 15$; Fig. 1A; table 1). At $10 \mu\text{M}$ endosulfan, the second depolarization-evoked increase in $[Ca^{2+}]_i$ amounted to $0.9 \pm 0.07 \mu\text{M}$ ($n = 59$, $N = 5$; Fig. 3; table 1), which was $46 \pm 4\%$ compared to control (Table 1). This second depolarization-evoked increase in $[Ca^{2+}]_i$ was comparable to the first depolarization-evoked increase in $[Ca^{2+}]_i$, which was also $46 \pm 4\%$ compared with control (Table 1). At $10 \mu\text{M}$ cypermethrin, both the first and the second depolarization-evoked increases in $[Ca^{2+}]_i$ were completely inhibited (Fig. 3; table 1). Chlorpyrifos and chlorpyrifos-oxon also demonstrated comparable net increases in $[Ca^{2+}]_i$ during the first and second induced depolarization (Table 1). Carbaryl and imidacloprid were not able to change the second depolarization-evoked increase in $[Ca^{2+}]_i$ compared with control and these insecticides thus also demonstrated comparable net increases in $[Ca^{2+}]_i$ during the first and second depolarization (Fig. 3; Table 1).

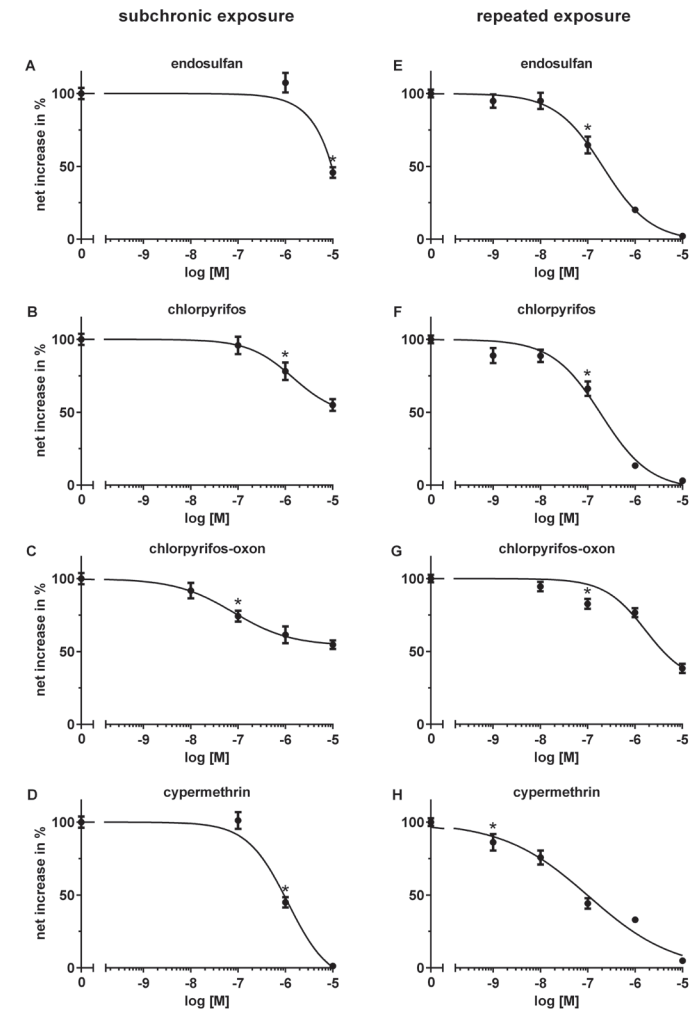


Figure 4: Concentration-response curves of inhibition of the depolarization-evoked increase in $[Ca^{2+}]_i$ by insecticides after 24h subchronic exposure (left) and after subsequent repeated exposure (right). The selected insecticides inhibit the depolarization-evoked increase in $[Ca^{2+}]_i$ concentration-dependently after 24h of subchronic exposure (A-D) and after subsequent repeated exposure (E-H) with the exception of carbaryl and imidacloprid (data not shown). Data represent mean \pm SEM ($n = 54-293$, $N = 4-23$). An asterisk indicates the lowest concentration that is significantly different from the control ($p < 0.05$).

Table 1: Net- and relative increases in $[Ca^{2+}]_i$ (expressed as mean \pm SEM (of n)) upon depolarization of cells subchronically exposed to insecticides for 24h.

Insecticide (10 μ M)	Net increase 1 st depolarization (μ M)	Net increase 2 nd depolarization (μ M)	Net increase 1 st depolarization compared to control (%)	Net increase 2 nd depolarization compared to control (%)	n/N
Control (0.1% DMSO)	2.1 \pm 0.08	1.9 \pm 0.07	100 \pm 4	100 \pm 4	212/5
Carbaryl	2.0 \pm 0.13	1.9 \pm 0.12	92 \pm 6	99 \pm 6	61/6
Imidacloprid	2.0 \pm 0.11	2.1 \pm 0.12	96 \pm 5	107 \pm 6	58/4
Endosulfan	1.0 \pm 0.08	0.9 \pm 0.07	46 \pm 4	46 \pm 4	59/5
Chlorpyrifos	1.2 \pm 0.09	1.1 \pm 0.07	55 \pm 4	58 \pm 4	59/5
Chlorpyrifos-oxon	1.2 \pm 0.06	1.2 \pm 0.06	55 \pm 3	65 \pm 3	64/6
Cypermethrin	0.03 \pm 0.00	0.05 \pm 0.01	1 \pm 0.2	3 \pm 0.3	65/4

8.3.3 Effects of repeated exposure (24h pre-exposure followed by an acute exposure) to insecticides on basal $[Ca^{2+}]_i$ and depolarization-evoked increase in $[Ca^{2+}]_i$ in PC12 cells

To investigate the effects of repeated exposure to insecticides, cells pre-exposed to insecticides for 24h were re-exposed acutely for 20 min starting 8 min after the first depolarization-evoked increase in $[Ca^{2+}]_i$ (see fig 1B for illustration). No changes in basal $[Ca^{2+}]_i$ were observed with the exception of 10 μ M endosulfan, which induced an increase in basal $[Ca^{2+}]_i$ of 71 \pm 13 nm in responding cells (41%; 25 out of 61 cells; Fig. 3).

The first depolarization-evoked increase in $[Ca^{2+}]_i$ in repeated exposure experiments was, as expected, comparable with the 24h subchronically exposed cells (Fig. 3). In control cells (0.1% DMSO), the first net depolarization-evoked increase in $[Ca^{2+}]_i$ amounted to 2.0 \pm 0.05 μ M and the second depolarization-evoked increase in $[Ca^{2+}]_i$ amounted to 1.4 \pm 0.04 μ M (n = 293, N = 23; Fig. 1B). Carbaryl induced a small but significant inhibition of the depolarization-evoked increase in $[Ca^{2+}]_i$ after repeated exposure at 10 μ M (87 \pm 6% compared with control; n = 62, N = 5; Fig. 3). When cells were exposed repeatedly to 10 μ M imidacloprid, no significant change in the depolarization-evoked increase was observed (105 \pm 6% compared with control; n = 65, N = 5; Fig. 3). In contrast, repeated exposure to endosulfan concentration-dependently inhibited the depolarization-evoked increase in $[Ca^{2+}]_i$ at 0.1 μ M (65 \pm 6%, n = 71, N = 5; Fig. 4E) and resulted in a nearly complete inhibition at 10 μ M (2 \pm 0.3%, n = 61,

N = 6; Figs. 3 and 4E). Chlorpyrifos also concentration-dependently reduced the depolarization-evoked increase in $[Ca^{2+}]_i$ at 0.1 μ M (66 \pm 5%; n = 65, N = 5; Fig. 4F) and induced a nearly complete inhibition at 10 μ M (3 \pm 0.4%; n = 61, N = 5; Figs. 3 and 4F). Chlorpyrifos-oxon induced a significant inhibition at 0.1 μ M (83 \pm 3%; n = 62, N = 5; Fig. 4G) and inhibited the depolarization-evoked increase to 38 \pm 3% of control at 10 μ M (n = 62, N = 6; Figs. 3 and 4G). Cypermethrin inhibited the depolarization-evoked increase in $[Ca^{2+}]_i$ concentration-dependently at 1 nM (86 \pm 6%; n = 83, N = 5; Fig. 4H) and inhibited the depolarization-evoked increase to 5 \pm 0.6% at 10 μ M (n = 74, N = 5; Figs. 3 and 4H).

8.3.4 Effects of exposure to insecticides on basal $[Ca^{2+}]_i$ and depolarization-evoked increase in $[Ca^{2+}]_i$ in rat primary cortical cells

In control rat primary cortical cells, basal $[Ca^{2+}]_i$ was low and stable following acute exposure to 0.1% DMSO (113 \pm 3 nM, n = 101, N = 17; data not shown). Acute exposure to 10 μ M chlorpyrifos induced an increase in basal $[Ca^{2+}]_i$ of 107 \pm 15 nM in responding cells (90%; 41 out of 45 cells; data not shown). Interestingly, upon exposure of cells to endosulfan or cypermethrin, continuous oscillations in basal $[Ca^{2+}]_i$ were observed (Fig. 5). No changes in basal $[Ca^{2+}]_i$ were observed for 10 μ M chlorpyrifos-oxon upon acute exposure (data not shown).

Due to the observed continuous oscillations upon exposure to endosulfan or cypermethrin, inhibition of VGCCs could not be accurately determined as the oscillations could influence the sensitivity to the K^+ -induced depolarization and hampers reliable quantification of the inhibitory effects. Therefore, effects on the depolarization-evoked increase in $[Ca^{2+}]_i$ were only qualified for chlorpyrifos and chlorpyrifos-oxon.

Upon depolarization of control (0.1% DMSO) primary cells with high K^+ -containing saline, $[Ca^{2+}]_i$ increased rapidly and transiently to 1.5 \pm 0.08 μ M (n = 101, N = 17; data not shown). Following 20 min of exposure to 0.1% DMSO, the depolarization-evoked increase in $[Ca^{2+}]_i$ amounted to 1.0 \pm 0.05 μ M (n = 101, N = 17; data not shown). Following acute exposure to chlorpyrifos, the depolarization-evoked increase in $[Ca^{2+}]_i$ amounted to 116 \pm 7% of control at 0.1 μ M (n = 40, N = 6), and was significantly reduced to 62 \pm 4% of control at 1 μ M (n = 56, N = 5) and to 81 \pm 7% of control at 10 μ M (n = 45, N = 7; Fig. 6). Upon acute exposure to chlorpyrifos-oxon, the

depolarization-evoked increase in $[Ca^{2+}]_i$ amounted to $90 \pm 8\%$ of control at $0.1 \mu\text{M}$ ($n = 25$, $N = 4$), and was significantly reduced to $44 \pm 5\%$ of control at $1 \mu\text{M}$ ($n = 47$, $N = 6$) and to $67 \pm 7\%$ of control at $10 \mu\text{M}$ ($n = 43$, $N = 4$; data not shown).

To compare the effects of acute, subchronic and repeated exposure scenarios in PC12 cells with effects in primary cortical cells, primary cortical cells were also subchronically and repeatedly exposed to chlorpyrifos. In control primary cortical cells, basal $[Ca^{2+}]_i$ was low and stable following subchronic and repeated exposure to 0.1% DMSO ($107 \pm 4 \text{ nM}$, $n = 82$, $N = 7$; $125 \pm 3 \text{ nM}$, $n = 58$, $N = 5$, respectively; data not shown). In control cells subchronically exposed to 0.1% DMSO, depolarization-evoked increase in $[Ca^{2+}]_i$ amounted to $0.8 \pm 0.05 \mu\text{M}$ ($n = 82$, $N = 7$; data not shown). In control repeated exposure experiments, depolarization-evoked increase in $[Ca^{2+}]_i$ after the second exposure amounted to $0.7 \pm 0.04 \mu\text{M}$ ($n = 58$, $N = 5$; data not shown). The depolarization-evoked increase in $[Ca^{2+}]_i$ after subchronic exposure to chlorpyrifos was largely unchanged ($89 \pm 9\%$ at $1 \mu\text{M}$; $n = 43$, $N = 6$; and $104 \pm 10\%$ at $10 \mu\text{M}$; $n = 46$, $N = 4$; Fig. 6). However, following a second, repeated exposure, chlorpyrifos did reduce the depolarization-evoked increase in $[Ca^{2+}]_i$ significantly to $74 \pm 6\%$ at $1 \mu\text{M}$ ($n = 46$, $N = 5$) and to $61 \pm 3\%$ at $10 \mu\text{M}$ ($n = 41$, $N = 5$; Fig. 6).

8.4 DISCUSSION

Previously, we have demonstrated that insecticides from different classes acutely inhibit VGCCs. In the current study, we demonstrate that insecticides also inhibit VGCCs after subchronic and repeated exposure which are more relevant exposure scenarios for neurotoxicity testing because exposure to insecticides is generally (sub)chronically and repeatedly. Also, studies have previously shown that prolonged insecticide exposure may change the potency of insecticides for neurotoxicity (e.g. Cao et al, 2014; Slotkin and Seidler, 2008). This study demonstrates that the potency of most insecticides for inhibition of VGCCs is comparable for acute and repeated exposure and also that the potency of insecticides for inhibition of VGCCs is lower in subchronic exposure conditions. In addition, the inhibition of VGCCs appeared not or slowly reversible.

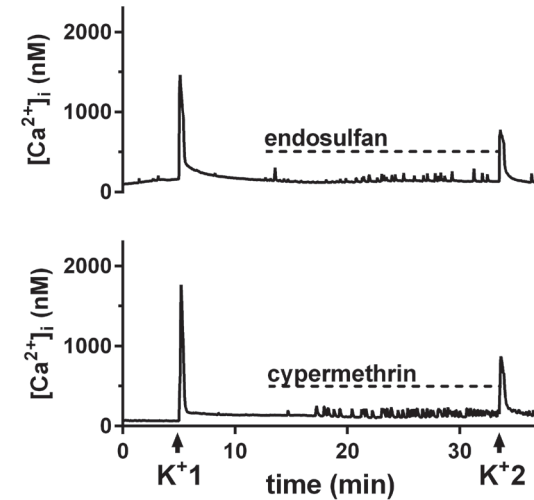


Figure 5: Representative recordings of $[Ca^{2+}]_i$ from individual primary cortical cells exposed acute to endosulfan ($10 \mu\text{M}$) or cypermethrin ($1 \mu\text{M}$). Primary cortical cells were exposed for 20 min (acute) to endosulfan or cypermethrin as indicated by the dashed line in the recordings. Cells were depolarized at 5 and 33.3 min as indicated by K^+1 and K^+2 .

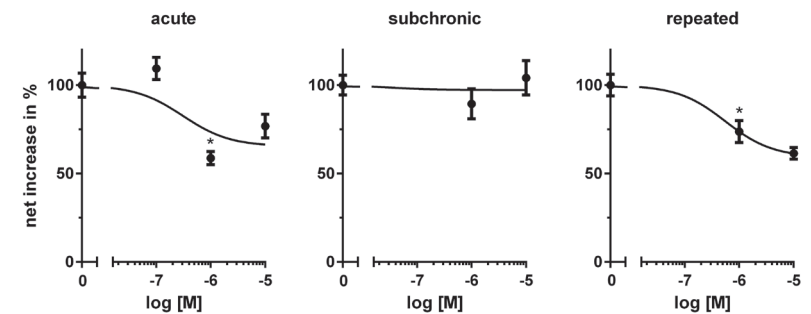


Figure 6: Concentration-response curves of inhibition of the depolarization-evoked increase in $[Ca^{2+}]_i$ by chlorpyrifos after acute (left), 24h subchronic exposure (middle) and after subsequent repeated exposure (right) in primary cortical cells. Chlorpyrifos inhibits the depolarization-evoked increase in $[Ca^{2+}]_i$ concentration-dependently after acute and repeated exposure. Data represent mean \pm SEM ($n = 40-101$, $N = 4-17$). An asterisk indicates the lowest concentration that is significantly different from the control ($p < 0.05$).

The observation of not or slowly reversible inhibition of VGCCs in subchronic exposure conditions suggests that a single subchronic (24h) exposure could have prolonged consequences for VGCCs function. Prolonged effects of insecticides on neurotoxicological targets have been reported before *in vitro*, e.g., a decrease in GABA_A receptor function by long-term (6 days) dieldrin exposure (Babot et al., 2007). Also, *in vivo* studies indicated that subacute and repeated exposure to chlorpyrifos could result in persistent effects on neurotoxicological endpoints, e.g., neurobiochemistry and neurobehavior were permanently changed by chlorpyrifos in animals (e.g., Chakraborti et al., 1993, Moser et al., 2005). We therefore hypothesized that the not or slowly reversible inhibition of VGCCs could affect the response upon subsequent repeated exposure, in particular for persistent and bioaccumulative chemicals like endosulfan. Our experiments demonstrate that repeated exposure indeed augmented the insecticide-induced inhibition of VGCC. However, our experiments with repeated exposure conditions also reveal that cypermethrin, chlorpyrifos-oxon, and endosulfan are basically equipotent in inhibiting VGCCs in a repeated exposure condition compared with acute exposure (Table 2). Inhibitory concentrations of insecticides that induced a 20 or 50% inhibition (IC₂₀ and IC₅₀ respectively) in acute and repeated exposure conditions were generally in the same order of magnitude. The exception to this is chlorpyrifos, which was clearly more potent in the repeated exposure scenario compared with the acute exposure condition in PC12 cells (Table 2). Nevertheless, the results suggest that the difference in potency of insecticides for inhibition of VGCCs between the two exposure conditions was generally limited and that the effects induced by a preceding subchronic exposure hardly influence the degree of inhibition of VGCCs by a repeated, acute exposure.

The observed higher potency for chlorpyrifos after repeated exposure compared with acute exposure in PC12 cells are likely the result of adaptive mechanisms. As described, studies on subacute and repeated exposure to chlorpyrifos have shown persistent and permanent changes on neurotoxicological endpoints and we have demonstrated that the inhibition in VGCCs was not or slowly reversible. This suggests that adaptive mechanisms, such as gene expression, protein function, phosphorylation or ubiquitination of VGCCs and/or changes in VGCCs turnover (Lipscombe et al., 2013), may play a role in the availability, functionality, and/or binding affinity of VGCCs. However, it remains to be determined which adaptive

mechanisms are involved and why particularly for chlorpyrifos an increased inhibition of VGCCs was observed after repeated exposure compared to acute exposure.

Previously, we have compared the effective concentrations of the presumed primary modes of action of organophosphates, organochlorines, and pyrethroids with effective concentrations for acute inhibition of VGCCs by chlorpyrifos, endosulfan, and cypermethrin (Meijer et al., 2014b). This comparison suggested that effective concentrations for acute inhibition of VGCCs by insecticides were lower compared to effective concentrations of the presumed primary modes of action, with the exception of chlorpyrifos-oxon (Meijer et al., 2014a,b). In case of repeated exposure, effective concentrations for inhibition of VGCCs by insecticides are thus also lower compared with the effective concentrations of the presumed primary modes of action of insecticides, with the exception of chlorpyrifos-oxon (Table 2). In case of subchronic exposure, effective concentrations of chlorpyrifos, chlorpyrifos-oxon, and endosulfan were comparable or higher compared with the effective concentrations of the primary modes of action (Table 2). Although inhibition of VGCCs thus appears a sensitive endpoint, it must however be noted that for the different studies different experimental models were used. These different models may differ in sensitivity due to the expression of different ion channels and/or receptors and presence/absence of potential feedback mechanisms (e.g., *Xenopus* oocytes). Also, different exposure scenarios were used in these experimental models that, in combination with the different properties of the model, may have influenced the effective concentrations.

Notably, earlier studies on VGCCs demonstrated that beside a variety of insecticides (organophosphates, organochlorines, pyrethroids: Heusinkveld and Westerink, 2012; Hildebrand et al., 2004; Liu et al., 1994; Meijer et al., 2014a,b; Neal et al., 2010; Yan et al., 2011), fungicides (Heusinkveld et al., 2013), PCBs (Langeveld et al., 2012), and brominated and halogen-free flame retardants (Dingemans et al., 2009, 2010; Hendriks et al., 2014) and other neurotoxicants can acutely inhibit VGCCs. Because VGCCs are essential for the regulation of calcium signaling, which is crucial for proper neuronal cell function (Simms and Zamponi, 2014; Westerink, 2006), development (Leclerc et al., 2011), and survival (Zündorf and Reiser, 2011), the investigation of chemical-induced inhibition of VGCCs can be useful for screening chemicals for neurotoxicity. Obviously, chemicals

that specifically affect postsynaptic targets, such as the imidacloprid-induced modulation of nAChRs (Matsuda et al., 2009), may remain undetected. Consequently, a neurotoxicity screening battery should consist of a range of endpoints to include additional neurotoxicological targets. For this study, PC12 cells were used because they express L-, N-, and P/Q-type VGCCs (Dingemans et al., 2009). The observed complete inhibition of VGCCs by insecticides thus indicates that the insecticides inhibit all VGCCs types present in PC12 cells. Calcium channels in PC12 cells are comparable with neurons and PC12 cells are therefore a suitable model for screening for effects on VGCCs as a measure of neurotoxicity (Westerink, 2013). Also, we show that primary rat cortical cells are a less sensitive cell model for the investigation of effects specifically on VGCC inhibition. Primary rat cortical cells constitute a physiologically relevant model and these heterogeneous cultures form spontaneously active neuronal networks. However, effects on VGCCs can be thus obscured due to interaction with additional targets. Many chemicals have additional targets, such as VGSCs in case of cypermethrin and GABA receptors in case of endosulfan, which may cause, e.g., continuous oscillations in basal $[Ca^{2+}]_i$ that could interfere with the depolarization-evoked increase in $[Ca^{2+}]_i$. For chlorpyrifos exposure, no continuous oscillations in primary cortical cells were observed and effects of chlorpyrifos on VGCCs could be determined. These data show that chlorpyrifos induces a comparable rank order potency for the different exposure scenarios in PC12 cells and primary cortical cells. However, the level of inhibition in cortical cells was lower compared with the inhibition observed in PC12 cells. This may be due to the use of serum in the medium of primary cortical cells, potentially decreasing the free insecticide concentrations, but may also be explained by interactions between different types of neurons that express different ion channels and receptors. Taken together, the current data indicate that primary cortical neurons may not be sufficiently sensitive to reliably detect effects on VGCCs by insecticides. However, for the measurement of, e.g., electrical activity, spontaneously active primary cultures, such as primary cortical neurons, are preferred. Therefore, for each endpoint, the most appropriate cell model should be selected and consequently, within a battery of screening methods for neurotoxicity various cell types and lines should be used (Coecke et al., 2007; Westerink, 2013).

In conclusion, our data (together with other studies) demonstrate that VGCCs are an important target for screening insecticides (and other chemicals) for neurotoxicity. Inhibition of VGCCs could be part of a battery of functional *in vitro* neurotoxicity tests. Furthermore, our data indicate that investigation of effects of acute exposure to chemicals is generally sufficient to detect insecticide (or chemical)-induced inhibition of VGCCs. However, some differences in potency of insecticides for inhibition of VGCCs were observed between the exposure scenarios, which argues for the inclusion of repeated exposure conditions for specific studies.

Table 2: Summary of inhibitory concentrations of insecticides (in nM) that induced a 20% or 50% inhibition of VGCCs after subchronic (24h), repeated or acute exposure and inhibitory concentrations of insecticides that induced a 50% inhibition of their presumed primary modes of action.

Insecticides	Subchronic		Repeated		Acute ^{1,2*}		Primary mode of action ^{1,3,4,5,6}
	IC ₂₀	IC ₅₀	IC ₂₀	IC ₅₀	IC ₂₀	IC ₅₀	
Carbaryl	>10 ⁴	>10 ⁴	>10 ⁴	>10 ⁴	>10 ⁴	>10 ⁴	990
Imidacloprid	>10 ⁴	>10 ⁴	>10 ⁴	>10 ⁴	>10 ⁴	>10 ⁴	1000 (LOEC)
Endosulfan	3798	9440	42	206	215	362	400 and 1000
Chlorpyrifos	859	>10 ⁴	35	179	188	1331	>50 ⁴
Chlorpyrifos-oxon	54	>10 ⁴	659	3977	231	>10 ⁴	9
Cypermethrin	250	931	6	97	6	92	10 ⁴

Legend color code (nM):

≥10 ⁴
≥1000- <10 ⁴
≥100- <1000
≥10- <100
≥1- <10

¹ Meijer et al., 2014b: VGCCs inhibition and AChE inhibition

² Meijer et al., 2014c: VGCCs inhibition

³ Kimura-Kuroda et al., 2012: nAChR agonist

⁴ Vale et al., 2003: GABA-R inhibition

⁵ Huang and Casida, 1996: GABA-R inhibition

⁶ Meacham et al., 2008: modification VGSCs currents

* data were recalculated from treatment ratios (TR) to net Ca²⁺ for comparison

Acknowledgements

The authors acknowledge the European Commission [DENAMIC project; grant number FP7-ENV-2011-282957] and the Faculty of Veterinary Medicine of Utrecht University for funding, and the members of the Neurotoxicology Research Group for helpful discussions.

Funding

This work was supported by the European Commission [DENAMIC project; grant number FP7-ENV-2011-282957] and the Faculty of Veterinary Medicine of Utrecht University.

The authors declare to have no competing financial interests.

Handwritten physics notes and diagrams:

- $U = EB$
- low resistance: $R_1 = 13.5 \Omega$, $R_2 = 3 \Omega$, $R_3 = 20 \Omega$
- $F_A = \rho g V$, $w = D \uparrow$, $w = 0$
- $\vec{u} = \frac{y}{BC} \vec{e}_x + 0 \vec{e}_y + z \vec{e}_z$
- $P = \bar{S}$
- Graph of $\chi_w T$ vs w showing a peak labeled "Plank".
- $\omega^2 = \frac{mgL}{I}$; $T = \frac{2\pi}{\omega} = 2\pi \sqrt{\frac{I}{mgL}}$
- $x = \rho \cos \varphi$, $y = \rho \sin \varphi$
- $\rho = \sqrt{x^2 + y^2}$
- $q = \frac{h}{\lambda} = \frac{h}{\frac{v}{f}} = \frac{hf}{v}$
- $\frac{h}{\lambda} = \frac{10m}{\frac{v}{5m}} \rightarrow ?$
- Coordinate system: $x' = x_0 + mt'$, $y' = y_0 + nt'$, $z' = z_0 + pt'$
- Formula for σ 's
- 1) $T = \frac{t}{n}$
- 2) $v = \frac{c}{n}$
- 3) $\omega = \frac{2\pi}{T}$
- 4) $\lambda = \frac{v}{f}$
- 5) $T = \frac{2\pi}{\omega}$
- Diagram of a circuit with a battery, a resistor, and a capacitor.
- Diagram of a pendulum.
- Diagram of a spring-mass system.
- $\frac{d^2x}{dt^2} + \gamma \frac{dx}{dt} = 0$
- $I = \frac{U}{R}$
- $\downarrow \vec{D} = \text{const}$, $\uparrow \vec{a} = \text{const}$
- $D = \frac{p \cdot l}{S}$
- $S = ?$

Part IV

Ex vivo study



Chapter 9

EFFECTS OF A SINGLE, ORAL DOSE OF CHLORPYRIFOS DURING A CRITICAL PERIOD OF BRAIN DEVELOPMENT IN MICE ON HIPPOCAMPAL LONG-TERM POTENTIATION

Marieke Meijer, Remco H.S. Westerink

Institute for Risk Assessment Sciences, Utrecht University,
Utrecht, the Netherlands

ABSTRACT

Chlorpyrifos is a widely used insecticide associated with adverse health effects in animals and humans. There are indications that chlorpyrifos can affect synaptic plasticity. Therefore, the current study has investigated the effects of chlorpyrifos on long-term potentiation (LTP), which is an electrophysiological measure of synaptic plasticity and learning and memory.

Mice were exposed to a single oral dose of 1 or 10 mg/kg bw chlorpyrifos at PND10 and LTP was measured in hippocampal slices when mice were ~5 months of age. With a comparable exposure scenario, it was previously shown that chlorpyrifos can alter spontaneous behavior.

Our results show no decrease in LTP 0-60 min after LTP induction in animals exposed to a single dose of 1 and 10 mg/kg bw chlorpyrifos at PND10. However, interpretation of the results was hampered by the low amount of slices used for the study.

In conclusion, the data suggests that chlorpyrifos has no effects on LTP and that effects on LTP are not related to chlorpyrifos-induced effects on spontaneous behavior.

9.1 INTRODUCTION

Chlorpyrifos is a widely used insecticide that is well-known for its neurotoxic effects in mammals (Eaton et al., 2008). Several epidemiological studies have associated chlorpyrifos exposure with adverse health effects in humans (Eaton et al., 2008). Moreover, various animal studies have demonstrated that chlorpyrifos has effects on various neurobehavioral parameters, such as motor activity, habituation and cognition (e.g. Icenogle et al., 2004; Moser et al., 2005). Additionally, *in vitro* studies have shown various effects of chlorpyrifos on neur(on)al processes and functions, including inhibition of neurite outgrowth (e.g. Howard et al., 2005), nicotinic acetylcholine receptor (nAChR) function (Smulders et al., 2004) and voltage-gated calcium channels (VGCCs; Meijer et al., 2014a,b, 2015).

Interestingly, toxicogenomics studies have demonstrated that chlorpyrifos exposure can also change gene expression of proteins involved in long-term potentiation (LTP; Stapleton and Chan, 2009; Moreira et al., 2010), which suggests that chlorpyrifos can affect synaptic plasticity. As such, effects on synaptic plasticity could be an underlying mechanism for the observed neurobehavioral effects induced by chlorpyrifos. However, it is currently not clear if synaptic plasticity is altered in animals exposed to chlorpyrifos.

Therefore, in the present study the effects of chlorpyrifos on synaptic plasticity were studied by investigating the effects of chlorpyrifos on LTP. LTP is a measure of synaptic plasticity and learning and memory (e.g. Martin et al., 2000). In the current study, LTP is studied in hippocampal brain slices of mice of ~5 months of age, which were exposed to a single, oral dose of chlorpyrifos during a critical period of brain development. A comparable exposure paradigm with chlorpyrifos and various other neurotoxic chemicals has previously been shown to induce neurobehavioral effects in mice of 2 and 4 months of age (Lee et al., 2015a,b; Buratovic et al., 2014).

9.2 MATERIALS AND METHODS

9.2.1 Animals

Pregnant NMRI (Naval Medical Research Institute) mice, obtained from Scanbur (Sollentuna, Sweden) were housed individually in plastic cages (40 ´ 25 ´ 15 cm) in a room with an ambient temperature of 22°C and a 12/12h

light/dark cycle. The animals were fed standardized pellets (Lactamin, Stockholm, Sweden) and tap water ad libitum. The pregnant NMRI mice were checked for parturition twice daily (08.00 and 18.00h). The day of birth is designated day 0 (birth during the preceding night was designated day 0 when checked at 08.00h). Litter sizes were adjusted and standardized to 8-12 pups within the first 48h after birth by euthanizing excess pups. The litters contained pups of both sexes, in about equal numbers during the neonatal period, no separation with regard to sex was made in the pre-weanlings. At around 4 weeks of age, male and female mice were separated and the males of each litter were kept together and raised in groups of 4-7 in a room for males only, under conditions as described above. Only male mice were used in order to compare with previously performed animal studies.

On PND 10, neonatal mice were exposed to chlorpyrifos at 1.0 or 10 mg/kg bw. Chlorpyrifos, was purchased from Sigma (The Netherlands). Chlorpyrifos was dissolved in a mixture of egg lecithin (Merck, Darmstadt, Germany) and peanut oil (*Oleum arachidis*; 1:10) and then sonicated together with water to yield a 20% (w:w) fat emulsion vehicle and given orally in a volume of 10 ml/kg body weight via a metal gastric-tube. Control animals received a 20% fat emulsion vehicle in a volume of 10 ml/kg bw. Animals were housed and treated at Uppsala University, Sweden until 10 weeks of age. Next, they were shipped to the VU University Amsterdam, The Netherlands, for subsequent behavioral studies prior to the use of these animals for the current study.

9.2.2 Induction and measurement of long-term potentiation (LTP)

LTP as a measure of synaptic plasticity was measured as described previously (Végh et al., 2014). Mice ~4.5-6 months of age were sacrificed by decapitation without anesthesia. The brains were rapidly removed and placed in ice-cold slice buffer medium (124 mM NaCl, 3.3 mM KCl, 1.2 mM KH_2PO_4 , 7 mM MgSO_4 , 0.5 mM CaCl_2 , 20 mM NaHCO_3 and 10 mM glucose; constantly gassed with 95% O_2 and 5% CO_2). Next, coronal hippocampal slices of 400 μm thick were cut with a vibrating microtome (Thermo Scientific MH650v) in ice-cold slice buffer medium constantly gassed with 95% O_2 and 5% CO_2 . Slices were transferred to a chamber containing

artificial cerebrospinal fluid (aCSF; 124 mM NaCl, 3.3 mM KCl, 1.2 mM KH_2PO_4 , 1.3 mM MgSO_4 , 2.5 mM CaCl_2 , 20 mM NaHCO_3 and 10 mM glucose; constantly gassed with 95% O_2 and 5% CO_2) at room temperature for > 1h. Slices were placed on multi-electrode arrays (8x8) containing P5155 probes that were pre-coated with polyethylenimine (PEI; Sigma) for > 1h. The CA3-CA1 region of the slices were manually located on the probes with a microscope (SZ61; Olympus, Japan) followed by the addition of ~500 μL aCSF to the array. To prepare the slices for the measurements, the array with the slice was placed in a moist chamber (constantly gassed with 95% O_2 and 5% CO_2) for > 1h. Following incubation in the moist chamber, arrays were placed in a multi-electrode recording setup (MED64 system; Alpha Med Sciences, Tokyo, Japan) to record field excitatory postsynaptic potentials (fEPSPs) from multiple electrodes located on the stratum radiatum of the CA1. The Schaffer collateral pathway was stimulated with an external concentric bipolar electrode (CBCBG75; FH-Company, Bowdoin, ME) with an isolated Bipolar Current Stimulator (model 440b). A stimulus-response curve was measured to extrapolate a stimulation intensity that evoked a 50% fEPSP response from the maximum fEPSP response. After a stable baseline recording of 10 min, LTP was evoked by theta burst stimulation (TBS) with a 2 x 100 Hz stimulus of 1 s each with a 15 s interval. fEPSPs were recorded every 20 s for 60 min following the tetanus stimulation. During the entire recording, slices were constantly perfused with oxygenated aCSF containing 10 μM glycine and 10 μM bicuculline to enhance fEPSPs at a flow rate of 2 mL/min at room temperature.

9.2.3 Data analysis and statistics

LTP was calculated as the change in amplitude of the fEPSPs (Fig. 1) relative to the baseline of ~2 (1 - 3) electrodes located in the stratum radiatum. Slices were included in the analysis if 1) stable fEPSPs were obtained for 60 min after TBS induction, and 2) if the signal-noise ratio of fEPSPs were sufficient (assessed blindly by 2 researchers). Data are expressed as average \pm standard error of the mean (SEM) of 4 - 6 slices (*N*) per condition. Statistical significance was determined with an one-way ANOVA and posthoc *bonferroni* test. Data were considered statistically significant if $p < 0.05$.

9.3 RESULTS

9.3.1 Long-term potentiation (LTP)

Upon induction of LTP by tetanic burst stimulation (TBS; 2 x 100 Hz stimulus of 1 s), an immediate increase in the fEPSP amplitude was observed (Fig. 2A). Compared with the control, the fEPSP amplitude within the first 10 min after LTP induction was not significantly reduced in slices from animals treated with 1 and 10 mg/kg chlorpyrifos (control: $118 \pm 5\%$, $N = 4$; 1 mg/kg: $126 \pm 3\%$, $N = 6$; 10 mg/kg: $113 \pm 2\%$, $N = 4$; Fig. 2B). Also, for the remaining 50 min (divided in 10 min intervals) no significant reduction in LTP was observed between control and exposed animals. Also, when the results of slices from 10 mg/kg treated animals were compared with 1 mg/kg treated animals, no significant reduction in LTP was observed.

9.4 DISCUSSION

Previously, it has been shown that spontaneous behavior (locomotion and rearing activity) is reduced in mice exposed to a single dose of BDE-47 at PND10 when they are 2 or 4 months of age (Eriksson et al., 2001). Another study identified LTP as a possible underlying mechanism of these changes in spontaneous behavior (Dingemans et al., 2007). In addition, a comparable exposure scenario has demonstrated (long lasting) effects of chlorpyrifos on spontaneous behavior (Lee et al., 2015a). Therefore, for this study a comparable exposure scenario was used to investigate if changes in LTP could be observed at doses that alter spontaneous behavior. However, inhibition in LTP was not observed at 1 and 10 mg/kg bw, which suggests that changes in spontaneous behavior are not correlated with changes in LTP.

A minor, insignificant reduction was observed between 1 and 10 mg/kg bw chlorpyrifos from 0-30 min after LTP induction, which may suggest that at higher doses LTP may be further reduced. However, no solid conclusions can be drawn due to the limited amount of slices (low power) used for the analysis in this study. In addition, higher doses of chlorpyrifos are of less relevance for developmental exposure as chlorpyrifos exposure to developing organisms is generally low. On the other hand, a small effect at a low dose that induces an effect on LTP ~5 months after exposure to a single dose of chlorpyrifos could be of concern for neurodevelopment. It would demonstrate a long-lasting effect of chlorpyrifos on LTP that could

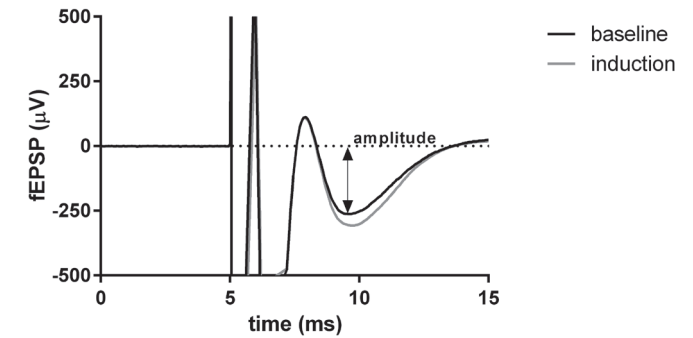


Figure 1: Example fEPSP during baseline recording (black line) and after TBS induction (grey line). The change in amplitude evoked by TBS was used to calculate the percentage LTP.

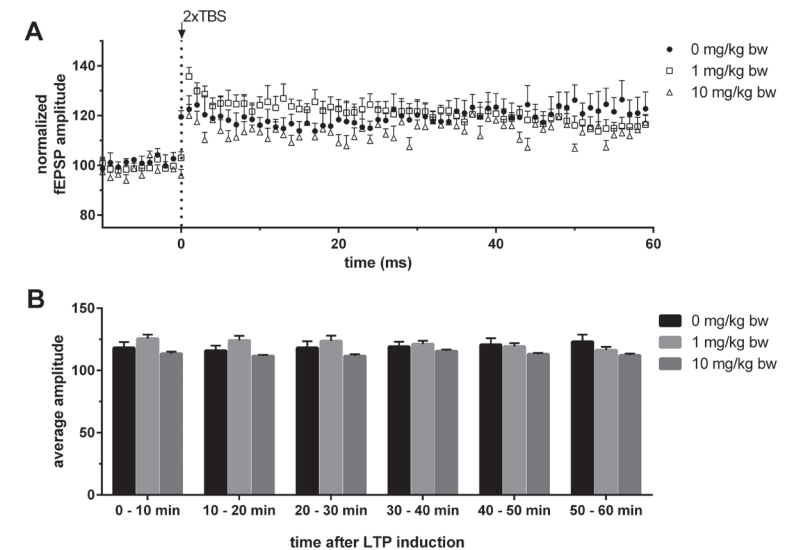


Figure 2: A) Normalized fEPSP amplitude data. After a 10 min baseline recording of fEPSPs, LTP was evoked by TBS and fEPSPs were recorded for another 60 min. Data are expressed as average \pm SEM relative to the baseline. For better graphical representation, only every third point in the timeline is shown. **B)** Average amplitude of fEPSPs after induction of LTP. Data are expressed as average \pm SEM ($N = 4-6$) of the baseline of a 10 min interval.

be of concern considering that neurodevelopment is a tightly regulated process and small changes in neuronal functions may contribute to altered neuronal function later in life (e.g. Rice and Barone Jr., 2000). Interestingly, a comparable study (Lee et al., 2015a) showed that CaMKII was decreased after 24h of exposure to chlorpyrifos but was no longer decreased after 4 months (despite long lasting changes in behavior). Considering the importance of CaMKII for LTP, this may suggest that LTP could be affected early after exposure, but is no longer affected in animals 5 months of age.

In this study, slices exposed to the vehicle control showed a relatively small increase in LTP (~20% increase in fEPSP after TBS) compared with other LTP experiments, which show an effect of ~50-100% (e.g. Freret et al., 2012). The experimental conditions used for this study were previously established for C57BL/6 mice (Végh et al., 2014). However, it has been shown that different mouse strains have different LTP responses (e.g. Nguyen et al., 2000) and the NMRI mice may have a lower LTP response compared with other mouse strains. However, previous studies with NMRI mice measured high(er) LTP responses (Freret et al., 2012), though, comparison with the current study is difficult as the studies differed in type of TBS, recording method and in the age of the animals used. Altogether, the small induction of LTP in control animals in this study indicate that the signal-noise ratio and low amount of slices are not sufficient to detect subtle effects on learning and memory in mice.

In conclusion, the current study has demonstrated that chlorpyrifos induces no changes in LTP in mice of ~5 months of age exposed to a single dose of 1 or 10 mg/kg bw chlorpyrifos at PND10. This study has used a comparable exposure scenario with a previous study that has demonstrated that chlorpyrifos alters spontaneous behavior (Lee et al., 2015a), suggesting that changes in LTP are not correlated with alterations in spontaneous behavior and that likely other underlying mechanisms play a role.

Acknowledgements

The authors thank P. Eriksson, I. Lee, and H. Viberg for providing and exposing the animals, M.M.L. Dingemans, T. Hamers, R.E. van Kesteren, P.E.G. Leonards, and R.M. Meredith for helpful discussions and M.M.L. Dingemans, T. Heistek, R. van der Loo, M. Loos, A.J. Timmermans, and R. Wijnands for excellent technical assistance.

Handwritten physics notes and diagrams:

- $U = \epsilon B$
- low resistance: $R_1 = 13.5 \Omega$, $R_2 = 3 \Omega$, $R_3 = 20 \Omega$
- $F_A = \rho g V$, $w = D \uparrow$, $w = 0$
- $z = u$
- $P = \bar{S}$
- Graph: $X_{w,T}$ vs w , labeled "Plank".
- $\omega = h \frac{c}{\lambda_0}$
- $w^2 = \frac{mgL}{I}$; $T = \frac{2\pi}{\omega} = 2\pi \sqrt{\frac{I}{mgL}}$
- $x = \rho \cos \varphi$, $y = \rho \sin \varphi$
- $\rho = \sqrt{x^2 + y^2}$
- $q = \frac{h}{\lambda} = \frac{h}{v \cdot t} = \frac{h}{v} \cdot \frac{1}{t}$
- $\frac{h}{v} = \frac{10m}{v} \rightarrow ?$
- $x' = x_0 + mt'$
- $y' = y_0 + nt'$
- $z' = z_0 + pt'$
- Formula for s
- 1) $T = \frac{t}{n}$
- 2) $v = \frac{c}{n}$
- 3) $w = \frac{v}{\lambda}$
- 4) $T = \frac{1}{f}$
- 5) $v = \frac{2\pi r}{T}$
- Diagram: A circuit with a battery, a resistor, and a capacitor.
- Diagram: A vector diagram showing \vec{v} and \vec{a} .
- Diagram: A diagram of a pendulum or similar system.
- Diagram: A diagram of a spring-mass system.
- Diagram: A diagram of a circuit with a battery and a resistor.
- Diagram: A diagram of a circuit with a battery and a resistor.
- $I = \frac{U}{R}$
- $\downarrow \vec{v} = \text{const}$
- $\uparrow \vec{a} = \text{const}$
- $D = \frac{p \cdot l}{\dots}$
- $S = ?$

Part V

Summary, discussion, and recommendations



Chapter 10

SUMMARY AND DISCUSSION

Chemical legislation requires that safety information of chemicals is obtained with studies performed according to specific guidelines. Studies described in these guidelines are generally *in vivo* studies. Due to the REACH regulation, more animal studies for regulatory safety studies are needed in the coming years unless suitable alternatives become available. In addition, regulatory neurotoxicity tests have been criticized for their low sensitivity and the large amount of animals, time and money that are needed to perform these studies (e.g. Coecke et al., 2007; Vorhees and Makris, 2015). There is thus a need for sensitive regulatory neurotoxicity tests that are fast, cheap and require (no or) less animals (Bal-Price et al., 2008, 2010; Coecke et al., 2007). Therefore, in this thesis several *in vitro* targets and methods for the development of *in vitro* screening tools for (developmental) neurotoxicity have been investigated as part of the EU project DENAMIC.

10.1 TARGETS AND ASSAYS FOR SCREENING FOR NEUROTOXICITY

In this thesis, *in vitro* methods for the investigation of chemical-induced oxidative stress, neurotransmitter release and calcium homeostasis were evaluated. Considering their relevance for proper neuronal function, these endpoints are very suitable for chemical neurotoxicity screening. Before these endpoints can be used for neurotoxicity testing *in vitro*, methods for the detection of chemical-induced effects on these endpoints should be carefully evaluated.

10.1.1 Cell viability

To identify concentrations below which specific effects on neurotoxicity can be detected in PC12 cells, cell viability studies were performed (concentration-range finding; chapter 2).

An active and a passive measure of cytotoxicity was included as differences in sensitivity between assays exist. For example, a cell could have low mitochondrial activity, but still have an intact membrane. An active measure of cytotoxicity may indicate mitochondrial dysfunction rather than actual cytotoxicity and could thus be a less reliable measure of cytotoxicity compared with a passive measure. On the other hand, passive assays could be considered less sensitive compared with active measures of cytotoxicity. Due to such differences in sensitivity between

cell viability assays, different measures of cell viability should be used for concentration-range finding studies.

Effects on cell viability were not observed for most chemicals or only at high concentrations (10-100 μM), with the exception of the developmental neurotoxicant methylmercury (MeHg) and the metabolite of the brominated flame retardant BDE-47, 6-OH-BDE-47. MeHg increased the mitochondrial activity already at 0.1 μM and decreased membrane integrity at $\geq 1 \mu\text{M}$. Therefore, for further studies maximum test concentrations of 10 μM (with the exception of MeHg: tested at 0.1 μM) of the chemicals of interest were used to prevent confounding of the results by cytotoxicity.

10.1.2 Oxidative stress

The H_2DCFDA and $\text{BODIPY}^{\circledast}581/591$ C11 assays were evaluated in this thesis as possible candidates for the investigation of chemical-induced oxidative stress (chapter 3). ROS are important indicators of oxidative stress and dyes designed to detect ROS should be able to quickly react with the different types of ROS. H_2DCFDA can react with ROS, but is also easily converted to its fluorescent compound by exposure to the air. Moreover, it was demonstrated here that H_2DCFDA is also prone to interfere with (extracellular) chemicals. Altogether, ROS detection with H_2DCFDA is associated with potential pitfalls and must be carefully applied when used for the detection of chemical-induced oxidative stress.

Possibly, the detection of damage to DNA, protein or lipids by oxidative stress is a more stable measurement of oxidative stress. Therefore, $\text{BODIPY}^{\circledast}581/591$ C11, a lipid peroxidation sensor with potential for real-time detection of lipid peroxidation, was evaluated. However, $\text{BODIPY}^{\circledast}581/591$ C11 could not be applied as a lipid peroxidation sensor in our set-up. This may have been due to the formation of excimers (dimers) by $\text{BODIPY}^{\circledast}581/591$ C11 that quench the fluorescent signal (Drummen et al., 2002). A frequently used assay for the detection of lipid peroxidation is the TBARS assay, which is based on the reaction of thiobarbituric acid with malondialdehyde (MDA), a peroxidized lipid product. However, thiobarbituric acid non-specifically binds MDA and thiobarbituric acid-based assays are therefore prone to false-positives. On the other hand, MDA can be detected with antibodies (e.g. with an ELISA), though these methods are expensive and generally not high-throughput. Besides MDA, other lipid peroxidation products could be formed and detection of lipid

peroxidation solely based on MDA could result in false-negatives (Moore and Roberts, 1998). In conclusion, current assays to assess oxidative stress are associated with potential pitfalls and other assays that investigate oxidative stress should therefore be identified and evaluated.

10.1.3 Neurotransmission

Neurotransmitter release

Neuronal cells communicate via neurotransmission, which involves the release of neurotransmitters in the synaptic cleft and is thus essential for proper neuronal communication (e.g. Sarter et al., 2007). Neurotransmitter release depends on proper function of signaling pathways regulated by various receptors and ion channels (such as VGCCs) and is an integrated endpoint for the investigation of chemical-induced neurotoxicity. It is a fast and dynamic process and real-time detection methods should be able to rapidly detect neurotransmitters. Methods for the detection of dopamine exist, though are time consuming, such as HPLC and amperometry, and are not suitable for high-throughput real-time detection of dopamine release. In this thesis, several methods for the *in vitro* detection of real-time dopamine release were evaluated (chapter 4). Particularly, fluorescent false neurotransmitters (FFNs) were evaluated for their potential use to study chemical-induced neurotransmitter release. FFNs are normally used in combination with high resolution microscopy, such as confocal microscopy. However, FFNs (and other evaluated methods) appeared not suitable for the detection of dopamine in biological samples when used with e.g. plate readers or 2D fluorescence microscopy, which can be applied with high(er) throughput but have low(er) sensitivity. Potentially, dopamine could be detected with electrodes (amperometry) in a high-throughput manner and this is currently under development in other laboratories (Wang et al., 2014; Wang and Ewing, 2014). In conclusion, no high-throughput and real-time assays for neurotransmitter release exists up to now. Therefore, additional studies are needed to identify reliable tools and methods for the investigation of chemical-induced alterations in neurotransmitter release.

Calcium homeostasis

Generally, real-time kinetic changes in calcium homeostasis are measured by either a plate reader-based method or a fluorescence microscopy-based method. However, plate reader-based methods have been criticized

because of their low(er) temporal and spatial resolution, low(er) sensitivity and potential pitfalls and artifacts (Heusinkveld and Westerink, 2011; Westerink and Hondebrink, 2010). In this thesis, a direct comparison was made between results obtained in a plate reader- and a fluorescence microscopy-based method (chapter 5). A test set of four chemicals was used to investigate acute chemical-induced changes in basal $[Ca^{2+}]_i$ and depolarization-evoked increase in $[Ca^{2+}]_i$ with both methods. Results obtained with the plate reader-based method did not show consistent changes in basal $[Ca^{2+}]_i$ or in the depolarization-evoked increase in $[Ca^{2+}]_i$ for the test compounds. In contrast, the fluorescence microscopy-based method demonstrated that three out of four chemicals induced an increase in basal $[Ca^{2+}]_i$ and that all four chemicals inhibited the depolarization-evoked increase in $[Ca^{2+}]_i$. Consequently, the plate reader-based method did not identify any of the test chemicals as neurotoxic compared to the fluorescence microscopy-based method, which did identify all chemicals as neurotoxic. Considering the high-temporal and spatial resolution of fluorescence microscopy and the lack of effects observed in the plate reader-based method, all other studies in this thesis on calcium homeostasis were performed with a fluorescence microscopy-based method.

This thesis has extensively investigated the effects of insecticides on calcium homeostasis (chapters 6, 7 and 8). As mentioned earlier, effects on calcium homeostasis were investigated since it plays an essential role in neuronal function. Moreover, it has previously been demonstrated that different types of chemicals such as PBDEs, PCBs, and the organochlorine insecticide lindane can increase basal $[Ca^{2+}]_i$ in neuronal cells (Dingemans et al., 2009, 2010; Heusinkveld et al., 2010; Langeveld et al., 2012). In addition, these chemicals were also shown to inhibit VGCCs (Dingemans et al., 2009, 2010; Heusinkveld et al., 2010; Langeveld et al., 2012). Several drugs of abuse, azole fungicides and the organochlorine insecticide dieldrin did not increase basal $[Ca^{2+}]_i$, but were able to inhibit VGCCs (Heusinkveld et al., 2013; Heusinkveld and Westerink, 2012; Hondebrink et al., 2012). In our studies, we extended on these findings and demonstrated that calcium homeostasis is a target for neurotoxic insecticides and could be used for neurotoxicity screening studies. It was demonstrated that different types of insecticides (organophosphates, organochlorines, pyrethroids) can acutely change basal $[Ca^{2+}]_i$ and/or acutely inhibit VGCCs at low concentrations. Specifically, the organophosphates chlorpyrifos, its

metabolite chlorpyrifos-oxon and the organochlorine insecticide endosulfan were able to increase basal $[Ca^{2+}]_i$ at 10 μ M in a subpopulation of PC12 cells. The organochlorine endosulfan, the organophosphates chlorpyrifos, chlorpyrifos-oxon, and parathion and the pyrethroids (α -cypermethrin) were able to inhibit VGCCs at concentrations \leq 10 μ M. The carbamate carbaryl, the neonicotinoid imidacloprid and the organophosphates paraoxon-ethyl and -methyl were not able to increase basal $[Ca^{2+}]_i$ or inhibit VGCCs. Moreover, it was shown that for screening for effects on VGCCs an acute exposure scenario is often sufficient since, with the exception of chlorpyrifos, a subchronic and a repeated exposure scenario did not increase the insecticide-induced inhibition of VGCCs (table 1).

Humans are generally exposed to a mixture of compounds rather than to individual insecticides. Therefore, this thesis has investigated the effects of mixtures of insecticides on calcium homeostasis (chapter 6 and 7). LOECs and NOECs were combined to constitute binary mixtures of organophosphates and carbaryl. A binary LOEC mixture of chlorpyrifos and its metabolite chlorpyrifos-oxon, and a binary LOEC mixture of chlorpyrifos and parathion suggested that additivity does not apply for binary mixtures of organophosphates for effects on VGCCs (chapter 6). In contrast, binary equipotent IC_{20} mixtures of different types of insecticides have indicated additive inhibition of VGCCs (chapter 7). This is comparable with data on binary mixtures ofazole fungicides, which also have indicated additive inhibition of VGCCs (Heusinkveld et al., 2013). A tertiary IC_{20} mixture of different types of insecticides indicated less than additive inhibition of VGCCs. In summary, for chemicals with common modes of action, additivity could be expected (chapter 7), though this was not observed when organophosphates were combined or in a tertiary mixture of insecticides (chapter 6 and 7). The data indicates that the effects of mixtures should be included in risk assessment to account for additive effects.

10.1.4 Other targets and methods for neurotoxicity screening of chemicals

Many other potential neuronal processes and functions exist that could be used as a target to study chemical-induced neurotoxicity. Different classes of insecticides are known for a particular mode of action, which could be studied *in vitro*. For example, organophosphates and carbamates are well-

known as inhibitors of AChE activity and AChE activity by chemicals could be assessed *in vitro* (chapter 6). Also, the function of GABA and nAChR receptors, well-known targets of respectively (alicyclic) organochlorines and neonicotinoids, can be studied *in vitro* (Kimura-Kuroda et al., 2012; Vale et al., 2003). These well-known targets for different types of neurotoxicants are thus suitable endpoints to screen for neurotoxicity *in vitro*.

An important function of the nervous system is neurotransmission (e.g. Dolan and Grasby, 1994; Ko and Strafella, 2012; Retz et al., 1996). It depends on proper function of different components of the cell, such as neurotransmitter receptors, VGCCs and other ion channels. In addition to calcium homeostasis and neurotransmitter release, chemical-induced changes in electrical activity could be used as an integrated measure of neurotoxicity. Multiple studies have investigated chemical-induced effects on electrical activity by means of multi-electrode arrays (MEA's) as measure of neurotoxicity (Alloisio et al., 2015; Dingemans et al., *unpublished*; Duarte et al., *unpublished*; de Groot et al., 2016; Hogberg et al., 2011; Hondebrink et al., *unpublished*; LeFew et al., 2013; McConnell et al., 2012) and showed that numerous neurotoxic chemicals can alter electrical activity. In addition, it was indicated that with these MEA's chemical-induced effects can be reliably measured at different laboratories (Novellino et al., 2011). Chemical-induced effects on electrical activity could thus be reliably studied with MEA's and this is a suitable method to study neurotoxicity *in vitro*.

The methods described in this thesis assess mainly functional measures of neurotoxicity. In addition to functional measures of neurotoxicity, also morphological measures of neurotoxicity exist, such as neurite outgrowth (e.g. Harrill et al., 2013). However, morphological endpoints are considered less sensitive compared to functional endpoints as functional processes are likely disturbed before morphological alterations are present (Bal-Price et al., 2008). Nevertheless, morphological endpoints are important endpoints, particularly for the study of developmental neurotoxicity. Differentiation of neur(on)al cells plays an important role in developmental neurotoxicity and effects of chemicals on differentiation could be studied with these morphological assays.

10.1.5 Cell models

For the study of neurotoxicity *in vitro*, different cell models can be used. For the study of chemical-induced effects on calcium homeostasis, PC12 cells are a suitable model since they have comparable calcium homeostasis with neurons (Dingemans et al., 2009; Heusinkveld et al., 2010; Westerink and Ewing, 2008). Primary cultures appeared less suitable to investigate effects on VGCCs, since the depolarization-evoked increase in $[Ca^{2+}]_i$ mediated via VGCCs is biased by the spontaneous electrical activity of these cells (chapter 8). Moreover, primary cultures of brain tissue are heterogeneous and the different cells can vary in their expression of VGCCs. However, to study chemical-induced effects on electrical activity primary cultures are preferred since, in contrast to PC12 cells, they can form axons, dendrites and heterogeneous networks that are spontaneously active. Taken together, for the investigation of a specific neurotoxic mechanism an appropriate cell model should be selected (Westerink, 2013).

10.2 USE AND ISSUES OF *IN VITRO* ASSAYS FOR SCREENING FOR NEUROTOXICITY

Already from the 1990's there has been concern that *in vivo* studies are not sufficient for chemical risk assessment. Several issues concerning the use of *in vitro* methods for risk assessment have also been raised (e.g. Tilson, 1990) and requirements for *in vitro* techniques as alternatives for neurotoxicity studies have been discussed (Costa, 1998; Harry et al., 1998; Walum et al., 1994). Up to now, *in vitro* neurotoxicity methods have not been used for regulatory safety studies and requirements for *in vitro* (developmental) neurotoxicity studies are still being discussed (e.g. Crofton et al., 2012; de Groot et al., 2013; van Thriel et al., 2012).

Neurotoxicity tests with animals generally evaluate chemical-induced changes in behavior. The altered behavior is the result of a complex interplay of chemical-induced molecular and cellular changes in the animal. Therefore, the molecular and cellular changes underlying the altered behavior are likely (partly) present at lower concentrations compared to those needed to observe changes in behavior. Thus, effects of low-dose chemical exposure may remain undetected if behavior is used as an endpoint for (developmental) neurotoxicity. *In vitro* assays can detect these chemical-induced molecular and cellular changes and may increase

the sensitivity of the detection of (developmental) neurotoxicity (e.g. Coecke et al., 2007; Vorhees and Makris, 2015). Therefore, *in vitro* studies have the potential to replace or significantly reduce *in vivo* behavioral neurotoxicity studies. However, *in vitro* assays lack the complexity of organisms and changes *in vitro* are not directly linked to neurotoxic effects *in vivo*. The nervous system is very complex and neuronal cells consists of numerous receptors, transporters and other components that could be targets for neurotoxicity. Obviously, a single *in vitro* assay is not sufficient to replace an *in vivo* study.

10.2.1 Batteries of *in vitro* tests

Since a single *in vitro* assay is not sufficient to replace an *in vivo* study, test batteries of *in vitro* tests could be used. For an *in vitro* neurotoxicity test battery, relevant targets of neurotoxicants should be identified and investigated. Key processes and key functions of the nervous system that are essential for proper function of the nervous system have already been well-investigated. Therefore, assuming that alterations in key processes and functions of the nervous system are adverse effects, an *in vitro* screening approach of chemicals for neurotoxicity could focus on these essential processes and functions. For example, VGCCs are well-known to be essential for proper neurotransmitter release (e.g. Iwasaki and Takahashi, 1998; Westerink, 2006), neuronal signaling (Gadbut et al., 1991), neuronal migration (Komuro and Rakic, 1992, 1998) and neuronal development (e.g. Arnhold et al., 2000; Chameau et al., 1999). Chemical-induced alterations in VGCCs could thus be a strong indication of neurotoxicity. Although key functions of the nervous system are numerous (only a few could be investigated in this thesis), common key targets for neurotoxicity should be identified and included in *in vitro* test batteries.

10.2.2 Adverse Outcome Pathways (AOPs)

From a regulatory perspective, a change in a particular *in vitro* mechanism does not necessarily mean that a neurotoxic effect will be detected *in vivo*. To establish a relation between molecular and cellular changes and adverse health outcomes a framework has been developed, Adverse Outcome Pathways (AOPs; Vinken, 2013). In an AOP, a connection is established between a molecular initiating event (MIE), key events (KEs) at the molecular, cellular and organ level, and effects in the organism and

eventually at population level. Up to now, several AOPs for neurotoxicity have been developed/suggested (Bal-price et al., 2015). In these AOPs, chemical-induced alterations in e.g. calcium homeostasis, ROS production, apoptosis, ATP production, mitochondrial function, or calcium dependent-signaling have been linked with impaired neuronal morphology, neuronal signaling, followed by neurodegeneration and altered network function, resulting in deficits in e.g. behavior, learning and memory (Bal-price et al., 2015). Interestingly, many AOPs report a disruption of calcium homeostasis as a key event, which indicates that calcium homeostasis should be considered as a key target for screening chemicals for neurotoxicity.

10.2.3 Extrapolation from the *in vitro* to the *in vivo* situation

In human risk assessment, usually results of *in vivo* studies are extrapolated to compare with the human situation. To this end, NOECs obtained in *in vivo* studies are generally multiplied by a safety factor 100 (10x10 to account for species differences and interspecies variation) and compared with human exposure concentrations. Previously, this approach was also applied to *in vitro* data and demonstrated that systemic concentrations in an occupational setting are higher compared with those that induce an effect *in vitro* (chapter 7). However, *in vitro* exposure represents a direct exposure of the applied chemical to neurons. In contrast, in humans/ animals absorption, distribution, metabolism and excretion (ADME) play an important role in the actual target concentration after e.g. oral exposure. Thus, *in vitro* concentrations are not directly comparable with human exposure levels. To correlate the *in vitro* and *in vivo* exposure and effect concentrations, physiologically-based pharmacokinetic (PBPK) models can be used to calculate circulating systemic levels in e.g. blood (e.g. Croom et al., 2015; Forsby and Blaauboer, 2007). Furthermore, assays should have some metabolic activity and/or assays should be performed to obtain information on metabolite formation. These metabolites should be screened for neurotoxicity as well.

To understand the relationship and bridge the gap between *in vitro* and *in vivo* studies, an *ex vivo* study was performed in this thesis (chapter 9). Long-term potentiation (LTP) was measured in mice treated with chlorpyrifos in a manner and at doses that were previously shown to affect spontaneous behavior in mice. No correlation between LTP and spontaneous behavior was

found. These data suggests that deficits in LTP are not involved or cannot be directly correlated to chlorpyrifos-induced effects on spontaneous behavior (chapter 9). However, the interpretation of LTP data was hampered by the low number of slices, and some subtle effects may have been detected if LTP would have been measured in a larger number of slices. Taken together, acute effects of chlorpyrifos on VGCCs observed *in vitro*, (chapter 6 and 7) do not seem related to an effect on LTP when assessed five months after exposure.

For *in vitro* assays, commonly used cell models are from animal origin and data still need to be extrapolated to the human situation. Currently, cell models from human origin are under investigation to develop cell models more closely related to the human situation (e.g. Baumann et al., 2015; Malik et al., 2014). Though human cell models are promising (Schwartz et al., 2015), more research is needed to improve the time and cost effectiveness of these human cell cultures. Moreover, new issues arising with these cultures must be addressed, such as ethical issues, reproducibility and genetic variation.

In conclusion, *in vitro* assays have the potential to replace *in vivo* assays. Chemical-induced molecular, biochemical and neurophysiological effects have been extensively investigated *in vitro* and the application of these *in vitro* assays for regulatory purposes has been extensively discussed. Previously, flame retardants were screened for their effects on several *in vitro* endpoints (oxidative stress, calcium homeostasis and nAChR function; Hendriks et al., 2014). Of these endpoints, calcium homeostasis appeared to be one of the most sensitive endpoints. A rank order of potency for flame retardants on these endpoints was established. Consequently, this rank order identified flame retardants with a low neurotoxic potential that could be considered as safer alternatives for the well-known neurotoxic brominated flame retardants (Hendriks et al., 2014). Effect concentrations obtained with comparable *in vitro* screening studies, combined with information on systemic exposure concentrations, could be used to calculate Margin Of Exposures (MOE; Chapter 7). This MOE approach can be used to prioritize chemicals for neurotoxicity studies.

In general, there is still a lack of confidence among regulatory authorities with respect to the predictive power and reliability of *in vitro* assays for human neurotoxicity. Nevertheless, some of the existing *in vitro* assays may already play an important role in prioritizing chemicals for neurotoxicity.

10.3 RECOMMENDATIONS FOR FUTURE RESEARCH:

Develop an *in vitro* test battery for neurotoxicity testing to identify priority neurotoxic chemicals (for schematic overview, see Fig. 1).

This test battery should include:

- General measures of toxicity, such as cell viability and metabolic activity.
- Key functions of the nervous system. These can be divided in:
 - Morphological endpoints, such as neurite outgrowth and synaptogenesis.
 - Functional endpoints, such as calcium homeostasis, electrical activity, oxidative stress, receptor and channel function (such as nACh-Rs, GABA-Rs, VGSCs, VGCCs).

Issues that should be taken into account in such a test battery include:

- *In vitro* assays incorporated in this test battery should be carefully evaluated prior to use for *in vitro* neurotoxicity screening purposes. In this thesis, we have demonstrated that methods should be carefully evaluated before being used to investigate chemical-induced neurotoxicity.
- For risk assessment purposes, information on ADME should be obtained. If metabolites are formed, these should be tested for neurotoxicity as well.
- Information on systemic human exposure concentrations should be obtained to determine a MOE for prioritizing neurotoxic chemicals.
- Effects of mixtures should be included in risk assessment. Additivity may be assumed, though, chemicals could interact and when combined cause non-additive effects and increased toxicity.

Table 1: Overview of NOECs, LOECs, IC₂₀s and IC₅₀s for inhibition of VGCCs and LOECs for increase in basal [Ca²⁺]_i by insecticides (in μM) after acute (20 min), subchronic (24h) or repeated exposure (24h and a second, 20 min exposure).

insecticide class	insecticide	exposure	NOEC	LOEC	IC ₂₀	IC ₅₀	LOEC basal [Ca ²⁺] _i	
organophosphates	chlorpyrifos	acute	0.01	0.1	0.08	0.899	10 ⁴	
		subchronic	0.1	1	0.859	>10 ⁴	>10 ⁴	
		repeated	0.01	0.1	0.035	0.179	>10 ⁴	
	chlorpyrifos-oxon	acute	0.1	1	0.231	>10 ⁴	10	
		subchronic	0.01	0.1	0.054	>10 ⁴	>10 ⁴	
		repeated	0.01	0.1	0.659	3.977	>10 ⁴	
	parathion	acute	1	3	2.6	4.1	>10 ⁴	
		paraoxon-ethyl	acute	10	>10 ⁴	>10 ⁴	>10 ⁴	>10 ⁴
		paraoxon-methyl	acute	1	10	>10 ⁴	>10 ⁴	>10 ⁴
organochlorines	endosulfan	acute	0.01	0.1	0.12	0.25	10	
		subchronic	1	10	3.798	9.440	>10 ⁴	
		repeated	0.01	0.1	0.042	0.206	10	
pyrethroids	cypermethrin	acute	0.001	0.01	0.009	0.078	>10 ⁴	
		subchronic	0.1	1	0.250	0.931	>10 ⁴	
		repeated	-	0.001	0.006	0.097	>10 ⁴	
carbamates	alpha-cypermethrin	Acute	0.01	0.1	0.03	0.239	>10 ⁴	
		carbaryl	acute	≥10 ⁴	10	>10 ⁴	>10 ⁴	>10 ⁴
			subchronic	≥10 ⁴	>10 ⁴	>10 ⁴	>10 ⁴	>10 ⁴
neonicotinoid	imidacloprid	repeated	≥10 ⁴	>10 ⁴	>10 ⁴	>10 ⁴	>10 ⁴	
		acute	≥10 ⁴	10	>10 ⁴	>10 ⁴	>10 ⁴	
		subchronic	≥10 ⁴	>10 ⁴	>10 ⁴	>10 ⁴	>10 ⁴	
		repeated	≥10 ⁴	>10 ⁴	>10 ⁴	>10 ⁴	>10 ⁴	

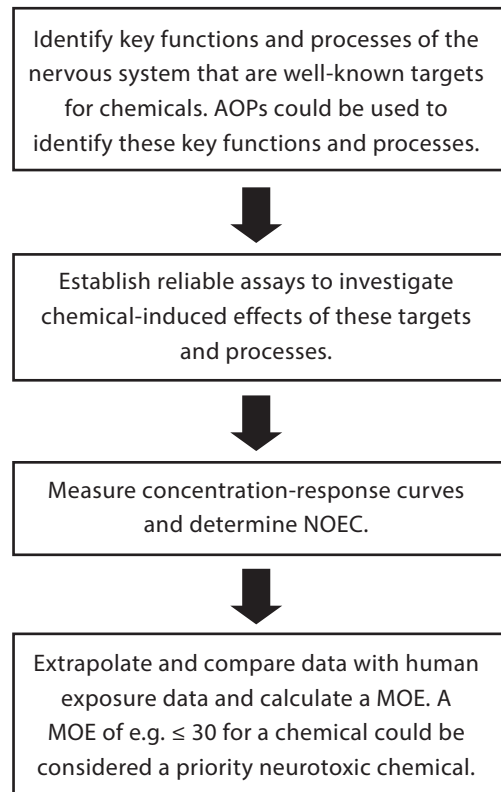


Figure 1: Schematic overview of steps needed to develop and use *in vitro* test batteries for risk assessment purposes.

REFERENCES

- Abou-Donia, M. B., Goldstein, L. B., Bullman, S., Tu, T., Khan, W. A., Dechkovskaia, A. M., et al. (2008). Imidacloprid induces neurobehavioral deficits and increases expression of glial fibrillary acidic protein in the motor cortex and hippocampus in offspring rats following in utero exposure. *Journal of Toxicology and Environmental Health, Part A*, 71(2), 119-130. doi:10.1080/15287390701613140
- Adigun, A. A., Ryde, I. T., Seidler, F. J., & Slotkin, T. A. (2010a). Organophosphate exposure during a critical developmental stage reprograms adenylyl cyclase signaling in PC12 cells. *Brain Research*, 1329, 36-44. doi:10.1016/j.brainres.2010.03.025
- Adigun, A. A., Seidler, F. J., & Slotkin, T. A. (2010b). Disparate developmental neurotoxicants converge on the cyclic AMP signaling cascade, revealed by transcriptional profiles *in vitro* and *in vivo*. *Brain Research*, 1316, 1-16. doi:10.1016/j.brainres.2009.12.025
- Agrawal, S., Singh, A., Tripathi, P., Mishra, M., Singh, P. K., & Singh, M. P. (2015). Cypermethrin-induced nigrostriatal dopaminergic neurodegeneration alters the mitochondrial function: A proteomics study. *Molecular Neurobiology*, 51(2), 448-65. doi:10.1007/s12035-014-8696-7
- Alloisio, S., Nobile, M., & Novellino, A. (2015). Multiparametric characterisation of neuronal network activity for *in vitro* agrochemical neurotoxicity assessment. *Neurotoxicology*, 48, 152-65. doi:10.1016/j.neuro.2015.03.013
- Arnhold, S., Andressen, C., Angelov, D. N., Vajna, R., Volsen, S. G., Hescheler, J., et al. (2000). Embryonic stem-cell derived neurones express a maturation dependent pattern of voltage-gated calcium channels and calcium-binding proteins. *International Journal of Developmental Neuroscience*, 18(2-3), 201-12.
- Babot, Z., Vilaró, M. T., & Suñol, C. (2007). Long-term exposure to dieldrin reduces gamma-aminobutyric acid type A and N-methyl-D-aspartate receptor function in primary cultures of mouse cerebellar granule cells. *Journal of Neuroscience Research*, 85(16), 3687-3695. doi:10.1002/jnr.21433
- Bailey, J. M., Hutsell, B. A., & Newland, M. C. (2013). Dietary nimodipine delays the onset of methylmercury neurotoxicity in mice. *Neurotoxicology*, 37, 108-117. doi:10.1016/j.neuro.2013.03.011
- Bal-Price, A. K., Crofton, K. M., Sachana, M., Shafer, T. J., Behl, M., Forsby, A., et al. (2015). Putative adverse outcome pathways relevant to neurotoxicity. *Critical Reviews in Toxicology*, 45(1), 83-91. doi:10.3109/10408444.2014.981331
- Bal-Price, A. K., Hogberg, H. T., Buzanska, L., Lenas, P., van Vliet, E., & Hartung, T. (2010). *In vitro* developmental neurotoxicity (DNT) testing: Relevant models and endpoints. *Neurotoxicology*, 31(5), 545-54. doi:10.1016/j.neuro.2009.11.006
- Bal-Price, A. K., Suñol, C., Weiss, D. G., van Vliet, E., Westerink, R. H. S., & Costa, L. G. (2008). Application of *in vitro* neurotoxicity testing for regulatory purposes: Symposium III summary and research needs. *Neurotoxicology*, 29(3), 520-31. doi:10.1016/j.neuro.2008.02.008

- Bal, R., Erdogan, S., Theophilidis, G., Baydas, G., & Naziroglu, M. (2010). Assessing the effects of the neonicotinoid insecticide imidacloprid in the cholinergic synapses of the stellate cells of the mouse cochlear nucleus using whole-cell patch-clamp recording. *Neurotoxicology*, *31*(1), 113-120. doi:10.1016/j.neuro.2009.10.004
- Barr, D. B., Ananth, C. V., Yan, X., Lashley, S., Smulian, J. C., Ledoux, T. A., et al. (2010). Pesticide concentrations in maternal and umbilical cord sera and their relation to birth outcomes in a population of pregnant women and newborns in new jersey. *Science of the Total Environment*, *408*(4), 790-795. doi:http://dx.doi.org/10.1016/j.scitotenv.2009.10.007
- Baumann, J., Gassmann, K., Masjosthusmann, S., de Boer, D., Bendt, F., Giersiefer, S., et al. (2015). Comparative human and rat neurospheres reveal species differences in chemical effects on neurodevelopmental key events. *Archives of Toxicology*, doi:10.1007/s00204-015-1568-8
- Berridge, M. J., Bootman, M. D., & Roderick, H. L. (2003). Calcium signalling: Dynamics, homeostasis and remodelling. *Nature Reviews. Molecular Cell Biology*, *4*(7), 517-529.
- Betancourt, A. M., Burgess, S. C., & Carr, R. L. (2006). Effect of developmental exposure to chlorpyrifos on the expression of neurotrophin growth factors and cell-specific markers in neonatal rat brain. *Toxicological Sciences*, *92*(2), 500-506. doi:10.1093/toxsci/kfl004
- Boix, J., Cauli, O., Leslie, H., & Felipo, V. (2011). Differential long-term effects of developmental exposure to polychlorinated biphenyls 52, 138 or 180 on motor activity and neurotransmission. gender dependence and mechanisms involved. *Neurochemistry International*, *58*(1), 69-77. doi:10.1016/j.neuint.2010.10.014
- Bopp, S. K., & Lettieri, T. (2008). Comparison of four different colorimetric and fluorometric cytotoxicity assays in a zebrafish liver cell line. *BMC Pharmacology*, *8*, 8. doi:10.1186/1471-2210-8-8
- Boucher, O., Simard, M. N., Muckle, G., Rouget, F., Kadhel, P., Bataille, H., et al. (2013). Exposure to an organochlorine pesticide (chlordecone) and development of 18-month-old infants. *Neurotoxicology*, *35*, 162-8. doi:10.1016/j.neuro.2013.01.007
- Breier, J. M., Gassmann, K., Kayser, R., Stegeman, H., de Groot, D., Fritsche, E., et al. (2010). Neural progenitor cells as models for high-throughput screens of developmental neurotoxicity: State of the science. *Neurotoxicology and Teratology*, *32*(1), 4-15. doi:10.1016/j.ntt.2009.06.005
- Bressler, J., Kim, K. A., Chakraborti, T., & Goldstein, G. (1999). Molecular mechanisms of lead neurotoxicity. *Neurochemical Research*, *24*(4), 595-600.
- Buratovic, S., Viberg, H., Fredriksson, A., & Eriksson, P. (2014). Developmental exposure to the polybrominated diphenyl ether PBDE 209: Neurobehavioural and neuroprotein analysis in adult male and female mice. *Environmental Toxicology and Pharmacology*, *38*(2), 570-85. doi:10.1016/j.etap.2014.08.010
- Burr, S. A., & Ray, D. E. (2004). Structure-activity and interaction effects of 14 different pyrethroids on voltage-gated chloride ion channels. *Toxicological Sciences*, *77*(2), 341-6. doi:10.1093/toxsci/kfh027
- Cali, T., Ottolini, D., & Brini, M. (2014). Calcium signaling in parkinson's disease. *Cell and Tissue Research*, *357*(2), 439-54. doi:10.1007/s00441-014-1866-0
- Cao, Z., Cui, Y., Nguyen, H. M., Jenkins, D. P., Wulff, H., & Pessah, I. N. (2014). Nanomolar bifenthrin alters synchronous Ca²⁺ oscillations and cortical neuron development independent of sodium channel activity. *Molecular Pharmacology*, *85*(4), 630-639. doi:10.1124/mol.113.090076
- Cao, Z., Shafer, T. J., & Murray, T. F. (2011). Mechanisms of pyrethroid insecticide-induced stimulation of calcium influx in neocortical neurons. *The Journal of Pharmacology and Experimental Therapeutics*, *336*(1), 197-205. doi:10.1124/jpet.110.171850
- Carr, R. L., Chambers, H. W., Guarisco, J. A., Richardson, J. R., Tang, J., & Chambers, J. E. (2001). Effects of repeated oral postnatal exposure to chlorpyrifos on open-field behavior in juvenile rats. *Toxicological Sciences*, *59*(2), 260-267. doi:10.1093/toxsci/59.2.260
- Casabar, R. C. T., Das, P. C., Dekrey, G. K., Gardiner, C. S., Cao, Y., Rose, R. L., et al. (2010). Endosulfan induces CYP2B6 and CYP3A4 by activating the pregnane X receptor. *Toxicology and Applied Pharmacology*, *245*(3), 335-43. doi:10.1016/j.taap.2010.03.017
- Chakraborti, T. K., Farrar, J. D., & Pope, C. N. (1993). Comparative neurochemical and neurobehavioral effects of repeated chlorpyrifos exposures in young and adult rats. *Pharmacology, Biochemistry and Behavior*, *46*(1), 219-224.
- Chameau, P., Lucas, P., Melliti, K., Bournaud, R., & Shimahara, T. (1999). Development of multiple calcium channel types in cultured mouse hippocampal neurons. *Neuroscience*, *90*(2), 383-8.
- Chang, P. A., Wu, Y. J., Li, W., & Leng, X. F. (2006). Effect of carbamate esters on neurite outgrowth in differentiating human SK-N-SH neuroblastoma cells. *Chemico-Biological Interactions*, *159*(1), 65-72. doi:10.1016/j.cbi.2005.09.005
- Chen, A., Dietrich, K. N., Huo, X., & Ho, S. (2011). Developmental neurotoxicants in e-waste: An emerging health concern. *Environmental Health Perspectives*, *119*(4), 431-8. doi:10.1289/ehp.1002452
- Choi, J. S., & Soderlund, D. M. (2006). Structure-activity relationships for the action of 11 pyrethroid insecticides on rat na v 1.8 sodium channels expressed in xenopus oocytes. *Toxicology and Applied Pharmacology*, *211*(3), 233-44. doi:10.1016/j.taap.2005.06.022
- Clarkson, T. W., & Magos, L. (2006). The toxicology of mercury and its chemical compounds. *Critical Reviews in Toxicology*, *36*(8), 609-62. doi:10.1080/10408440600845619
- Coats, J. R. (1990). Mechanisms of toxic action and structure-activity relationships for organochlorine and synthetic pyrethroid insecticides. *Environmental Health Perspectives*, *87*, 255-262.
- Coecke, S., Eskes, C., Gartlon, J., Kinsner, A., Price, A., van Vliet, E., et al. (2006). The value of alternative testing for neurotoxicity in the context of regulatory needs. *Environmental Toxicology and Pharmacology*, *21*(2), 153-167. doi:10.1016/j.etap.2005.07.006

- Coecke, S., Goldberg, A. M., Allen, S., Buzanska, L., Calamandrei, G., Crofton, K., et al. (2007). Workgroup report: Incorporating *in vitro* alternative methods for developmental neurotoxicity into international hazard and risk assessment strategies. *Environmental Health Perspectives*, 115(6), 924-931. doi:10.1289/ehp.9427
- Costa, L. G., de Laat, R., Tagliaferri, S., & Pellacani, C. (2014). A mechanistic view of polybrominated diphenyl ether (PBDE) developmental neurotoxicity. *Toxicology Letters*, 230(2), 282-94. doi:10.1016/j.toxlet.2013.11.011
- Costa, L. G. (1998). Neurotoxicity testing: A discussion of *in vitro* alternatives. *Environmental Health Perspectives*, 106 Suppl 2, 505-10.
- Crofton, K. M., & Reiter, L. W. (1988). The effects of type I and II pyrethroids on motor activity and the acoustic startle response in the rat. *Fundamental and Applied Toxicology*, 10(4), 624-34.
- Crofton, K. M., Mundy, W. R., & Shafer, T. J. (2012). Developmental neurotoxicity testing: A path forward. *Congenital Anomalies*, 52(3), 140-6. doi:10.1111/j.1741-4520.2012.00377.x
- Croom, E. L., Shafer, T. J., Evans, M. V., Mundy, W. R., Eklund, C. R., Johnstone, A. F., et al. (2015). Improving *in vitro* to *in vivo* extrapolation by incorporating toxicokinetic measurements: A case study of lindane-induced neurotoxicity. *Toxicology and Applied Pharmacology*, 283(1), 9-19. doi:10.1016/j.taap.2014.11.006
- Crosby, E. B., Bailey, J. M., Oliveri, A. N., & Levin, E. D. (2015). Neurobehavioral impairments caused by developmental imidacloprid exposure in zebrafish. *Neurotoxicology and Teratology*, 49, 81-90. doi:10.1016/j.ntt.2015.04.006
- Crumpton, T. L., Seidler, F. J., & Slotkin, T. A. (2000). Is oxidative stress involved in the developmental neurotoxicity of chlorpyrifos? *Developmental Brain Research*, 121(2), 189-195. doi:http://dx.doi.org.proxy.library.uu.nl/10.1016/S0165-3806(00)00045-6
- Dai, D. F., Chiao, Y. A., Marcinek, D. J., Szeto, H. H., & Rabinovitch, P. S. (2014). Mitochondrial oxidative stress in aging and healthspan. *Longevity & Healthspan*, 3, 6. doi:10.1186/2046-2395-3-6
- Dalvie, M. A., Africa, A., Solomons, A., London, L., Brouwer, D., & Kromhout, H. (2009). Pesticide exposure and blood endosulfan levels after first season spray amongst farm workers in the western cape, south africa. *Journal of Environmental Science and Health. Part B. Pesticides, Food Contaminants, and Agricultural Wastes*, 44(3), 271-277. doi:10.1080/03601230902728351
- Dam, K., Seidler, F. J., & Slotkin, T. A. (2000). Chlorpyrifos exposure during a critical neonatal period elicits gender-selective deficits in the development of coordination skills and locomotor activity. *Developmental Brain Research*, 121(2), 179-187. doi:10.1016/S0165-3806(00)00044-4
- Das, K. P., & Barone Jr., S. (1999). Neuronal differentiation in PC12 cells is inhibited by chlorpyrifos and its metabolites: Is acetylcholinesterase inhibition the site of action? *Toxicology and Applied Pharmacology*, 160(3), 217-230. doi:10.1006/taap.1999.8767
- de Groot, M. W. G. D. M., van Kleef, R. G. D. M., de Groot, A., & Westerink, R. H. S. (2016). *In vitro* developmental neurotoxicity following chronic exposure to 50 hz extremely low-frequency electromagnetic fields in primary rat cortical cultures. *Toxicological Sciences*, 149(2), 433-440. doi:10.1093/toxsci/kfv242
- de Groot, M. W. G. D. M., Westerink, R. H. S., & Dingemans, M. M. L. (2013). Don't judge a neuron only by its cover: Neuronal function in *in vitro* developmental neurotoxicity testing. *Toxicological Sciences*, 132(1), 1-7. doi:10.1093/toxsci/kfs269
- de Groot, M. W. G. D. M., & Westerink, R. H. S. (2014). Chemically-induced oxidative stress increases the vulnerability of PC12 cells to rotenone-induced toxicity. *Neurotoxicology*, 43, 102-9. doi:10.1016/j.neuro.2014.02.008
- Di Virgilio, F., Steinberg, T. H., & Silverstein, S. C. (1990). Inhibition of fura-2 sequestration and secretion with organic anion transport blockers. *Cell Calcium*, 11(2-3), 57-62. doi:10.1016/0143-4160(90)90059-4
- Dingemans, M. M. L., Ramakers, G. M. J., Gardoni, F., van Kleef, R. G. D. M., Bergman, A., Di Luca, M., et al. (2007). Neonatal exposure to brominated flame retardant BDE-47 reduces long-term potentiation and postsynaptic protein levels in mouse hippocampus. *Environmental Health Perspectives*, 115(6), 865-70. doi:10.1289/ehp.9860
- Dingemans, M. M. L., Heusinkveld, H. J., de Groot, A., Bergman, Å., van den Berg, M., & Westerink, R. H. S. (2009). Hexabromocyclododecane inhibits depolarization-induced increase in intracellular calcium levels and neurotransmitter release in PC12 cells. *Toxicological Sciences*, 107(2), 490-497. doi:10.1093/toxsci/kfn249
- Dingemans, M. M. L., van den Berg, M., Bergman, Å., & Westerink, R. H. S. (2010). Calcium-related processes involved in the inhibition of depolarization-evoked calcium increase by hydroxylated PBDEs in PC12 cells. *Toxicological Sciences*, 114(2), 302-309. doi:10.1093/toxsci/kfp310
- Dolan, R. J., & Grasby, P. M. (1994). Exploring the functional role of monoaminergic neurotransmission. A method for exploring neurotransmitter dysfunction in psychiatric disorders. *British Journal of Psychiatry*, 164(5), 575-80.
- Drummen, G. P. C., van Liebergen, L. C. M., op den Kamp, J. A. F., & Post, J. (2002). C11-BODIPY(581/591), an oxidation-sensitive fluorescent lipid peroxidation probe: (micro) spectroscopic characterization and validation of methodology. *Free Radical Biology & Medicine*, 33(4), 473-490.
- Eaton, D. L., Daroff, R. B., Autrup, H., Bridges, J., Buffler, P., Costa, L. G., et al. (2008). Review of the toxicology of chlorpyrifos with an emphasis on human exposure and neurodevelopment. *Critical Reviews in Toxicology*, 38, 1-125. doi:10.1080/10408440802272158
- Egorova, P., Popugaeva, E., & Bezprozvanny, I. (2015). Disturbed calcium signaling in spinocerebellar ataxias and alzheimer's disease. *Seminars in Cell & Developmental Biology*, 40, 127-33. doi:10.1016/j.semcdb.2015.03.010

- Eriksson, P., Jakobsson, E., & Fredriksson, A. (2001). Brominated flame retardants: A novel class of developmental neurotoxicants in our environment? *Environmental Health Perspectives*, 109(9), 903-8.
- Eskenazi, B., Rosas, L. G., Marks, A. R., Bradman, A., Harley, K., Holland, N., et al. (2008). Pesticide toxicity and the developing brain. *Basic & Clinical Pharmacology & Toxicology*, 102(2), 228-36. doi:10.1111/j.1742-7843.2007.00171.x
- Eskenazi, B., Harley, K., Bradman, A., Weltzien, E., Jewell, N. P., Barr, D. B., et al. (2004). Association of *in utero* organophosphate pesticide exposure and fetal growth and length of gestation in an agricultural population. *Environmental Health Perspectives*, 112(10), 1116-1124.
- Estevan, C., Vilanova, E., & Sogorb, M. A. (2013). Chlorpyrifos and its metabolites alter gene expression at non-cytotoxic concentrations in D3 mouse embryonic stem cells under *in vitro* differentiation: Considerations for embryotoxic risk assessment. *Toxicology Letters*, 217(1), 14-22. doi:10.1016/j.toxlet.2012.11.026
- European Chemicals Agency (ECHA, 2015) <http://echa.europa.eu/regulations/reach/evaluation> (visited online 10-11-2015)
- European Chemicals Agency (ECHA, 2015) <http://echa.europa.eu/en/support/oecd-eu-test-guidelines> (visited online 10-11-2015)
- European commission, European Union. (EC EU, 2015). http://ec.europa.eu/growth/sectors/chemicals/reach/index_en.htm (visited online 10-11-2015)
- European Food Safety Authority. (EFSA, 2013). The 2010 European Union Report on Pesticide Residues in Food. *EFSA Journal* 2013, 11(3), 3130-3938. doi:10.2903/j.efsa.2013.3130
- European Food Safety Authority. (EFSA, 2014). The 2012 European Union Report on Pesticide Residues in Food. *EFSA Journal* 2014, 12(12), 3942-4098. doi:10.2903/j.efsa.2014.3942
- European Food Safety Authority. (EFSA, 2015). The 2013 European Union Report on Pesticide Residues in Food. *EFSA Journal* 2015, 13(3), 4038-4207. doi:10.2903/j.efsa.2015.4038
- Flaskos, J., Fowler, M. J., Teurtrie, C., & Hargreaves, A. J. (1999). The effects of carbaryl and trichlorphon on differentiating mouse N2a neuroblastoma cells. *Toxicology Letters*, 110(1-2), 79-84.
- Flaskos, J. (2012). The developmental neurotoxicity of organophosphorus insecticides: A direct role for the oxon metabolites. *Toxicology Letters*, 209(1), 86-93. doi:10.1016/j.toxlet.2011.11.026
- Forns, J., Lertxundi, N., Aranbarri, A., Murcia, M., Gascon, M., Martinez, D., et al. (2012). Prenatal exposure to organochlorine compounds and neuropsychological development up to two years of life. *Environment International*, 45, 72-7. doi:10.1016/j.envint.2012.04.009
- Forsby, A., & Blaauboer, B. J. (2007). Integration of *in vitro* neurotoxicity data with biokinetic modelling for the estimation of *in vivo* neurotoxicity. *Human & Experimental Toxicology*, 26(4), 333-8. doi:10.1177/0960327106072994
- Freeborn, D. L., McDaniel, K. L., Moser, V. C., & Herr, D. W. (2015). Use of electroencephalography (EEG) to assess CNS changes produced by pesticides with different modes of action: Effects of permethrin, deltamethrin, fipronil, imidacloprid, carbaryl, and triadimefon. *Toxicology and Applied Pharmacology*, 282(2), 184-94. doi:10.1016/j.taap.2014.11.011
- Freret, T., Billard, J. M., Schumann-Bard, P., Dutar, P., Dauphin, F., Boulouard, M., et al. (2012). Rescue of cognitive aging by long-lasting environmental enrichment exposure initiated before median lifespan. *Neurobiology of Aging*, 33(5), 1005.e1-1005.e10. doi:10.1016/j.neurobiolaging.2011.09.028
- Gadbut, A. P., Cash, S. A., Noble, J. A., Radice, T. R., & Weyhenmeyer, J. A. (1991). The effect of Ca²⁺ channel antagonists (cadmium, omega-conotoxin GIVA, and nitrendipine) on the release of angiotensin II from fetal rat brain *in vitro*. *Neuroscience Letters*, 123(1), 91-4.
- Garcia, S. J., Seidler, F. J., Crumpton, T. L., & Slotkin, T. A. (2001). Does the developmental neurotoxicity of chlorpyrifos involve glial targets? macromolecule synthesis, adenylyl cyclase signaling, nuclear transcription factors, and formation of reactive oxygen in C6 glioma cells. *Brain Research*, 891(1-2), 54-68.
- Garcia, S. J., Seidler, F. J., & Slotkin, T. A. (2005). Developmental neurotoxicity of chlorpyrifos: Targeting glial cells. *Environmental Toxicology and Pharmacology*, 19(3), 455-61. doi:10.1016/j.etap.2004.12.007
- Giray, B., Gürbay, A., & Hincal, F. (2001). Cypermethrin-induced oxidative stress in rat brain and liver is prevented by vitamin E or allopurinol. *Toxicology Letters*, 118(3), 139-46.
- Greene, L. A., & Tischler, A. S. (1976). Establishment of a noradrenergic clonal line of rat adrenal pheochromocytoma cells which respond to nerve growth factor. *Proceedings of the National Academy of Sciences*, 73(7), 2424-2428.
- Gubernator, N., Zhang, H., Staal, R. G. W., Mosharov, E., Pereira, D., Yue, M., et al. (2009). Fluorescent false neurotransmitters visualize dopamine release from individual presynaptic terminals. *Science*, 324(5933), 1441-1444. doi:10.1126/science.1172278
- Guizzetti, M., Pathak, S., Giordano, G., & Costa, L. G. (2005). Effect of organophosphorus insecticides and their metabolites on astroglial cell proliferation. *Toxicology*, 215(3), 182-90. doi:10.1016/j.tox.2005.07.004
- Han, Y., Cao, D., Li, X., Zhang, R., Yu, F., Ren, Y., et al. (2014). Attenuation of γ -aminobutyric acid (GABA) transaminase activity contributes to GABA increase in the cerebral cortex of mice exposed to β -cypermethrin. *Human & Experimental Toxicology*, 33(3), 317-24. doi:10.1177/0960327113497770
- Harrill, J. A., Robinette, B. L., Freudenrich, T., & Mundy, W. R. (2013). Use of high content image analyses to detect chemical-mediated effects on neurite sub-populations in primary rat cortical neurons. *Neurotoxicology*, 34, 61-73. doi:10.1016/j.neuro.2012.10.013
- Harry, G. J., Billingsley, M., Bruinink, A., Campbell, I. L., Classen, W., Dorman, D. C., et al. (1998). *In vitro* techniques for the assessment of neurotoxicity. *Environmental Health Perspectives*, 106 Suppl 1, 131-58.

- Hendriks, H. S., Meijer, M., Muilwijk, M., van den Berg, M., & Westerink, R. H. S. (2014). A comparison of the *in vitro* cyto- and neurotoxicity of brominated and halogen-free flame retardants: Prioritization in search for safe(r) alternatives. *Archives of Toxicology*, *88*(4), 857-69. doi:10.1007/s00204-013-1187-1
- Hendriks, H. S., van Kleef, R. G. D. M., van den Berg, M., & Westerink, R. H. S. (2012). Multiple novel modes of action involved in the *in vitro* neurotoxic effects of tetrabromobisphenol-A. *Toxicological Sciences*, *128*(1), 235-246. doi:10.1093/toxsci/kfs136
- Herbstman, J. B., Sjödin, A., Kurzon, M., Lederman, S. A., Jones, R. S., Rauh, V., et al. (2010). Prenatal exposure to PBDEs and neurodevelopment. *Environmental Health Perspectives*, *118*(5), 712-9. doi:10.1289/ehp.0901340
- Heusinkveld, H. J., Thomas, G. O., Lamot, I., van den Berg, M., Kroese, A. B. A., & Westerink, R. H. S. (2010). Dual actions of lindane (γ -hexachlorocyclohexane) on calcium homeostasis and exocytosis in rat PC12 cells. *Toxicology and Applied Pharmacology*, *248*(1), 12-19. doi:10.1016/j.taap.2010.06.013
- Heusinkveld, H. J., Molendijk, J., van den Berg, M., & Westerink, R. H. S. (2013). Azole fungicides disturb intracellular Ca^{2+} in an additive manner in dopaminergic PC12 cells. *Toxicological Sciences*, *134*(2), 374-381. doi:10.1093/toxsci/kft119
- Heusinkveld, H. J., & Westerink, R. H. S. (2011). Caveats and limitations of plate reader-based high-throughput kinetic measurements of intracellular calcium levels. *Toxicology and Applied Pharmacology*, *255*(1), 1-8. doi:10.1016/j.taap.2011.05.020
- Heusinkveld, H. J., & Westerink, R. H. S. (2012). Organochlorine insecticides lindane and dieldrin and their binary mixture disturb calcium homeostasis in dopaminergic PC12 cells. *Environmental Science & Technology*, *46*(3), 1842-1848. doi:10.1021/es203303r
- Hildebrand, M. E., McRory, J. E., Snutch, T. P., & Stea, A. (2004). Mammalian voltage-gated calcium channels are potently blocked by the pyrethroid insecticide allethrin. *Journal of Pharmacology and Experimental Therapeutics*, *308*(3), 805-813. doi:10.1124/jpet.103.058792
- Hoffman, K., Webster, T. F., Weisskopf, M. G., Weinberg, J., & Vieira, V. M. (2010). Exposure to polyfluoroalkyl chemicals and attention deficit/hyperactivity disorder in U.S. children 12-15 years of age. *Environmental Health Perspectives*, *118*(12), 1762-7. doi:10.1289/ehp.1001898
- Hogberg, H. T., Sobanski, T., Novellino, A., Whelan, M., Weiss, D. G., & Bal-Price, A. K. (2011). Application of micro-electrode arrays (MEAs) as an emerging technology for developmental neurotoxicity: Evaluation of domoic acid-induced effects in primary cultures of rat cortical neurons. *Neurotoxicology*, *32*(1), 158-68. doi:10.1016/j.neuro.2010.10.007
- Hondebrink, L., Meulenbelt, J., Rietjens, S., Meijer, M., Westerink, R. H. S. (2012). Methamphetamine, amphetamine, MDMA ('ecstasy'), MDA and mCPP modulate electrical and cholinergic input in PC12 cells. *Neurotoxicology*, *33*(2), 255-260. doi:10.1016/j.neuro.2011.09.003
- Hondebrink, L., Meulenbelt, J., Meijer, M., van den Berg, M., & Westerink, R. H. S. (2011). High concentrations of MDMA ('ecstasy') and its metabolite MDA inhibit calcium influx and depolarization-evoked vesicular dopamine release in PC12 cells. *Neuropharmacology*, *61*(1-2), 202-8. doi:10.1016/j.neuropharm.2011.03.028
- Howard, A. S., Bucelli, R., Jett, D. A., Bruun, D., Yang, D., & Lein, P. J. (2005). Chlorpyrifos exerts opposing effects on axonal and dendritic growth in primary neuronal cultures. *Toxicology and Applied Pharmacology*, *207*(2), 112-24. doi:10.1016/j.taap.2004.12.008
- Huang, J., & Casida, J. E. (1996). Characterization of [3H]ethynylbicycloorthobenzoate ([3H]EBOB) binding and the action of insecticides on the gamma-aminobutyric acid-gated chloride channel in cultured cerebellar granule neurons. *Journal of Pharmacology and Experimental Therapeutics*, *279*(3), 1191-1196.
- Icenogle, L., Christopher, N. C., Blackwelder, W. P., Caldwell, D. P., Qiao, D., Seidler, F. J., et al. (2004). Behavioral alterations in adolescent and adult rats caused by a brief subtoxic exposure to chlorpyrifos during neurulation. *Neurotoxicology and Teratology*, *26*(1), 95-101. doi:10.1016/j.ntt.2003.09.001
- Iwasaki, S., & Takahashi, T. (1998). Developmental changes in calcium channel types mediating synaptic transmission in rat auditory brainstem. *Journal of Physiology*, *509*(2), 419-23.
- Jacobson, J. L., & Jacobson, S. W. (1996). Intellectual impairment in children exposed to polychlorinated biphenyls in utero. *The New England Journal of Medicine*, *335*(11), 783-9. doi:10.1056/NEJM199609123351104
- Jameson, R. R., Seidler, F. J., Qiao, D., & Slotkin, T. A. (2006). Chlorpyrifos affects phenotypic outcomes in a model of mammalian neurodevelopment: Critical stages targeting differentiation in PC12 cells. *Environmental Health Perspectives*, *114*(5), 667-672.
- Jia, Z., & Misra, H. P. (2007). Reactive oxygen species in *in vitro* pesticide-induced neuronal cell (SH-SY5Y) cytotoxicity: Role of NF κ B and caspase-3. *Free Radical Biology and Medicine*, *42*(2), 288-298. doi:http://dx.doi.org/10.1016/j.freeradbiomed.2006.10.047
- Johnson, S., Nguyen, V., & Coder, D. (2013). Assessment of cell viability. *Current Protocols in Cytometry*, Chapter 9, Unit 9. doi:10.1002/0471142956.cy0902s64
- Kakko, I., Toimela, T., & Tähti, H. (2004). The toxicity of pyrethroid compounds in neural cell cultures studied with total ATP, mitochondrial enzyme activity and microscopic photographing. *Environmental Toxicology and Pharmacology*, *15*(2-3), 95-102. doi:10.1016/j.etap.2003.11.005
- Keil, A. P., Daniels, J. L., & Hertz-Picciotto, I. (2014). Autism spectrum disorder, flea and tick medication, and adjustments for exposure misclassification: The CHARGE (Childhood autism risks from genetics and environment) case-control study. *Environmental Health*, *13*(1), 3. doi:10.1186/1476-069X-13-3
- Kimura-Kuroda, J., Komuta, Y., Kuroda, Y., Hayashi, M., & Kawano, H. (2012). Nicotine-like effects of the neonicotinoid insecticides acetamiprid and imidacloprid on cerebellar neurons from neonatal rats. *Plos One*, *7*(2), 1-11. doi:10.1371/journal.pone.0032432

- Ko, J. H., & Strafella, A. P. (2012). Dopaminergic neurotransmission in the human brain: New lessons from perturbation and imaging. *The Neuroscientist*, *18*(2), 149-68. doi:10.1177/1073858411401413
- Komuro, H., & Rakic, P. (1992). Selective role of N-type calcium channels in neuronal migration. *Science*, *257*(5071), 806-9.
- Komuro, H., & Rakic, P. (1998). Orchestration of neuronal migration by activity of ion channels, neurotransmitter receptors, and intracellular Ca²⁺ fluctuations. *Journal of Neurobiology*, *37*(1), 110-30.
- Langeveld, W. T., Meijer, M., & Westerink, R. H. S. (2012). Differential effects of 20 Non-Dioxin-like PCBs on basal and depolarization-evoked intracellular calcium levels in PC12 cells. *Toxicological Sciences*, *126*(2), 487-496. doi:10.1093/toxsci/kfr346
- Larsson, M., Weiss, B., Janson, S., Sundell, J., & Bornehag, C. G. (2009). Associations between indoor environmental factors and parental-reported autistic spectrum disorders in children 6-8 years of age. *Neurotoxicology*, *30*(5), 822-31. doi:10.1016/j.neuro.2009.01.011
- Leclerc, C., Néant, I., & Moreau, M. (2011). Early neural development in vertebrates is also a matter of calcium. *Biochimie*, *93*(12), 2102-2111. doi:10.1016/j.biochi.2011.06.032
- Lee, I., Eriksson, P., Fredriksson, A., Buratovic, S., & Viberg, H. (2015a). Developmental neurotoxic effects of two pesticides: Behavior and biomolecular studies on chlorpyrifos and carbaryl. *Toxicology and Applied Pharmacology*, *288*(3), 429-38. doi:10.1016/j.taap.2015.08.014
- Lee, I., Eriksson, P., Fredriksson, A., Buratovic, S., & Viberg, H. (2015b). Developmental neurotoxic effects of two pesticides: Behavior and neuroprotein studies on endosulfan and cypermethrin. *Toxicology*, *335*, 1-10. doi:10.1016/j.tox.2015.06.010
- Lee, J. E., Park, J. H., Shin, I. C., & Koh, H. C. (2012). Reactive oxygen species regulated mitochondria-mediated apoptosis in PC12 cells exposed to chlorpyrifos. *Toxicology and Applied Pharmacology*, *263*(2), 148-62. doi:10.1016/j.taap.2012.06.005
- Lee, M., Gubernator, N. G., Sulzer, D., & Sames, D. (2010). Development of pH-responsive fluorescent false neurotransmitters. *Journal of the American Chemical Society*, *132*(26), 8828-8830. doi:10.1021/ja101740k
- Lefew, W. R., McConnell, E. R., Crooks, J. L., & Shafer, T. J. (2013). Evaluation of microelectrode array data using bayesian modeling as an approach to screening and prioritization for neurotoxicity testing. *Neurotoxicology*, *36*, 34-41. doi:10.1016/j.neuro.2013.02.006
- Leng, G., Gries, W., & Selim, S. (2006). Biomarker of pyrethrum exposure. *Toxicology Letters*, *162*(2-3 SPEC. ISS.), 195-201.
- Li, P., Ann, J., & Akk, G. (2011). Activation and modulation of human $\alpha 4\beta 2$ nicotinic acetylcholine receptors by the neonicotinoids clothianidin and imidacloprid. *Journal of Neuroscience Research*, *89*(8), 1295-301. doi:10.1002/jnr.22644
- Lipscombe, D., Allen, S. E., & Toro, C. P. (2013). Control of neuronal voltage-gated calcium ion channels from RNA to protein. *Trends in Neurosciences*, *36*(10), 598-609. doi:10.1016/j.tins.2013.06.008
- Liu, P. S., Kao, L. S., & Lin, M. K. (1994). Organophosphates inhibit catecholamine secretion and calcium influx in bovine adrenal chromaffin cells. *Toxicology*, *90*(1-2), 81-91.
- Lynch, G., & Schubert, P. (1980). The use of *in vitro* brain slices for multidisciplinary studies of synaptic function. *Annual Review of Neuroscience*, *3*, 1-22. doi:10.1146/annurev.ne.03.030180.000245
- Mackenzie Ross, S., McManus, I. C., Harrison, V., & Mason, O. (2013). Neurobehavioral problems following low-level exposure to organophosphate pesticides: A systematic and meta-analytic review. *Critical Reviews in Toxicology*, *43*(1), 21-44. doi:10.3109/10408444.2012.738645
- Magnani, E., & Bettini, E. (2000). Resazurin detection of energy metabolism changes in serum-starved PC12 cells and of neuroprotective agent effect. *Brain Research Protocols*, *5*(3), 266-72.
- Makris, S. L., & Vorhees, C. V. (2015). Assessment of learning, memory and attention in developmental neurotoxicity regulatory studies: Introduction. *Neurotoxicology and Teratology*, *52*(A), 62-7. doi:10.1016/j.ntt.2015.05.010
- Malik, N., Efthymiou, A. G., Mather, K., Chester, N., Wang, X., Nath, A., et al. (2014). Compounds with species and cell type specific toxicity identified in a 2000 compound drug screen of neural stem cells and rat mixed cortical neurons. *Neurotoxicology*, *45*, 192-200. doi:10.1016/j.neuro.2014.10.007
- Malkiewicz, K., Koterak, M., Folkesson, R., Brzezinski, J., Winblad, B., Szutowski, M., et al. (2006). Cypermethrin alters glial fibrillary acidic protein levels in the rat brain. *Environmental Toxicology and Pharmacology*, *21*(1), 51-5. doi:10.1016/j.etap.2005.06.005
- Marinovich, M., Ghilardi, F., & Galli, C. L. (1996). Effect of pesticide mixtures on *in vitro* nervous cells: Comparison with single pesticides. *Toxicology*, *108*(3), 201-206. doi:http://dx.doi.org/10.1016/0300-483X(96)03303-3
- Martin, S. J., Grimwood, P. D., & Morris, R. G. (2000). Synaptic plasticity and memory: An evaluation of the hypothesis. *Annual Review of Neuroscience*, *23*, 649-711. doi:10.1146/annurev.neuro.23.1.649
- Matsuda, K., Kanaoka, S., Akamatsu, M., & Sattelle, D. B. (2009). Diverse actions and target-site selectivity of neonicotinoids: Structural insights. *Molecular Pharmacology*, *76*(1), 1-10. doi:10.1124/mol.109.055186
- Mattson, M. (2007). Calcium and neurodegeneration. *Aging Cell*, *6*(3), 337-350. doi:10.1111/j.1474-9726.2007.00275.x
- Maurya, S. K., Mishra, J., Abbas, S., & Bandyopadhyay, S. (2015). Cypermethrin stimulates GSK3 β -dependent A β and p-tau proteins and cognitive loss in young rats: Reduced HB-EGF signaling and downstream neuroinflammation as critical regulators. *Molecular Neurobiology*, doi:10.1007/s12035-014-9061-6
- McConnell, E. R., McClain, M. A., Ross, J., Lefew, W. R., & Shafer, T. J. (2012). Evaluation of multi-well microelectrode arrays for neurotoxicity screening using a chemical training set. *Neurotoxicology*, *33*(5), 1048-57. doi:10.1016/j.neuro.2012.05.001

- McDaniel, K. L., & Moser, V. C. (1993). Utility of a neurobehavioral screening battery for differentiating the effects of two pyrethroids, permethrin and cypermethrin. *Neurotoxicology and Teratology*, *15*(2), 71-83.
- McDaniel, K. L., Padilla, S., Marshall, R. S., Phillips, P. M., Podhorniak, L., Qian, Y., et al. (2007). Comparison of acute neurobehavioral and cholinesterase inhibitory effects of N-methylcarbamates in rat. *Toxicological Sciences*, *98*(2), 552-60. doi:10.1093/toxsci/kfm114
- Meacham, C. A., Brodfuehrer, P. D., Watkins, J. A., & Shafer, T. J. (2008). Developmentally-regulated sodium channel subunits are differentially sensitive to α -cyano containing pyrethroids. *Toxicology and Applied Pharmacology*, *231*(3), 273-281. doi:http://dx.doi.org/10.1016/j.taap.2008.04.017
- Mehrani, H., & Golmanesh, L. (2008). Changes in mRNA and protein levels of nicotinic acetylcholine receptors in diazoxon exposed PC12 cells. *Toxicology in Vitro*, *22*(5), 1257-1263. doi:http://dx.doi.org/10.1016/j.tiv.2008.04.013
- Meijer, M., Brandsema, J. A. R., Nieuwenhuis, D., Wijnolts, F. M. J., Dingemans, M. M. L., & Westerink, R. H. S. (2015). Inhibition of voltage-gated calcium channels after subchronic and repeated exposure of PC12 cells to different classes of insecticides. *Toxicological Sciences*, *147*(2), 607-17. doi:10.1093/toxsci/kfv154
- Meijer, M., Dingemans, M. M. L., van den Berg, M., & Westerink, R. H. S. (2014a). Inhibition of voltage-gated calcium channels as common mode of action for (mixtures of) distinct classes of insecticides. *Toxicological Sciences*, *141*(1), 103-11. doi:10.1093/toxsci/kfu110
- Meijer, M., Hamers, T., & Westerink, R. H. S. (2014b). Acute disturbance of calcium homeostasis in PC12 cells as a novel mechanism of action for (sub)micromolar concentrations of organophosphate insecticides. *Neurotoxicology*, *43*, 110-116. doi:10.1016/j.neuro.2014.01.008
- Meijer, M., Hendriks, H., Heusinkveld, H., Langeveld, W., & Westerink, R. H. S. (2014c). Comparison of plate reader-based methods with fluorescence microscopy for measurements of intracellular calcium levels for the assessment of *in vitro* neurotoxicity. *Neurotoxicology*, *45C*, 31-37. doi:10.1016/j.neuro.2014.09.001
- Milton, V., & Sweeney, S. (2012). Oxidative stress in synapse development and function. *Developmental Neurobiology*, *72*(1), 100-10. doi:10.1002/dneu.20957
- Miodovnik, A. (2011). Environmental neurotoxicants and developing brain. *The Mount Sinai Journal of Medicine, New York*, *78*(1), 58-77. doi:10.1002/msj.20237
- Moore, K., & Roberts, L. J. (1998). Measurement of lipid peroxidation. *Free Radical Research*, *28*(6), 659-71
- Moreira, E. G., Yu, X., Robinson, J. F., Griffith, W., Hong, S. W., Beyer, R. P., et al. (2010). Toxicogenomic profiling in maternal and fetal rodent brains following gestational exposure to chlorpyrifos. *Toxicology and Applied Pharmacology*, *245*(3), 310-25. doi:10.1016/j.taap.2010.03.015
- Moser, V. C., Phillips, P. M., McDaniel, K. L., Marshall, R. S., Hunter, D. L., & Padilla, S. (2005). Neurobehavioral effects of chronic dietary and repeated high-level spike exposure to chlorpyrifos in rats. *Toxicological Sciences*, *86*(2), 375-386. doi:10.1093/toxsci/kfi199
- Moser, V. C. (1995). Comparisons of the acute effects of cholinesterase inhibitors using a neurobehavioral screening battery in rats. *Neurotoxicology and Teratology*, *17*(6), 617-625. doi:10.1016/0892-0362(95)02002-0
- Moser, V. C., McDaniel, K. L., Phillips, P. M., & Lowit, A. B. (2010). Time-course, dose-response, and age comparative sensitivity of N-methyl carbamates in rats. *Toxicological Sciences*, *114*(1), 113-123. doi:10.1093/toxsci/kfp286
- Moser, V. C., Phillips, P. M., & McDaniel, K. L. (2015). Assessment of biochemical and behavioral effects of carbaryl and methomyl in brown-norway rats from preweaning to senescence. *Toxicology*, *331*(0), 1-13. doi:http://dx.doi.org/10.1016/j.tox.2015.02.006
- Mrema, E. J., Rubino, F. M., Brambilla, G., Moretto, A., Tsatsakis, A. M., & Colosio, C. (2013). Persistent organochlorinated pesticides and mechanisms of their toxicity. *Toxicology*, *307*, 74-88. doi:10.1016/j.tox.2012.11.015
- Muñoz-Quezada, M. T., Lucero, B. A., Barr, D. B., Steenland, K., Levy, K., Ryan, P. B., et al. (2013). Neurodevelopmental effects in children associated with exposure to organophosphate pesticides: A systematic review. *Neurotoxicology*, *39*, 158-168. doi:http://dx.doi.org/10.1016/j.neuro.2013.09.003
- Nagata, K., Huang, C. S., Song, J. H., & Narahashi, T. (1997). Direct actions of anticholinesterases on the neuronal nicotinic acetylcholine receptor channels. *Brain Research*, *769*(2), 211-218. doi:10.1016/S0006-8993(97)00707-5
- Nasuti, C., Gabbianelli, R., Falcioni, M. L., Di Stefano, A., Sozio, P., & Cantalamessa, F. (2007). Dopaminergic system modulation, behavioral changes, and oxidative stress after neonatal administration of pyrethroids. *Toxicology*, *229*(3), 194-205. doi:10.1016/j.tox.2006.10.015
- Neal, A. P., Yuan, Y., & Atchison, W. D. (2010). Allethrin differentially modulates voltage-gated calcium channel subtypes in rat PC12 cells. *Toxicological Sciences*, *116*(2), 604-613. doi:10.1093/toxsci/kfq139
- Nguyen, P. V., Abel, T., Kandel, E. R., & Bourtochouladze, R. (2000). Strain-dependent differences in LTP and hippocampus-dependent memory in inbred mice. *Learning & Memory*, *7*(3), 170-9.
- Novellino, A., Scelfo, B., Palosaari, T., Price, A., Sobanski, T., Shafer, T. J., et al. (2011). Development of micro-electrode array based tests for neurotoxicity: Assessment of interlaboratory reproducibility with neuroactive chemicals. *Frontiers in Neuroengineering*, *4*, 4. doi:10.3389/fneng.2011.00004
- Organisation for Economic Co-operation and Development (OECD, 2015a) http://www.oecd-ilibrary.org/environment/oecd-guidelines-for-the-testing-of-chemicals-section-4-health-effects_20745788 (visited online 10-11-2015)
- Organisation for Economic Co-operation and Development (OECD, 2015b) http://www.oecd-ilibrary.org/environment/test-no-443-extended-one-generation-reproductive-toxicity-study_9789264122550-en (visited online 10-11-2015)
- Organisation for Economic Co-operation and Development (OECD, 2015c) http://www.oecd-ilibrary.org/environment/test-no-426-developmental-neurotoxicity-study_9789264067394-en (visited online 10-11-2015)

- Organisation for Economic Co-operation and Development (OECD, 2015d) http://www.oecd-ilibrary.org/environment/test-no-424-neurotoxicity-study-in-rodents_9789264071025-en (visited online 10-11-2015)
- Ostrea, E. M. Jr, Reyes, A., Villanueva-Uy, E., Pacifico, R., Benitez, B., Ramos, E., et al. (2012). Fetal exposure to propoxur and abnormal child neurodevelopment at 2 years of age. *Neurotoxicology*, 33(4), 669-75. doi:10.1016/j.neuro.2011.11.006
- Oulhote, Y., & Bouchard, M. F. (2013). Urinary metabolites of organophosphate and pyrethroid pesticides and behavioral problems in canadian children. *Environmental Health Perspectives*, 121(11-12), 1378-84. doi:10.1289/ehp.1306667
- Padilla, S., Marshall, R. S., Hunter, D. L., Oxendine, S., Moser, V. C., Southerland, S. B., et al. (2005). Neurochemical effects of chronic dietary and repeated high-level acute exposure to chlorpyrifos in rats. *Toxicological Sciences*, 88(1), 161-71. doi:10.1093/toxsci/kfi274
- Park, H., Park, J., Sovcikova, E., Kocan, A., Linderholm, L., Bergman, A., et al. (2009). Exposure to hydroxylated polychlorinated biphenyls (OH-PCBs) in the prenatal period and subsequent neurodevelopment in eastern slovakia. *Environmental Health Perspectives*, 117(10), 1600-6. doi:10.1289/ehp.0900611
- Peele, D. B., & Crofton, K. M. (1987). Pyrethroid effects on schedule-controlled behavior: Time and dosage relationships. *Neurotoxicology and Teratology*, 9(5), 387-94.
- Pereira, V. M., Bortolotto, J. W., Kist, L. W., Azevedo, M. B. d., Fritsch, R. S., Oliveira Rda, L., et al. (2012). Endosulfan exposure inhibits brain AChE activity and impairs swimming performance in adult zebrafish (danio rerio). *Neurotoxicology*, 33(3), 469-475. doi:10.1016/j.neuro.2012.03.005
- Phung, D. T., Connell, D., Miller, G., & Chu, C. (2012). Probabilistic assessment of chlorpyrifos exposure to rice farmers in vietnam. *Journal of Exposure Science and Environmental Epidemiology*, 22(4), 417-423. doi:10.1038/jes.2012.32
- Popa Wagner, A., Mitran, S., Sivanesan, S., Chang, E., & Buga, A. (2013). ROS and brain diseases: The good, the bad, and the ugly. *Oxidative Medicine and Cellular Longevity*, 2013, 963520. doi:10.1155/2013/963520
- Qiao, D., Seidler, F. J., & Slotkin, T. A. (2001). Developmental neurotoxicity of chlorpyrifos modeled in vitro: Comparative effects of metabolites and other cholinesterase inhibitors on DNA synthesis in PC12 and C6 cells. *Environmental Health Perspectives*, 109(9), 909-13.
- Qiao, D., Seidler, F. J., & Slotkin, T. A. (2005). Oxidative mechanisms contributing to the developmental neurotoxicity of nicotine and chlorpyrifos. *Toxicology and Applied Pharmacology*, 206(1), 17-26. doi:10.1016/j.taap.2004.11.003
- Qiao, D., Seidler, F. J., Tate, C. A., Cousins, M. M., & Slotkin, T. A. (2003). Fetal chlorpyrifos exposure: Adverse effects on brain cell development and cholinergic biomarkers emerge postnatally and continue into adolescence and adulthood. *Environmental Health Perspectives*, 111(4), 536.
- Rao, M. R., Kanji, V. K., & Sekhar, V. (1999). Pesticide induced changes of nitric oxide synthase in rat brain in vitro. *Drug and Chemical Toxicology*, 22(2), 411-20. doi:10.3109/01480549909017844
- Raszewski, G., Lemieszek, M. K., Lukawski, K., Juszczak, M., & Rzeski, W. (2015). Chlorpyrifos and cypermethrin induce apoptosis in human neuroblastoma cell line SH-SY5Y. *Basic & Clinical Pharmacology & Toxicology*, 116(2), 158-67. doi:10.1111/bcpt.12285
- Rauh, V., Arunajadai, S., Horton, M., Perera, F., Hoepner, L., Barr, D. B., et al. (2011). Seven-year neurodevelopmental scores and prenatal exposure to chlorpyrifos, a common agricultural pesticide. *Environmental Health Perspectives*, 119(8), 1196-1201. doi:10.1289/ehp.1003160
- Repetto, G., del Peso, A., & Zurita, J. L. (2008). Neutral red uptake assay for the estimation of cell viability/cytotoxicity. *Nature Protocols*, 3(7), 1125-31. doi:10.1038/nprot.2008.75
- Retz, W., Kornhuber, J., & Riederer, P. (1996). Neurotransmission and the ontogeny of human brain. *Journal of Neural Transmission*, 103(4), 403-19.
- Ricceri, L., Venerosi, A., Capone, F., Cometa, M. F., Lorenzini, P., Fortuna, S., et al. (2006). Developmental neurotoxicity of organophosphorous pesticides: Fetal and neonatal exposure to chlorpyrifos alters sex-specific behaviors at adulthood in mice. *Toxicological Sciences*, 93(1), 105-113. doi:10.1093/toxsci/kfl032
- Rice, D., & Barone, S. (2000). Critical periods of vulnerability for the developing nervous system: Evidence from humans and animal models. *Environmental Health Perspectives*, 108 Suppl 3, 511-33.
- Richendrer, H., Pelkowski, S. D., Colwill, R. M., & Créton, R. (2012). Developmental sub-chronic exposure to chlorpyrifos reduces anxiety-related behavior in zebrafish larvae. *Neurotoxicology and Teratology*, 34(4), 458-65. doi:10.1016/j.nt.2012.04.010
- Robbins, N., Koch, S. E., Tranter, M., & Rubinstein, J. (2012). The history and future of probenecid. *Cardiovascular Toxicology*, 12(1), 1-9. doi:10.1007/s12012-011-9145-8
- Roberts, E. M., English, P. B., Grether, J. K., Windham, G. C., Somberg, L., & Wolff, C. (2007). Maternal residence near agricultural pesticide applications and autism spectrum disorders among children in the california central valley. *Environmental Health Perspectives*, 115(10), 1482-9. doi:10.1289/ehp.10168
- Rodriguez, P. C., Pereira, D. B., Borgkvist, A., Wong, M. Y., Barnard, C., Sonders, M. S., et al. (2013). Fluorescent dopamine tracer resolves individual dopaminergic synapses and their activity in the brain. *Proceedings of the National Academy of Sciences of the United States of America*, 110(3), 870-875. doi:10.1073/pnas.1213569110
- Ross, G. (2004). The public health implications of polychlorinated biphenyls (PCBs) in the environment. *Ecotoxicology and Environmental Safety*, 59(3), 275-91. doi:10.1016/j.ecoenv.2004.06.003
- Roze, E., Meijer, L., Bakker, A., Van Braeckel, Koenraad N. J. A., Sauer, P. J. J., & Bos, A. F. (2009). Prenatal exposure to organohalogens, including brominated flame retardants, influences motor, cognitive, and behavioral performance at school age. *Environmental Health Perspectives*, 117(12), 1953-8. doi:10.1289/ehp.0901015

- Sachana, M., Flaskos, J., Alexaki, E., Glynn, P., & Hargreaves, A. J. (2001). The toxicity of chlorpyrifos towards differentiating mouse N2a neuroblastoma cells. *Toxicology in Vitro*, *15*(4-5), 369-72.
- Sachana, M., Flaskos, J., Sidiropoulou, E., Yavari, C. A., & Hargreaves, A. J. (2008). Inhibition of extension outgrowth in differentiating rat C6 glioma cells by chlorpyrifos and chlorpyrifos oxon: Effects on microtubule proteins. *Toxicology in Vitro*, *22*(5), 1387-91. doi:10.1016/j.tiv.2008.02.022
- Sachana, M., Flaskos, J., & Hargreaves, A. J. (2005). Effects of chlorpyrifos and chlorpyrifos-methyl on the outgrowth of axon-like processes, tubulin, and GAP-43 in N2a cells. *Toxicology Mechanisms and Methods*, *15*(6), 405-10. doi:10.1080/15376520500194767
- Sagiv, S. K., Nugent, J. K., Brazelton, T. B., Choi, A. L., Tolbert, P. E., Altshul, L. M., et al. (2008). Prenatal organochlorine exposure and measures of behavior in infancy using the neonatal behavioral assessment scale (NBAS). *Environmental Health Perspectives*, *116*(5), 666-73. doi:10.1289/ehp.10553
- Sagiv, S. K., Thurston, S. W., Bellinger, D. C., Tolbert, P. E., Altshul, L. M., & Korrick, S. A. (2010). Prenatal organochlorine exposure and behaviors associated with attention deficit hyperactivity disorder in school-aged children. *American Journal of Epidemiology*, *171*(5), 593-601. doi:10.1093/aje/kwp427
- Sarter, M., Bruno, J. P., & Parikh, V. (2007). Abnormal neurotransmitter release underlying behavioral and cognitive disorders: Toward concepts of dynamic and function-specific dysregulation. *Neuropsychopharmacology*, *32*(7), 1452-61. doi:10.1038/sj.npp.1301285
- Saulsbury, M. D., Heyliger, S. O., Wang, K., & Johnson, D. J. (2009). Chlorpyrifos induces oxidative stress in oligodendrocyte progenitor cells. *Toxicology*, *259*(1-2), 1-9. doi:10.1016/j.tox.2008.12.026
- Schuh, R., Lein, P., Beckles, R., & Jett, D. (2002). Noncholinesterase mechanisms of chlorpyrifos neurotoxicity: Altered phosphorylation of Ca²⁺/cAMP response element binding protein in cultured neurons. *Toxicology and Applied Pharmacology*, *182*(2), 176-85.
- Schwartz, M. P., Hou, Z., Propson, N. E., Zhang, J., Engstrom, C. J., Santos Costa, V., et al. (2015). Human pluripotent stem cell-derived neural constructs for predicting neural toxicity. *Proceedings of the National Academy of Sciences of the United States of America*, *112*(40), 12516-21. doi:10.1073/pnas.1516645112
- Scremin, O. U., Chialvo, D. R., Lavarello, S., Berra, H. H., & Lucero, M. A. (2011). The environmental pollutant endosulfan disrupts cerebral cortical function at low doses. *Neurotoxicology*, *32*(1), 31-37. doi:http://dx.doi.org/10.1016/j.neuro.2010.12.001
- Shelton, J. F., Geraghty, E. M., Tancredi, D. J., Delwiche, L. D., Schmidt, R. J., Ritz, B., et al. (2014). Neurodevelopmental disorders and prenatal residential proximity to agricultural pesticides: The CHARGE study. *Environmental Health Perspectives*, *122*(10), 1103-9. doi:10.1289/ehp.1307044
- Silva de Assis, H. C., Nicaretta, L., Marques, M. C. A., Crestani, S., Soares, K. C., Olmedo, D., et al. (2011). Anticholinesterase activity of endosulfan in wistar rats. *Bulletin of Environmental Contamination and Toxicology*, *86*(4), 368-72. doi:10.1007/s00128-011-0227-x
- Silva, M. H., & Beauvais, S. L. (2010). Human health risk assessment of endosulfan. I: Toxicology and hazard identification. *Regulatory Toxicology and Pharmacology*, *56*(1), 4-17. doi:http://dx.doi.org/10.1016/j.yrtph.2009.08.013
- Simms, B., & Zamponi, G. (2014). Neuronal voltage-gated calcium channels: Structure, function, and dysfunction. *Neuron*, *82*(1), 24-45. doi:10.1016/j.neuron.2014.03.016
- Singleton, S. T., Lein, P. J., Farahat, F. M., Farahat, T., Bonner, M. R., Knaak, J. B., et al. (2013). Characterization of α -cypermethrin exposure in egyptian agricultural workers. *International Journal of Hygiene and Environmental Health*, doi:10.1016/j.ijheh.2013.10.003
- Sledge, D., Yen, J., Morton, T., Dishaw, L., Petro, A., Donerly, S., et al. (2011). Critical duration of exposure for developmental chlorpyrifos-induced neurobehavioral toxicity. *Neurotoxicology and Teratology*, *33*(6), 742-51. doi:10.1016/j.ntt.2011.06.005
- Slotkin, T. A., Lobner, D., & Seidler, F. J. (2010). Transcriptional profiles for glutamate transporters reveal differences between organophosphates but similarities with unrelated neurotoxicants. *Brain Research Bulletin*, *83*(1-2), 76-83. doi:10.1016/j.brainresbull.2010.06.010
- Slotkin, T. A., MacKillop, E. A., Ryde, I. T., & Seidler, F. J. (2007a). Ameliorating the developmental neurotoxicity of chlorpyrifos: A mechanisms-based approach in PC12 cells. *Environmental Health Perspectives*, *115*(9), 1306-1313. doi:10.1289/ehp.10194
- Slotkin, T. A., MacKillop, E. A., Ryde, I. T., Tate, C. A., & Seidler, F. J. (2007b). Screening for developmental neurotoxicity using PC12 cells: Comparisons of organophosphates with a carbamate, an organochlorine, and divalent nickel. *Environmental Health Perspectives*, *115*(1), 93-101.
- Slotkin, T. A., & Seidler, F. J. (2008). Developmental neurotoxicants target neurodifferentiation into the serotonin phenotype: Chlorpyrifos, diazinon, dieldrin and divalent nickel. *Toxicology and Applied Pharmacology*, *233*(2), 211-219. doi:http://dx.doi.org/10.1016/j.taap.2008.08.020
- Slotkin, T. A., & Seidler, F. J. (2009a). Oxidative and excitatory mechanisms of developmental neurotoxicity: Transcriptional profiles for chlorpyrifos, diazinon, dieldrin, and divalent nickel in PC12 cells. *Environmental Health Perspectives*, *117*(4), 587-96. doi:10.1289/ehp.0800251
- Slotkin, T. A., & Seidler, F. J. (2009b). Transcriptional profiles reveal similarities and differences in the effects of developmental neurotoxicants on differentiation into neurotransmitter phenotypes in PC12 cells. *Brain Research Bulletin*, *78*(4-5), 211-25. doi:10.1016/j.brainresbull.2008.08.021
- Slotkin, T. A., & Seidler, F. J. (2011). Developmental exposure to organophosphates triggers transcriptional changes in genes associated with parkinson's disease *in vitro* and *in vivo*. *Brain Research Bulletin*, *86*(5-6), 340-7. doi:10.1016/j.brainresbull.2011.09.017
- Slotkin, T. A., & Seidler, F. J. (2012). Developmental neurotoxicity of organophosphates targets cell cycle and apoptosis, revealed by transcriptional profiles *in vivo* and *in vitro*. *Neurotoxicology and Teratology*, *34*(2), 232-41. doi:10.1016/j.ntt.2011.12.001

- Smulders, C. J. G. M., Bueters, T. J. H., Vailati, S., van Kleef, R. G. D. M., & Vijverberg, H. P. M. (2004). Block of neuronal nicotinic acetylcholine receptors by organophosphate insecticides. *Toxicological Sciences*, *82*(2), 545-54. doi:10.1093/toxsci/kfh269
- Smulders, C. J. G. M., Bueters, T. J. H., van Kleef, R. G. D. M., & Vijverberg, H. P. M. (2003). Selective effects of carbamate pesticides on rat neuronal nicotinic acetylcholine receptors and rat brain acetylcholinesterase. *Toxicology and Applied Pharmacology*, *193*(2), 139-146. doi:10.1016/j.taap.2003.07.011
- Soderlund, D. M. (2012). Molecular mechanisms of pyrethroid insecticide neurotoxicity: Recent advances. *Archives of Toxicology*, *86*(2), 165-181. doi:10.1007/s00204-011-0726-x
- Stanley, K. A., Curtis, L. R., Massey Simonich, S. L., & Tanguay, R. L. (2009). Endosulfan I and endosulfan sulfate disrupts zebrafish embryonic development. *Aquatic Toxicology*, *95*(4), 355-361. doi:http://dx.doi.org/10.1016/j.aquatox.2009.10.008
- Stapleton, A., & Chan, V. (2009). Subtoxic chlorpyrifos treatment resulted in differential expression of genes implicated in neurological functions and development. *Archives of Toxicology*, *83*(4), 319-33. doi:10.1007/s00204-008-0346-2
- The Molecular Probes Handbook. (2010). Chapter 18.2: Probes for reactive oxygen species including nitric oxide, generating and detecting reactive oxygen species; <http://www.lifetechnologies.com/nl/en/home/references/molecular-probes-the-handbook/probes-for-reactive-oxygen-species-including-nitric-oxide/generating-and-detecting-reactive-oxygen-species.html> (visited online 15-7-2014).
- Tilson, H. A. (1990). Neurotoxicology in the 1990s. *Neurotoxicology and Teratology*, *12*(4), 293-300.
- Timofeeva, O. A., Roegge, C. S., Seidler, F. J., Slotkin, T. A., & Levin, E. D. (2008). Persistent cognitive alterations in rats after early postnatal exposure to low doses of the organophosphate pesticide, diazinon. *Neurotoxicology and Teratology*, *30*(1), 38-45. doi:10.1016/j.ntt.2007.10.002
- Toescu, E. C., & Verkhatsky, A. (2007). The importance of being subtle: Small changes in calcium homeostasis control cognitive decline in normal aging. *Aging Cell*, *6*(3), 267-273. doi:10.1111/j.1474-9726.2007.00296.x
- Tomizawa, M., Lee, D. L., & Casida, J. E. (2000). Neonicotinoid insecticides: Molecular features conferring selectivity for insect versus mammalian nicotinic receptors. *Journal of Agricultural and Food Chemistry*, *48*(12), 6016-24.
- Tomizawa, M., & Casida, J. E. (2002). Desnitro-imidacloprid activates the extracellular signal-regulated kinase cascade via the nicotinic receptor and intracellular calcium mobilization in N1E-115 cells. *Toxicology and Applied Pharmacology*, *184*(3), 180-186. doi:http://dx.doi.org/10.1006/taap.2002.9503
- Tomizawa, M., & Casida, J. E. (2005). Neonicotinoid insecticide toxicology: Mechanisms of selective action. *Annual Review of Pharmacology and Toxicology*, *45*(1), 247-268. doi:10.1146/annurev.pharmtox.45.120403.095930
- Vale, C., Fonfra, E., Bujons, J., Messeguer, A., Rodriguez-Farr, E., & Suol, C. (2003). The organochlorine pesticides γ -hexachlorocyclohexane (lindane), α -endosulfan and dieldrin differentially interact with GABAA and glycine-gated chloride channels in primary cultures of cerebellar granule cells. *Neuroscience*, *117*(2), 397-403. doi:http://dx.doi.org/10.1016/S0306-4522(02)00875-8
- van Thriel, C., Westerink, R. H. S., Beste, C., Bale, A., Lein, P., & Leist, M. (2012). Translating neurobehavioural endpoints of developmental neurotoxicity tests into *in vitro* assays and readouts. *Neurotoxicology*, *33*(4), 911-24. doi:10.1016/j.neuro.2011.10.002
- Végh, M. J., Heldring, C. M., Kamphuis, W., Hijazi, S., Timmerman, A. J., Wan Li, K., et al. (2014). Reducing hippocampal extracellular matrix reverses early memory deficits in a mouse model of alzheimer's disease. *Acta Neuropathologica Communications*, *2*, 76. doi:10.1186/s40478-014-0076-z
- Vinken, M. (2013). The adverse outcome pathway concept: A pragmatic tool in toxicology. *Toxicology*, *312*, 158-65. doi:10.1016/j.tox.2013.08.011
- Vorhees, C. V., & Makris, S. L. (2015). Assessment of learning, memory, and attention in developmental neurotoxicity regulatory studies: Synthesis, commentary, and recommendations. *Neurotoxicology and Teratology*, *52*(A), 109-15. doi:10.1016/j.ntt.2015.10.004
- Wagner Schuman, M., Richardson, J., Auinger, P., Braun, J., Lanphear, B., Epstein, J., et al. (2015). Association of pyrethroid pesticide exposure with attention-deficit/hyperactivity disorder in a nationally representative sample of U.S. children. *Environmental Health*, *14*, 44. doi:10.1186/s12940-015-0030-y
- Walum, E., Clemedson, C., & Ekwall, B. (1994). Principles for the validation of *in vitro* toxicology test methods. *Toxicology in Vitro*, *8*(4), 807-12.
- Wang, J., Trouillon, R., Dunevall, J., & Ewing, A. (2014). Spatial resolution of single-cell exocytosis by microwell-based individually addressable thin film ultramicroelectrode arrays. *Analytical Chemistry*, *86*(9), 4515-20. doi:10.1021/ac500443q
- Wang, J., & Ewing, A. (2014). Simultaneous study of subcellular exocytosis with individually addressable multiple microelectrodes. *Analyst*, *139*(13), 3290-5. doi:10.1039/c4an00058g
- Weiner, M., Nemeč, M., Sheets, L., Sargent, D., & Breckenridge, C. (2009). Comparative functional observational battery study of twelve commercial pyrethroid insecticides in male rats following acute oral exposure. *Neurotoxicology*, *30* Suppl 1, S1-16. doi:10.1016/j.neuro.2009.08.014
- Westerink, R. H. S., & Ewing, A. G. (2008). The PC12 cell as model for neurosecretion. *Acta Physiologica*, *192*(2), 273-285. doi:10.1111/j.1748-1716.2007.01805.x
- Westerink, R. H. S. (2006). Targeting exocytosis: Ins and outs of the modulation of quantal dopamine release. *CNS & Neurological Disorders - Drug Targets*, *5*(1), 57-77.
- Westerink, R. H. S. (2013). Do we really want to REACH out to *in vitro*? *Neurotoxicology*, *39*(0), 169-172. doi:http://dx.doi.org/10.1016/j.neuro.2013.10.001

- Westerink, R. H. S., & Hondebrink, L. (2010). Are high-throughput measurements of intracellular calcium using plate-readers sufficiently accurate and reliable? *Toxicology and Applied Pharmacology*, 249(3), 247-248. doi:<http://dx.doi.org/10.1016/j.taap.2010.09.014>
- Westerink, R. H. S. (2014). Modulation of cell viability, oxidative stress, calcium homeostasis, and voltage- and ligand-gated ion channels as common mechanisms of action of (mixtures of) non-dioxin-like polychlorinated biphenyls and polybrominated diphenyl ethers. *Environmental Science and Pollution Research*, 21(10), 6373-83. doi:10.1007/s11356-013-1759-x
- Wilson, W. W., Shapiro, L., Bradner, J., & Caudle, W. M. (2014). Developmental exposure to the organochlorine insecticide endosulfan damages the nigrostriatal dopamine system in male offspring. *Neurotoxicology*, 44C, 279-287. doi:10.1016/j.neuro.2014.07.008
- Wolansky, M. J., Gennings, C., & Crofton, K. M. (2006). Relative potencies for acute effects of pyrethroids on motor function in rats. *Toxicological Sciences*, 89(1), 271-7. doi:10.1093/toxsci/kfj020
- Wolansky, M. J., & Harrill, J. A. (2008). Neurobehavioral toxicology of pyrethroid insecticides in adult animals: A critical review. *Neurotoxicology and Teratology*, 30(2), 55-78. doi:<http://dx.doi.org/10.1016/j.ntt.2007.10.005>
- Xu, F., Chang, X., Lou, D., Wu, Q., & Zhou, Z. (2012). Chlorpyrifos exposure causes alternation in dopamine metabolism in PC12 cells. *Toxicology Mechanisms and Methods*, 22(4), 309-14. doi:10.3109/15376516.2012.657260
- Yan, Y., Yang, Y., You, J., Yang, G., Xu, Y., Huang, N., et al. (2011). Permethrin modulates cholinergic mini-synaptic currents by partially blocking the calcium channel. *Toxicology Letters*, 201(3), 258-263. doi:10.1016/j.toxlet.2011.01.009
- Yang, D., Howard, A., Bruun, D., Aja Alemanj, M., Pickart, C., & Lein, P. (2008). Chlorpyrifos and chlorpyrifos-oxon inhibit axonal growth by interfering with the morphogenic activity of acetylcholinesterase. *Toxicology and Applied Pharmacology*, 228(1), 32-41. doi:10.1016/j.taap.2007.11.005
- Yu-Tao, T., Zhao-Wei, L., Yang, Y., Zhuo, Y., & Tao, Z. (2009). Effect of alpha-cypermethrin and theta-cypermethrin on delayed rectifier potassium currents in rat hippocampal neurons. *Neurotoxicology*, 30(2), 269-273. doi:<http://dx.doi.org/10.1016/j.neuro.2009.01.001>
- Zündorf, G., & Reiser, G. (2011). Calcium dysregulation and homeostasis of neural calcium in the molecular mechanisms of neurodegenerative diseases provide multiple targets for neuroprotection. *Antioxidants & Redox Signaling*, 14(7), 1275-1288. doi:10.1089/ars.2010.3359
- Zurich, M., Honegger, P., Schilter, B., Costa, L. G., & Monnet Tschudi, F. (2004). Involvement of glial cells in the neurotoxicity of parathion and chlorpyrifos. *Toxicology and Applied Pharmacology*, 201(2), 97-104. doi:10.1016/j.taap.2004.05.003

APPENDICES

NEDERLANDSE SAMENVATTING

Regelgeving voor het testen van chemicaliën op veiligheid

Om mens en milieu te beschermen is in de ontwikkelde landen de productie, het gebruik en het toepassen van chemicaliën gereguleerd. In Europa zijn verschillende regels omtrent chemicaliën vervangen door één regulering, genaamd REACH. REACH staat voor registratie, evaluatie en administratie van chemicaliën. De vorige wetgeving van de Europese Unie (EU) maakte onderscheid tussen "bestaande" (chemicaliën gerapporteerd op de Europese markt tussen 1971 en 1981; > 100.000 chemicaliën) en "nieuwe" chemicaliën (chemicaliën geïntroduceerd op de markt na 1981; > 3.800). Deze wet vereiste dat alleen nieuwe chemicaliën op veiligheid getest moesten worden voordat zij toegestaan worden op de markt. Dit is in tegenstelling met de nieuwe REACH regulering die vereist dat bedrijven veiligheidsinformatie leveren van alle chemicaliën die geproduceerd of geïmporteerd worden in grote volumes (> 1000 kg/jaar). Dit heeft tot gevolg dat meer veiligheids (toxiciteit) testen nodig zijn die volgens bepaalde richtlijnen uitgevoerd moeten zijn. Deze richtlijnen zijn gemaakt door de OECD (organisatie voor economische samenwerking en ontwikkeling; OECD) en beschrijven met name dierstudies (*in vivo* studies). Een voorbeeld van zo een '*in vivo*' studie is beschreven in OECD richtlijn 443. Deze richtlijn beschrijft een studie voor het evalueren van reproductie- en ontwikkelingseffecten van chemicaliënblootstelling voor- en na de geboorte, en systemische toxiciteit in zwangere en borstvoedende vrouwen en in hun nageslacht. Daarnaast kunnen studies, die uitgevoerd worden volgens deze richtlijn, een indicatie geven van andere typen toxiciteit. Als er indicaties zijn van door chemicaliën veroorzaakte toxiciteit aan het zenuwstelsel (neurotoxiciteit), dan moet er een extra studie worden uitgevoerd volgens de OECD richtlijn 426 of 424. Deze richtlijnen onderzoeken het effect van stoffen op respectievelijk het ontwikkelend en volwassen zenuwstelsel. De studies beschreven door testrichtlijnen 426 en 424 evalueren specifiek effecten van stoffen op gedragsveranderingen in cognitieve, sensorische en beweeg functies en veranderingen in de neuropathologie van dieren. Met de resultaten van deze studies wordt de veiligheid van chemicaliën geëvalueerd door het Europese chemicaliën agentschap (ECHA) of door de lidstaten.

Het DENAMIC (beoordeling van ontwikkelings neurotoxiciteit van mengsels in kinderen) project

Er zijn steeds meer zorgen dat de huidige regelgevende studies voor het vaststellen van mogelijke (ontwikkelings) neurotoxiciteit niet gevoelig genoeg zijn. Er zijn voornamelijk zorgen dat blootstellingen in onze leefomgeving aan lage niveaus van neurotoxische stoffen en mengsels daarvan, bijdragen aan de toename in leer- en ontwikkelingsstoornissen. Er zijn verschillende epidemiologische studies die indiceren dat blootstelling aan bekende neurotoxische stoffen de neuronale ontwikkeling in kinderen kan verstoren. Bij het onderzoek hiernaar worden veel proefdieren gebruikt, bij de huidige studies ten minste 80 dieren per experiment, ook zijn deze onderzoeken duur en kosten ze veel tijd (28 dagen tot 1 jaar). Hierdoor is de behoefte ontstaan aan betere (gevoeligere, goedkopere en snellere) en dier-vrije (*in vitro*) ontwikkelings- neurotoxiciteit studies die risico's voor de mens meer accuraat voorspellen. Het doel van het DENAMIC project was om methoden te ontwikkelen voor het screenen van chemicaliën op neurotoxiciteit om met deze methoden de handhaving van de EU wetgeving voor de identificatie van (potentiële) neurotoxische stoffen te ondersteunen en te verbeteren.

Het DENAMIC project bestaat uit twee delen; blootstelling/epidemiologie en het karakteriseren van gevaren. Deze delen worden samen gebruikt voor de risicobeoordeling. Het in dit proefschrift beschreven onderzoek was onderdeel van het karakteriseren van gevaren en focuste op de ontwikkeling van methoden voor het detecteren van neurotoxiciteit *in vitro*. Binnen het DENAMIC project zijn verschillende insecticiden (middelen voor het bestrijden van insecten) geselecteerd die bekend staan om hun neurotoxiciteit en aanwezigheid op voedsel. Er zijn verschillende insecticiden die op basis van werkingsmechanisme en moleculaire structuur gecategoriseerd zijn in verschillende klassen. Als referentie insecticiden binnen het DENAMIC project zijn endosulfan (een organochlorine), chlorpyrifos (een organofosfaat), cypermethrin (een pyrethroïde) en carbaryl (een carbamaat) geselecteerd. Daarnaast zijn imidacloprid (een neonicotinoïd), parathion, paraoxon-ethyl (metaboliet van parathion), paraoxon-methyl (metaboliet van methyl parathion) en chlorpyrifos-oxon (metaboliet van chlorpyrifos;organofosfaten) bestudeerd in dit proefschrift.

Aangrijpingspunten voor de detectie van neurotoxiciteit

Als onderdeel van het EU project DENAMIC zijn proefdier-vrije (*in vitro*) screenings methoden voor (ontwikkelings)neurotoxiciteit onderzocht. Voor dit proefschrift zijn verschillende neurotoxische aangrijpingspunten en methoden in deze *in vitro*-modellen onderzocht.

De onderzochte aangrijpingspunten en testen voor het screenen van neurotoxiciteit zijn: oxidatieve stress, neurotransmitter afgifte en calcium homeostase. Door de relevantie van deze processen voor neuronale functie, zijn deze eindpunten zeer geschikt voor het bepalen van neurotoxiciteit van stoffen. Voordat deze eindpunten gebruikt kunnen worden voor het '*in vitro*' bepalen van neurotoxiciteit, moeten de methoden voor de detectie van effecten van stoffen op deze eindpunten goed geëvalueerd worden.

Als eerste is in dit proefschrift onderzocht bij welke concentraties de stoffen cellen kunnen doden (cel toxiciteit). Dit is gedaan om te bepalen bij welke concentraties specifieke neurotoxische effecten verwacht kunnen worden. Dit wordt ook wel een concentratie-bereik studie genoemd (hoofdstuk 2). Effecten op cel toxiciteit werden niet ontdekt voor de meeste chemicaliën of alleen bij hoge concentraties (10-100 μM). Voor verdere studies zijn daarom maximale test concentraties van 10 μM gebruikt om te voorkomen dat de resultaten beïnvloed worden door cel toxiciteit.

Oxidatieve stress en neurotransmitter afgifte

In dit proefschrift zijn verschillende methoden geëvalueerd voor het meten van oxidatieve stress en neurotransmitter afgifte. Er zijn geen geschikte methoden gevonden om effecten van insecticiden op deze processen betrouwbaar te onderzoeken. Om betrouwbaardere methoden te ontwikkelen voor het testen van effecten van stoffen op oxidatieve stress en neurotransmitter afgifte wordt daarom meer onderzoek aangeraden

Calcium homeostase

Over het algemeen worden directe veranderingen in calcium homeostase gemeten met een plate reader-gebaseerde methode of met een fluorescentie microscopie-gebaseerde methode. Vanwege de lage(re) gevoeligheid, tijd en ruimtelijke resolutie en mogelijke valkuilen en artefacten is er kritiek op plate-reader-gebaseerde methoden. In dit proefschrift is een directe vergelijking gemaakt tussen resultaten verkregen met een plate reader- en een fluorescentie microscopie-gebaseerde

methode (hoofdstuk 5). Deze vergelijking heeft aangetoond dat de plate reader-gebaseerde methode niet geschikt is voor het testen van stoffen op neurotoxiciteit *in vitro*. Omdat fluorescentie microscopie een hoge-tijd en ruimtelijke resolutie heeft, zijn alle overige studies met fluorescentie microscopie uitgevoerd.

Voor dit proefschrift is uitgebreid onderzocht wat de effecten van insecticiden op calcium homeostase zijn (hoofdstukken 6, 7 en 8). Zoals eerder genoemd, zijn effecten op calcium homeostase onderzocht omdat zij een belangrijke rol spelen in neuronale functie. Het is eerder aangetoond dat verschillende typen stoffen, zoals PBDEs, PCBs en de organochlorine insecticide lindaan, de basale calcium concentratie kunnen verhogen in neuronale cellen. Daarnaast is ook aangetoond dat deze stoffen VGCCs (lading-gemedieerde calcium kanalen) kunnen inhiberen. Verschillende drugs, azole fungiciden en de organochlorine dieldrin verhogen de basale calcium concentratie niet maar remden wel VGCCs. In onze studies breiden wij deze bevindingen uit en laten we zien dat calcium homeostase een neurotoxisch aangrijpingspunt is voor neurotoxische insecticiden en gebruikt kan worden voor het testen van stoffen op neurotoxiciteit *in vitro*. Dit proefschrift laat zien dat verschillende typen insecticiden (organofosfaten, organochlorinen en pyrethroiden) de basale calcium concentratie kunnen veranderen en/of VGCCs remmen bij lage concentraties ($\leq 10 \mu\text{M}$). De carbamaat carbaryl, de neonicotinoïd imidacloprid, en de organofosfaat paraoxon-ethyl en -methyl veranderen de basale calcium concentratie niet en remde ook VGCCs niet. Verder is aangetoond dat voor het testen van neurotoxiciteit door middel van effecten op VGCCs een acuut blootstellingsscenario meestal voldoende is omdat, met uitzondering van chlorpyrifos, een subchronische blootstelling en een herhaaldelijke blootstelling aan insecticiden geen toename in VGCC inhibitie lieten zien.

Mensen zijn meestal blootgesteld aan mengsels van stoffen in plaats van aan één stof. Dit proefschrift heeft daarom ook de effecten van mengsels op calcium homeostase (hoofdstuk 6 en 7) onderzocht. De laagste effect concentraties (LOECs) en de concentraties waarbij geen effecten (NOECs) op VGCCs gemeten zijn met organofosfaten en carbaryl, zijn gecombineerd om binaire mengsels te vormen. Een binair LOEC mengsel van chlorpyrifos en zijn metaboliet chlorpyrifos-oxon en een binair LOEC mengsel van chlorpyrifos en parathion suggereren dat additiviteit

niet van toepassing is voor binaire mengsels van organofosfaten voor effecten op VGCCs (hoofdstuk 6). In tegenstelling, binaire mengsels van verschillende typen insecticiden laten additieve inhibitie van VGCCs zien (hoofdstuk 7). Dit is vergelijkbaar met data van binaire mengsels van azole fungiciden, die ook additieve inhibitie van VGCCs laten zien. Een tertiair mengsel van verschillende typen insecticiden liet een minder dan additief effect van VGCCs zien. Samengenomen kan voor stoffen met hetzelfde werkingsmechanisme additiviteit worden verwacht (hoofdstuk 7), alhoewel dit niet gezien is bij de combinatie van organofosfaten of bij tertiaire mengsels van insecticiden (hoofdstukken 6 en 7). De data indiceert dat effecten van mengsels moeten worden meegenomen in de risicobeoordeling om rekening te houden met additiviteit.

Gebruik van *in vitro* testen voor het testen op neurotoxiciteit

Om *in vitro* studies te kunnen gebruiken voor regelgevende veiligheidsstudies, moeten effecten *in vitro* vertaald worden naar de situatie in de mens. Om de relatie te begrijpen, en de kloof tussen *in vitro* en *in vivo* studies te verkleinen is een *ex vivo* studie uitgevoerd in dit proefschrift (hoofdstuk 9). Lange-termijn potentiatie (LTP) werd gemeten in muizen behandeld met chlorpyrifos op een wijze en met doses waarvan eerder is aangetoond dat deze spontaan gedrag in muizen beïnvloeden. Er is geen correlatie tussen LTP en spontaan gedrag gevonden. Deze gegevens suggereren dat deficiënties in LTP niet betrokken zijn of niet direct gecorreleerd kunnen worden aan de effecten van chlorpyrifos op spontaan gedrag (hoofdstuk 9). Wel moet in gedachten gehouden worden dat de interpretatie van de LTP data gehinderd werd door het lage aantal metingen en dat mogelijk een aantal subtiele effecten gedetecteerd hadden kunnen worden als er meer metingen waren verricht. Bij elkaar genomen lijken de acute effecten van chlorpyrifos op VGCCs *in vitro* (hoofdstuk 6 en 7) geen verband te hebben met een effect op LTP.

Om *in vitro* data te vergelijken met de humane situatie wordt in dit proefschrift voorgesteld om humane blootstellingsconcentraties te vergelijken met de effect concentraties *in vitro*. Ook is beargumenteerd dat een enkele *in vitro* test niet representatief is voor de complexiteit van een *in vivo* studie en dat meerdere *in vitro* testen gebruikt moeten worden om te screenen voor effecten op verschillende neurotoxische aangrijpingspunten. Van mogelijke aangrijpingspunten om te screenen

op neurotoxiciteit blijkt calcium homeostase een geschikt en gevoelig aangrijpingspunt. In combinatie met andere *in vitro* testen waarmee effecten op andere belangrijke neurotoxische aangrijpingspunten kunnen worden bestudeerd en met informatie over humane blootstellingsconcentraties, kunnen *in vitro* testen mogelijk al gebruikt worden voor het prioriteren van stoffen voor neurotoxiciteit studies. In het algemeen is er nog steeds een gebrek aan vertrouwen bij de regelgevende instanties met betrekking tot de voorspelbaarheid en betrouwbaarheid van *in vitro* testen voor humane neurotoxiciteit. Toch heeft een aantal van de bestaande *in vitro* testen de potentie om al een belangrijke rol te spelen bij het prioriteren van stoffen voor neurotoxiciteit.

DANKWOORD

...als laatste onderdeel van mijn proefschrift rest dan nog het gebruikelijke dankwoord. Dit proefschrift had hier niet gelegen als ik er alleen voor had gestaan. Bij deze alvast aan iedereen die hier een bijdrage aan heeft gegeven in welke vorm dan ook: dank hiervoor!

In het bijzonder wil ik een aantal mensen bedanken voor hun bijdrage. Copromotor Remco, jij hebt een belangrijke rol gespeeld in mijn opleiding. Tijdens mijn master heb ik stage gelopen bij Laura, bij de neurotox groep en heb ik mij verder kunnen ontwikkelen tot wetenschapper en is mijn interesse in neurotox gegroeid. Daarnaast was jij mijn begeleider vanuit de universiteit bij mijn andere stage en masterscriptie en stelde jij mij daarna in de gelegenheid om bij de neurotox groep te komen werken, eerst als onderzoeksmedewerker en daarna als AiO. Verder had hier uiteraard een heel andere boekje gelegen zonder jouw steun en kritische blik. Bedankt hiervoor en succes met de lopende projecten en met het aanvragen van nieuwe projecten.

Martin, dank dat jij mijn promotor was en voor de vrijheid en het vertrouwen dat je in mij en Remco had om dit proefschrift tot stand te laten komen. Bedankt voor je waardevolle input aan verschillende hoofdstukken in dit proefschrift.

Milou, als sub-coördinator van het DENAMIC project wil ik jou graag bedanken dat ik als AiO onderdeel was van DENAMIC. Zonder DENAMIC had hier geen proefschrift gelegen en was ik niet naar de leuke en interessante project bijeenkomsten geweest waar ik veel van heb geleerd. Dank ook voor jouw bijdrage aan verschillende hoofdstukken, voor je kritische blik en feedback die zeker ten goede zijn gekomen aan de kwaliteit van dit proefschrift. Ik wens jou veel succes met je nieuwe project(en).

Mijn neurotox collega's, Harm, Laura, Alfons, Hester H., Fiona, Gina, Aart, Martje en alle neurotox studenten van de afgelopen vier jaar, mede door jullie heb ik een goede tijd als AiO gehad. Bedankt voor alle gezellige lunches, pizza-meetings, BBQs en uitjes! Gina en Fiona, zonder jullie had ik nooit een experiment kunnen starten (waar ligt dat ene stofje ook al weer?) en Aart, zonder jouw technische ondersteuning en macros zou ik

nu nog steeds bezig zijn met mijn experimenten en uitwerking van de data. Harm, Martje en Hester H., bedankt voor jullie gezelligheid, feedback op presentaties, discussies en het zijn van zulke goede voorbeeld-AiOs. Ik heb veel van jullie geleerd en ik vond het erg leuk en bijzonder om jullie promoties te mogen meemaken. Jullie hebben allemaal een mooi boekje afgeleverd. Succes met jullie verdere carrières!

Mathijs, Joske en Desirée, heel erg bedankt voor jullie bijdrages aan mijn proefschrift! Mathijs, welliswaar geen gepubliceerd artikel maar jouw bijdrage was wel essentieel voor het tot stand komen van een DENAMIC rapport en dus ook een hoofdstuk voor mijn proefschrift. Joske en Desirée, zonder jullie harde werken was er geen hoofdstuk 8 in dit proefschrift. Bedankt allemaal dat jullie je vrijwillig hebben laten opsluiten in het donker voor de calcium experimenten en voor jullie enthousiasme! Ik wens jullie veel succes met jullie carrières.

Mijn roomies, Jessica, Harm, Hester H., Hester P., Soheil, Martje en recentelijk ook Annick, Anke en Anne. Bedankt voor de gezelligheid maar ook voor een luisterend oor als het tegen- en meezit. Mede door jullie ging ik met veel plezier naar het werk! Jessica, wij hebben veel gezellige klets/ thee momentjes gehad. Ik vind het erg leuk dat we elkaar nog zien! Harm, Hester H. en Martje, ik vond het leuk dat we als (rare) NTX-ers met elkaar op een kamer zaten en dat we op die manier makkelijk NTX-gerelateerde zaken (in de breedste zin van het woord) konden bespreken. Harm, je hield je goed staande tussen alle vrouwen in de kamer en met jouw humor was er een goede sfeer. Hester H., jouw versieringen maakte het een stuk minder vervelend om te werken op feestdagen. Martje, SOT2014 was voor mij ook het hoogtepunt. Ik zal nooit vergeten dat wij samen op de Grand Canyon stonden! Hester P., wij zijn tegelijkertijd begonnen als AiOs bij het IRAS en ik vond het erg leuk om met jou ervaringen hierover uit te wisselen. Ik vind het bijzonder dat wij allebei op zo een korte tijd van elkaar gaan promoveren. Soheil, good luck with finishing your project. Annick, Anke en Anne, het was kort maar krachtig, heel veel succes met jullie projecten. Annick, ik hoop dat je rond de tijd van mijn promotie je nog steeds bij het IRAS werkt. Aan je enthousiasme zal het niet liggen.

Overige partners in crime Karin, Maarke, en Cyrina. Karin, ik vond onze reisjes naar SOT superleuk. Ook zal ik nooit de leuke promotie-filmpjes vergeten die wij samen in elkaar hebben gezet! Maarke, wij waren de pioniers in hardlopen na het werk (later ook met Hester P. en Cyrina). Door elkaar hadden we een stok achter de deur om ook echt te gaan hardlopen! Dank voor deze gezellige momenten! Ook was jij vaak de drijvende kracht achter het organiseren van leuke uitjes met AiOs. Jouw energie en doorzettingsvermogen is bewonderingswaardig. Cyrina, de indertijd best-geïntegreerde VFFT-er bij IRAS-Tox, ik vind het superleuk dat ik jou na de verhuizing naar het JDV heb leren kennen. Met jou heb ik tot het einde van mijn contract veel gezellige hardlooptmomentjes gehad en kon ik altijd bij jou terecht voor een luisterend oor en wijze raad. IRAS-meiden, ik hoop dat we nog steeds contact met elkaar houden, in ieder geval via de Vrouwenzaken-app.

Alle andere niet bij naam genoemde collega's wil ik uiteraard ook bedanken voor hun hulp, interesse en gezelligheid bij de koekjes, de pantry en IRAS-uitjes en feestjes!

Naast mijn collega's wil ik ook mijn vrienden en familie bedanken voor interesse in mijn onderzoek en voor het zorgen voor ontspanning naast het werk. Papa en mama, bedankt voor alle steun. Het is een fijn gevoel om te weten dat jullie deur altijd voor mij open staat.

Mijn langste en goede vriendin Chantal en mijn broer Thijs, jullie zijn allebei belangrijk in mijn leven en ik vind het fijn dat jullie mij bij zullen staan op deze voor mij bijzondere dag.

Last but not least, mijn steun en toeverlaat, Eko. Tegelijkertijd zijn wij begonnen aan ons werkend leven na onze studies. Ik vind het fijn dat je er altijd voor me bent en dat we slechte en goede momenten met elkaar kunnen delen. Ook houd je mij met beide benen op de grond en kan jij (bijna) alles weer goed maken met jouw hartelijke lach en wijze raad. Terima kasih atas dukunganmu. Semoga kita bisa memiliki banyak kenangan indah bersama. Aku bangga padamu, cintaku.

Marieke

ABOUT THE AUTHOR

Marieke Meijer

Marieke Meijer was born on April 2nd, 1988 in Beverwijk and grew up in Maarssen. She completed a bachelor education in biology in 2009 and continued with a master education in Toxicology and Environmental Health. During her masters, she did an internship at the Neurotoxicology Research Group, IRAS, with the supervision of Laura Hondebrink. Her work has resulted in two co-authored scientific publications. She performed her second internship at Xpand Biotechnology. After successfully completing a thesis with the supervision of Leo van der Ven at the RIVM, she obtained her master degree in 2011. Marieke was offered a job as a research assistant for four months at IRAS, which has resulted in one co-authored publication and was offered a job position as a PhD candidate at the Neurotoxicology Research Group. She started as a PhD candidate from January 1st, 2012 until December 2015 with the supervision of Dr. Remco H.S. Westerink and Prof. dr. Martin van den Berg. Her work has resulted in several reports for the European Union and four first-authored publications. Also, she completed several postgraduate courses needed to obtain a registration as European registered toxicologist. From April 2016 she will continue her career as an advisor/toxicologist at RPS.

LIST OF PUBLICATIONS

Meijer M, Brandsema JA, Nieuwenhuis D, Wijnolts FM, Dingemans MM, Westerink RHS. Inhibition of voltage-gated calcium channels after subchronic and repeated exposure of PC12 cells to different classes of insecticides. *Toxicol Sci.* **2015** 147(2):607-17. doi: 10.1093/toxsci/kfv154.

Meijer M, Hendriks HS, Heusinkveld HJ, Langeveld WT, Westerink RHS. Comparison of plate reader-based methods with fluorescence microscopy for measurements of intracellular calcium levels for the assessment of *in vitro* neurotoxicity. *Neurotoxicology.* **2014** 45C:31-37. doi: 10.1016/j.neuro.2014.09.001.

Meijer M, Dingemans MML, van den Berg M, Westerink RHS. Inhibition of voltage-gated calcium channels as common mode of action for (mixtures of) distinct classes of insecticides. *Toxicol Sci.* **2014** 141(1):103-11. doi: 10.1093/toxsci/kfu110.

Meijer M, Hamers T, Westerink RHS. Acute disturbance of calcium homeostasis in PC12 cells as a novel mechanism of action for (sub)micromolar concentrations of organophosphate insecticides. *Neurotoxicology.* **2014** 43:110-6. doi: 10.1016/j.neuro.2014.01.008.

Hendriks HS, Meijer M, Muilwijk M, van den Berg M, Westerink RHS. A comparison of the *in vitro* cyto- and neurotoxicity of brominated and halogen-free flame retardants: prioritization in search for safe(r) alternatives. *Arch Toxicol.* **2014** 88(4):857-69. doi: 10.1007/s00204-013-1187-1.

Langeveld WT, Meijer M, Westerink RHS. Differential effects of 20 non-dioxin-like PCBs on basal and depolarization-evoked intracellular calcium levels in PC12 cells. *Toxicol Sci.* **2012** 126(2):487-96. doi:10.1093/toxsci/kfr346.

Hondebrink L, Meulenbelt J, Rietjens SJ, Meijer M, Westerink RHS. Methamphetamine, amphetamine, MDMA ('ecstasy'), MDA and mCPP modulate electrical and cholinergic input in PC12 cells. *Neurotoxicology.* **2012** 33(2):255-60. doi:10.1016/j.neuro.2011.09.003.

Hondebrink L, Meulenbelt J, Meijer M, van den Berg M, Westerink RHS. High concentrations of MDMA ('ecstasy') and its metabolite MDA inhibit calcium influx and depolarization-evoked vesicular dopamine release in PC12 cells. *Neuropharmacology.* **2011** 61(1-2):202-8. doi: 10.1016/j.neuropharm.2011.03.028.

